Catalytic Asymmetric Approaches to Nitrogen-Containing Bicycles



Yan Zhang

Somerville College

University of Oxford

A thesis submitted for the degree of

Doctor of Philosophy

Hilary 2023

Declaration

This thesis describes work carried out in the Chemistry Research Laboratory, University of Oxford, between October 2018 and November 2022 under the supervision of Prof. Stephen. P. Fletcher. This thesis is a result of my own work and has not been submitted for any other degree at this or any other university.

Yan Zhang

Acknowledgements

I would like to thank Prof. Stephen P. Fletcher with my sincerest gratitude for offering me a place in the group for my DPhil research. Thank you, Steve, for your guidance and support throughout my DPhil. The process from a BSc directly to a DPhil has not been easy, but the patience you had for me truly eased the confusion and I cannot thank you enough for all the happy problem-solving discussions and chats.

I am very grateful to Dr. Friedrich Wieland Goetzke, who has also supervised and guided me during my DPhil. Thank you for all the inspirations, ideas, lab tips, and kind reminders in these four years, thank you for always looking out for me. You are one of the best chemists and kindest people I have ever known.

I would like to thank all the Fletcher group members, old and new, for being my family in Oxford; and for all the kindness, friendship, help, advice you had given me as well as for all the karaoke songs and midnight drinks we have had together. You made my DPhil a lot easier.

Elena, Laszlo, Ke, Sourabh – thank you for being my good friends, for all the Chemistry advice and non–Chemistry chats, as well as the Wendy's and Chinese food we had together.

Thank you, David, for sharing the happy and bad moments in the lab.

Big thanks to Elias, Rob, Reece, Alex B., Alex H., Masha, Ivan and Josh: thank you all for making me feel no longer a stranger in the group.

Special thanks to Dr. Friedrich Wieland Goetzke, Dr. László Balázs, and Mr. Ke Liu for kindly proofreading my thesis, I cannot thank you more for your kindness and patience.

I am extremely grateful for my two viva assessors, Prof. Michael Willis and Prof. Jeremy Wulff, for their kind suggestions and the inspiring discussion we had during the viva. Thank you for your time and patience.

I also want to thank Prof. Alan C. Spivey and Dr. Mahesh Mohan at Imperial College London,

as you are mentors that enlightened and led me to this path of science, where I am able to learn more about Chemistry.

I would also like to thank my friends scattered around the world, Zifan Zhang, Xinjie Pan, Yuhan Jian, Yihuan Ma, Mengyao Wu, Yihan Wang, Yang Liu, Ziwei Zhang, Jiaqi Tian, Mengjun Gong, Zhiqian Wu, for all the stress-relieving chats, the great times, and the big laughs and smiles we had together. Friendship is one of the most important parts of one's life, and with you all, the part of mine is complete.

In the long path, one always needed inspirations and enthusiasm, therefore, I would like to thank Meiyun Lai, Seulgi Kang, Xijun Liu for their presence. Thank you for being the light.

Being a lucky person to be able to learn about something that I love, I feel that I am even luckier to have met someone who loves me and understands me. Thank you, Wenze, for being here for me during my highlights and the hardest times. Thank you for all the sunny days, full moons, scenery along the railways - and for the moments we shared, together or 9617 km apart. I cannot wait to walk down this mysterious path of life together with you.

Finally, my greatest gratitude to my parents, for their everlasting and unconditional love and support since I was born. Thank you for all the important decisions and suggestions that led me to the place I am at and thank you for understanding and backing me up even when I made bad decisions. I know that I am yet to mature and grow, but being your daughter is the greatest accomplishment of my life. Thank you for being the best parents and I owe you both a thousand hugs.

This thesis is dedicated to Xiaoqin Zhang and Binglun Sun, the greatest and most loving grandparents in the whole world. I miss you so much.

Life is an infinitely large puzzle, and thank you again to all that mentioned above, as you are the pieces that made me, someone who I am proud of today.

Abstract

In this thesis, we report a series of asymmetric rhodium-catalysed Suzuki-Miyaura cross-coupling reactions between nitrogen-containing bicycles and boron species. High stereoselectivity was observed on nortropane derivatised allyl chloride, while the reaction with quinuclidine species requires further optimisations.

In Chapter 1, we summarise recent development of catalytic asymmetric Suzuki-Miyaura cross-coupling reactions on cyclic products, specifically with rhodium catalysis with the establishment of multiple stereogenic centres. Next, the advancements in catalytic asymmetric synthesis of nitrogen-containing cyclic molecules by cross-coupling reactions were highlighted in the second section. Furthermore, an introduction was given on different types of asymmetric reactions, including Kinetic Resolution (KR), Dynamic Kinetic Resolution (DKR), and Dynamic Kinetic Asymmetric Transformation (DyKAT).

In Chapter 2, we present a highly enantio- and diastereoselective asymmetric Rh-catalysed Suzuki-Miyaura cross-coupling reactions of racemic nortropane-derived allylic chloride with aryl- and heteroaryl boronic pinacol esters. The reactions proceeded *via* a kinetic resolution process to afford highly enantioenriched bicyclic products and enantiopure allylic chloride. This method was applied in the first catalytic asymmetric synthesis of an intermediate of YZJ-1139(1), a potential insomnia treatment which completed Phase II trials. Further synthetic utility of enantiopure allyl chloride was demonstrated by highly enantiospecific S_N2' reactions with N-, O-, and S-containing nucleophiles.

In Chapter 3, we investigated the asymmetric Rh-catalysed arylation reactions between dehydroquinuclidine-derived substrates and aryl boronic acids. Various substrates including dehydroquinuclidine, its *N*-oxide derivative, and its nitrogen-borane complex were synthesised and tested subject to different conditions under rhodium-catalysis. The substrate exhibited reactivity and stereoselectivity but required further optimisations.

List of Abbreviations

°	Degrees
α	Alpha
δ	Chemical shift in ppm
λ	Wavelength
μ	Micro-
ν	Wavenumber
Ac	Acetyl or acetate
Aq.	Aqueous
Ar	Aryl
Atm	Atmospheric pressure
BINAP	(2,2′-bis(diphenylphosphino)-1,1′-binaphthyl)
Bn	Benzyl
Boc	Tert-butoxy carbonyl
Br.	Broad
c	Centi-
C	Celsius
C_3-TunePhos	1,13-Bis(diphenylphosphino)-7,8-dihydro-6H dibenzo[f,h][1,5]dioxonin
Cl-MeO-BIPHEP	(5,5′-Dichloro-6,6′-dimethoxy-1,1′-biphenyl)-2,2′-diyl-bis(diphenylphosphine)
cod	1,5–Cyclooctadiene
COSY	Correlation spectroscopy experiment
Cy	Cyclohexyl
d	Doublet (NMR)
dd	Doublet of doublets (NMR)
ddd	Doublet of doublets of doublets (NMR)
DBU	1,8-Diazabicyclo[5.4.0]undec-7-ene
DIPA	Diisopropylamine
DMAP	4-Dimethylaminopyridine
DME	Dimethoxyethane
DM-SEGPHOS	5,5′−Bis[di(3,5-xylyl)phosphino]-4,4′-bi-1,3-benzodioxole

DMSO	Dimethyl sulfoxide
dppf	(1,1'-Bis(diphenylphosphino)ferrocene)
d.r.	Diasteromeric ratio
DTBM-SEGPHOS	5,5′-Bis[di(3,5-di-tert-butyl-4-methoxyphenyl)phosphino]-4,4′-bi-1,3-benzodioxole
DyKAT	Dynamic kinetic transformation
ee	Enantiomeric excess
eq.	Equivalent(s)
e.r.	Enantiomeric ratio
Et	Ethyl
ESI	Electrospray ionisation
FC	Flash column chromatography
g	Gram(s)
GC	Gas chromatography
h	Hour(s)
HPLC	High pressure liquid chromatography
HRMS	High-resolution mass spectrometry
HSQC	Heteronuclear single quantum coherence
Hz	Hertz
IR	Infrared spectroscopy
J	J-coupling constants in Hz (NMR)
Josiphos	2-(Diphenylphosphino)ferrocenyl]ethyldicyclohexylphosphine
KHMDS	Potassium hexamethyldisilazane
KR	Kinetic resolution
L	Litre
m	multiplet (NMR)
M	Molar/Molarity
Me	Methyl
Mes	Mesityl
min.	Minute(s)
mmol	Millimoles
Ms	Methanesulfonyl
MS	Mass spectroscopy

m.p.	Melting point
m/z	Mass to charge ratio
NCS	N–Chlorosuccinimide
NHC	*N*–Hetereocyclic carbene
NMR	Nuclear magnetic resonance
p	Pentet (NMR)
Ph	Phenyl
Pin	Pinacol
ppm	Parts per million (NMR)
P-Phos	2,2′,6,6′-Tetramethoxy-4,4′-bis(diphenylphosphino)-3,3′-bipyridine
q	Quartet (NMR)
RhAAAr	Rhordium-catalysed Asymmetric Allylic Arylation
s	Singlet (NMR) or Strong (IR)
Sat	Saturated
SEGPHOS	5,5′-Bis(diphenylphosphino)-4,4′-bi-1,3-benzodioxole
SFC	Supercritical fluid chromatography
SM	Suzuki-Miyaura
S_N1	Unimolecular nucleophilic substitution
S_N2	Bimolecuar nucleophilic substitution
S_N2'	Bimolecuar nucleophilic substitution with allylic rearrangement
sp	Orbital hybridisation: 1:1 p:s character
sp^2	Orbital hybridisation: 2:1 p:s character
sp^3	Orbital hybridisation: 3:1 p:s character
t	Triplet (NMR)
TA	Tropane Alkaloids
*t*Bu	*tert*-Butyl
TA	Tropane alkaloids
Tf	Trifluoromethanesulfonate
TFA	Trifluoroacetic acid
TFAA	Trifluoroacetic anhydride
THF	Tetrahydrofuran
TMS	Trimethylsilyl
UHP	Urea hydrogen peroxide

Xylyl-P-Phos	2,2′,6,6′-Tetramethoxy-4,4′-bis[di(3,5-xylyl)phosphino]-3,3′-bipyridine
wt	Weight

Table of Contents

Chapter 1: Catalytic Asymmetric Reactions of Cyclic Compounds

1.1 Asymmetric Suzuki-Miyaura Cross-Coupling Reactions On Cyclic Compounds **1**

1.1.1 Asymmetric SM $C(sp^2)$–$C(sp^2)$ Coupling Reactions On Cyclic Substrates **4**

1.1.2 Asymmetric SM $C(sp^3)$–$C(sp^2)$/$C(sp^3)$ Coupling Reactions On Cyclic Substrates **9**

1.2 Nitrogen–Heterocycle Synthesis by Asymmetric Cross-coupling **17**

1.2.1 Asymmetric Coupling Reactions Towards Nitrogen-containing Heteroaromatics **17**

1.2.2 Asymmetric Coupling Reactions Towards Saturated Nitrogen Heterocycles **20**

Chapter 2: Synthesis of Nortropanes *via* Rh-catalysed Asymmetric Allylic Arylation

2.1 Project Background **24**

2.1.1 Synthesis of Chiral Tropane Derivatives from the Chiral Pool **27**

2.1.2 Synthesis of Chiral Tropane Derivatives by Desymmetrisation **29**

2.1.3 Enantioselective Synthesis of Tropane Scaffold **31**

2.2 Project Aims **34**

2.3 Results and Discussion **36**

2.3.1 Substrate Synthesis **36**

2.3.2 Reaction Optimisation **38**

2.3.3 Design of Experiments **42**

2.3.4 Synthesis and Tests of Other Substrates **44**

2.3.5 Mechanistic Experiments **50**

2.3.6 Reaction Scope **53**

2.3.7 Product Derivatisation **55**

2.4 Conclusion and Future Work **58**

Chapter 3: Synthesis of Quinuclidines *via* Rh-Catalysed Asymmetric Arylation

3.1 Project Background **61**

3.1.1 Synthesis of Enantioenriched Quinuclidine Rings by Cyclisation **64**

3.1.2 Synthesis of Enantioenriched Quinuclidine Rings by Modifications on Ring Substituents **66**

3.2 Project Aims **69**

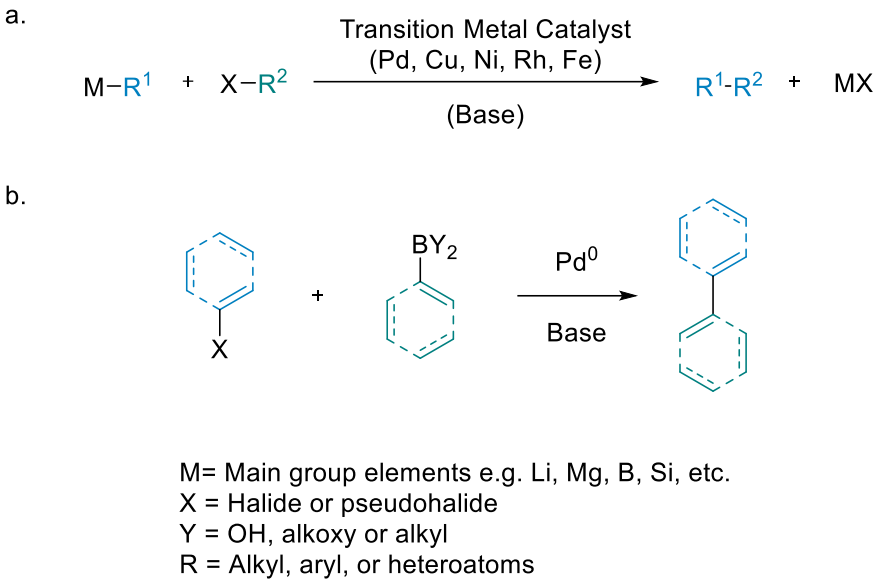
3.3 Results and Discussion **72**

3.3.1 Substrate Synthesis **72**
3.3.2 Rh-Catalysed Arylation Reaction **76**
3.3.3 Synthesis and Tests of Other Substrates **81**
3.4 Conclusion and Future Work **87**
Chapter 4: Experimental Procedures
4.1 General Information **90**
4.2 Chapter 2 Procedures **92**
4.2.1 Substrate Synthesis **92**
4.2.2 Rh-Catalysed Allylic Arylation Reactions **117**
4.2.3 Product Characterisations **118**
4.2.4 Upscale and Derivatisation of Product **144**
4.2.5 Derivatisation of Enantiopure Allyl Chloride **147**
4.2.6 Calculation of Apparent *S*-Factors **151**
4.2.7 X-Ray Crystallographic Analysis **153**
4.3 Chapter 3 Procedures **157**
4.3.1 Substrate Synthesis **157**
4.3.2 Rh-Catalysed Asymmetric Arylation Reactions **164**
Chapter 5: References **167**

Chapter 1: Catalytic Asymmetric Reactions of Cyclic Compounds

1.1 Asymmetric Suzuki-Miyaura Cross-coupling Reactions On Cyclic Substrates

Aromatic and aliphatic carbocycles and heterocycles are important building blocks in countless naturally occurring molecules and drugs, hence synthetic methods assembling cyclic components in an efficient manner has been among the top research areas of interest in organic chemistry. [1] Cross-coupling is one of the most efficient and reliable methods for building new cyclic molecules by joining two fragments with the formation of new C–C bonds. Two types of substrates are involved in cross-coupling reactions: the nucleophilic coupling partner, typically being organometallic species; and the electrophile, often being sp^2-hybridised organohalides or organo-pseudohalides (Scheme 1.1.1a). [2-4]



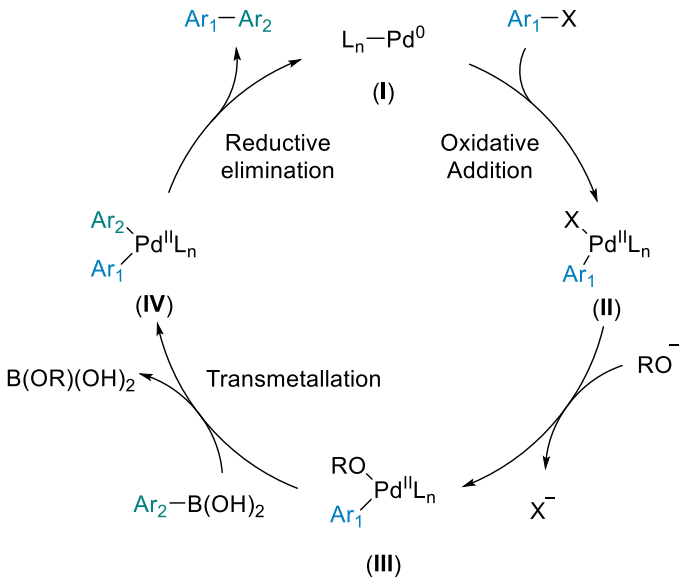
Scheme 1.1.1 a. General cross-coupling reactions. **b**. Classical Suzuki-Miyaura cross-coupling reactions.

These cross-coupling reactions often require use of transition metal catalysts, and different classes of catalysts include Pd, Cu, Ni, Rh, Fe. Among all, palladium is the most frequently used catalyst due to its high functional group tolerance. [5] In some cross-coupling reactions, the addition of base is required. Significant advancement in cross-coupling reactions took place in the 1970s with the developments in transition metal catalysis, with major contributions being

made in the area by chemists including Heck, [6] Kumada, [7] Sonogashira, [8] Negishi, [9] Stille, [10] Suzuki, and Miyaura. [11-13]

Suzuki-Miyaura (SM) cross-coupling reactions utilise organoboron compounds with organic (pseudo)halides as the two fragments, and the reaction operates under the presence of Pd catalyst and base. Among various cross-coupling reactions, SM reactions stand out as one of the most strategically important reactions to construct biaryls (Scheme 1.1.1b), and they have been widely applied for poly-olefins, styrenes and substituted biphenyl synthesis. [14] This reaction was first reported by Suzuki and Miyaura in 1979, and the importance of this robust method was recognised by the award of a Nobel Prize in Chemistry to Akira Suzuki. The award was jointly won by Richard F. Heck and Ei-ichi Negishi for their contribution in Pd-catalysed cross-coupling reactions. [15]

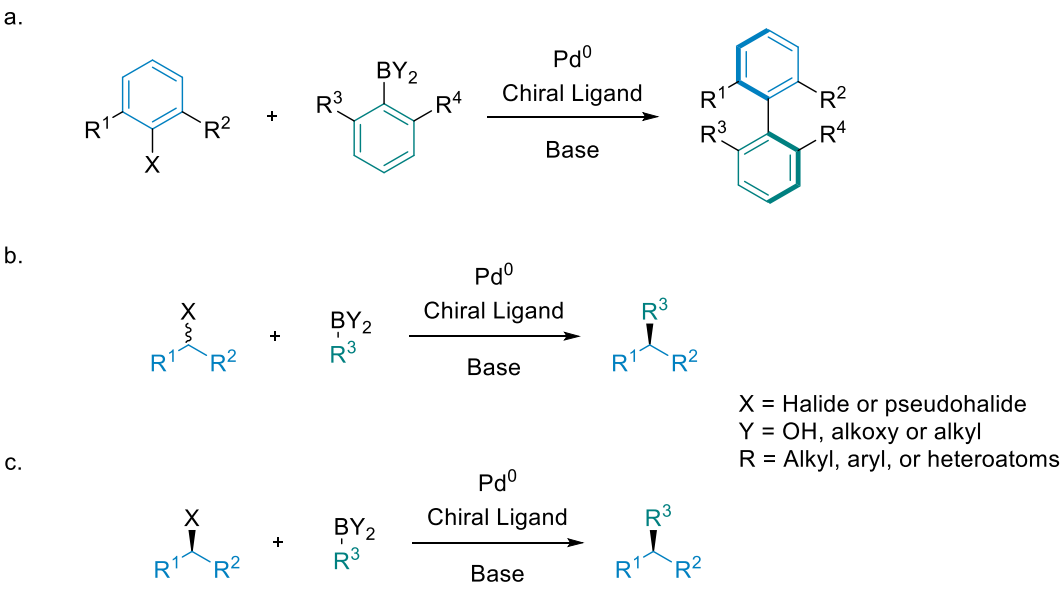
The reason that SM cross-coupling reactions are widely applied in various areas of chemistry is because of its high functional group tolerance, and predictable chemoselectivity. Furthermore, the easy access, low toxicity, and bench stability of most organoboron compounds added to the practicability of the reaction.[16] The mechanism of Suzuki-Miyaura cross-coupling reactions is similar to other cross-coupling reactions, where oxidative addition of aryl (pseudo)halide to the palladium(0) complex occurs first to give an aryl palladium(II) intermediate. Next, transmetallation of the organoboron species takes place with the assistance of base to form the diaryl palladium(II) complex. Finally, reductive elimination occurs to give the biaryl product, regenerating the palladium(0) catalyst for the next catalytic cycle (Scheme 1.1.2).



Scheme 1.1.2 Generic catalytic cycle for palladium-catalysed Suzuki-Miyaura cross-couplings.

Even with its wide application in organic synthetic chemistry, certain drawbacks of classical SM cross-coupling reactions exist. The main disadvantage of the reaction is that the flatness of aryl substrates tends to result in lower molecular complexity in comparison to saturated substrates, as classical SM reactions mostly generate new C–C bonds between sp^2 hybridised carbon centres. As it was noted that higher levels of carbon saturation and three-dimensionality in the target molecule as well as the presence with chiral carbon correlate with success throughout different phases of drug discovery, work has been done in developing catalytic asymmetric SM cross-coupling reactions that afford products with more chiral elements. [17-19] Catalytic asymmetric SM coupling reactions generally afford enantio- and diastereo-enriched products using chiral ligands alongside the Pd catalyst, and they could generally be divided into three different categories (Scheme 1.1.3).

The first approach establishes product with axial, planar, or point chirality by building new $C(sp^2)$–$C(sp^2)$ bonds (Scheme 1.1.3a); the other method generally involves desymmetrisation or enantioconvergent reaction, coupling substrates with sp^3 hybridised carbon centres and generating stereogenic centres in the product (Scheme 1.1.3b); the third approach utilises enantioenriched substrate and the stereochemistry is preserved in the reaction.



Scheme 1.1.3 Catalytic asymmetric Suzuki-Miyaura cross-coupling. **a**. Asymmetric SM reactions constructing axially chiral biaryl products. **b**. Asymmetric SM reactions constructing stereogenic centres. **c**. Asymmetric SM reactions on enantioenriched substrates.

Below in sections of Chapter 1.1, the recent advancements in asymmetric Suzuki-Miyaura cross-coupling reactions on cyclic substrates on the first two types of asymmetric reactions towards enantioenriched cyclic products will be introduced. Examples for the third approach will be given in Chapter 1.2.2.

1.1.1 Asymmetric SM C(sp^2)–C(sp^2) Coupling Reactions On Cyclic Substrates

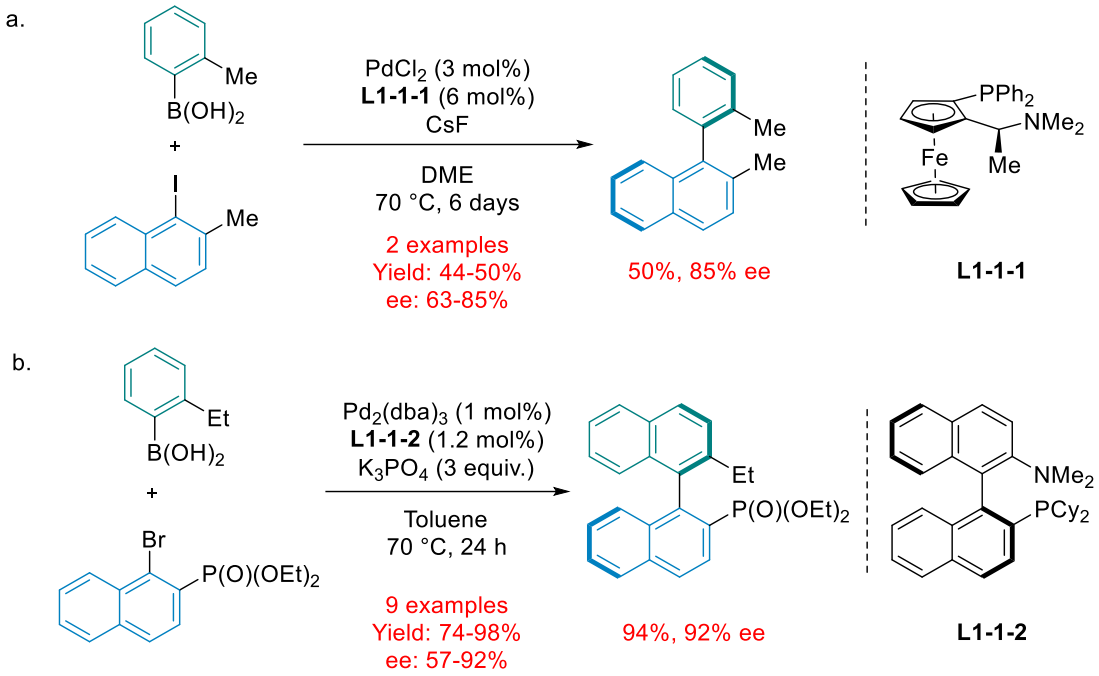
Atropisomers are stereoisomers of axially chiral compounds, where the axial chirality arises from a chemical bond with restricted rotation due to high steric hindrance of ring substituents in biaryls. [20] Axial chirality is present in many bioactive natural products with cyclic components including vancomycin, Gossypol and Steganacin. [21-23] In addition, axial chirality plays a crucial part in asymmetric catalysis, as an important element in many chiral ligands including BINAP and BINOL derivatives. [24]

Atropisomer synthesis has been achieved by various methods including resolution of racemates, kinetic thermodynamic resolution of certain stereoisomers, derivatisation of diastereomeric species, enantioselective desymmetrisation of prochiral biaryls, and asymmetric cross-coupling reactions. [25] The first transition metal catalysed asymmetric synthesis of atropisomers was achieved in 1988 *via* Ni-catalysed Kumada coupling reaction by Hayashi group with high enantioselectivity. This work inspired following transition metal catalysed coupling reactions constructing C(sp^2)–C(sp^2) bonds, including catalytic asymmetric Suzuki-Miyaura cross-coupling reactions which remain one of the most reliable methods to synthesise atropisomers. [25-26]

Pioneering reports on asymmetric SM cross-coupling reaction were made by Cammidge group and Buchwald group independently in 2000 (Scheme 1.1.4). [27-28] Cammidge and Crépy reported the asymmetric SM coupling reaction between aryl halides and aryl boronates under Pd(0) catalysis to form disubstituted binaphthalene derivatives, and two different products could be synthesised in up to 85% ee (Scheme 1.1.4a). [27] The best enantioselectivity was achieved using a ferrocene-type ligand (**L1-1-1** in Scheme 1.1.4a).

In the same year, Buchwald and Yin reported an asymmetric Pd(0)-catalysed SM cross-coupling reaction using a substituted aryl boronic acid and an *ortho*-phosphonate-substituted aryl halide. In the enantioselective reaction, an axially chiral monosphosphine-type ligand,

KenPhos (**L1-1-2**) was used to give nine different chiral biaryl atropisomers in up to 92% ee (Scheme 1.1.4b). Later, they performed DFT calculations and results indicated that the phosphonate group on aryl halide was acting as directing group, and the origin of enantioselectivity was secondary interactions between the oxygen on the phosphonate group and the hydrogen on the ligand and the aryl boronic acid. [29]



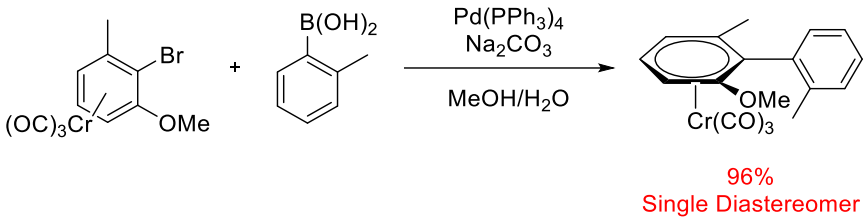
Scheme 1.1.4 First examples of asymmetric Suzuki-Miyaura cross-couplings. **a**. Asymmetric Suzuki-Miyaura reaction reported by Cammidge and Crépy. **b**. Asymmetric Suzuki-Miyaura reaction reported by Buchwald and Yin.

Initial works by Buchwald and Cammidge laid the foundation for following investigations on asymmetric SM coupling towards atropisomeric products. Since then, both diastereoselective and enantioselective cross-coupling reactions with good stereoselectivities have been reported, and some of the examples will be introduced below. [30]

Diastereoselective C(sp^2)–C(sp^2) SM Cross-Coupling

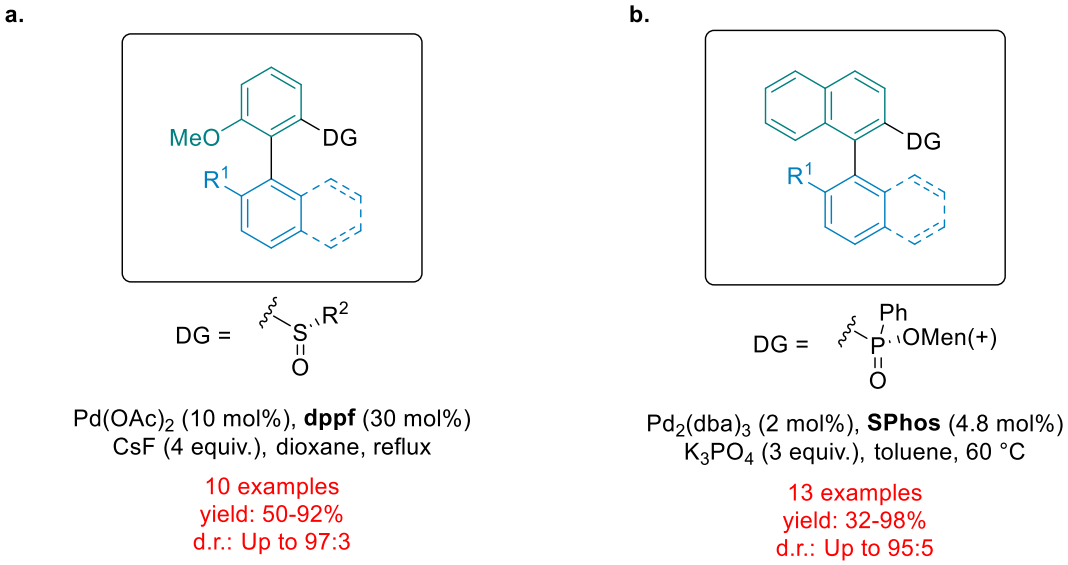
Diastereoselective SM cross-coupling reactions generally achieve stereocontrol by one of the two ways: in the first method, the existing planar chirality on substrate induces the axial chirality, and the second controls chirality with established chiral centres in chiral auxiliaries or directing groups on *ortho* positions. [25] Preliminary works for the first method include

diastereoselective SM coupling reactions using planar chromium complexes by Uemura in 1994 (Scheme 1.1.5). The reaction gave good yield and diastereoselectivity. [31-32] Nelson later reported reactions using chiral η^6–Cr complex with different substitution on the arene ring. [33] This methodology was applied in the total syntheses of vancomycin, Korupensamine A and Steganacin derivatives. [23, 34-36]



Scheme 1.1.5 An example in Uemura's diastereselective SM cross-coupling reaction.

For the second method, work was devoted to expanding the scope of possible chiral directing groups and auxiliaries. Diastereoselective SM coupling using substrates with different directing groups including chiral sulfoxide, chiral phosphinate and aminopropyl have been reported by Colobert (Scheme 1.1.6a), [37] and Yang (Scheme 1.1.6b) with generally good yields and stereoselectivities. [38-39] The applicability of the methodology could also be shown in the synthesis of naphthylisoquinoline alkaloids. [40]



Scheme 1.1.6 Diastereoselective SM cross-coupling with various directing groups. **a**. Colobert's reaction using chiral sulfoxide as directing group. **b**. Yang's work using chiral phosphinate as directing group.

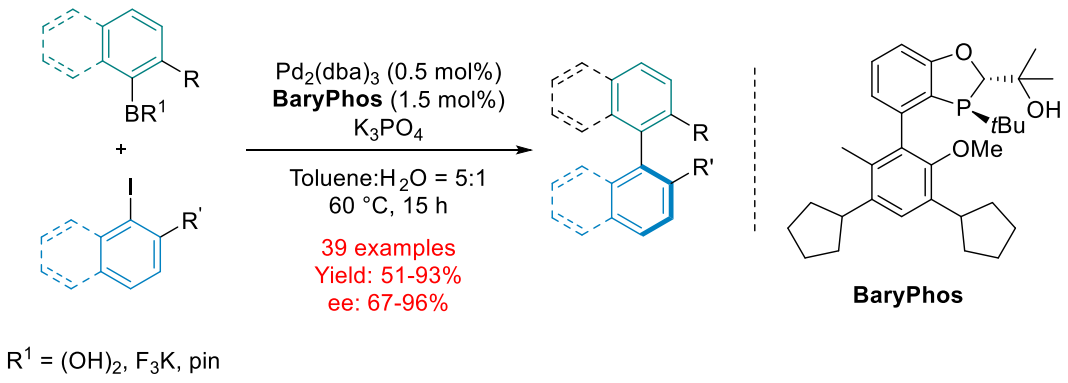
As removal of chiral auxiliaries is generally required as an extra step in diastereoselective SM coupling reactions, catalytic enantioselective approaches provided another efficient method for atropisomer synthesis. Advancements in enantioselective $C(sp^2)$–$C(sp^2)$ cross-coupling reactions will be summarised below.

Enantioselective $C(sp^2)$–$C(sp^2)$ SM Cross-Coupling

Catalytic enantioselective SM coupling reactions generally require an achiral directing group to favour one of the atropisomers by secondary interactions in the transition state. An example of asymmetric synthesis of 2,2'-dimethyl binaphthalene was reported by Jensen and coworkers, and the highest ee was only 54% without the presence of any other directing groups. [41] This supports the theory proposed by Qiu and Buchwald that the secondary interactions between the directing group and the catalyst are crucial for enantiocontrol of the reaction. [30]

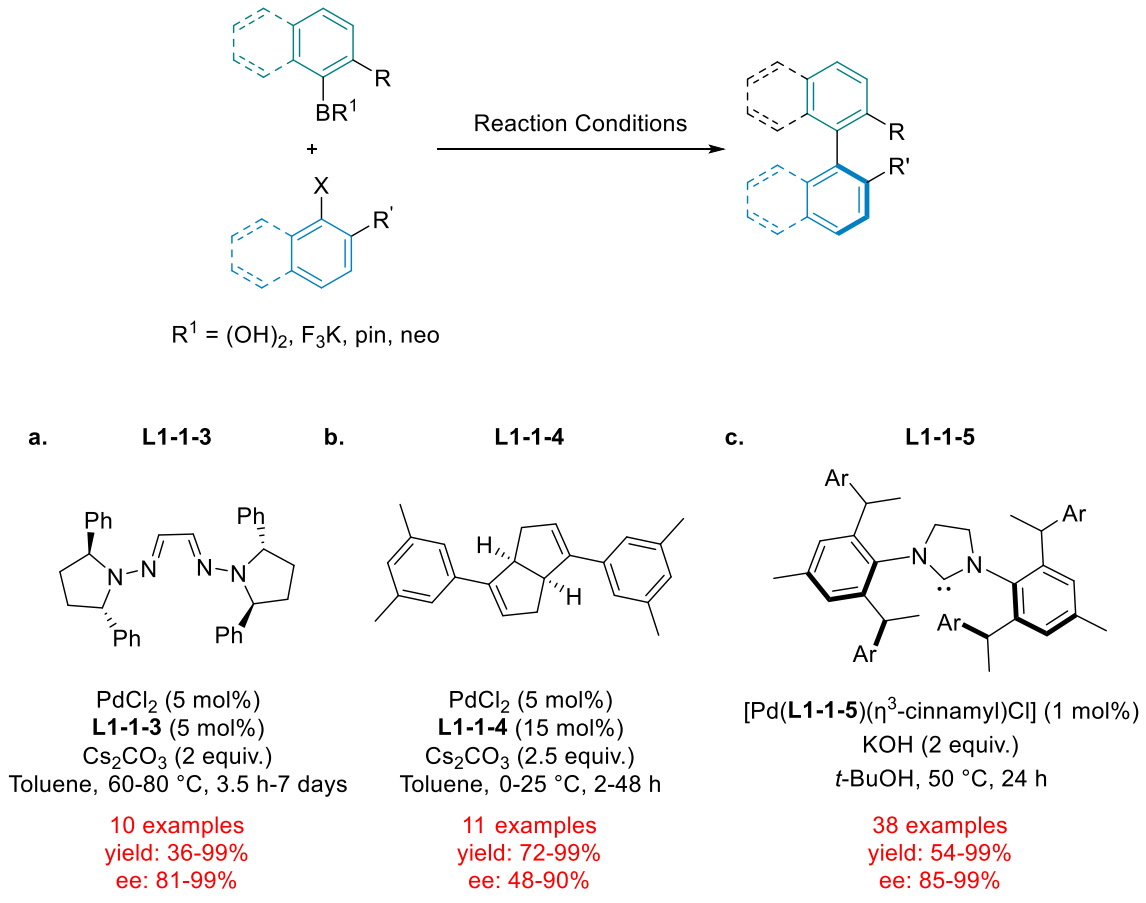
Later, the Buchwald group was able to extend their previous substrate scope to various aryl halides with amide directing groups achieving yield up to 92% and ee up to 94%. [29] Furthermore, phosphonate esters, formyl group, phosphine oxide, and triflates were all reported as efficient directing groups in the work of Qiu, Wu and Zhang, and Tang. [42-43]

As both the directing group and the ligand are crucial for reaction stereoselectivity, different ligands were investigated. Tang's group successfully reported several different enantioselective SM coupling reactions using various P-stereogenic ligands, including a highly efficient monophosphine ligand, BaryPhos, achieving moderate to excellent enantioselectivity with broad scope (Scheme 1.1.7). [22, 44-46]



Scheme 1.1.7 Tang's enantioselective SM cross-coupling using BaryPhos ligand.

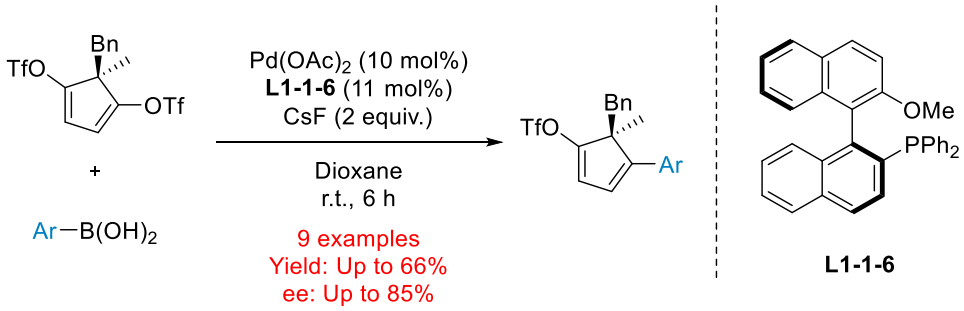
Even though asymmetric SM cross-coupling reactions rely heavily on phosphorus-based ligands, reactions using non-phosphorus-based ligands were reported. In 2008, Fernández and Lassaletta reported the enantioselective synthesis of unfunctionalized biaryls using C_2-symmetric bis-hydrazones ligand with very good enantioselectivity. Long reaction times were required for this reaction (Scheme 1.1.8a). [47] Diene ligands could be used, as described in work by Lin and coworkers, achieving good yield and up to 90% ee of atropisomeric biaryls (Scheme 1.1.8b). [48] *N*-hetereocyclic carbenes (NHCs) were also used as ligands by Shi *et. al.*, allowing good enantioselectivity to be achieved with various electrophiles including aryl chloride, bromide, and triflates, and different nucleophiles including boronic acids and esters (Scheme 1.1.8c). [49]



Scheme 1.1.8 Enantioselective SM cross-coupling with non-phosphorus-based ligands. **a**. Fernández and Lassaletta's work using bis-hydrazone ligands. **b**. Lin's work using dienes. **c**. Shi's work using NHC ligands.

Desymmetrisation of Prochiral Substrates

Apart from diastereoselective and enantioselective cross-coupling reactions, desymmetrisation of prochiral bis-(pseudo)halides and metallocenes was also used as an alternative strategy towards atropisomeric products. An example of this methodology is demonstrated by the work of Willis and coworkers using cyclopentadiene-derived *meso*-bistriflate substrate with Pd catalysis, obtaining moderate to good yield and enantioselectivity with various aryl- and hetereoaryl nucleophiles (Scheme 1.1.9). [50] Work by Kündig and coworkers showed another example on desymmetrisation of *meso*-tricarbonylchromium 1,4-dibromonaphthalenes towards products with planar chirality. [51] In Kündig's reaction, both monoarylation and bisarylation took place, and the monoarylation product was formed as the major product in high ee of over 90%.



Scheme 1.1.9 Willis's desymmetrisation of *meso*-bistriflate substrate.

1.1.2 Asymmetric SM C(sp^3)–C(sp^3)/C(sp^2) Coupling Reactions On Cyclic Substrates

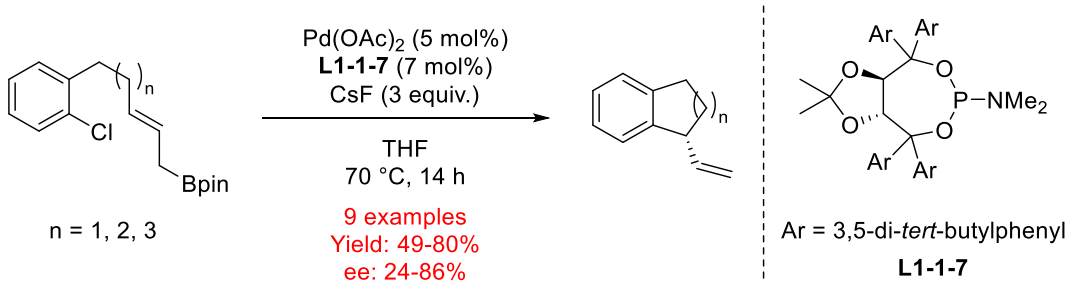
Generally, cross-coupling reactions on sp^3 hybridised carbon centre are more challenging than on sp^2 hybridised carbon centres. This is typically because of the slower transmetallation and potential side reactions including β-hydride elimination. [52] Various transition metals could be used as catalysts in the asymmetric SM C(sp^2)–C(sp^3) and C(sp^3)–C(sp^3) cross-coupling reactions, and examples towards enantioenriched cyclic compounds will be introduced below with highlights on Rh-catalysis.

Pd Catalysis

Palladium has naturally become one of the common catalysts in both non-asymmetric and asymmetric Suzuki-Miyaura cross-coupling reactions. A lot of early asymmetric SM cross-

coupling reactions involve linear substrates, posing regioselectivity issues where both branched and linear coupling products could be formed. Examples of these reactions include Miyaura's asymmetric allylation of alkenyl and aryl bromides, [53-54] Morken's work on achiral geminal bis(pinacolboronates), [55] Buchwald group's work on highly regioselective SM coupling of allylboronates and aryl bromides. [56] These reactions will not be discussed here in detail.

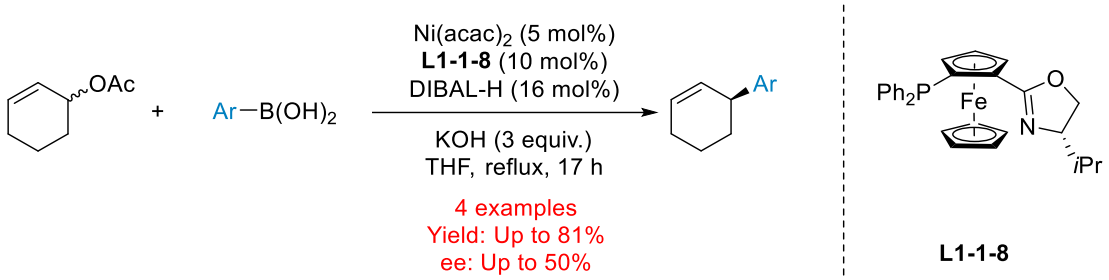
One example of Pd-catalysed enantioselective SM cross-coupling reactions constructing C(sp^2)–C(sp^3) bonds on cyclic substrate was reported by the Morken group, where they performed an efficient Pd-catalysed intramolecular cross-coupling reaction to give enantioenriched carbocyclic products from an aryl chloride substrate with a tethered allylboronate group using a TADDOL-based phosphonamidite ligand **L1-1-7** (Scheme 1.1.10). [57] The reaction could be applied to afford five, six, and seven-membered carbocyclic rings, and a single regioisomer was isolated in the reaction with good yield and moderate ee. In the reaction, it was proposed that allyl equilibration of the adduct occurred during transmetallation to form a common palladacycle intermediate, and the following reductive elimination step was the stereochemistry determining step, as the polarity and the *Z*/*E* stereochemistry of the double bond in substrate had negligible effect on the enantioselectivity of the reaction.



Scheme 1.1.10 Morken's work on enantioselective intramolecular Pd-catalysed SM coupling.

Ni Catalysis

Nickel as a type of more earth-abundant and cheaper transition metal compared to palladium, naturally became a common alternative as the catalyst in asymmetric SM cross-coupling reactions, especially in construction of C(sp^3)–C(sp^3) bonds. Uemura and coworkers reported an early example of Ni-catalysed enantioselective SM cross-coupling on racemic monocyclic allylic acetate, albeit with limited substrate scope and low stereocontrol (Scheme 1.1.11). [58]



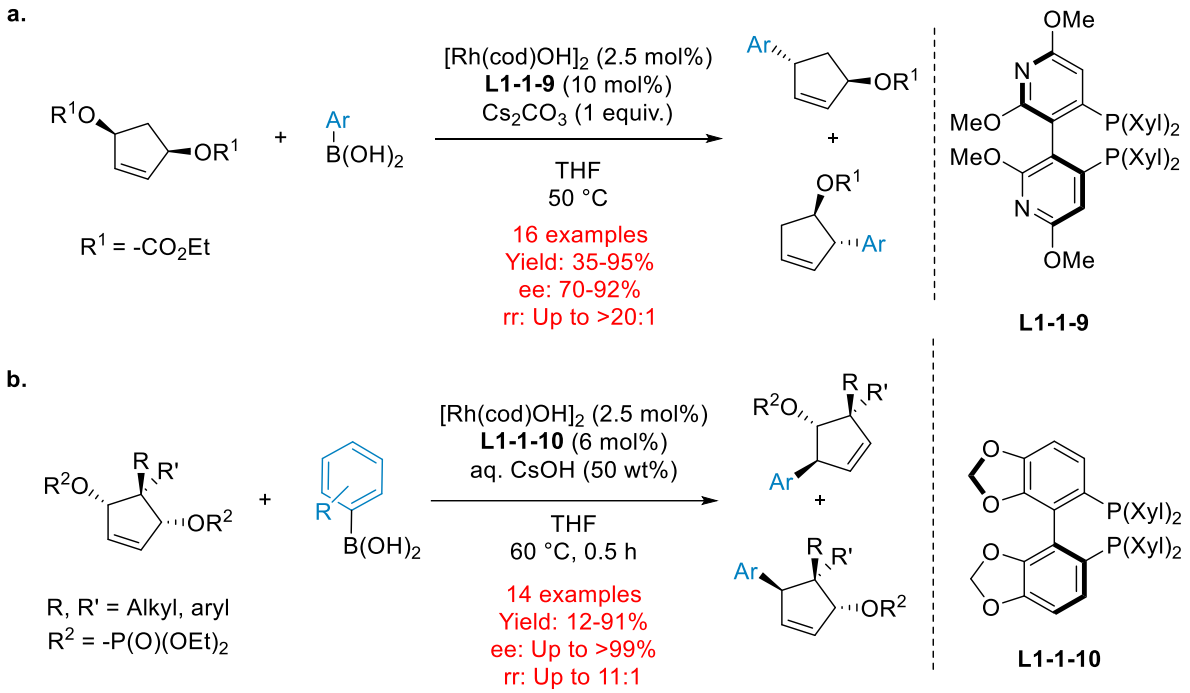
Scheme 1.1.11 Uemura's work on enantioselective Ni-catalysed SM coupling.

Later, Fu's group made significant contributions to the area of asymmetric Ni-catalysed SM cross-coupling reactions, and reported numerous examples with high stereocontrol, as a high proportion of these reactions used acyclic substrates, they will not be discussed here in detail. [59-65]

Rh Catalysis

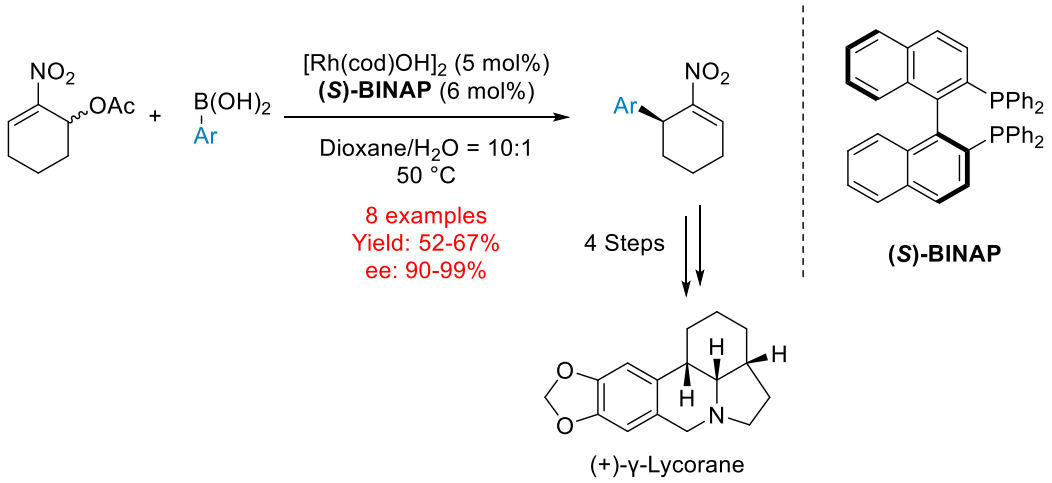
Over the past decades, rhodium was discovered as an efficient catalyst for the construction of C–C bonds, due to its special reactivity and selectivity as well as its tolerance of water in reaction environment. [66] Both asymmetric arylation and SM cross-coupling reactions forming $C(sp^2)$–$C(sp^3)$ bonds were reported, and the Lautens group was one of the first explorers of the area, where they used *meso*-biscarbonates with various functionalised aryl boronic acid nucleophiles to obtain arylation products with good yields and stereoselectivities in 2006 (Scheme 1.1.12a) and 2010. [67-68] The choice of ligand was found to affect the regioselectivity in the reaction. [67-68]

Later, the Fletcher group successfully extended the reaction scope in prior works onto *meso*-phosphonates (Scheme 1.1.12b). Excellent enantioselectivities (generally >99%) with moderate to good yields were observed, and in addition to Lautens' prior investigations, hetereoaryl boronic acid nucleophiles containing N-, S-, O-atoms were also tolerated with moderate regioselectivity and excellent enantioselectivity, albeit in poor yields. [69]



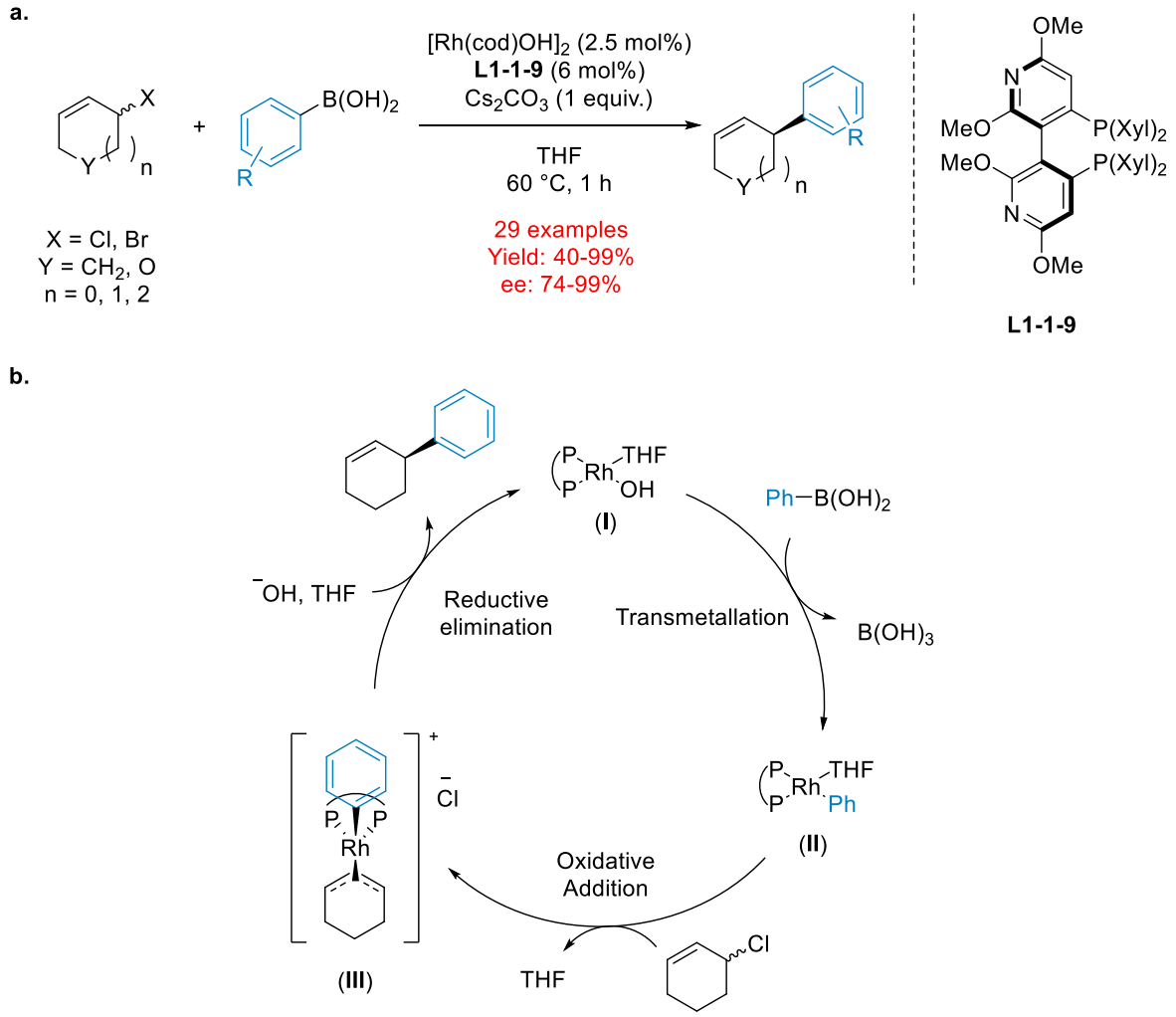
Scheme 1.1.12 Rh-catalysed asymmetric arylations on *meso*-compounds. **a**. Lautens' work on *meso*-biscarbonates. **b**. Jacques' work on *meso*-bisphosphonates.

With Rh-catalysed asymmetric reactions reported on *meso*-compounds, reactions were also reported starting from racemic substrates. Work by Gong and coworkers represented an early example using racemic cyclic substrate with Rh-catalysis, where the reaction proceeded *via* an enantioselective conjugate addition of the aryl group onto the substrate followed by elimination of the acetate group (Scheme 1.1.13). [70] Moderate yields were obtained with high ee up to 99%, and the reaction could be applied into the total synthesis of **(+)**-γ-Lycorane.



Scheme 1.1.13 Gong's work on Rh-catalysed asymmetric nitroallylation of racemic cyclic allylic acetate.

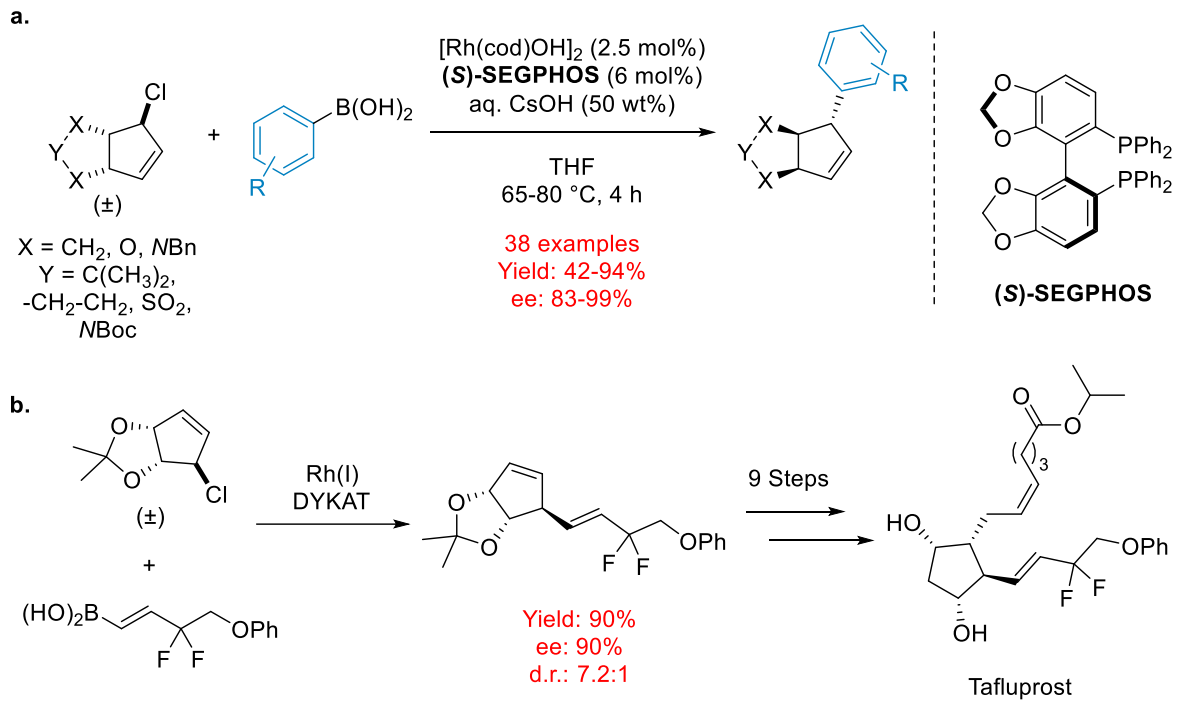
In 2015, the Fletcher group reported a highly efficient SM cross-coupling reaction between aryl and allyl boronic acids and monocyclic allylic halides (Cl and Br) with up to 99% yield and up to 99% ee (Scheme 1.1.14a). Mechanistic studies revealed that the reaction proceeded *via* a DyKAT type II process, where both enantiomers of the substrate undergo oxidative addition to form a common *meso*-Rh-complex, and stereoselective reductive elimination occurs next, which sets the stereochemistry of the product to afford highly enantioenriched coupling products (Scheme 1.1.14b).



Scheme 1.1.14 Rh-catalysed asymmetric SM cross-coupling on racemic cyclic allylic halides by Fletcher and coworkers. **a**. Reported reaction using monocyclic substrate. **b**. Proposed reaction mechanism.

Later in 2019, the group successfully applied this methodology on a racemic bicyclic allylic chloride tolerating oxygen and protected nitrogen in the bicycle (Scheme 1.1.15a). [71] Like the reaction with monocyclic allylic halides, this reaction also operates as a DyKAT process to

afford various products with electronically different boronic acids giving high yield, enantioselectivity and diastereoselectivity. The reaction would be an efficient way to construct enantioenriched bicyclic structures with up to five contiguous stereogenic centres. In the group's following work, the broad applicability of this reaction was demonstrated with the total synthesis of Tafluprost (Scheme 1.1.5b), carbocyclic C-nucleosides, as well as prostaglandin F2α. [72-74]

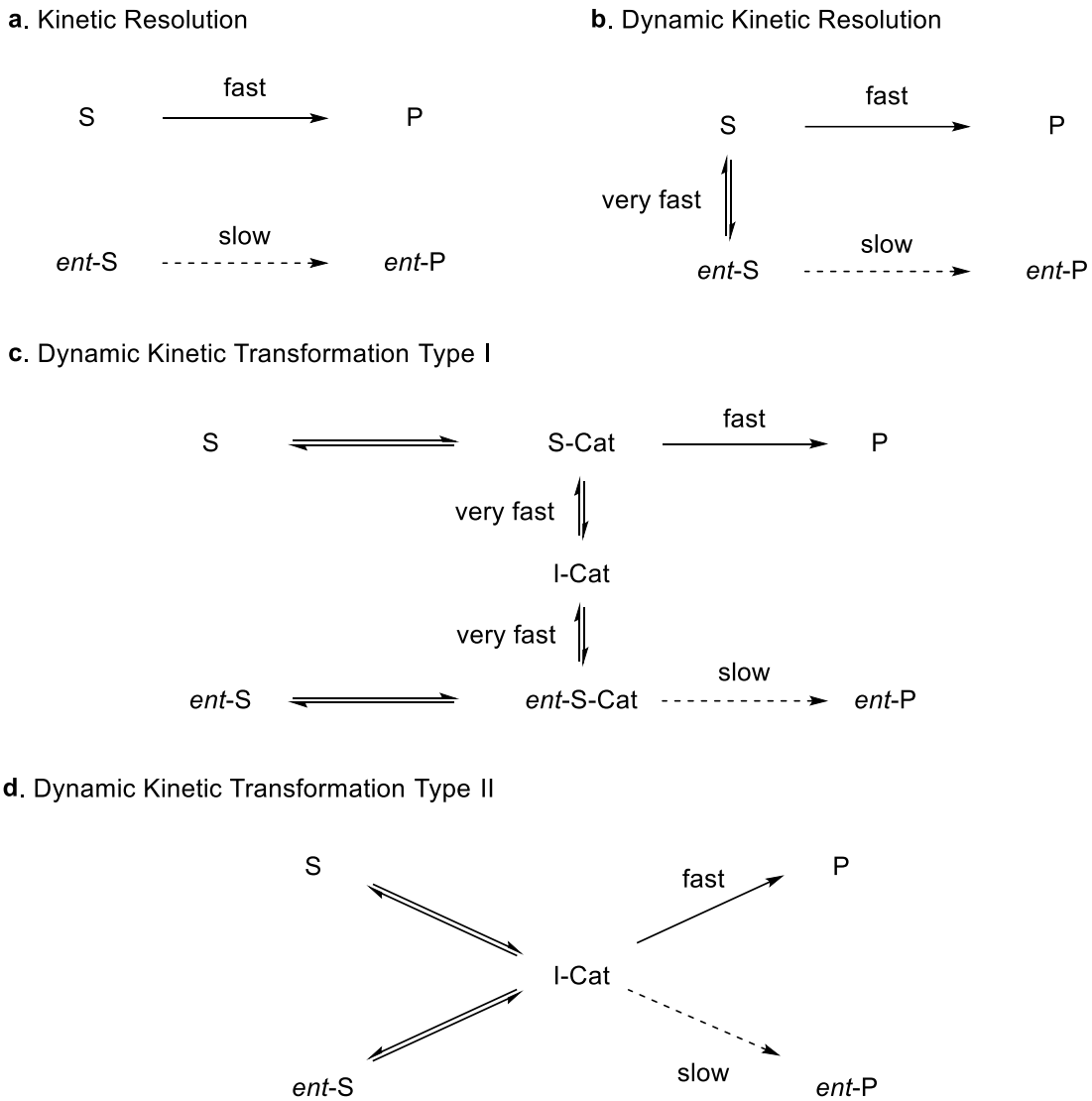


Scheme 1.1.15 a. Rh-catalysed asymmetric SM cross-coupling on racemic bicyclic allylic chlorides by Fletcher and coworkers. **b**. Transformation of product to Tafluprost.

Both reactions reported by the Fletcher group shown above were operating as a DyKAT process. DyKAT and DKR are efficient processes which circumvents the drawback of 50% theoretical yield limitation in a KR process. These procedures will be introduced in detail in the following section.

DyKAT, DKR, and KR Processes

Kinetic resolution occurs when two enantiomers of the substrate react with different rates in a reaction, therefore resulting in enantioenriched product from the more reactive enantiomer, together with an enantioenriched sample of the less reactive substrate enantiomer. The ideal kinetic resolution occurs when only one enantiomer reacts, resulting in maximum theoretical yield of 50% of product P and unreactive enantiomer *ent*-S, with both being enantiopure (Scheme 1.1.16a).



Scheme 1.1.16 a. Kinetic Resolution. **b**. Dynamic Kinetic Resolution. **c**. Type I Dynamic Kinetic Transformation. **d**. Type II Dynamic Kinetic Transformation.

For DKR reactions, there is also a significant difference in reaction rate between two substrate

enantiomers, however, racemisation occurs at a faster rate relative to the asymmetric transformation rate, therefore, it is possible to convert 100% of the starting material to a single enantiopure product (Scheme 1.1.16b).

DyKAT process is similar to DKR process in the way that a single enantiopure product could be achieved theoretically with 100% yield. The difference of DyKAT to DKR is that in DyKAT reactions, no racemisation of substrate enantiomers takes place, but either rapid racemisation of diastereomeric catalytic intermediates occur (Type I DyKAT, Scheme 1.1.16c), or a common pseudo-achiral intermediate is formed from both enantiomers of the substrate (Type II DyKAT, Scheme 1.1.16d).

Other Transition Metal Catalysis (Cu, Fe, Ir)

Asymmetric SM cross-coupling reactions using other transition metal catalysts were also reported, and examples include copper, cobalt, iron, and iridium. The first reported Cu-catalysed asymmetric SM cross-coupling reaction by Liu and coworkers builds $C(sp^3)–C(sp^2)$ bonds between aryl- or heteroarylboronates with secondary alkyl halides. [75] The reaction provides a wide range of substrates and operates *via* a radical pathway. Another example involving radical pathways was reported by Nakamura and coworkers using Fe-catalysis on racemic alkyl bromides, albeit with moderate enantioselectivity. [76]

Iridium appeared to be a powerful tool and exhibits high regioselectivity in asymmetric allylic substitution reactions on acyclic substrates, and numerous examples were reported in good yield and high regio- and enantioselectivities by Carreira, Yang, and others. [77-78] As most reactions utilising these transition metal catalysts involve acyclic substrates, they will not be introduced here in detail.

1.2 Nitrogen-Heterocycle Synthesis by Asymmetric Cross-Coupling

Heterocycles are important moieties in medicinal chemistry, especially the nitrogen-containing cyclic compounds, which are among the most significant structural components of naturally occurring products and pharmaceuticals. [79] According to the analysis of the US FDA pharmaceuticals database in 2020, nearly 75% unique small-molecule drugs contain a nitrogen heterocycle. [79-80] Therefore, diversifying and extending the scope of asymmetric synthesis of nitrogen hetereocycles became a prioritised target.

However, in comparison to the tremendous advancements in cross-coupling reactions on carbocycles, synthesis of nitrogen-heterocycles *via* cross-coupling are relatively under-developed. Even though numerous non-asymmetric examples have been reported with good yields using heteroaryl boronic acids or heteroaryl halides since the end of 20th century, asymmetric cross-coupling reactions towards enantioenriched nitrogen hetereocycles remain scarce due to multiple reasons. [81-99]

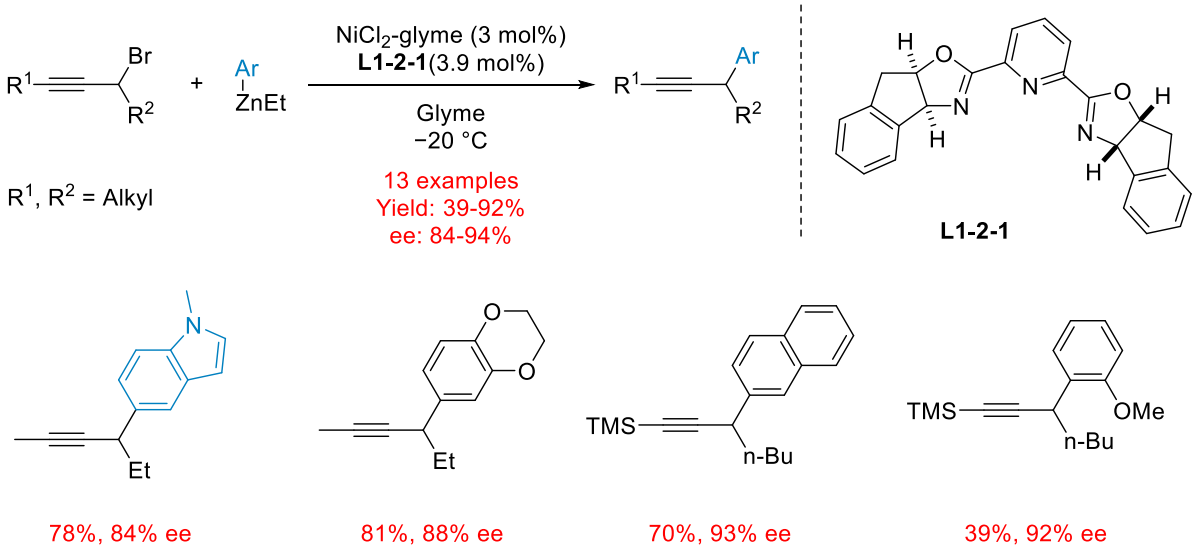
To begin with, it is generally known that unprotected nitrogen atom binds strongly with the transition metal catalyst, leading to deactivation of the catalyst and inferior stereoselectivity. This leads to the necessity of a protecting group on nitrogen, and the choice of protecting group could potentially affect the reaction due to their different steric and electronic effects. In addition, the extra steps of protection and deprotection during synthesis could be problematic, including the loss of yield and possibly affecting other existing functional groups on substrate. Furthermore, some nitrogen-containing substrates are not chemically stable which could undergo decomposition in the catalytic reaction. [100-101]

Nevertheless, several asymmetric cross-coupling reactions were reported using nitrogen-heteroaromatic cycles, most being pyridine and quinoline based substrates, and a few examples will be summarised below in Chapter 1.2.1.

1.2.1 Asymmetric Coupling Reactions Towards Nitrogen-Containing Heteroaromatics

The Fu group had previously successfully reported catalytic asymmetric cross-coupling of organozinc, organosilane and organoboron compounds with racemic secondary alkyl

electrophiles using chiral Ni complex catalysis. [60, 102-105] Later in 2008, they were able to extend this methodology to secondary propargylic halides, and in this reaction, one nitrogen-containing heterocycle example was reported with 78% yield and 84% ee (Scheme 1.2.1). [106]

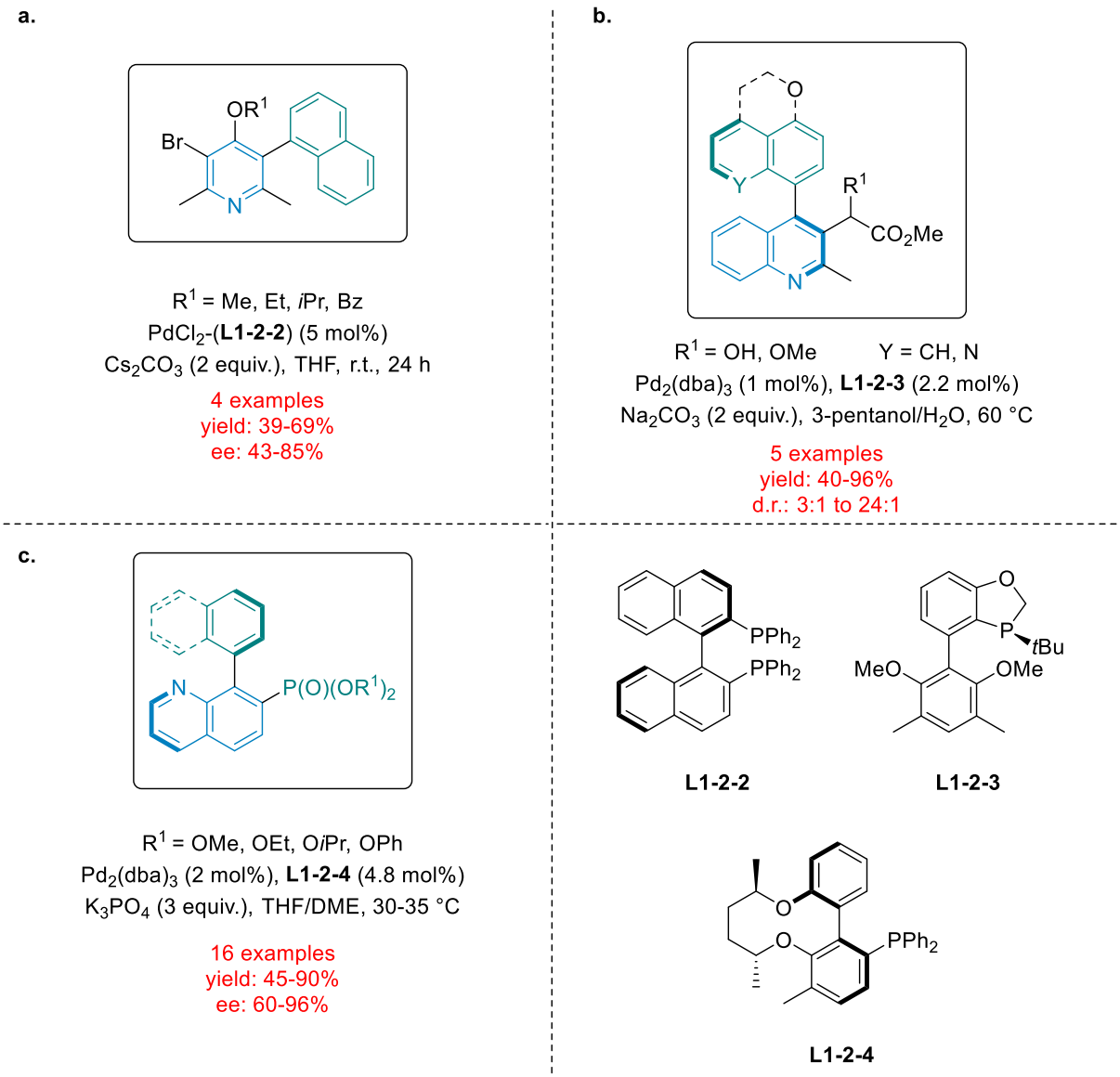


Scheme 1.2.1 Fu's work on asymmetric Ni-catalysed Negishi coupling using racemic propargylic halides.

In 2016, an asymmetric SM coupling reaction constructing atropisomeric mono-naphthyl substituted pyridine derivatives was reported by Czarnocki and coworkers. [107] The reaction used 3-pyridine type substrates and $PdCl_2$ and BINAP (**L1-2-2**) as catalyst. Moderate yields and enantioselectivites with limited scope were obtained in the reaction (Scheme 1.2.2a).

Another diastereoselective SM coupling of 4-chloroquinoline was reported in the same year by Haddad and coworkers, moderate to good yield and good diastereoselectivity of up to 24:1 was reported using $Pd_2(dba)_3$ and a P-stereogenic ligand **L1-2-3**, with relatively limited scope of only five examples (Scheme 1.2.2b). [108]

Subsequently in 2017, Qiu and coworkers were able to apply asymmetric SM coupling on 8-bromoquinolines. Palladium catalyst and bridged monophosphine ligand (**L1-2-4**) was used and the reaction scope was extended to 16 different examples giving good yields and enantioselectivities (Scheme 1.2.2c). [109] Extension of this work was reported in 2019 performing similar reaction on 3-bromopyridine type substrates with an amide directing group, and 17 different products could be obtained in good yields and ee. [110]

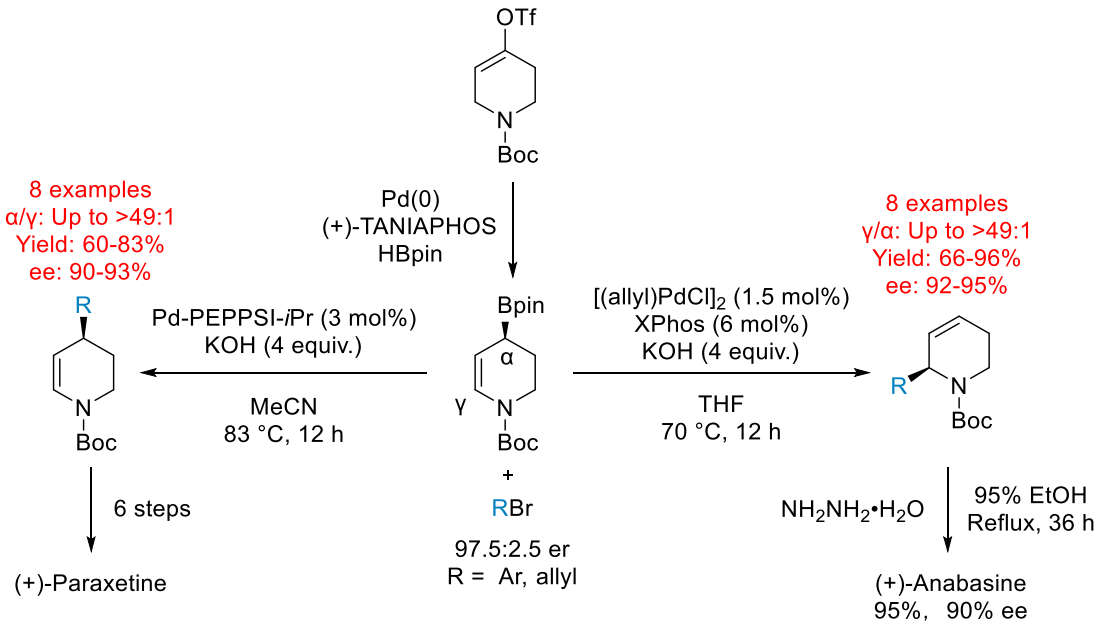


Scheme 1.2.2 Examples of asymmetric coupling towards nitrogen heterocycles. **a**. Czarnocki's work in 2016. **b**. Haddad's work in 2016. **c**. Qiu's work in 2017.

In comparison to asymmetric cross-coupling reactions reported on nitrogen-containing heteroaromatic substrates as shown above, significantly fewer reports on saturated nitrogen heterocycles were given, even though these are among the most prevalent structural subunits in biologically and pharmaceutically active agents. [79, 111-112] A few asymmetric coupling reactions towards enantioenriched saturated aza-heterocycles will be summarised below in Chapter 1.2.2.

1.2.2 Asymmetric Coupling Reactions Towards Saturated Nitrogen Heterocycles

Herein, we will list a few examples on the asymmetric coupling reactions towards non-aromatic nitrogen-containing heterocycles. In 2014, the Hall group reported a stereospecific and regiodivergent Pd-catalysed SM cross-coupling reaction to synthesise chiral heterocycles including 2- and 4-substituted dihydropyrans and dehydropiperidines in high stereoselectivities (Scheme 1.2.3). [113] This reaction proceeded *via* a two-step sequence, firstly the enantioselective isomerisation of the hetereocyclic alkenyl triflate to give the enantioenriched boronic pinacol ester, followed by the catalyst-controlled regioselective enantiospecific SM cross-coupling reaction, affording the desired stereoisomer with moderate to high regioselectivity, good yield, and very good enantioselectivity. This reaction is an example of the third type of asymmetric cross-coupling reaction summarised in Scheme 1.1.3, where stereochemistry is pre-established in the enantioenriched substrate, and the cross-coupling step reacts stereospecifically to give the product.

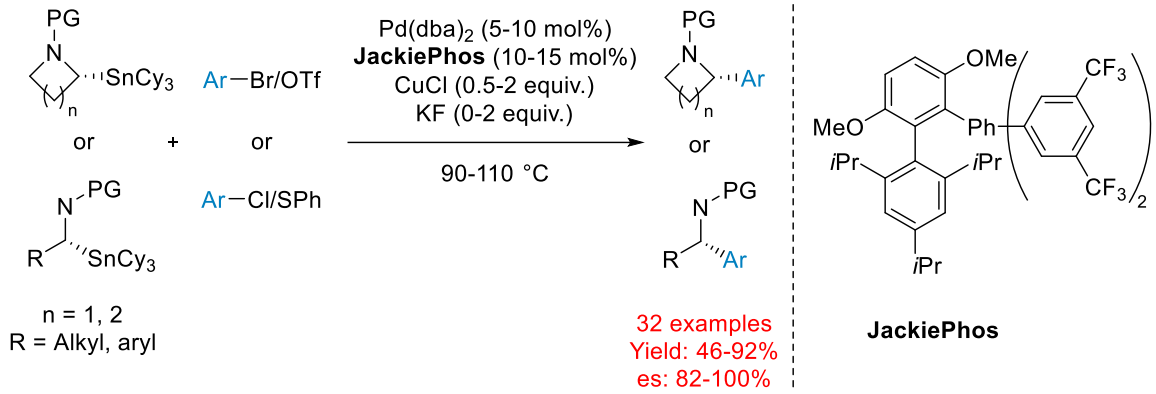


Scheme 1.2.3 Hall's work on stereospecific SM coupling to chiral hetereocycles.

In their reaction, 32 examples were reported with dehydropiperidyl and dihydropyranyl boronates (16 examples for each substrate). The utility of this methodology is illustrated by the synthesis of different bioactive piperidines including (+)-anabasine and (+)-paroxetine (Scheme 1.2.3).

Another example of the third type of asymmetric cross-coupling reaction was reported by the

Biscoe group in 2020. [114] The reaction involves a Pd-catalysed Stille cross-coupling reaction on α-stannylated amines affording enantioenriched pyrrolidine, azetidine and open-chain amine products in good to high yield and high enantiospecificity (Scheme 1.2.4). The reaction required prior synthesis of the *R* enantiomer of the α-stannylated amines, and the applicability of this methodology is demonstrated by the transformation of the coupling product to CDK8 inhibitor derivatives which would act as a potential target for cancer therapeutics. [114-117]

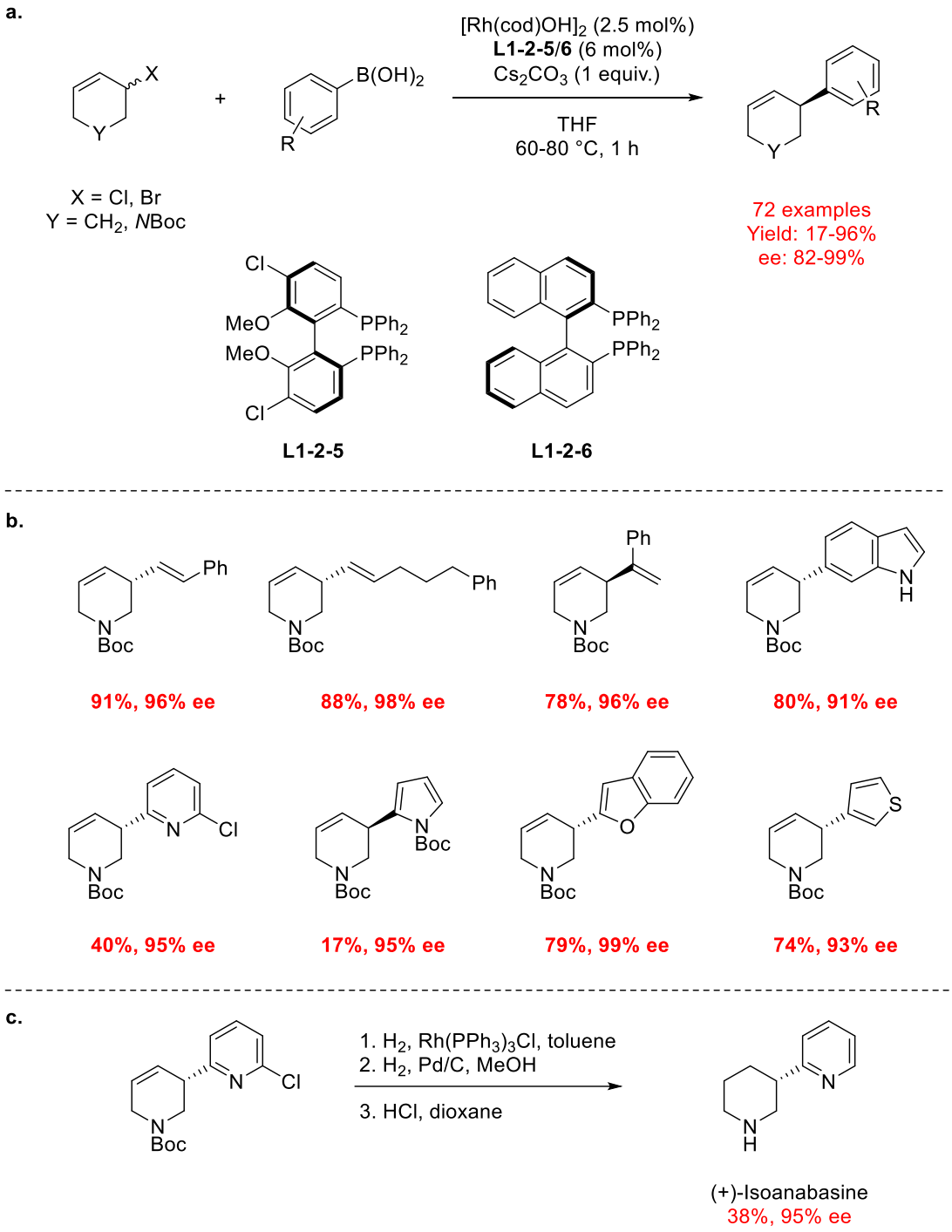


Scheme 1.2.4 Biscoe's work on stereospecific Pd-catalysed Stille coupling reaction towards enantioenriched pyrrolidine, azetidine and open-chain amine products.

Other types of stereoselective asymmetric cross-coupling reactions were also reported on saturated nitrogen-containing heterocycles. An example was reported by the Fletcher group in 2017, where they were able to extend the methodology on racemic mono-carbocyclic allylic halide reported in 2015, [118] onto the racemic nitrogen-containing monocyclic allylic halide (Scheme 1.2.5a). [119]

This reaction works well with various boronic acids including aryl, vinyl, heteroaromatics, and hetereocycles, and very good yields and enantioselectivity could be achieved (Scheme 1.2.5b).

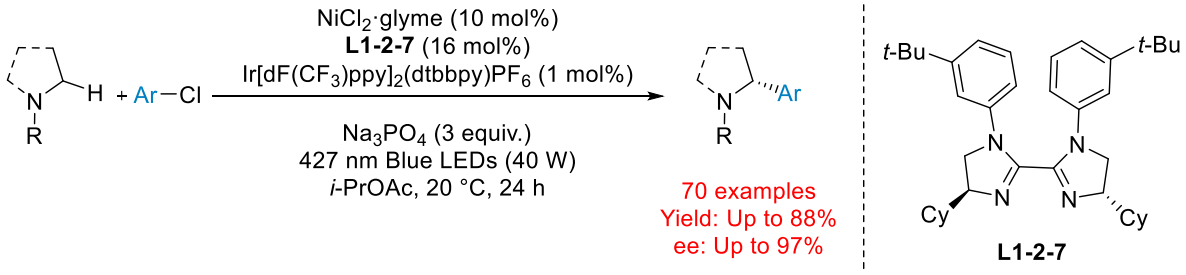
In the reaction, it was demonstrated that even though the pyridine boronic acids gave no reactivity, substrate with halogen substitution on the *ortho*-position exhibited reactivity and good enantioselectivity, and the halogen atom could be then utilised to facilitate further reactions. The applicability of this methodology was demonstrated by the synthesis of isoanabasine (Scheme 1.2.5c), preclamol, and niraparib which is an anticancer agent approved for medical use in US and EU in 2017. [120]



Scheme 1.2.5 Fletcher group's Rh-catalysed SM coupling on nitrogen-containing cycle. **a**. Reaction conditions. **b**. Examples of reaction with hetereoaryl- and vinylboronic acids. **c**. Transformation of coupling product to (+)-isoanabasine.

In 2022, another reaction using Ni/photoredox dual catalysis was reported by the Huo group, where direct enantioselective α-arylation of saturated azacycles and acyclic N-alkyl benzamides was achieved. [121] In the reaction, the hydrogen atom transfer ability of photoeliminated chloride radicals was exploited to transform azacycles to α-amino alkyl

radicals, which then undergoes enantioselective cross-coupling with aryl halides. The scope of the reaction is broad with 70 examples reported, tolerating electronically and sterically different aryl and heteroaryl electrophiles, as well as 5, 6, 7, 8-membered ring aza-heterocyclic nucleophiles and acyclic secondary amine nucleophiles with good yield and high enantioselectivity. Mechanistic studies were done, suggesting that the Ni catalyst is crucial in the reaction, responsible for generating chlorine radical, capturing α-amino radical, cross-coupling, and asymmetric induction.



Scheme 1.2.6 Huo's work on enantioselective Ni/photoredox catalysed coupling towards α–Heteroaryl amines.

Since the end of 20th century, significant advancements were made in the field of asymmetric Suzuki-Miyaura cross-coupling reactions using various transition metal catalysts towards enantioenriched carbo- and heterocycles. However, in comparison to the catalytic asymmetric synthesis of carbon-based cyclic molecules, asymmetric reactions synthesising heterocycles are limited, especially for saturated nitrogen containing heterocycles synthesis. Consequently, we aimed to explore the possibility to develop methodology for non-aromatic aza-heterocycles substrates, to circumvent the current limitations of scope and allow high efficiency of synthesis towards bioactive molecules by catalytic asymmetric cross-coupling reactions.

Chapter 2: Synthesis of Nortropanes *via* Asymmetric Rh-Catalysed Allylic Arylation

Sections of this chapter are published in *ACS Catal.* 2022, 12, 8995–9002 *[122]*

I contributed to this chapter by carrying out all experimental work and by writing the manuscript for publication with contributions from F. W. Goetzke and Stephen P. Fletcher. F. W. Goetzke contributed to this chapter by joint project conception with Stephen P. Fletcher, by co-supervision, planning, and analysing of experiments with Yan Zhang. K. E. Christensen contributed to this chapter by carrying out X-ray crystallography measurements shown in Chapter 4.2.7. Stephen P. Fletcher guided the research.

2.1 Project Background

Tropane alkaloids (TA) represent a well-recognised family of nitrogen-containing heterocycles which are commonly found in pharmaceutical agents. [123-125] The scaffold is characterised by the 8-aza-bicyclo[3.2.1]octane core, and the tropane alkaloids appear as either 3α-tropanole esters, known as tropines, or 3β-tropanoles which are known as pseudotropines (Figure 2.1.1). [126-127] Over 200 different TAs have been identified, and they could be categorised as three different groups: coca alkaloids including cocaine, tropane alkaloids including hyoscyamine and scopolamine, as well as the polyhydroxylated nortropane alkaloids like calystegines (Figure 2.1.1). [128]

Even though with high structural similarities, tropane alkaloids display a wide range of biological and pharmaceutical properties, which were exploited long even before the elucidation of the structure of tropane. For example, scopolamine and cocaine display strong dosage-dependent psychoactive and hallucinogenic effects, while atropine, which is used as anticholinergic and stimulant, is effective in treatment of neurological and psychiatric disorders such as Parkinson's disease and depression. [129-130]

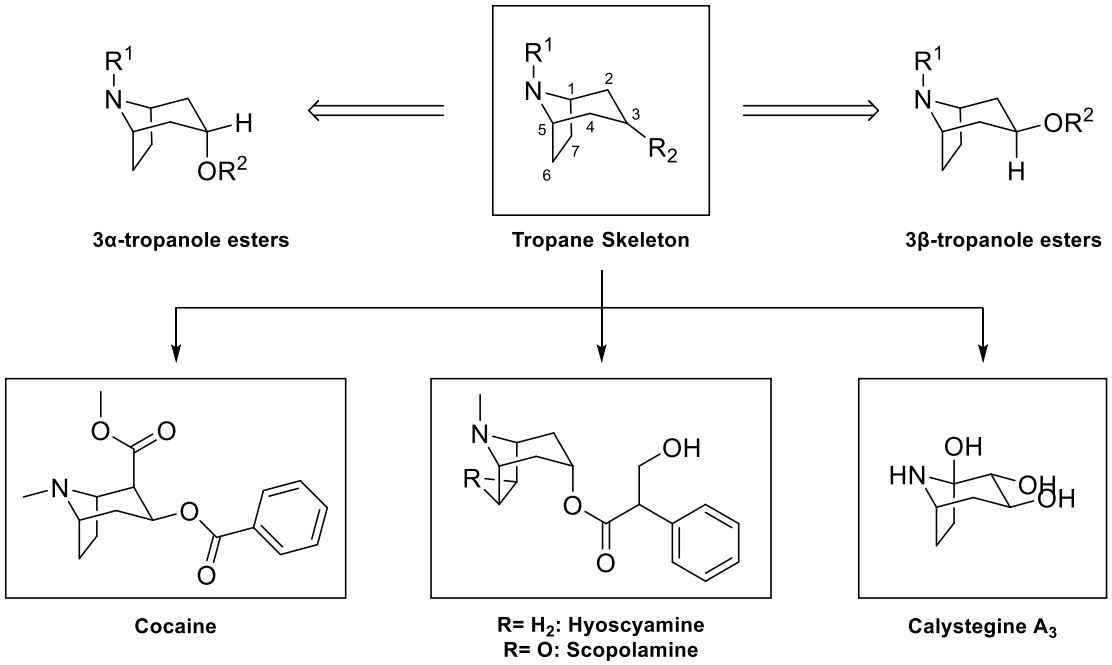
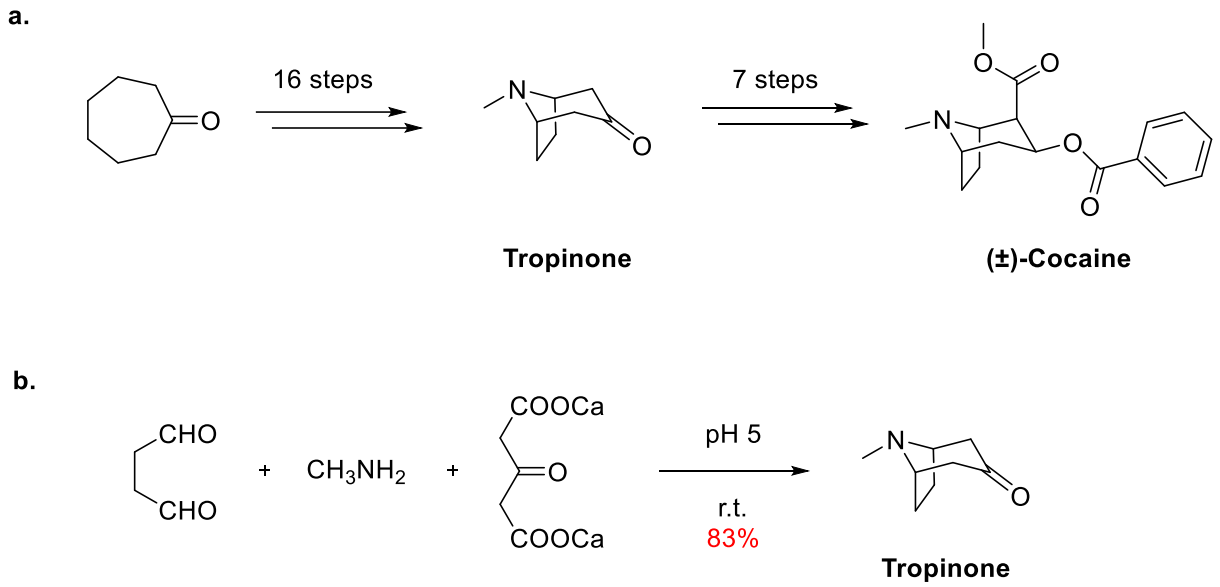


Figure 2.1.1 Structure of tropane skeleton and examples from three major groups of TA.

Historically, extraction from plants was the main method to access tropane alkaloids. Since the first isolation of cocaine in 1860 by Niemann, [127] the interesting and unique bioactivity of tropane alkaloids has inspired the development of different synthetic routes towards chiral derivatives of tropane. In 1901, Willstätter's work represented a milestone of this field, reporting the first elucidation of structure and the synthesis of cocaine *via* a 23-step synthesis from cycloheptanone (Figure 2.1.2a). [131] In this procedure, tropinone was synthesised in 16 steps as an intermediate with 0.75% yield. Robinson's work in 1917, utilising an intramolecular double Mannich method with succinaldehyde, methylamine and calcium salt of acetonedicarboxylic acid, represented the first biomimetic synthesis of tropinone. [132] His work was later improved by Schöpf *et al.* by using a pH 5 buffer solution and replacing succinaldehyde with a more accessible and stable synthetic equivalent, 2,5-dimethoxytetrahydrofuran. [133-134] The synthetic efficiency of tropinone synthesis was raised significantly compared to Willstätter's work, with the yield reaching 83% (Figure 2.1.2b).



Scheme 2.1.2 a. Willstätter's synthesis of tropinone and cocaine. **b**. Robinson-Schöpf synthesis of tropinone.

This basic principle in the synthesis of tropinone discovered by Willstätter, Robinson and Schöpf were later applied by other researchers for the synthesis of various tropane derivatives. [135-136] Modifications on the Robinson-Schöpf synthesis of tropinone have also been made to achieve various new ways of tropinone synthesis, affording racemic tropane derivatives, where the desired stereoisomer could be obtained by resolution at later stage.

Apart from resolution, a large proportion of the nonracemic tropane derivatives were obtained by derivatisation of naturally occurring TAs. By using this approach, the product scope is limited by the number of existing naturally occurring tropane derivatives. Therefore, a more general method of stereoselective synthesis was pursued, and more desirably, allowing the synthesis of different chiral tropane alkaloids *via* the same route.

Synthetic routes towards enantioenriched tropane derivatives have now been extensively explored, and most synthetic methods usually rely on one of the following approaches:

1. Use of naturally occurring enantiopure molecules to install stereogenic centres, i.e. from the chiral pool,
2. Desymmetrisation of *meso* tropinone derivatives using stoichiometric chiral lithium amide bases,

3. Enantioselective synthesis of the tropane scaffold where the stereochemical information is introduced concomitantly with the formation of the bicycle, including the use of chiral auxiliaries and asymmetric catalytic approaches. [125, 137]

Biosynthesis method also have been explored in the last few decades but will not be introduced here in detail. In the following sections, we will discuss the existing method for the synthesis of chiral tropane alkaloids.

2.1.1 Synthesis of Chiral Tropane Derivatives from the Chiral Pool

As the scope for chiral tropane molecules obtained by derivatising cocaine and related tropane alkaloids are intrinsically limited, it is desirable to extend the scope of the chiral pool to other non-tropane molecules. Alternative syntheses of tropanes from the chiral pool was investigated, where non-tropane-based molecules with established stereochemistry were used as starting materials. [137]

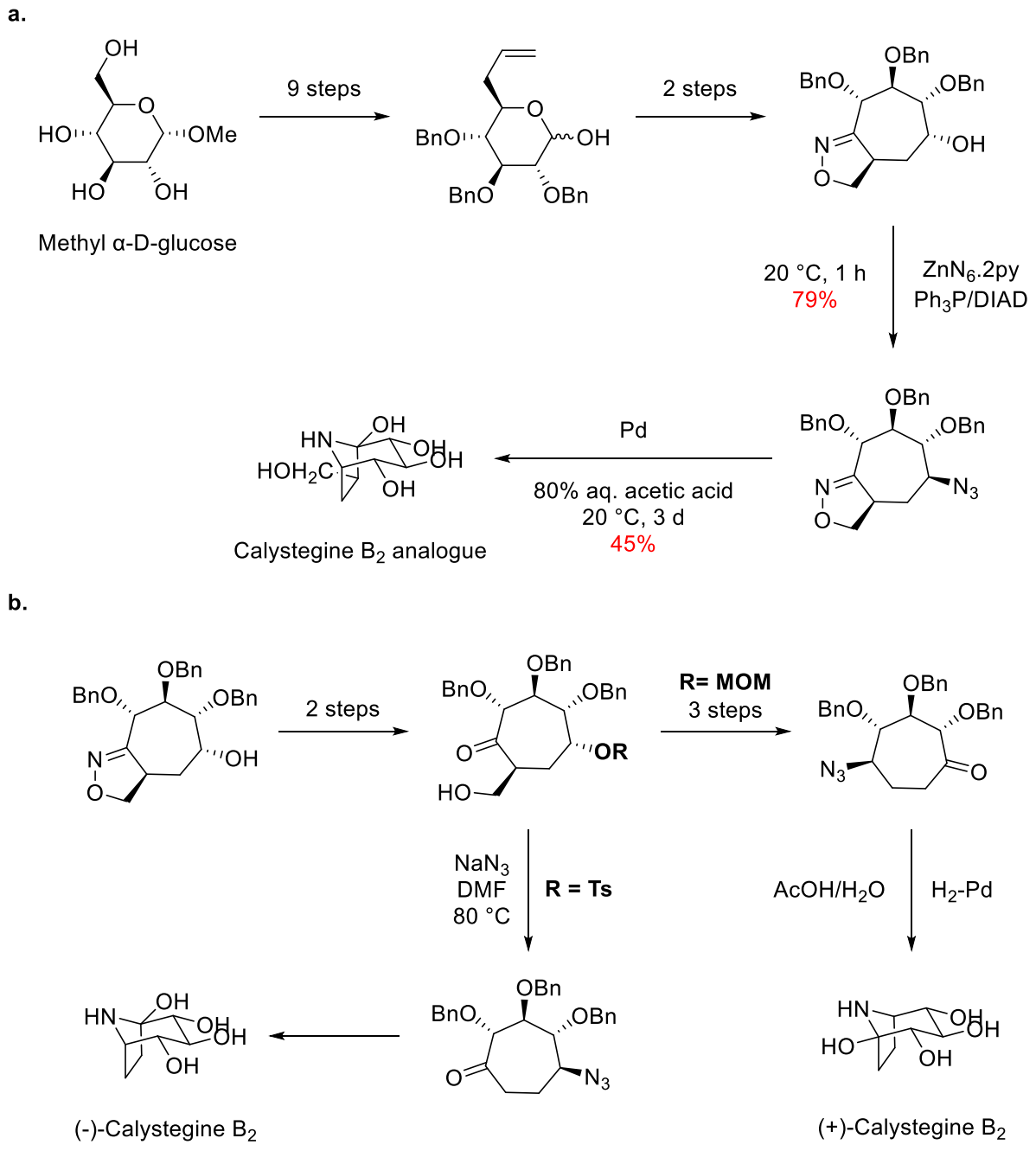
Due to the structural resemblance between certain tropane alkaloids with carbohydrates, numerous syntheses were reported starting from chiral carbohydrates, amino acids, and α-hydroxy acids. [137] Monosaccharides were one of the first types of molecules used in the chiral pool approach due to their striking similarities with calystegines. Sugars including $_D$-glucose, $_D$-galactose and $_D$-mannose are commonly used in tropane synthesis.

In 1992, Duclos and co-workers reported a reaction sequence starting from methyl α-$_D$-glucose molecule to access an analogue of calystegine B_2. [138] The reaction started from derivatisation of methyl α-$_D$-glucose to the pyranose, followed by formation of the oxime and a crucial step of intramolecular [3+2] cycloaddition to give rise to the seven-membered ring, finally, reductive ring-opening and a concomitant cyclisation occurred to give the analogue of calystegine B_2 (Scheme 2.1.3a). In addition, extension of this method could be demonstrated by synthesis of both enantiomers of calystegine B_2 from derivatisation of an intermediate in the previous route (Scheme 2.1.3b).

Following Duclos's work, different approaches towards the tropane backbone using the chiral sugar molecules have been found, including ring expansion, tandem reactions, and ring-closing metathesis. Throughout these reactions, different calystegine derivatives including B_2, B_3, and

B_4 have been synthesised, albeit typically in low yield. [139-142]

Besides carbohydrates, other commonly utilised synthetic precursors from the chiral pool involve amino acids like $_D$- and $_L$-glutamic acid and $_L$-pyroglutamic acid for ferruginine synthesis, as well as α-hydroxy acids including malic acid, tartaric acid and quinic acid. [143-146]



Scheme 2.1.3 Duclos' synthesis of calystegine B_2 and its analogue from methyl α-$_D$-glucose. **a**. Synthesis of calystegine B_2 analogue. **b**. Synthesis of both enantiomers of calystegine B_2.

The advantages for the chiral pool approach include easier and cheaper access of precursors

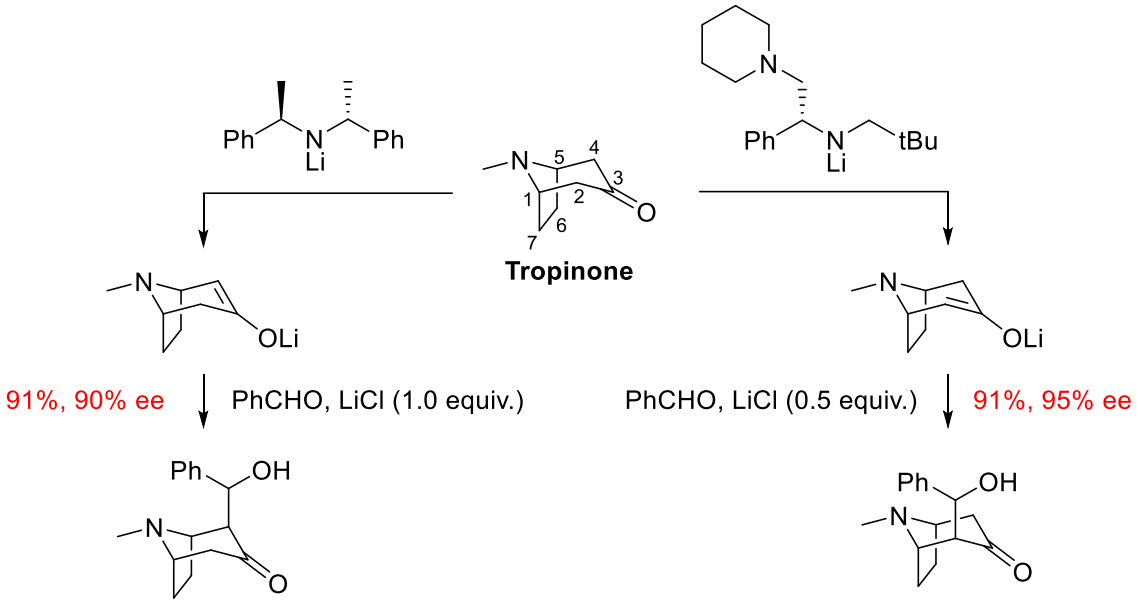
compared to cocaine derivatisation, and the possibility for the establishment of multiple stereocentres simultaneously with the formation of the ring. However, certain drawbacks still exist. Firstly, as the starting molecules are chiral, the stereochemistry of the target molecule is determined by the stereochemistry of the substrate, and the scope of accessible products would be limited. Secondly, synthetic precursors from the chiral pool are either five- or six-membered rings, and so they typically require ring expansion to achieve the seven-membered ring tropane scaffold, which might involve loss of stereochemistry during synthesis. Thirdly, the final products are generally obtained in low yields due to the long sequences of derivatisation steps required. [137] Therefore, developing other stereoselective methods for chiral tropane synthesis, ideally circumventing the limitations of the chiral pool approach by developing new reactions that can use non-chiral starting material became an attractive strategy.

2.1.2 Synthesis of Chiral Tropane Derivatives by Desymmetrisation

With the development of asymmetric reactions towards enantioenriched tropanes, synthesis from seven-membered ring substrates structurally similar to tropane also became an attractive strategy. Robinson's contribution to tropinone synthesis allowed high efficiency of the process, making tropinone readily available to chemists with affordable price. With the C_S symmetry point group, tropinone is prochiral, hence stereoselective desymmetrisation of the *meso* molecule to form the enolate would be a powerful method for tropane derivatives synthesis.

Majewski and co-workers firstly reported their investigation on the desymmetrisation of tropinone in 1991. [147] The reaction proceeded by breaking of symmetry *via* lithium enolate formation using a chiral lithium amide reagent, followed by an aldol reaction with an electrophile at the β carbon to form the product.

During investigation, they discovered that the type of electrophile determined the outcome of the reaction among three possibilities: for benzaldehyde, β-addition occurs to give the aldol product with high stereoselectivity (examples shown in Scheme 2.1.4), while oxygen-substitution was observed with other electrophiles and pyrimidone ring opening was also found to occur in some circumstances (examples not shown). [148-151] In addition, the stereoselectivity for C2 and C4 deprotonation is dependent on the lithium amide base used. The presence of LiCl was found essential to maintain high enantioselectivity.



Scheme 2.1.4 Majewski's work on stereoselective deprotonation of tropinone.

Their preliminary results inspired follow-up work using other chiral lithium amides and these methods were applied in the synthesis of different tropane-derivatised natural product precursors including (−)-knightinol, (+)-ferruginine, (+)-cocaine. [148-149, 152-153] In addition, this enantioselective deprotonation/aldol methodology was later employed by other groups, and by modifying the *N*-substitution as well as the tropane backbone ring, they were able to extend the scope to product a wider array of other tropane-derivatised products. [154-156]

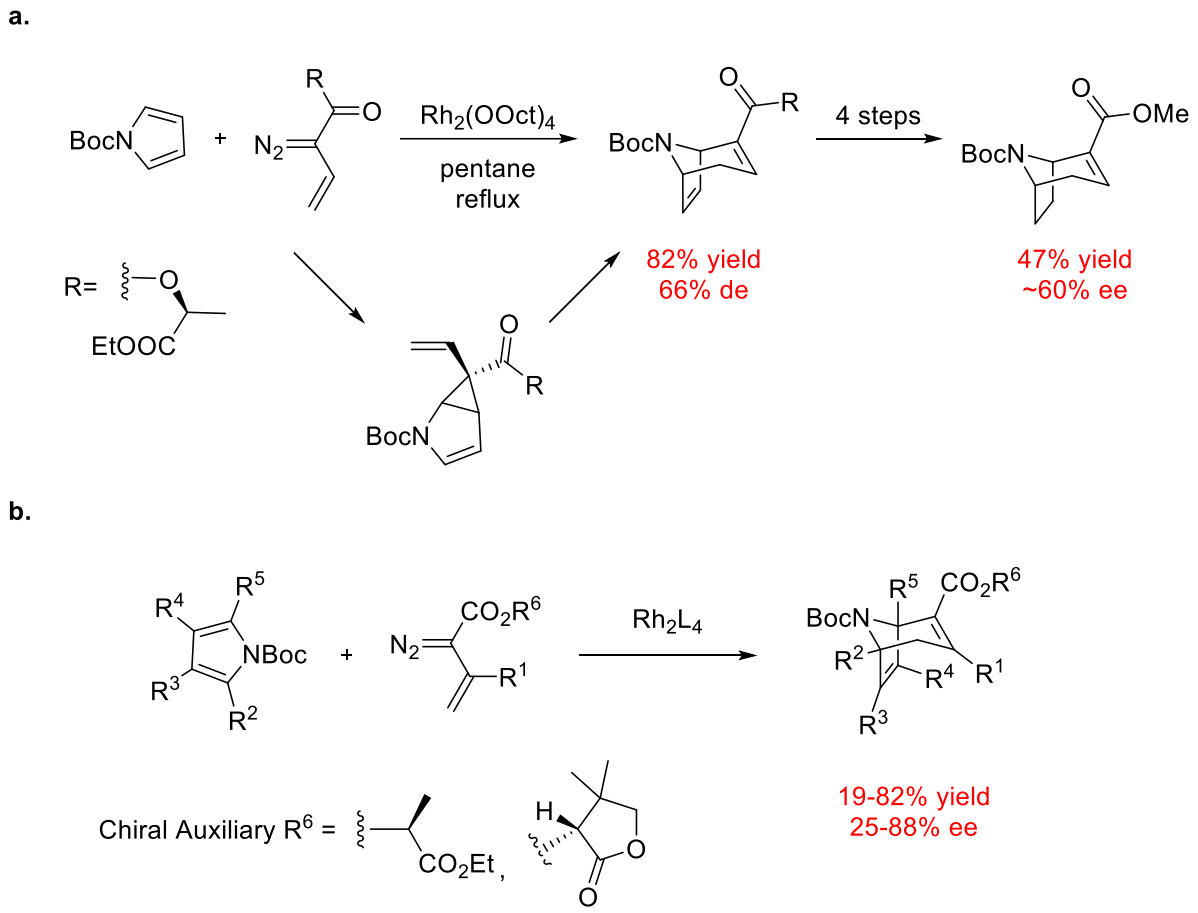
In summary, this approach was able to circumvent the scope limitations inherent in starting from chiral pool molecules by using an easily accessible prochiral tropinone. However, testing and adjustments of the structure and chirality of lithium amide base are required to achieve specific regio- and stereoselectivity. Apart from the previous two methods introduced above, a third complementary approach for the enantioselective synthesis for chiral tropane derivatives is summarised in the section below, where chiral catalysts and auxiliaries are used in up to stoichiometric amounts, with the stereochemistry being set concomitantly with the formation of tropane ring.

2.1.3 Enantioselective Synthesis of Tropane Scaffold

The enantioselective synthesis of tropane scaffold can be achieved by several different methods, including the use of chiral auxiliaries and chiral catalysts to set the stereochemistry during the reactions. Chiral auxiliaries are defined as enantiomerically enriched molecules which can be easily attached to the prochiral substrate and subsequently recovered from the diastereomeric product, and are responsible for the stereoselectivity of the reaction. [137] The majority of asymmetric reactions in tropane synthesis using chiral auxiliaries are cycloaddition reactions between olefins and azomethine ylides. [125]

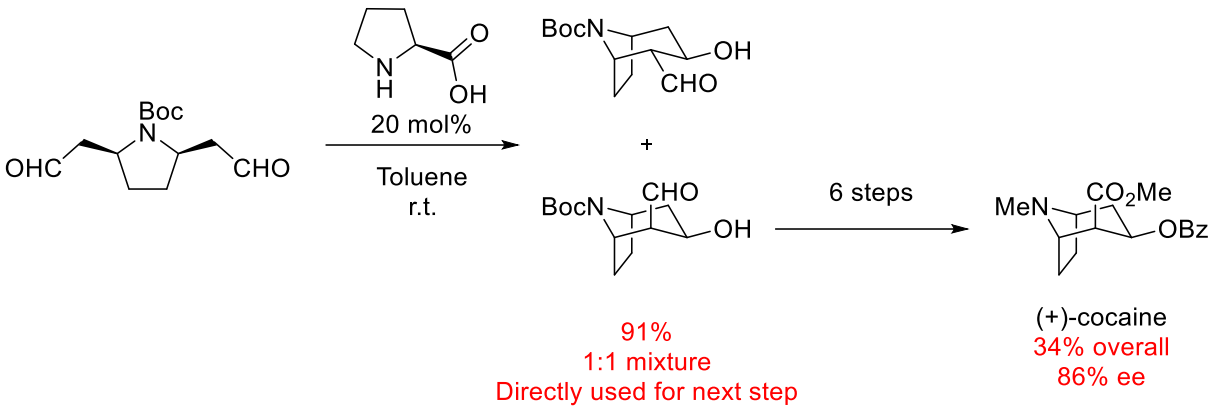
Likewise, the asymmetric reactions towards enantioenriched tropane derivatives using chiral catalysts are mainly cyclisation or cycloaddition reactions, and the catalysts that were commonly used include transition metal catalyst as well as organocatalysts including the amino acids, and NHCs. [125, 157-158]

Davies and co-workers discovered the reaction between *N*-Boc protected pyrrole and Rh(II)-stabilised vinylcarbenoids, where a chiral auxiliary was used to achieve stereocontrol in the reaction. A tandem reaction was observed by cyclopropanation to form a pyrrolinocyclopropane intermediate, the tropane scaffold is formed in the next step by Cope rearrangement with 82% yield and 66% de (Scheme 2.1.5a). [159] Among the reaction, opposite enantioselectivity was observed during the reaction when (*R*)-pantolactone and (*S*)-lactate were used as the chiral auxiliary, which provided asymmetric induction during cyclopropanation. Later in 1997, Davies group reported the same reaction on substituted pyrroles to form functionalised tropane scaffolds with up to 82% yield and up to 88% ee, and the synthetic utility of the reaction was demonstrated through the asymmetric synthesis of (−)-anhydroecgonine methyl ester and (−)-ferruginine. [160]



Scheme 2.1.5 Davies' work on enantioselective synthesis of tropane derivatives **a**. Initial work on the reaction. **b**. Follow-up work on enantioselective synthesis of functionalised tropane.

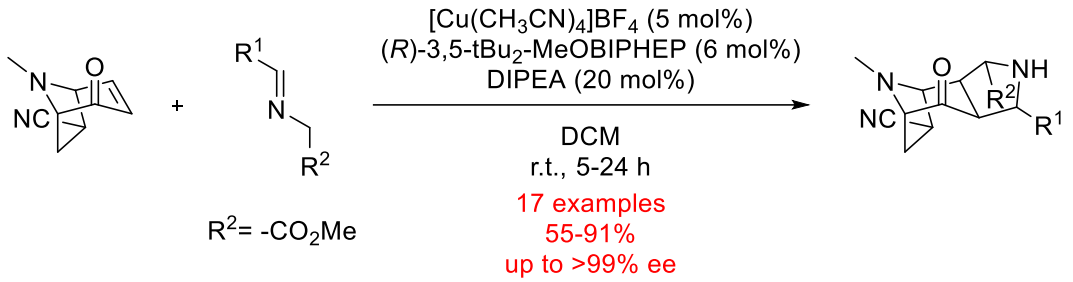
Other catalytic enantioselective approaches generally apply transition metal catalysts including palladium, copper, chromium, cobalt, gold catalysts, and organocatalytic methods are also known. [157, 161-163] An example of the enantioselective synthesis of (+)-cocaine was reported by Mans group using proline catalysis as shown in Scheme 2.1.6. [157] Unlike most enantioselective synthesis of tropane molecules which proceeded by cycloadditions, this reaction was an intramolecular aldol reaction. Other tropane derivatives including (+)-ferruginine, (−)-Bao Gong Teng A, and other substituted tropane scaffolds were successfully synthesised with moderate to high ee with various asymmetric catalytic reactions. [157-158, 162-168]



Scheme 2.1.6 Mans group's work on enantioselective synthesis of (+)-cocaine by proline catalysis.

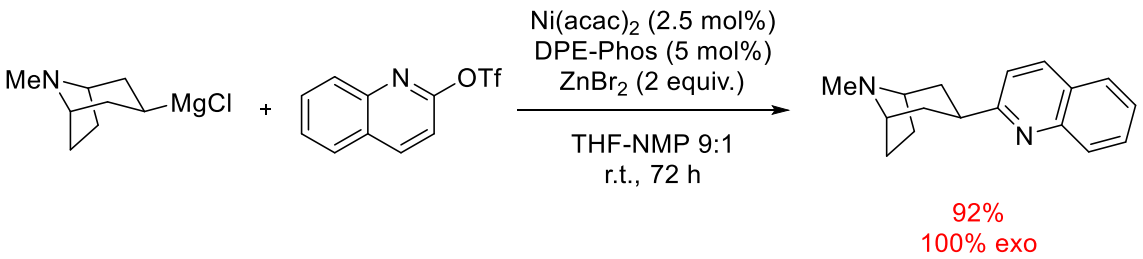
2.2 Project Aims

Tropane derivatives display a range of various biological and pharmaceutical properties, hence there has been a demand for the asymmetric synthesis of chiral tropane derivatives. With the existing approaches for enantioselective synthesis of tropane discussed above in Chapter 2.1, we realised that the catalytic asymmetric approaches from racemic tropane are highly limited with one example reported by Waldmann and coworkers. [169] They established a highly enantio- and diastereo-selective strategy on the enantiodivergent synthesis of natural product derivatives using racemic tropane (Scheme 2.2.1). The reaction proceeded *via* a Cu(I)-catalysed [3+2] cycloaddition.



Scheme 2.2.1 Waldmann's work on Cu-catalysed [3+2] cycloaddition with racemic tropane.

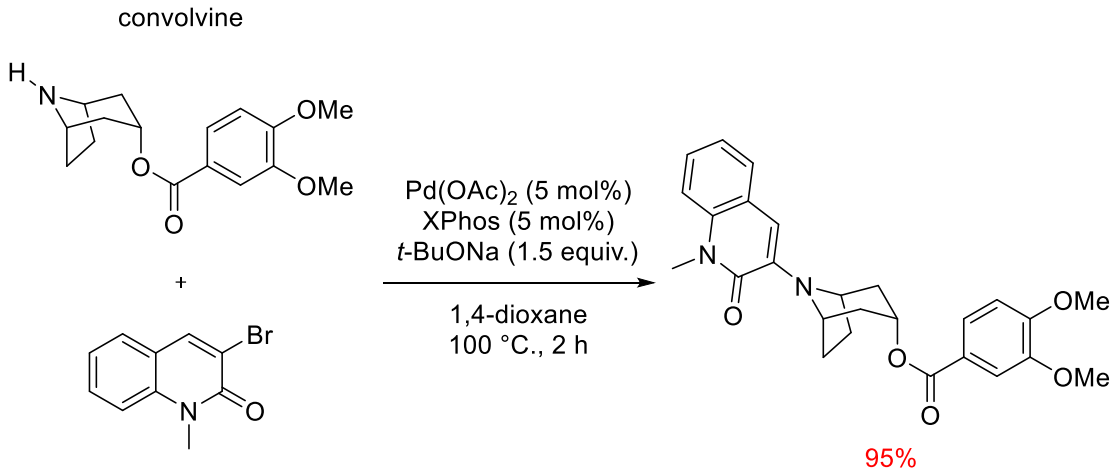
No catalytic asymmetric cross-coupling reactions on racemic tropanes are known, and the few existing cross-coupling reactions with tropanes were generally non-asymmetric using *meso* tropane substrates. One Ni-catalysed Negishi cross-coupling reaction constructing new C–C bond on tropane was reported by the Knochel group, and the reaction only afforded a *meso*-tropane derivative from the *meso* tropane derived Grignard reagent (Scheme 2.2.2). [170]



Scheme 2.2.2 Ni-catalysed cross-coupling reaction on *meso* tropane substrate by Knochel group.

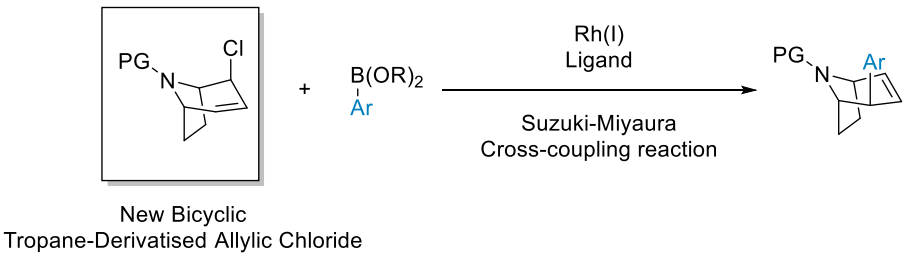
Another interesting example was reported by the Messaoudi group which performed a Pd-

catalysed C(sp^2)–N Buchwald–Hartwig cross-coupling using a *meso*-tropane derivatised substrate, convolvine (Scheme 2.2.3). [171] The reaction provided route with various aryl- and heteroaryl substitutions on the nitrogen atom, enabling access to unknown convolvine type products which could potentially become new Hsp90 inhibitors.



Scheme 2.2.3 Pd-catalysed Buchwald–Hartwig cross-coupling reaction on tropane derivative by the Messaoudi group.

Hence, we set out to find new catalytic asymmetric cross-coupling reactions for the synthesis of chiral tropane derivatives. The new reactions would ideally be efficient and highly stereoselective, while utilising racemic tropane substrates, unlike previous methods. The Fletcher group had previously reported highly stereoselective Rh-catalysed Suzuki-Miyaura type cross-coupling reactions on both mono- and bi-cyclic allylic halides, in which the racemic substrates are converted to a single enantiomer of the cross-coupling product (Chapter 1.1.2 and 1.2.2). Therefore, we wondered if we could apply a related strategy to the catalytic asymmetric synthesis of sterically congested bicyclic *N*-heterocycles, and by that develop an asymmetric cross-coupling approach to the nortropane scaffold as shown in Scheme 2.2.4.



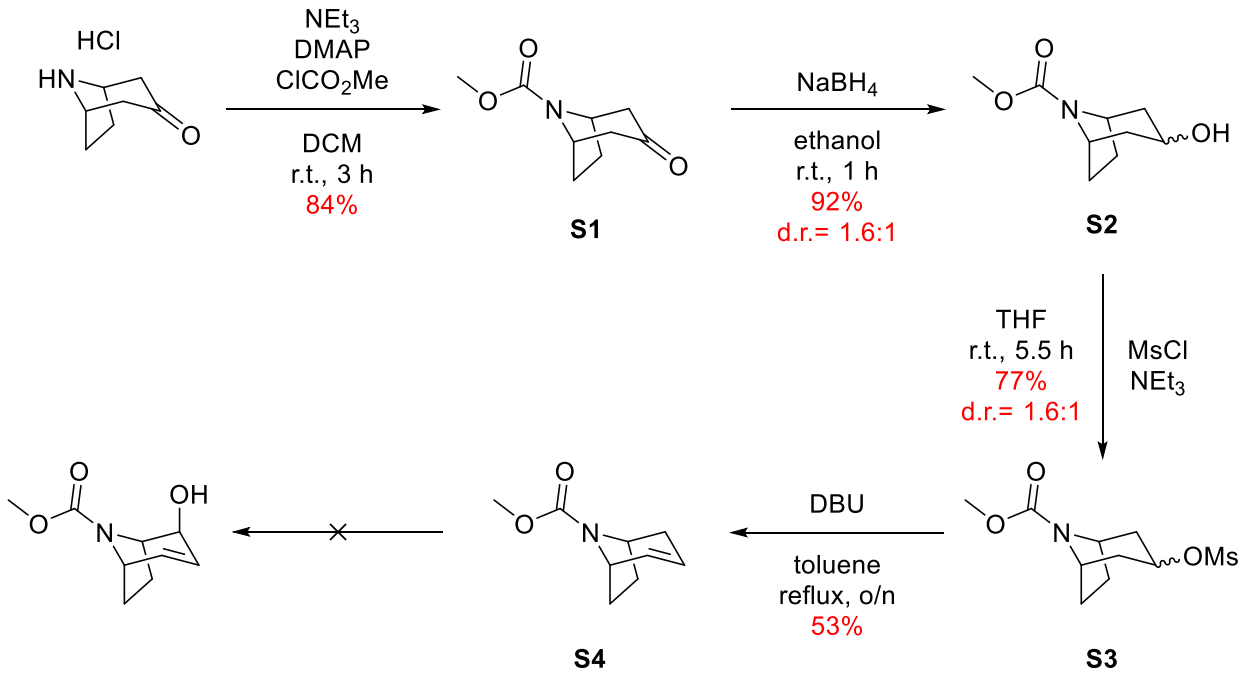
Scheme 2.2.4 Proposed Rh-catalysed asymmetric allylic arylation reaction.

This project aims to apply Rh-catalysed cross-coupling reaction conditions to racemic tropane-derived allylic chloride. First, we developed the synthesis of a nortropane-derived allylic chloride derived from a commercial building block. Then, we developed a highly enantio- and diastereoselective cross-coupling protocol, studied the reaction mechanism and showed the synthetic utility of the building blocks.

2.3 Results and Discussion

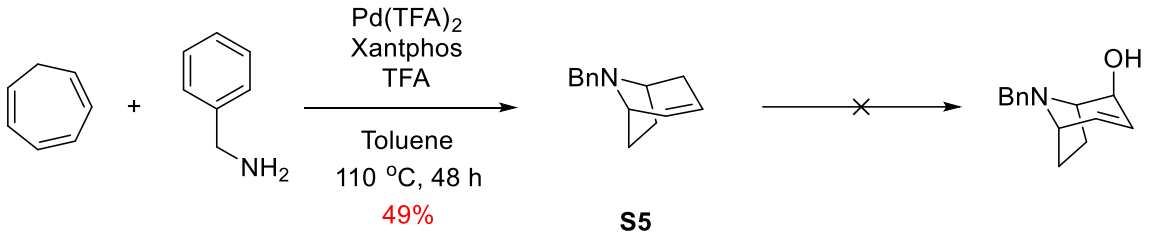
2.3.1 Substrate Synthesis

First, we investigated the synthesis of the racemic nortropane-derived allylic chloride substrate. Various substrates were proposed, and different routes were attempted, and synthesis with methyl carbamate, benzyl, and Cbz as the *N*-protecting group were tested first. We started with the synthesis of methyl carbamate protected substrate from commercially available nortropinone hydrochloride. The first four steps were successful, but after testing the direct allylic oxidation using SeO_2 and the epoxidation + ring opening approach using urea hydrogen peroxide (UHP), we could not obtain the allylic alcohol and **S4** was recovered from the reaction (Scheme 2.3.1).



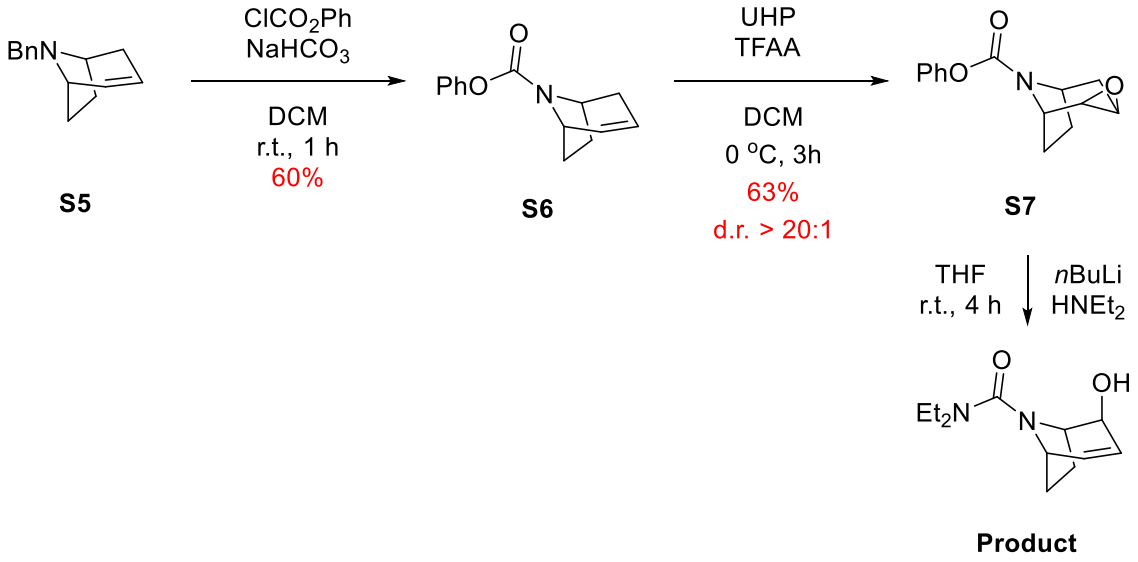
Scheme 2.3.1 Overview of synthesis route of methyl carbamate protected substrate.

Next, attempts were made to synthesise the benzyl-protected substrate using Hartwig's procedure, [172] proceeding *via* intermolecular hydroamination of a cycloheptatriene with a subsequent intramolecular transannular hydroamination of a diene. However, after both allylic oxidation methods including SeO_2 allylic oxidation and UHP epoxidation being tested, the oxidation step on **S5** did not proceed, and **S5** was recovered from the reaction (Scheme 2.3.2).



Scheme 2.3.2 Overview of synthesis of benzyl protected substrate.

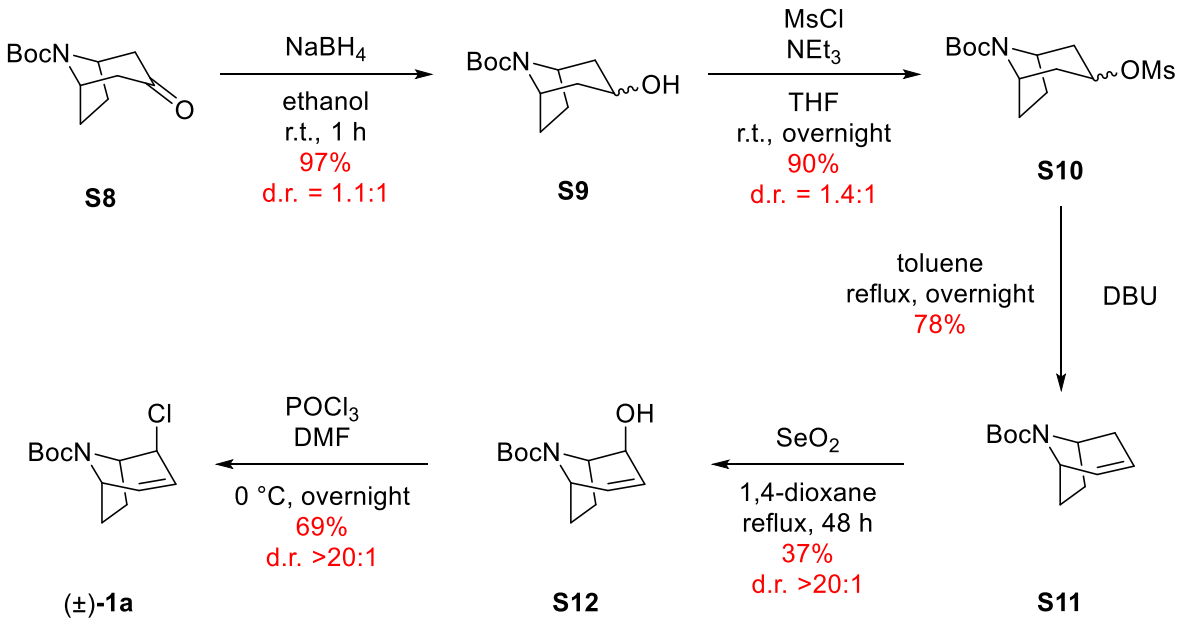
Then, phenyl carbamate was tested as an alternative protecting group. Even though direct SeO_2 allylic oxidation did not proceed on **S6**, epoxidation afforded the epoxide **S7** successfully. However, even though sequential ring opening on **S7** proceeded to form the allylic alcohol on the ring, we did not successfully synthesise the desired phenyl carbamate protected allylic alcohol. Alternatively, nucleophilic attack of the lithium amide occurred at the carbonyl to afford a urea moiety (Scheme 2.3.3). Our postulation was that relatively low steric hindrance of the phenyl ring at the C=O carbon position as well as the stability of the phenoxide facilitated the nucleophilic attack at the carbonyl. No further investigations were made on this route.



Scheme 2.3.3 Overview of synthesis of phenyl carbamate protected substrate.

Finally, we succeeded in the synthesis of *N*-Boc protected allyl chloride derived from nortropane (Scheme 2.3.4). To synthesise the nortropane-derived allyl chloride, we started from commercially available nortropinone **S8**. $NaBH_4$ reduction gave the corresponding alcohol **S9** with approximately 1.1:1 d.r.. The alcohol **S9** was activated with methanesulfonyl chloride to **S10** with 1.4:1 d.r. and 90% yield, which was then eliminated to give the alkene **S11**. Different

methods were attempted to oxidise the allylic position of the alkene, including direct allylic oxidation with SeO_2 and epoxidation followed by ring-opening. Allylic oxidation exhibited a better overall yield of 37% and perfect diastereocontrol with >20:1 d.r., hence was utilised as the synthesis route to give **S12**. Compound **S12** was subjected to chlorination conditions to afford the substrate (±)-**1a** with 69% yield and >20:1 d.r..



Scheme 2.3.4 Synthesis of nortropane-derived allyl chloride (±)-**1a**.

The route proved to work at multi-gram scales, except for the allylic oxidation step, where the reaction gave inferior yields on scales using more than 1.2 g of **S11**. Higher concentrations and different equivalents of SeO_2 were tested in the reaction, which were found to be harmful for yield compared to the standard conditions (shown in Chapter 4.2.1). We hypothesised that the temperature control in larger reaction vessels caused lower yields. In order to circumvent this scale-up problem, we performed multiple 1.2 g reactions in parallel. The relatively lone 5-step synthesis provided an overall yield of 17%, and possible optimisation could be sought to shorten the route or improved the yield.

2.3.2 Reaction Optimisation

With the nortropane-derived allylic chloride substrate (±)-**1a** in hand, we went on to test the Rh-catalysed cross-coupling reaction. Using Rh-catalysed Suzuki-Miyaura cross-couplings reaction conditions established by our group, [71] the reaction of allyl chloride (±)-**1a** with

phenylboronic acid **2aa** afforded cross-coupling product **3a** in 94% enantiomeric excess as a single diastereomer (>20:1), albeit only in 28% yield (Table 2.3.1, Entry 1). After quenching the reaction, we observed unreacted allyl chloride (+)-**1a** in the reaction as well as the hydrolysis product forming the allylic alcohol **S12**.

To optimise the yield and enantiomeric excess of the reaction, we extensively examined a series of factors including solvent, temperature, ligand, base, boronic acid derivatives, equivalents of substrate and base, concentration, catalyst loading and additives.

First, temperature effects were examined, and we found that increase in temperature resulted in both inferior yield and ee (Table 2.3.1, Entry 2). We also found out that increasing the number of equivalents of the coupling partner gave a 1.5-fold increase in yield to 43% with a 1% increase in ee to 95% (Table 2.3.1, Entry 3).

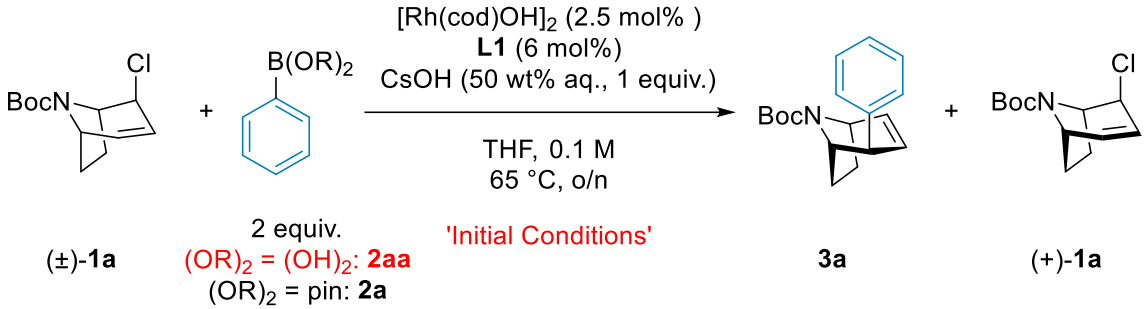
We then proceeded to screen some common solvent for Rh-catalysed cross-coupling reactions used by the group, including toluene and 1,4-dioxane, but none exhibited higher reactivity (Table 2.3.1, Entries 4-6). A frequently used base for Rh-catalysis, Cs_2CO_3, was tested and displayed similar reactivity but slightly lower ee (Table 2.3.1, Entry 7).

Furthermore, various bisphophine ligands were screened, among all, (*S*)-SEGPHOS **L1** gave superior results compared to all other ligands (Table 2.3.1, Entries 8-14). Finally, we found out by substituting the coupling partner with phenyl boronic pinacol ester **2a**, as well as increasing number of equivalents of both the coupling partner and the base, we successfully obtained product **3a** with 48% yield and 94% ee (Table 2.3.1, Entry 15). Doubling the catalyst loading did not give rise to improved yield (Table 2.3.1, Entry 16).

Later in reaction optimisation, other substrates were synthesised with various protecting groups. Firstly, the methyl carbamate protected substrate (±)-**1b** was synthesised by deprotection of the *N*-Boc group on (±)-**1a** with TFA and re-protection using methyl chloroformate (Scheme 2.3.5).

The methyl carbamate protected substrate (±)-**1b** was tested using optimal conditions from previous screening, and the reaction afforded coupling product **3ab** with 57% yield and 94% ee, albeit a significantly lower d.r. of 5.1:1 (Table 2.3.2, Entry 1).

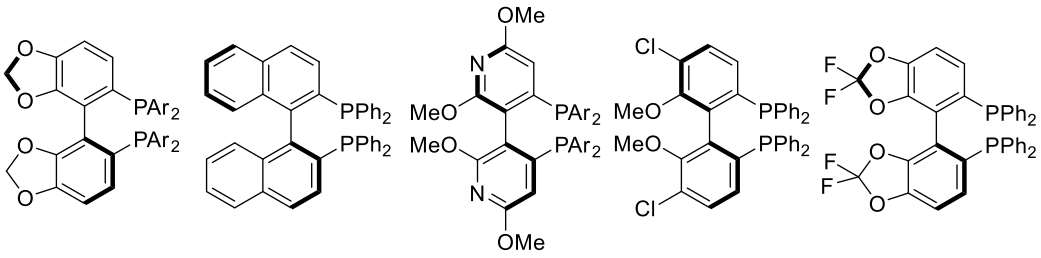
Table 2.3.1 Optimisation of Rh-catalysed reaction of (±)-**1a**



(±)-**1a** | 2 equiv. (OR)$_2$ = (OH)$_2$: **2aa** (OR)$_2$ = pin: **2a** | 'Initial Conditions' | **3a** | (+)-**1a**

Entry	Deviation from initial conditions	Yield /%[a]	ee/%[b]	d.r.[c]
1	-	28	94	>20:1
2	80 °C	10	83	>20:1
3	**2aa** (3 equiv.)	43	95	>20:1
4	**2aa** (3 equiv.), 1,4-dioxane as solvent	33	93	>20:1
5	**2aa** (3 equiv.), toluene as solvent	38	90	>20:1
6	**2aa** (3 equiv.), toluene as solvent, 80 °C	43	93	>20:1
7	**2aa** (3 equiv.), Cs_2CO_3 as base	43	93	>20:1
8	**L2** as ligand	23	81	>20:1
9	**L3** as ligand	35	89	>20:1
10	**L4** as ligand	8	83	>20:1
11	**2aa** (3 equiv.), **L5** as ligand	11	89	>20:1
12	**2aa** (3 equiv.), **L6** as ligand	0	-	-
13	**2aa** (3 equiv.), **L7** as ligand	23	92	>20:1
14	**2aa** (3 equiv.), **L8** as ligand	11	92	>20:1
15	**2a** (3 equiv.), CsOH (2.5 equiv.)	48	94	>20:1
16	**2a** (3 equiv.), CsOH (2.5 equiv.), double catalyst loading	43	93	>20:1

a. Isolated yield. **b**. Enantiomeric excess determined by Supercritical Fluid Chromatography (SFC) analysis on a chiral non-racemic stationary phase. **c**. Diastereomeric ratio determined by integration of ^{1}H NMR spectra.



L1: Ar = Ph
L5: Ar = Xyl
L6: Ar = DTBM

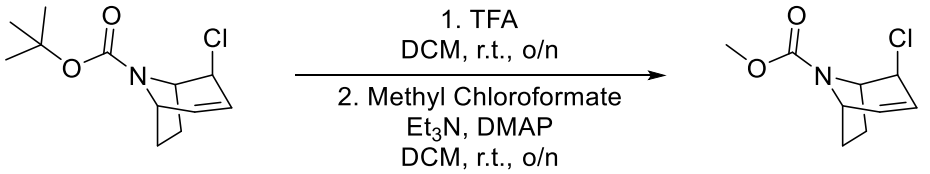
L2

L3: Ar = Xyl
L8: Ar = Ph

L4

L7

Even though with lower steric bulk in the methyl carbamate protected substrate compared to *N*-Boc, the *exo*-diastereomer was not favoured in the reaction of **1b**, which contradicted with our expectation. Therefore, our postulation was that due to the lower steric bulk of the methyl carbamate, the barrier of rotation is lower, resulting in lower chances of coordination of the carbonyl group with the Rh-complex. As the coordination was possibly responsible for the *exo*-conformation in the product, significantly lower diastereoselectivity was achieved.



(±)-**1a**

(±)-**1b**
Quantitative Yield

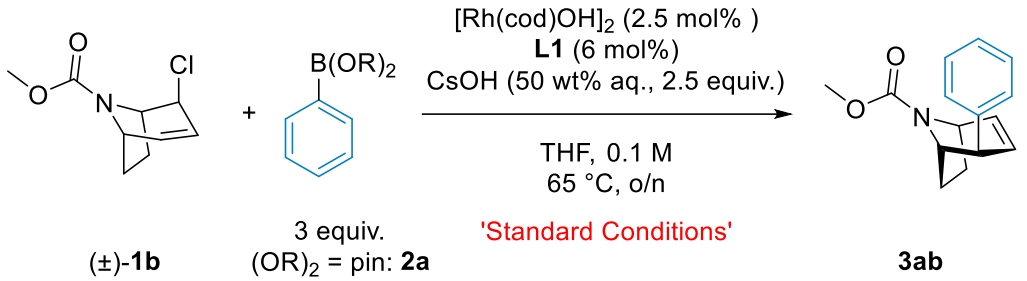
Scheme 2.3.5 Synthesis of (±)-**1b**.

In order to optimise the diastereomeric ratio and the yield, we screened the influence of coupling partner, solvent, and temperature. Two different coupling partners including triphenylboroxin and potassium phenyl trifluoroborate were tested, showing lower performance than phenyl boronic pinacol ester (Table 2.3.2, Entries 2-3). Again, we tried the effect of further increasing the number of equivalents of the coupling partner to 5 equiv., but observed no significant increase in yield, potentially representing that apparent increase in yield could only be resulted from increase in both the equivalents of the coupling partner and the base (Table 2.3.2, Entry 4).

Subsequently, we tried replacing the base to $CsOH \cdot H_2O$ to reduce the reactivity inhibition by hydrolysis, but only observed a significant drop in both the yield to 22% and ee to 71% (Table 2.3.2, Entry 5). Furthermore, to explore the effects of lower temperature on reaction, we stirred

the reaction overnight at 40 °C, but observed no conversion to the product, indicating that lower temperature impaired reactivity (Table 2.3.2, Entry 6). However, heating the reaction up to 100 °C in 1,4-dioxane with increased equivalents of **2a** and base did not improve the reactivity as we expected, in addition to a much poorer ee, either with CsOH or Cs_2CO_3 (Table 2.3.2, Entries 7-8).

Table 2.3.2 Selected Optimisation Results of Rh-catalysed reaction of (±)-**1b**



Entry	Deviation from standard conditions	Yield /%[a]	ee/%[b]	d.r.[c]
1	-	57	94	5.1:1
2	Triphenylboroxin instead of **2a**	53	96	5.2:1
3	Ph-BF_3K instead of **2a**	n.r.	-	-
4	**2a** (5 equiv.)	53	96	4.7:1
5	$CsOH{\cdot}H_2O$ as base	22	71	6.2:1
6	40 °C	-	-	-
7	1,4-dioxane, 100 °C, **2a** (5 equiv.), CsOH (4 equiv.)	25	67	5.5:1
8	1,4-dioxane, 100 °C, **2a** (5 equiv.), Cs_2CO_3 (4 equiv.)	11	20	-

a. Isolated yield. **b**. Enantiomeric excess determined by Supercritical Fluid Chromatography (SFC) analysis on a chiral non-racemic stationary phase. **c**. Diastereomeric ratio determined by integration of ^{1}H NMR spectra.

2.3.3 Design of Experiments

As the effects of different factors on the reactivity and stereoselectivity remained unclear after a series of optimisation, we performed Design of Experiments (DoE) using the methyl carbamate substrate in the reaction to uncover and quantify how different factors would jointly affect the output. Continuous factors including temperature, number of equivalents of the coupling partner and base; and categorical factors including base and solvent were input into a

statistical software (JMP®), and 16 experiments were automatically generated as shown in Table 2.3.3. Experiments were performed accordingly and the results of yields and ee were used to calculate the correlation between different factors and the results.

The correlation between input and output were calculated by the software and presented below as a prediction profiler. The X-axis represented the different factors, while the Y-axis presented three results, including the desirability, the yields, and the ee of the corresponding factor (Figure 2.3.1).

Table 2.3.3 Design of Experiment Results for (±)-**1b**

Entry	Solvent	Temperature/°C	Base	Equiv. of 2a	Yield /% [a]	ee/% [b]
1	Dioxane	65	RbOH (4 equiv.)	1	7	24
2	THF	65	CsOH (1 equiv.)	3	40	98
3	Dioxane	50	CsOH (4 equiv.)	2	25	95
4	THF	50	LiO*t*Bu (4 equiv.)	4	14	45
5	Toluene	80	NaOMe (4 equiv.)	3	34	88
6	Toluene	50	CsOH (2 equiv.)	1	4	62
7	Toluene	65	LiO*t*Bu (3 equiv.)	2	11	85
8	THF	50	NaOMe (3 equiv.)	1	27	99
9	Dioxane	50	LiO*t*Bu (2 equiv.)	3	5	35
10	Dioxane	80	CsOH (3 equiv.)	4	57	90
11	Toluene	50	RbOH (1 equiv.)	4	9	75
12	Dioxane	65	NaOMe(2 equiv.)	4	3	61
13	THF	80	RbOH (2 equiv.)	2	19	72
14	Dioxane	50	RbOH (3 equiv.)	3	7	84
15	Dioxane	50	NaOMe(1 equiv.)	2	4	21
16	Dioxane	80	LiO*t*Bu(1 equiv.)	1	10	3

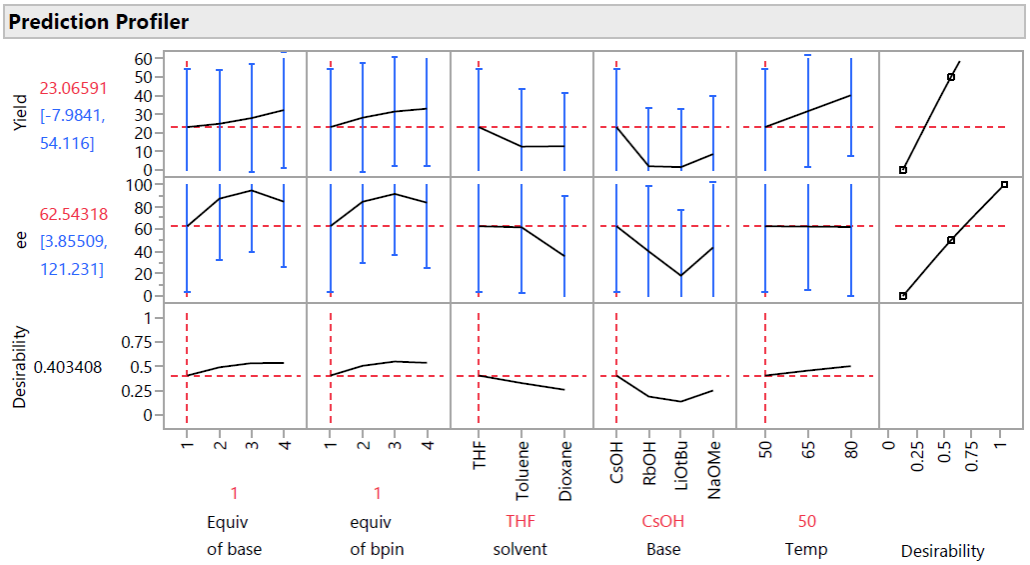
a. Isolated yield as mixture with minor diastereomer. **b**. Enantiomeric excess determined by Supercritical Fluid Chromatography (SFC) analysis on a chiral non-racemic stationary phase.

From the plot, we would be able to see that the higher number of equivalents of coupling partner and base is more desirable for the reaction, while no other factors gave predominant effects. Consequently, we took the best conditions from DoE, with 4 equivalents of **2a** and 3 equivalents of CsOH and brought it for further optimisations, affording **3ab** with 63% yield and 95% ee with 4.8:1 d.r. (Table 2.3.4, Entry 1).

Given the superior performance of THF as solvent for the reaction, we tested some other ethereal solvents shown below in Table 2.3.4. Di-isopropyl ether and 2,2-dimethoxypropane exhibited incompatibility with the reaction and did not give rise to the formation of a viable

Rh-ligand complex (Table 2.3.4, Entries 2-3). Dimethoxyethane and cyclopentyl methyl ether gave slightly lower yield than THF, while 2-methyl tetrahydrofuran gave a yield slightly lower than 67% yield and 95% ee (Table 2.3.4, Entries 4-6). The yields are shown with < due to the contamination of product by grease.

Figure 2.3.1 Design of Experiment fit model prediction profiler generated by JMP software.

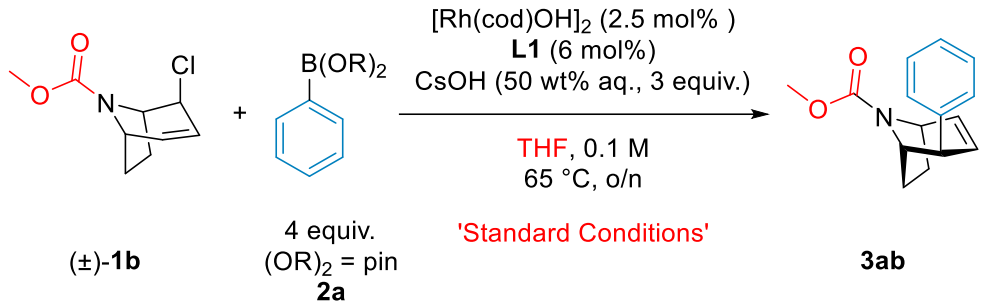


Nevertheless, no further improvement in d.r. was observed. With the optimised conditions, the d.r. of the product was ~ 4.9:1, indicating a comparable actual yield of the desired diastereomer to the yield for *N*-Boc substrate. Furthermore, different diastereomers afforded in the reaction were inseparable from each other, complicating further transformations on the substrate.

2.3.4 Synthesis and Tests of Other Substrates

Consequently, we went on to test other substrates with different leaving groups and protecting groups. The benzyl protected allyl chloride (±)-**1c**, the unprotected substrate (±)-**1d**, and ammonium salt (±)-**1e** were synthesised using similar methods to (±)-**1b**. Among these substrates, the benzyl protected substrate (±)-**1c** gave < 30% conversion as well as poor diastereoselectivity in crude NMR spectra, hence was not isolated and investigated in depth (Table 2.3.4, Entry 7). For the other two substrates, the cross-coupling reaction of (±)-**1d** gave trace product with only 79% ee, while (±)-**1e** gave rise to a significantly poorer ee of only 20% (Table 2.3.4, Entries 8-9). Neither product was isolated due to low yield.

Table 2.3.4 Selection solvent and leaving group screening results of Rh-catalysed reactions



Entry	Deviation from standard conditions	Yield /%[a]	ee/%[b]	d.r.[c]
1	-	63	93	4.8:1
2	Di-isopropyl ether as solvent	-	-	-
3	2,2-Dimethoxypropane as solvent	-	-	-
4	Dimethoxyethane as solvent	<55	93	5.0:1
5	Cyclopentyl methyl ether as solvent	<50	92	4.7:1
6	2-Methyl THF as solvent	<67	95	4.9:1
7	(±)-**1c** (PG = Benzyl)	<30	-	-
8	(±)-**1d** (PG = H)	<10	79	N.D.
9	(±)-**1e** (PG = H_2Cl)	N.D.	<20%	N.D.

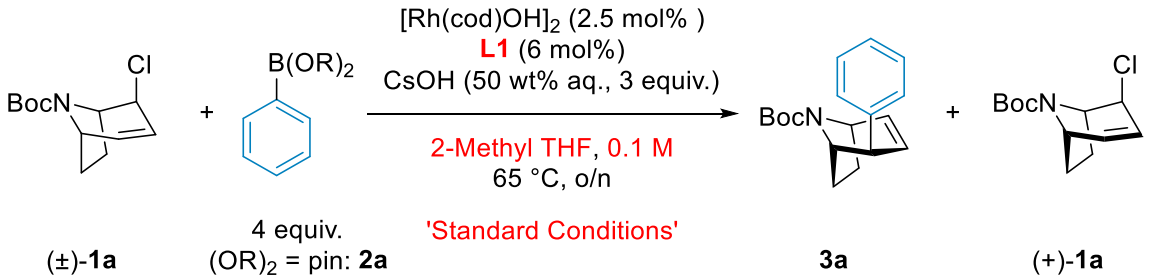
a. Isolated yield. **b**. Enantiomeric excess determined by Supercritical Fluid Chromatography (SFC) analysis on a chiral non-racemic stationary phase. **c**. Diastereomeric ratio determined by integration of ^{1}H NMR spectra.

Subsequently, we decided to continue further optimisation reactions with the *N*-Boc substrate (±)-**1a**. The optimal reaction conditions for the methyl carbamate substrate were used on the *N*-Boc substrate, and **3a** was obtained with 51% yield and 93% ee (Table 2.3.5, Entry 1). The reaction was subjected to further screening and the optimisation results were summarised below.

To list the noticeable improvements, we first found that doubling the reaction concentration from 0.1 M to 0.2 M led to a higher yield of 54% with 91% ee (Table 2.3.5, Entry 2). In addition, 2-methyl-THF was replaced with THF as the latter being a more easily accessible and cheaper solvent while giving comparable yield of 53% and ee of 93% (Table 2.3.5, Entry 3). Further ligand screening was also performed (Table 2.3.5, Entries 4-7), but we observed no improvement in yield.

As after extensive screening, the yield remained around 50%, hence we attempted to recover the remaining allyl chloride from the reaction and measured its ee. The allyl chloride (+)-**1a** was recovered with >99% ee, hinting that unlike the previous DyKAT Rh-catalysed cross-coupling reactions reported by the group, [71, 118] this reaction was likely proceeding *via* a kinetic resolution process.

Table 2.3.5 Selected Optimisation Results of Rh-catalysed reaction with (±)-**1a**



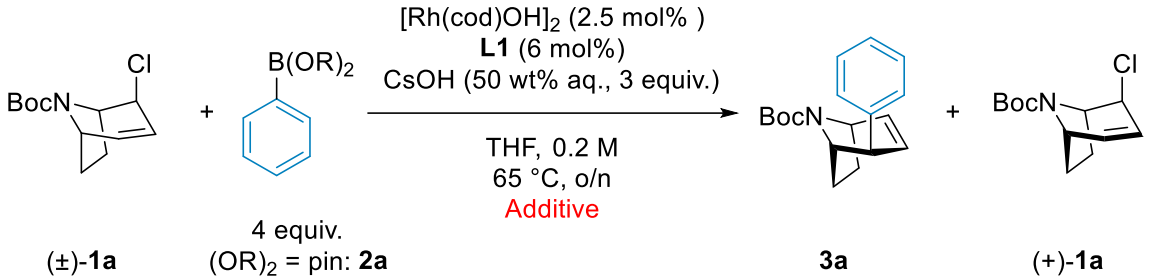
Entry	Deviation from standard conditions	Yield /%[a]	ee/%[b]	d.r.[c]
1	2-Methyl THF as solvent	51	93	>20:1
2	2-Methyl THF as solvent, 0.2 M concentration	54	91	>20:1
3	0.2 M concentration	53	93	>20:1
4	**L4** as ligand	39	86	>20:1
5	**L7** as ligand	47	94	>20:1
7	**L8** as ligand	47	94	>20:1

a. Isolated yield. **b**. Enantiomeric excess determined by Supercritical Fluid Chromatography (SFC) analysis on a chiral non-racemic stationary phase. **c**. Diastereomeric ratio determined by integration of ^{1}H NMR spectra.

We then looked at the possibility to switch the reaction pathway from a KR to DKR, thus circumventing the 50% yield for **3a**. To address this challenge, we explored different conditions trying to racemise the allyl chloride. We started by trying out addition of organic and inorganic salts to the reaction mixture. The salts tested including copper iodide, tetrabutylammonium chloride, iron(III) chloride, potassium iodide did not harm the reactivity or stereoselectivity of the reaction , but also did not racemise **1a** as expected (Table 2.3.6, Entries 1-4). The addition of silver and palladium species gave rise to noticeable racemisation of **1a**, but also induced significant inhibition on either reactivity (29% and 18% yield with Ag_2O addition and $Pd(PPh_3)_4$ addition, Table 2.3.6, Entries 5-6) or stereoselectivity (64% ee with $PdCl_2(MeCN)_2$

addition, Table 2.3.6, Entry 7).

Table 2.3.6 Selected Optimisation Results for different additives



Entry	Additive	Yield /%[a]	ee/%[b]	d.r.[c]	Yield of **1a**/%[a]	ee of **1a**/%[b]
1	10 mol% CuI, additional 10 mol% **L1**	56	95	>20:1	22	>99
2	50 mol% nBu$_4$N$^+$Cl$^-$	54	93	>20:1	17	>99
3	10 mol% $FeCl_3$	51	90	>20:1	-	>99
4	10 mol% KI	55	93	>20:1	22	>98
5	10 mol% Ag_2O	29	94	>20:1	<58[d]	39
6	5 mol% $Pd(PPh_3)_4$, 15 mol% dppf	18	95	>20:1	<14[d]	88
7	5 mol% $PdCl_2(MeCN)_2$	47	64	>20:1	34	90

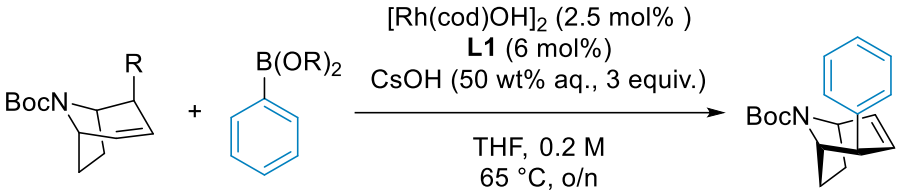
a. Isolated yield. **b**. Enantiomeric excess determined by Supercritical Fluid Chromatography (SFC) analysis on a chiral non-racemic stationary phase. **c**. Diastereomeric ratio determined by integration of ^{1}H NMR spectra. **d**. Conversion determined by integration of ^{1}H NMR spectra.

During additive screening, racemisation of (+)-**1a** was only observed with Ag_2O, while no increase in yield of product **3a** being observed, and no other additives were able to racemise **1a**. Therefore, we went on to explore the effects of the substrate leaving group on the reaction pathway. Substrates with different leaving groups including fluoride, bromide, diethyl phosphate, acetate, ethyl carbonate and phenyl carbonate ((±)-**1f** – (±)-**1k**) were synthesised from either the allyl chloride or allyl alcohol (detailed synthesis shown in Chapter 4.2.1). The new substrates were tested in the Rh reaction and results were summarised in Table 2.3.7. The allylic triflate synthesis was also attempted but was unsuccessful due to poor stability of the target substrate.

Among these substrates, allyl fluoride and bromide showed significantly poorer stability

compared to allyl chloride **1a**, and both experienced decomposition at room temperature. Both substrates gave poor yields and ee (Table 2.3.7, Entries 1-2). Other substrates, including the allyl carbonate, acetate, and the phosphate underwent hydrolysis and afforded <10% product after overnight reaction.

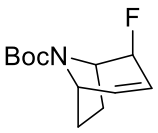
Table 2.3.7 Leaving group screening results



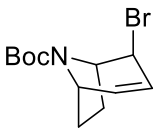
(±)-**1f** – **1k** 4 equiv. $(OR)_2$ = pin: **2a** **3a**

Entry	Substrate	Yield /%[a]	ee/%[b]	d.r.[c]
1	(±)-**1f**	30	18	>20:1
2	(±)-**1g**	10	78	>20:1
3	(±)-**1h**	<5	-	-
4	(±)-**1i**	<5	-	-
5	(±)-**1j**	<5	-	-
7	(±)-**1k**	<5	-	-

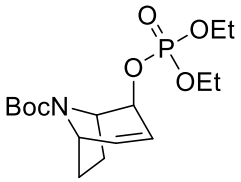
a. Isolated yield. **b**. Enantiomeric excess determined by Supercritical Fluid Chromatography (SFC) analysis on a chiral non-racemic stationary phase. **c**. Diastereomeric ratio determined by integration of ^{1}H NMR spectra.



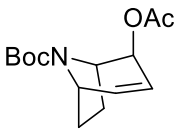
(±)-**1f**



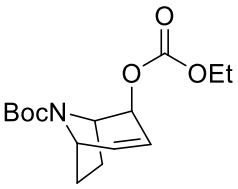
(±)-**1g**



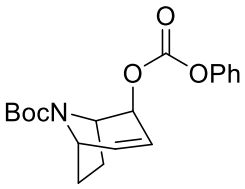
(±)-**1h**



(±)-**1i**

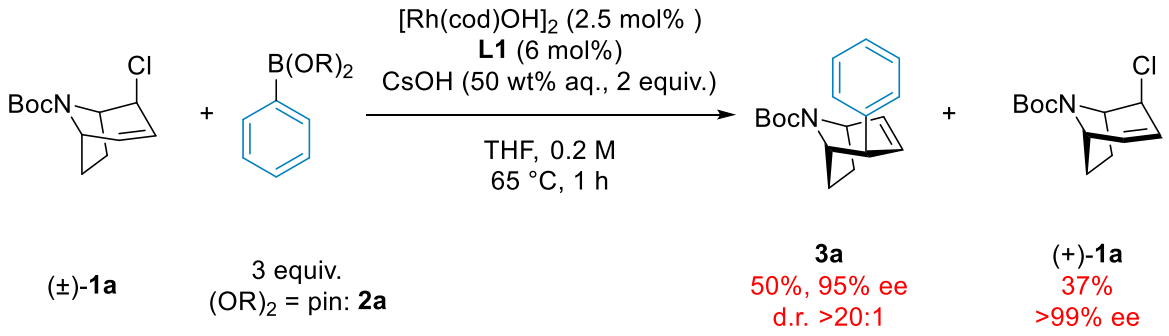


(±)-**1j**



(±)-**1k**

Subsequently, we monitored the course of reaction in time by performing a kinetic reaction. To our surprise, we found out that the reaction reached over 40% conversion in less than 30 min, and hydrolysis products could be observed from 45 min onwards. Therefore, to allow higher conversion towards product **3a** while maintaining the ee of both **3a** and recovered allyl chloride **1a**, the standard reaction time was set at 1 h. Furthermore, as difficult purification was observed due to the high content of phenyl boronic pinacol ester present in the reaction which eluted together with product on silica columns, the equivalents of base and the pinacol ester were also reduced by 1 equivalent from 3 equivalents of base with 4 equivalents of Bpin to 2 equivalents of base with 3 equivalents of Bpin to allow easier purification. This set of conditions were set and used as the optimal conditions for further scope reactions giving 50% yield and 95% ee in 1 h (Scheme 2.3.6).



Scheme 2.3.6 Optimal conditions for Rh-catalysed Suzuki-Miyaura cross-coupling reaction of (±)-**1a**.

2.3.5 Mechanistic Experiments

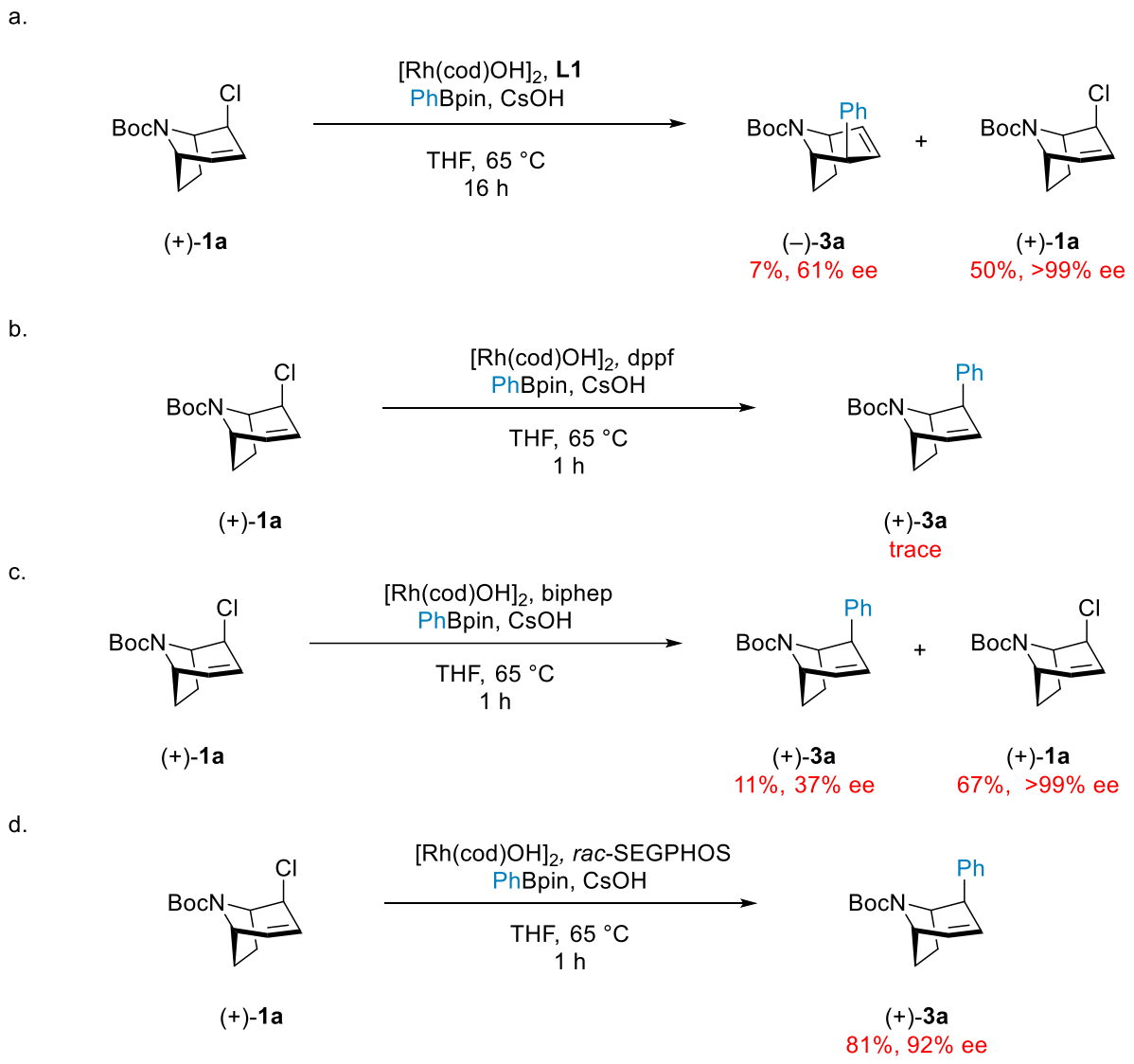
During optimisation, we found out that the reaction was proceeding *via* kinetic resolution. Attempts to switch the reaction pathway from KR to DKR by changing the substrate leaving group and additive screening were unsuccessful. Due to the intrinsically limited yield at 50 % of a KR process, we speculate that catalyst deactivation and decomposition of the pinacol ester would also play a part in limiting conversion. To distinguish if catalyst deactivation and pinacol ester decomposition was responsible for the low yield, and to elucidate the mechanism of this kinetic resolution process, we performed a few mechanistic reactions with both enantiopure and racemic **1a**.

Firstly, we performed the reaction under standard conditions with enantiopure allyl chloride (+)-**1a**. The reaction was allowed to stir overnight, and small amounts of the coupling product was isolated at 7% yield, albeit surprisingly at only 60% ee. 50% of the enantiopure allyl chloride was recovered, while the rest of the substate was subject to hydrolysis (Scheme 2.3.7a).

This result indicated that, the reaction proceeded in a different way from the previous DyKAT process developed by the group where both enantiomers of the substrate form a common symmetric Rh-π-allyl intermediate from oxidative addition. We proposed a possible mechanism of the reaction (Scheme 2.3.8a) where transmetallation occurs first, followed by the *syn* oxidative addition of the reactive enantiomer (–)-**1a** which potentially undergoes σ-π-σ isomerisation, and reductive elimination then occurs to give product **3a**. As shown by the first mechanistic experiment, during the reaction of this racemic nortropane-derived allyl chloride substrate **1a** with (*S*)-SEGPHOS as the ligand, the oxidative addition of (+)-**1a** either does not occur or does not give the same intermediate as the other enantiomer (Scheme 2.3.8a), and product formation *via* (+)-**1a** is slow.

In order to test if oxidative addition (–)-**1a** would result in the formation of *meso* π-complex, which would result in complete loss in stereochemical information upon oxidative addition, we subjected the cross-coupling reaction with enantiopure allyl chloride (+)-**1a** using achiral ligands. We started by testing dppf as the ligand, and very low conversion was observed (Scheme 2.3.7b). To confirm that the conversion was not limited by the intrinsic low reactivity of the substrate with ligand, we went on the test a phosphine-based ligand, and biphep was introduced. Under those conditions, we obtained (+)-**3a** in 11% yield and 37% ee (Scheme

2.3.7c). The significant loss in ee in the reaction with biphep suggests that reductive elimination is at least partially enantio-determining and is controlled by the ligand when SEGPHOS is used. We attribute the partial, but not complete loss in stereochemical information in the experiment with biphep, to either σ-π-σ isomerisation mechanism (Scheme 2.3.8b), which occurs at a rate similar to reductive elimination, or to a lack of selectivity amongst different oxidative addition type pathways, S_N2' or S_N1, when biphep is used.

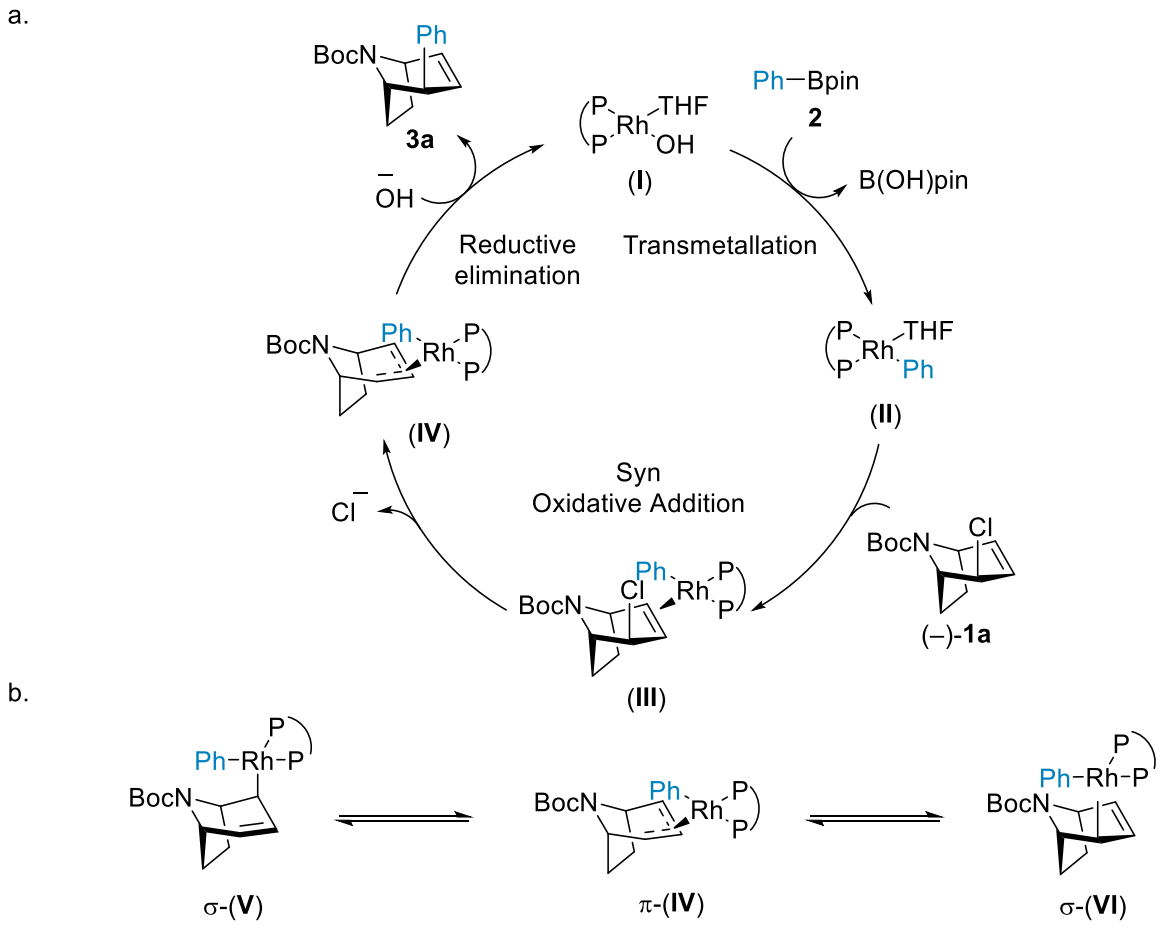


Scheme 2.3.7 Mechanistic experiments on Rh-catalysed Allylic Arylation of (±)-**1a**. **a**. Reaction with enantiopure (+)-**1a**. **b**. Reaction with enantiopure (+)-**1a** and dppf as ligand. **c**. Reaction with enantiopure (+)-**1a** and biphep as ligand. **d**. Reaction with enantiopure (+)-**1a** and *rac*-SEGPHOS as ligand.

Using *rac*-SEGPHOS as the ligand in the reaction with enantiopure (+)-**1a**, we obtained (+)-

3a in 81% yield and 92% ee (Scheme 2.3.7d). In analogy to the combination of racemic allyl chloride and enantiopure ligand, this experiment shows the strong matched effect between (+)-**1a** and (*R*)-SEGPHOS in the oxidative addition step (or (–)-**1a** and (*S*)-SEGPHOS – most likely for steric reasons, which ultimately results in a highly selective kinetic resolution.

To quantify the efficiency of the kinetic resolution process, we have calculated the *S*-factors of the reactions. However, as this reaction proceeded with a partial DyKAT character, meaningful quantification could not be completely achieved, therefore, the table of calculated apparent S-factor values are included in Chapter 4.2.6.



Scheme 2.3.8 a. Proposed mechanism of the reaction. **b**. Equilibration between two Rh-σ complexes.

2.3.6 Reaction Scope

After mechanistic investigations, we went on to study the scope. A range of aryl boronic pinacol esters with electron-withdrawing and donating substituents at *para*- and *meta*-positions yielded the desired coupling products typically in 40–50% yield (Scheme 2.3.9, **3a**–**3h**, **3l**–**3o**) and >94% ee as single diastereomers (>20:1 d.r.). These examples included various aryl halides, alkoxy groups, ester, and an aryl silane, which are useful intermediates for further transformations.

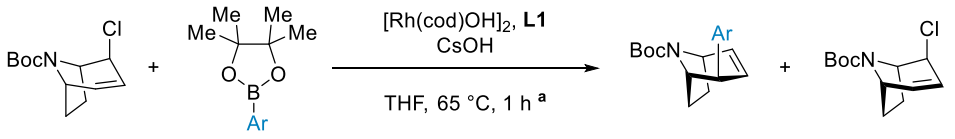
More challenging coupling partners featuring an iodide, cyano, or acetyl group (**3i**–**3k**) resulted in diminished yields but consistently high enantioselectivity. We observed only trace product formed with 2-methylphenylboronic pinacol ester (**2u**), likely due to sterics and/or competitive protodeborylation. [173]

We went on to test a range of heteroaryl boronic pinacol esters. 2-Furanyl- and 2-chloropyridyl-boronic pinacol esters performed well with yields over 40% and high enantioselectivities (**3p**, **3q**). However, 3-furanylboronic pinacol esters gave only 15% yield, likely due to rapid protodeborylation ─ a common problem with heterocyclic boronic acids and esters. [174]

Interestingly, a few examples gave >50% yield (**3l** and **3p** gave 59 and 56% yield, respectively), which varied in both steric and electronic properties. We have briefly investigated but still do not fully understand the reason behind this phenomenon. Furthermore, the yield of reaction to give **3p** was found to further improve upon scale-up (Chapter 2.3.5).

The absolute and relative stereochemistries of the product and resolved allyl chloride (Scheme 2.3.10) were determined by single-crystal X-ray diffraction of **3p** and (+)-**1a**.

Scheme 2.3.9 Scope of Reaction

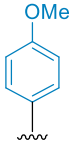


(±)-**1a** **2a-u** **3a-u** (+)-**1a**

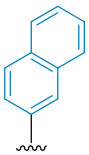
3a
50%, 95% ee



3b
44%, 96% ee



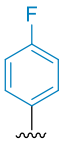
3c
32%, 94% ee



3d
51%, 95% ee



3e
44%, 94% ee



3f
49%, 98% ee[b]



3g
47%, 96% ee



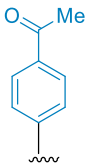
3h
39%, 96% ee



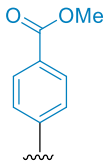
3i
22%, 96% ee



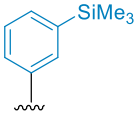
3j
23%, 97% ee[c, d]



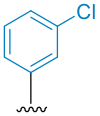
3k
19%, 98% ee



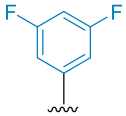
3l
59%, 96% ee



3o
46%, 97% ee



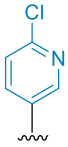
3m
38%, 96% ee



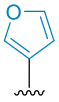
3n
49%, 97% ee



3p
56%, 97% ee[e]



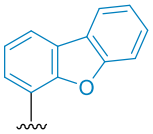
3q
42%, 97% ee[e]



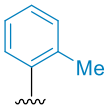
3r
15%, 98% ee[d, e]



3s
44%, 88% ee[d, e]

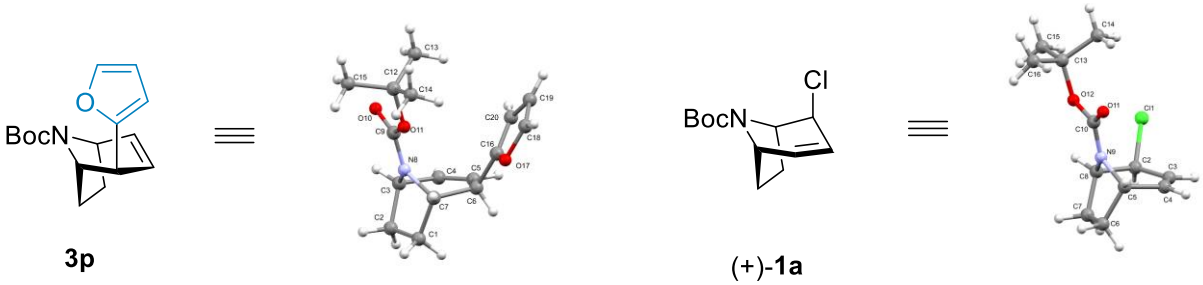


3t
21%, 88% ee[e]



3u
trace

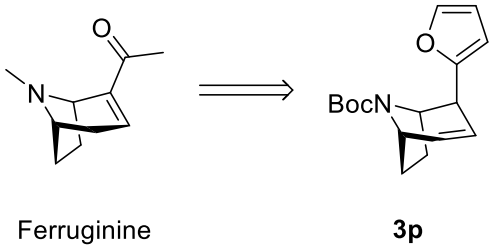
a. Rh[(cod)OH]$_2$ (2.5 mol %), **L1** (6 mol %), (±)-**1a** (0.2 mmol, 1.0 equiv), **2** (3.0 equiv), CsOH (50 wt % aq.; 2.0 equiv), THF (0.2 M), 65 °C, 1 h. All yields presented are isolated yields. Enantiomeric excess determined by supercritical fluid chromatography (SFC) analysis on a chiral nonracemic stationary phase. Single diastereomer (>20:1) obtained unless stated. **b**. 4 h. **c**. Dioxane instead of THF, 80 °C overnight. **d**. 3j: 18:1 d.r., 3r: 17:1 d.r., 3s: 19:1 d.r. **e**. 2 h.



Scheme 2.3.10 Relative and absolute stereochemistry of **3p** and (+)-**1a** by single-crystal X-ray diffraction.

2.3.7 Product Derivatisation

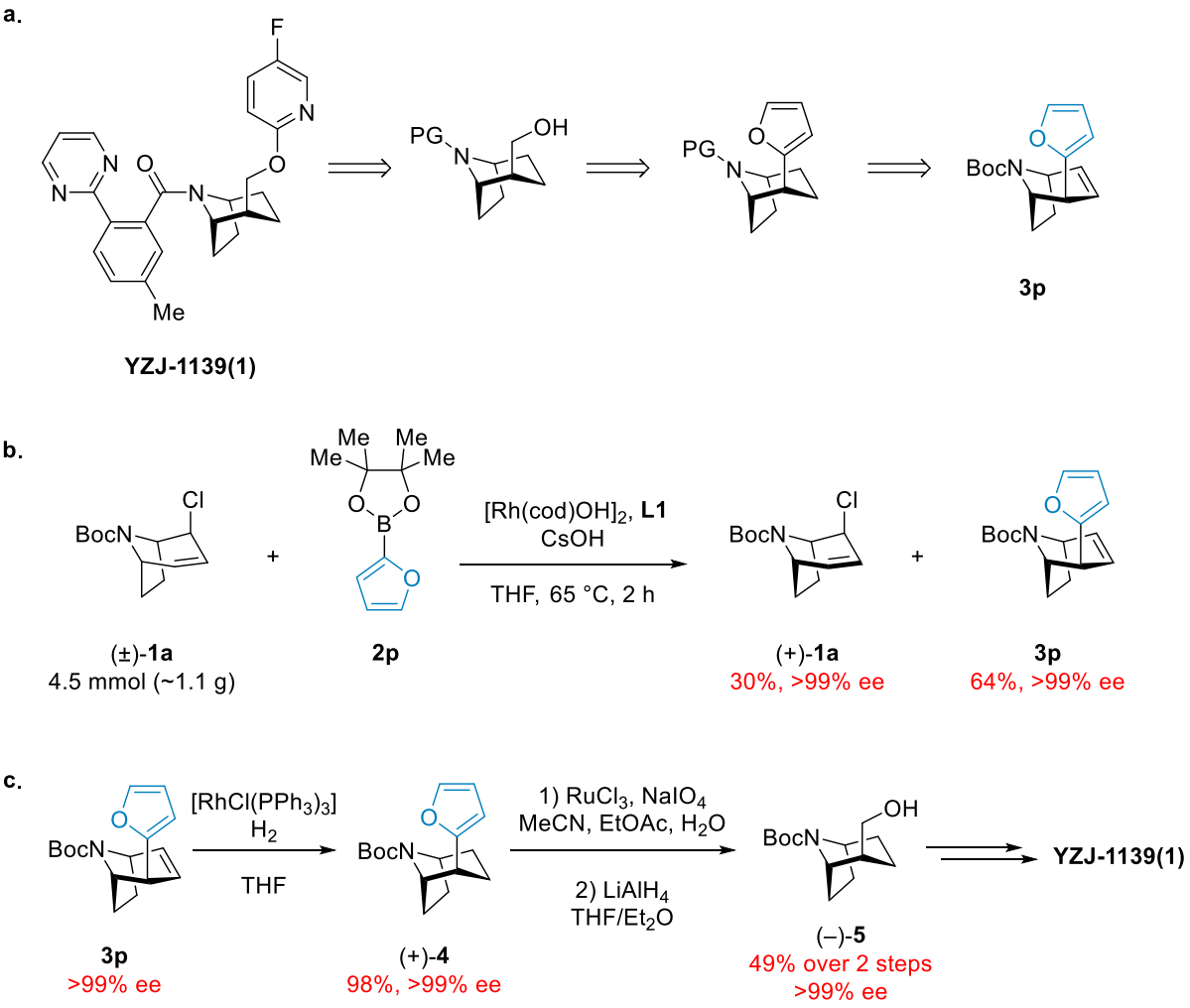
To demonstrate the synthetic utility of this method, we explored potential synthetic applications of the cross-coupling products from the reaction. Due to the presence of the C=C double bond and the furan ring on product **3p** being a carbonyl group equivalent, we explored various reaction conditions to convert the product into ferruginine (Scheme 2.3.11). However, initial attempts for transformation to ferruginine including the isomerisation of the C=C double bond were unsuccessful. Heating up to over 100 °C only induced partial substrate decomposition, while metal catalysis was also ineffective. Therefore, further potential synthetic applications were proposed.



Scheme 2.3.11 Proposed product transformation from **3p** to ferruginine.

A novel orexin receptor antagonist, YZJ-1139(1) came to our attention. This molecule had passed the Phase II clinical trials and proven to be effective for insomnia treatment. [175] To the best of our knowledge, the synthesis of YZJ-1139(1) was only previously reported by a process chemistry group, and in their approach, preparative HPLC separation of the enantiomers or a chiral auxiliary approach were used. [176] We envisioned applying our Rh-catalysed Suzuki-Miyaura cross-coupling approach for the precursor synthesis of YZJ-1139(1) would provide a modular route towards the target drug and derivatives.

Retrosynthesis was performed from target (Scheme 2.3.12a), showing that the deprotection and re-protection on nitrogen together with removal of pyridine substitution on oxygen could afford the alcohol, which is the synthetic precursor of YZJ-1139(1). The alcohol could be synthesised by the reduction of carboxylic acid, which could be obtained by oxidative cleavage of the furan ring on the intermediate. Finally, this intermediate could be synthesised by the reduction of the C=C double bond from cross-coupling product **3p**.



Scheme 2.3.12 **a**. Retrosynthetic analysis of YZJ-1139(1). **b**. Scale-up of reaction. **c**. Transformation of cross-coupling product **3p**.

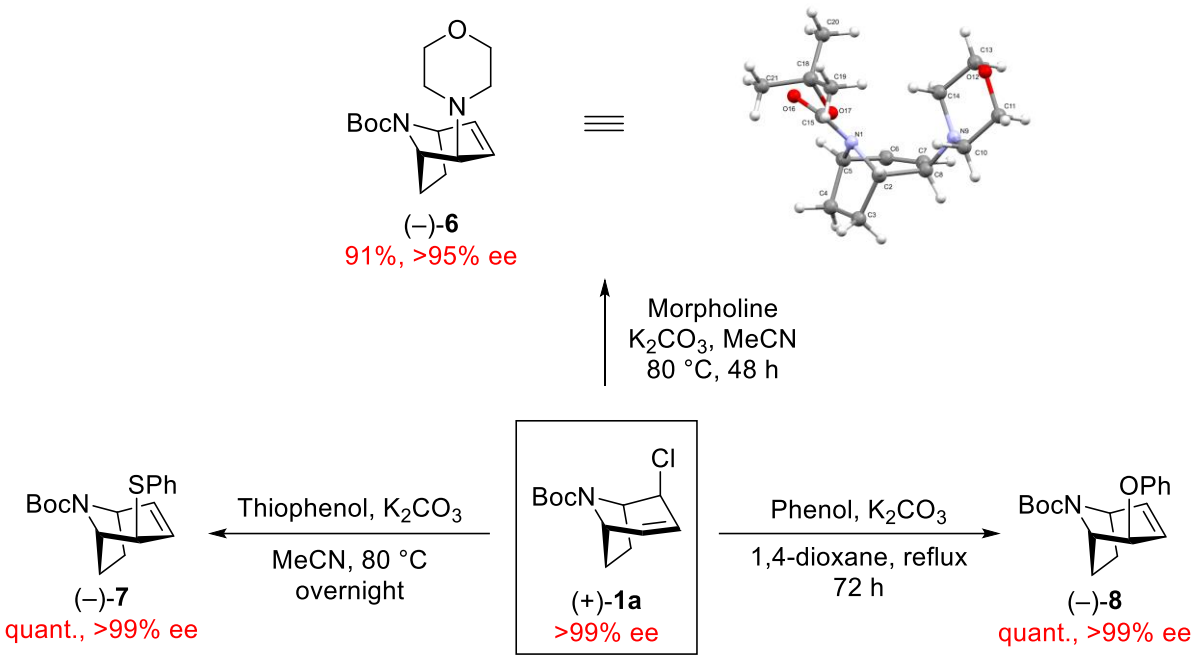
To effectively test the proposed route of transformation, we firstly performed the scale-up of the cross-coupling reaction. In a gram scale reaction between (±)-**1a** and 2-furanylboronic pinacol ester **2p** we observed a rise in both yield and enantioselectivity, where we isolated cross coupling product **3p** in 64% isolated yield and >99% ee (Scheme 2.3.12b). Our postulation was that the difference in the shape of furan ring induced the increased character of DyKAT in the

reaction pathway. The enantioenriched allyl chloride (+)-**1a** was isolated in 30% yield and >99% ee.

After successful attempts to scale up the cross-coupling reaction, we started testing the proposed synthetic route. Reduction of **3p** with Wilkinson's catalyst gave (+)-**4** in 98% yield and >99% ee. The furyl group was then converted into a hydroxymethyl group *via* a two-step oxidative cleavage / reduction protocol to give (–)-**5** in 49% yield, a previously reported intermediate in the synthesis of YZJ-1139(1) (Scheme 2.3.12c). Perfect enantioretention was observed throughout the three-step reaction.

Being a kinetic resolution process, synthetic access to enantiopure allyl chloride (+)-**1a** provided the opportunity to use **1a** as a building block for stereospecific reactions. Previously, our group reported a Cu-catalysed kinetic resolution reaction of a piperidine-derived allyl chloride, and the enantioenriched allyl chloride was used in enantiospecific substitution reactions with heteroatom-based nucleophiles. [177] We wondered if related substitutions with (+)-**1a** were possible. Several different substitution reactions were tested on (+)-**1a**.

The substitution with morpholine, thiophenol, and phenol gave (−)-**6**, (−)-**7**, and (−)-**8** in excellent yield and enantiospecificity (Scheme 2.3.13) respectively. Other enantiospecific substitution reactions with this substrate are likely possible. The absolute stereochemistry of (−)-**6** was determined by single-crystal X-ray diffraction, and this, combined with the knowledge of the absolute configuration of the starting material, indicates that the substitution reaction proceeds *via* a *syn*-S_N2' pathway (Scheme 2.3.13). The relative and absolute stereochemistry of (−)-**7** and (−)-**8** was assigned in analogy to (−)-**6**.



Scheme 2.3.13 Transformation of resolved allyl chloride (+)-**1a**.

2.4 Conclusion and Future Work

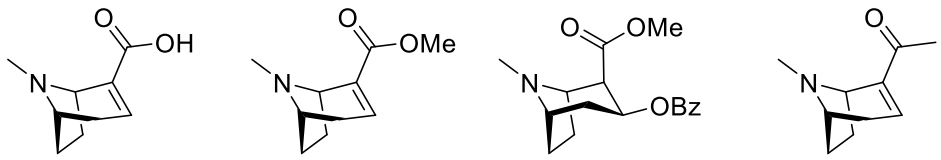
We have developed a highly enantio- and diastereoselective Rh-catalysed asymmetric Suzuki–Miyaura-type cross-coupling reactions between a racemic *N*-Boc-nortropane-derived allylic chloride and (hetero)aryl boronic esters. The reaction proceeds *via* an unexpected kinetic resolution, and the resolved enantiopure allyl chloride can undergo highly enantiospecific reactions with N-, O-, and S-containing nucleophiles. The method was applied in a highly stereoselective formal synthesis of YZJ-1139(1), a potential insomnia treatment that recently completed Phase II clinical trials. Our work represents a new asymmetric catalytic method for the synthesis of YZJ-1139(1) and related compounds.

Further investigations could be categorised in several different aspects. Firstly, we could explore further transformation reactions of the product to useful tropane derivatives. Potential targets from **3p** include ecogoniline, methylecgonidine, cocaine, and ferruginine (Scheme 2.4.1a). These molecules are structurally similar and could be accessed by first isomerising the C=C double bond, followed by oxidative cleavage of the ring, subsequently nucleophilic attack on the C=O with suitable Grignard or organolithium reagents, then final deprotection of the *N*-Boc protecting group and methylation on the nitrogen atom, potentially with further addition

onto the double bond to give the final products.

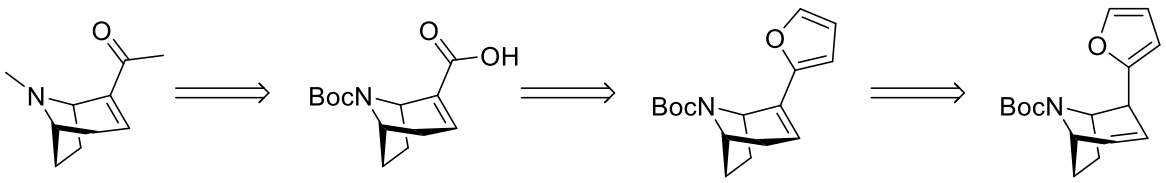
Previously we attempted transformation from **3p** towards ferruginine, the retrosynthetic analysis was done similarly as in Scheme 2.4.1b. We tested the isomerisation of the C=C double bond on **3p** by heating and transition metal catalysis, but no reactivity was observed towards isomerised product. As previously our attempts to synthesise ferruginine by transformation from cross-coupling product were unsuccessful, other potential methods of isomerisation could be investigated in the future. If the route is proven to be successful, we would be able to synthesise furruginine and other structurally similar tropane derivatives by simple substitution/addition reactions, as listed in Scheme 2.4.1a.

a.



Ecgonidine Methylecgonidine (*R*)-cocaine Ferruginine

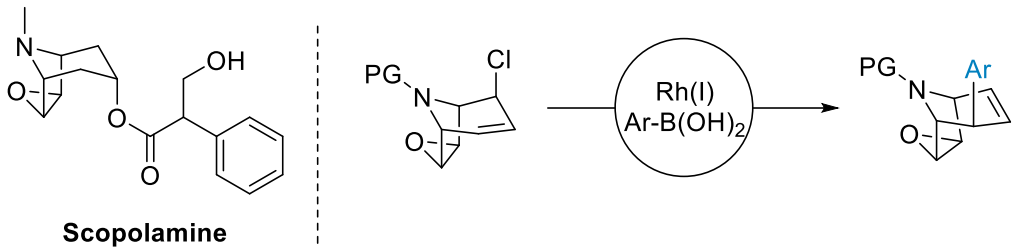
b.



Ferruginine **3p**

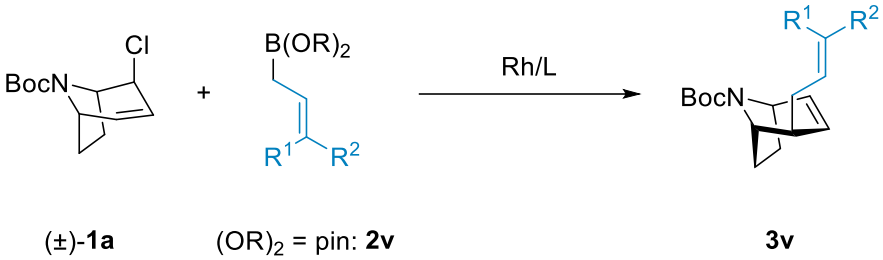
Scheme 2.4.1 Potential product transformation of **3p**. **a**. Possible target molecules for transformation. **b**. Proposed retrosynthetic pathway from **3p**.

Secondly, utilisation of other tropane-derivatised substrates could be tested. Potentially modifications could be made on the protecting group, as well as on the tropane backbone, including substitutions on C^6 and C^7 position in the back forming scopolamine-like products as shown in Scheme 2.4.2.



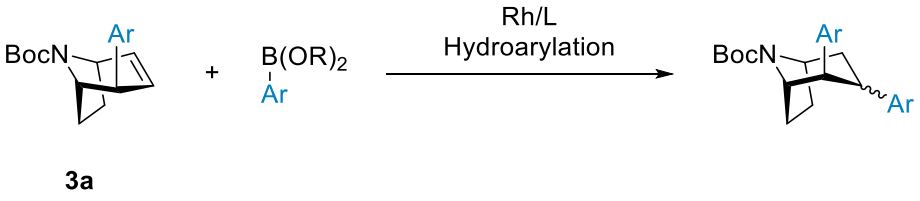
Scheme 2.4.2 Rh-catalysed cross-coupling reaction towards scopolamine derivatives.

Thirdly, as in this project, only aryl- and heteroaryl boronic species were tested as the coupling partner, we could test if non-aromatic coupling partners like vinyl and allyl boronic species could be used to achieve higher three-dimensionality as well as possibility of further product transformations (Scheme 2.4.3).



Scheme 2.4.3 Rh-catalysed cross-coupling reaction with vinyl boronic pinacol ester.

In addition, direct arylation could be attempt using the coupling product from the reaction towards the synthesis of tropane derivatives with higher structural complexity, as shown in Scheme 2.4.4.



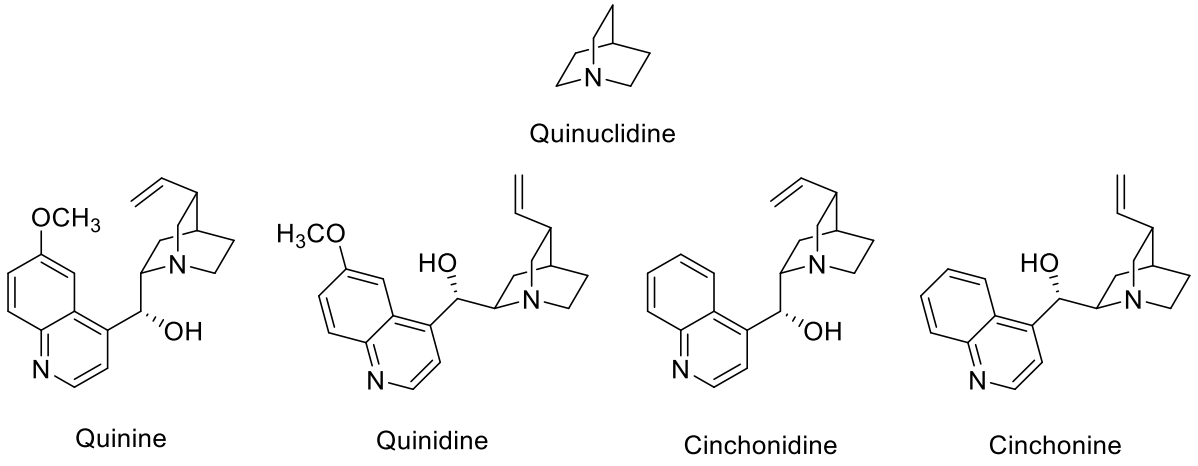
Scheme 2.4.4 Rh-catalysed arylation on **3a**.

Chapter 3: Synthesis of Quinuclidines *via* Rh-Catalysed Asymmetric Arylation

3.1 Project Background

Quinuclidine is a type of saturated bridged nitrogen-containing bicycle which is characterised by the l-azabicyclo[2.2.2]octane core. This results in high symmetry, low bond strain, structural rigidity, and high stability of quinuclidine. [178-179] In addition, in quinuclidine, the nitrogen atom is at the bridgehead position, restricting the conformational changes and the free rotations of the bonds in the ring. The sp^3 hybridised lone pair on nitrogen atom in quinuclidine is less sterically hindered in comparison to other tertiary amines and *N*-substituted pyridines. Therefore, quinuclidine is similar to some tertiary amines with high basicity and nucleophilicity with the pKa value of 11.0 for its conjugate acid. [180-181] However, the relatively free sp^3 hybridised lone pair differentiates quinuclidine to other tertiary amines in the way that even with low molecular weight of 111.19 $g \cdot mol^{-1}$, quinuclidine exists as a volatile crystalline solid susceptible to sublimation, but with a melting point surprisingly high at 158 °C. [182]

Quinuclidine derivatives display a wide range of pharmacological and biological activities. [183-185] Examples of quinuclidine derivatives include quinine and quinidine, cinchonidine and cinchonine, each pair are diastereomers of each other but often referred to as pseudo-enantiomers (Scheme 3.1.1). These derivatives all belong to the cinchona alkaloid family, which are characterised by three main units: the quinuclidine backbone with a vinyl substituent, the quinoline ring, and the hydroxyl group. [184]



Scheme 3.1.1 Quinuclidine and its well-recognised derivatives.

The use of quinine can be dated back at least 400 years ago, [186] where it was firstly used as cinchona tree bark extracts to treat malaria. This identified the first antimalarial treatment and quinine remained the sole remedy for malaria for centuries. [187] While around 40% of the quinine produced goes into pharmaceuticals, the other 60% of quinine is used in the food industry, constituting the flavour component responsible for the bitter taste in tonic water. [188] Quinidine is an antiarrhythmic agent often used to treat heart rhythm disturbances. [189]

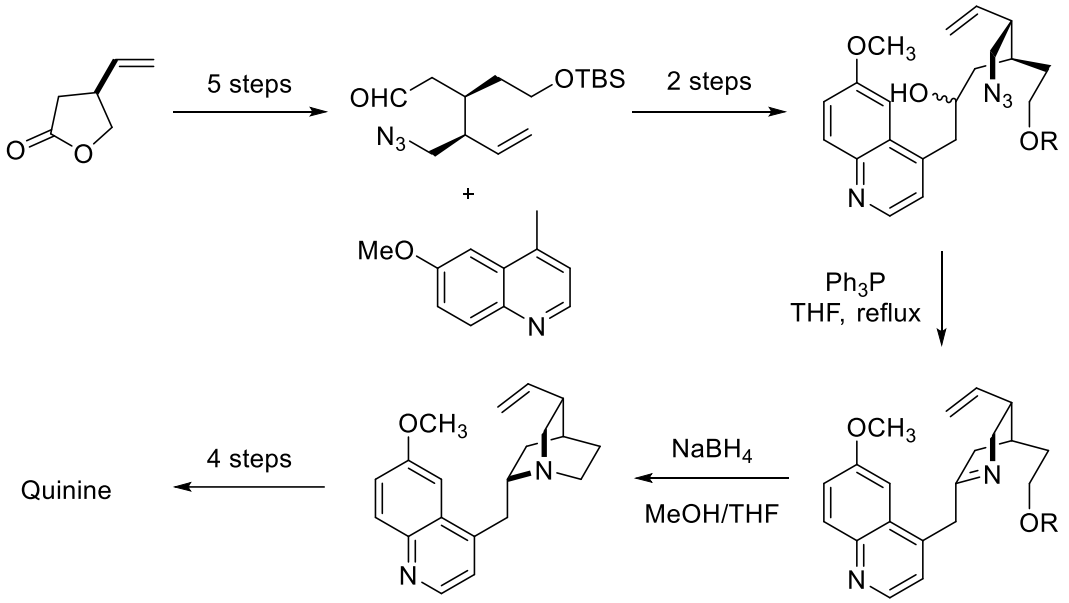
In addition, numerous chiral cinchona alkaloid derivatives are extensively used as chiral catalysts and ligands for asymmetric and photoredox catalysis. [190-191] A representative example of asymmetric reactions using quinuclidine as catalyst is the Sharpless asymmetric dihydroxylation, where use of pseudo-enantiomeric ligands from cinchona alkaloids gave opposite stereochemical induction. [192-195]

Up till now, quinine production still relied heavily on extraction from cinchona trees due to economical practicality. [196] Because of the high demand of quinine in various fields from pharmaceutical to asymmetric catalysis dating back centuries ago, extensive work has been done to explore synthetic routes towards quinine.

Historically, the first isolation of quinine from natural sources was done in 1820 by Pelletier and Caventou, [197] which paved the way for following successful isolation of other derivatives from the cinchona family: isolation of quinuclidine by Delondre and Henry in 1833, [198-199] cinchonidine isolation by Winckler in 1851, [188] and isolation of numerous other quinuclidine derivatives by 1884. [200-201] The correct molecular formula of quinine was proposed in 1854 by Strecker, [202] and the molecular connectivity was later established by Paul Rabe in 1907, [203] laying foundations for quinine synthesis.

Later in 1918, Paul Rabe and Karl Kindler proposed the first synthesis towards quinine from quinotoxine, which was later experimentally verified by Smith and coworkers in 2008, marking the first major step towards quinine synthesis. [204-206] In 1944, the first quinine total synthesis was reported by Woodward and Doering, synthesising the precursor homomeroquinene from 7-hydroxyisoquinoline. The reaction was not stereoselective and product was isolated as a mixture of *cis* and *trans* stereoisomers in roughly 1:1 ratio. [207-208] Numerous works have been done since, but were only able to establish up to three out of four stereogenic centres in the quinine target. [196] The first completely stereoselective synthesis of quinine was only reported

by Stork in 2001 (Scheme 3.1.2). [209]



Scheme 3.1.2 First stereoselective quinine synthesis by Stork *et. al*.

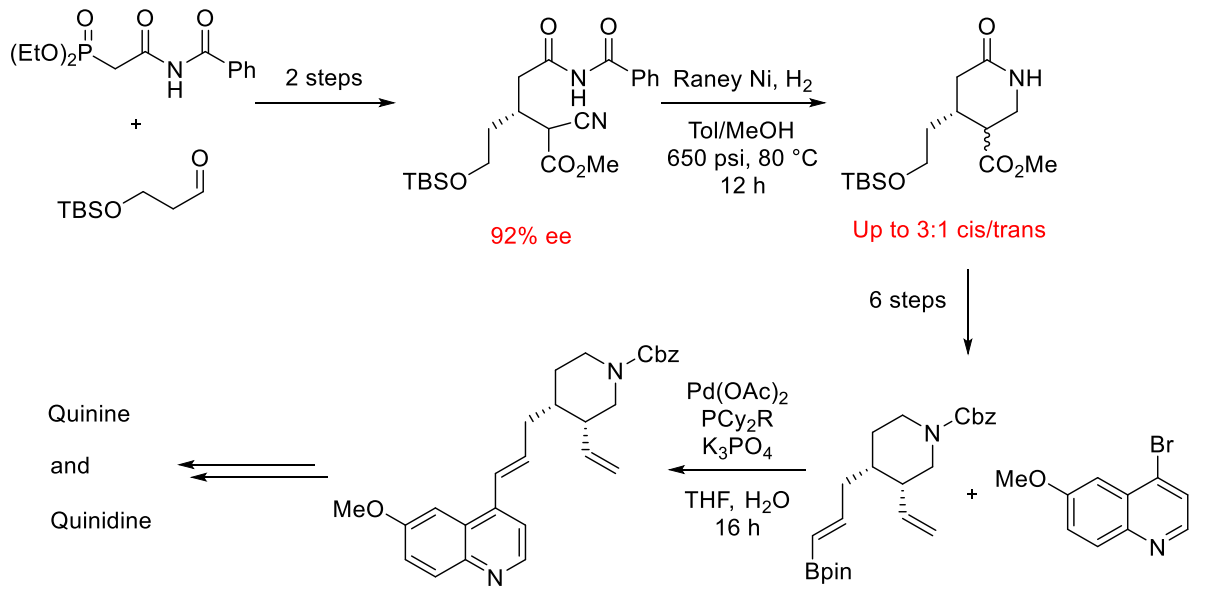
The century-long effort in synthesis of quinine from Rabe and Kindler's first synthesis of quinine to the first stereoselective synthesis of quinine by the Stork group implied the synthetic difficulty towards chiral quinine derivatives. With five stereogenic centres in the molecule, the stereocontrol of the reaction is vital to achieve the correct isomer. Consequently, stereoselective reactions towards quinine and its derivatives has attracted tremendous attention of synthetic organic chemists.

Stereoselective synthesis methods for cinchona alkaloids are similar to those for tropane synthesis, involving the use of chiral auxiliary, synthesis from the chiral pool, and catalytic methods. [183] Two categories could be summarised, where the first represents all reactions building up the chirality during quinuclidine ring synthesis by cyclisation or condensation; another method builds the chirality on the substituents on the quinuclidine ring, which are usually pre-installed before ring-closure. [178] Examples of these two methods will be introduced below.

3.1.1 Synthesis of Enantioenriched Quinuclidine Rings by Cyclisation

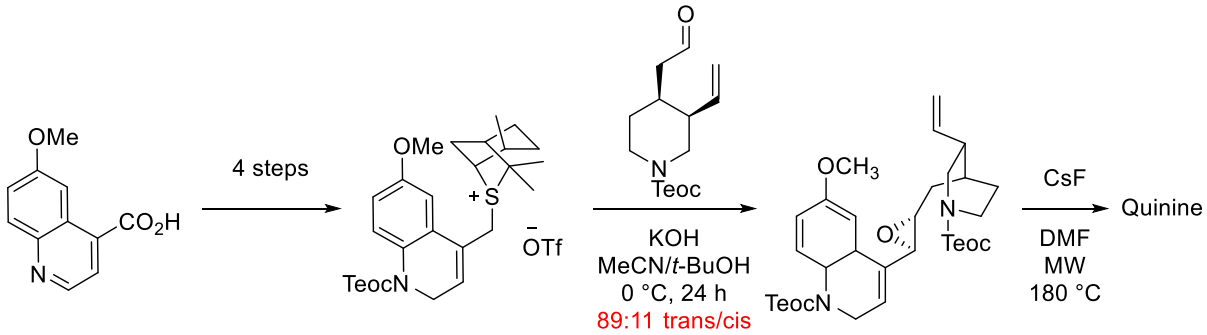
One of the well-known examples of stereoselective synthesis of quinuclidine derivatives is reported by Jacobsen and co-workers on the first catalytic asymmetric synthesis of quinine and quinidine (Scheme 3.1.3). [210]

This route started with a *trans*-Wittig olefination between phosphonate imide and an aldehyde, followed by asymmetric Michael addition, which was assisted by the next step of Raney Ni-mediated hydrogenation for cyclisation to form the lactam. Subsequently, LAH reduction, Wittig olefination, nitrogen protection, and Takai olefination of the aldehyde were performed to give the boronic pinacol ester. The Bpin ester then reacts with the quinoline derivative *via* a Suzuki-Miyaura cross-coupling reaction. The product then undergoes asymmetric epoxidation followed by stereoselective ring opening to form the C^8–N bond on quinuclidine ring. Stereoselective steps include the first Wittig olefination, where >50:1 *E*/*Z* ratio could be achieved; and the following asymmetric Michael addition and lactam cyclisation were also stereoselective with 92% ee and up to 3:1 d.r. achieved respectively; the final epoxidation and ring opening were also stereoselective to obtain final product of quinine and quinidine.



Scheme 3.1.3 Jacobsen's catalytic asymmetric synthesis of quinine and quinidine.

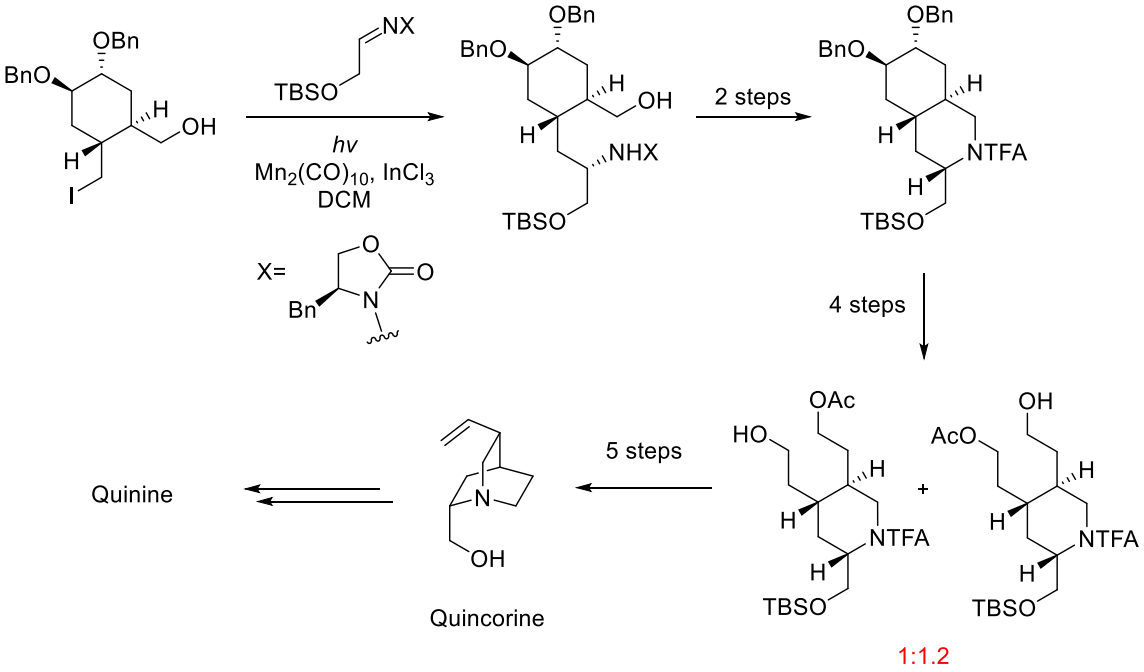
In 2010, Aggarwal and coworkers reported a convergent and stereoselective synthesis towards quinine and other cinchona alkaloids *via* chiral sulfur ylide epoxidation (Scheme 3.1.4). [211-212]



Scheme 3.1.4 Aggarwal's stereoseletive synthesis of quinine and quinidine.

The epoxidation was reasonably stereoselective with *trans/cis* ratio at 89:11, and synthesis of quinidine was also performed with sulfur ylide of the opposite stereochemistry being used.

Another interesting example was reported by Friestad *et. al*., using Mn-mediated radical addition towards the synthesis of quincorine and then formal synthesis of quinine with the aid of chiral auxiliary (Scheme 3.1.5). [213-214] The chiral auxiliary assisted the imine addition with high stereocontrol, which proceeded smoothly by auxiliary cleavage followed by annulation. Later in the reaction sequence, a regioisomeric mixture was obtained in 1:1.2 ratio, and a regio-convergent approach was adopted to convert both isomers to the TBS protected quincorine, which was later converted to quincorine and then quinine.



Scheme 3.1.5 Friestad's stereoselective synthesis of quinine.

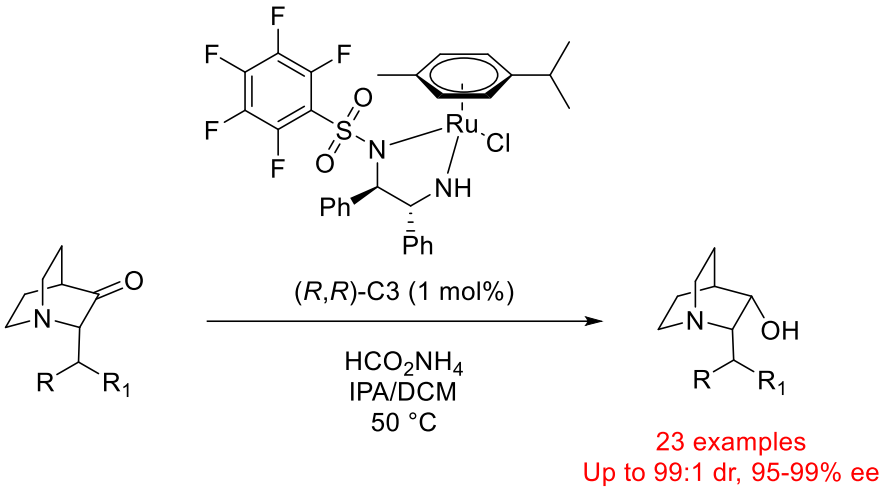
Apart from the reactions shown above, other stereoselective synthesis of quinine and derivatives were also reported, including Kobayashi's quinine synthesis from a chiral cyclic monoacetate, [215-216] Hatkeyama's organocatalytic synthesis of quinine and quinidine from benzylamine, [217] Webber and Krische's quinine synthesis *via* catalytic enone cycloallylation. [218] In these methods where the synthesis of chiral quinuclidine derivatives were performed by selective cyclisation to establish the ring, either chiral auxiliaries or chiral catalysts were used to assist the stereocontrol. In other cases, because of the existence of multiple stereocentres, it is generally more difficult to have complete stereocontrol over all chiral centres, as shown by Jacobsen's work where only up to 3:1 *cis*/*trans* ratio was achieved during the cyclisation step (Scheme 3.1.3). [192]

Therefore in the next section, we look at the other method for stereoselective synthesis of quinuclidine derivatives, where the quinuclidine scaffold is usually pre-established, and the chirality is built by modifications on substituents of quinuclidine ring.

3.1.2 Synthesis of Enantioenriched Quinuclidine Rings by Modifications on Ring Substituents

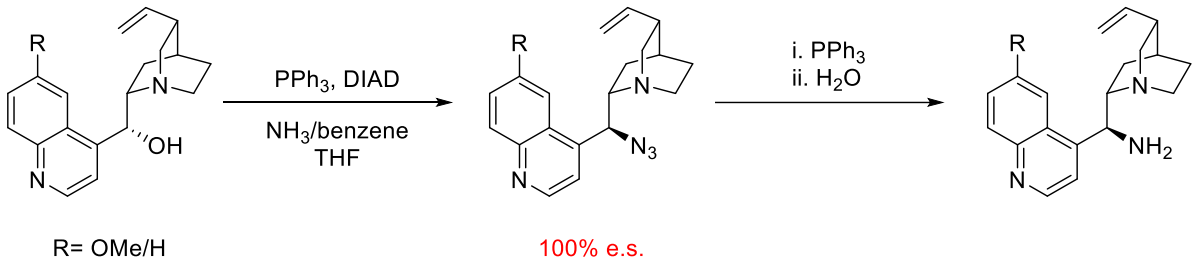
Another approach towards the synthesis of chiral quinuclidine derivatives is by controlling the stereochemistry on the substituents on the quinuclidine ring. With the fully saturated structure of quinuclidines, direct substitution onto the ring is extremely difficult, hence functional groups are usually present on the ring before ring-closure.

Among these groups, carboxyl and carbonyl derivatives, including quinuclidine-2-carboxylic acid, and quinuclidin-3-one, have been useful precursors, and an enantioselective synthesis of *cis*-3-quinuclidinols was reported by Wang by Ru-catalyzed asymmetric transfer hydrogenation *via* DKR (Scheme 3.1.6). [219] Ammonium formate was used in the reaction as the hydrogen donor, achieving up to 99% yields with excellent stereoselectivity of up to 99:1 d.r. and 95-99% ee.



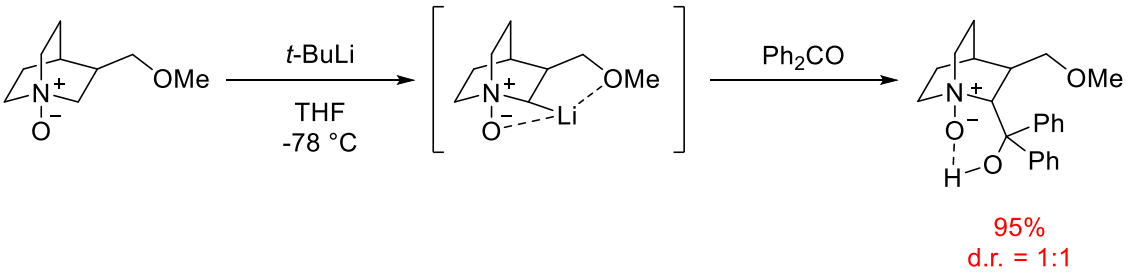
Scheme 3.1.6 Stereoselective synthesis of *cis*-3-quinuclidinols by Wang and coworkers.

Apart from modifying the carbonyl and carboxyl groups on the quinuclidine ring, variations could also be made on substituent groups on chiral quinuclidine derivatives from the chiral pool. An example was reported by Brunner and coworkers in 1995 which performed a Mitsunobu reaction on cinchonine and quinine to synthesise 9-amino(9-deoxy)cinchona alkaloids *via* an azide intermediate (Scheme 3.1.7). [220] The reaction proceeded through a Mitsunobu reaction resulting in complete inversion of stereochemistry at C^9, giving the corresponding azide and product with opposite stereochemistry at C^9 to the starting molecule.



Scheme 3.1.7 Stereoselective synthesis of 9-amino(9-deoxy)cinchona alkaloids by Brunner and coworkers.

Even though functionalisation on quinuclidine ring remained scarce, the O'Neil group reported a directed lithiation of the quinuclidine *N*-oxide to access 2,3-difunctionalised quinuclidine derivatives (Scheme 3.1.8). [221] Quinuclidine *N*-oxide was treated with *t*-BuLi to give the 2-lithio equivalent, which was then trapped with different aromatic aldehydes. This methodology could also be extended to the quinuclidine enamine *N*-oxide and nitrogen-borane complex, allowing further transformation towards chiral quinuclidine derivatives. [222]



Scheme 3.1.8 Synthesis of 2,3-difunctionalised quinuclidines from *N*-oxide by O'Neil group.

These methods listed above are some examples for synthesis of chiral quinuclidine molecules by modifications on the substituents of the ring. The scope for available substrates for these methods remain relatively limited, hence there has been rising demand on new asymmetric methodologies directly from quinuclidine substrates.

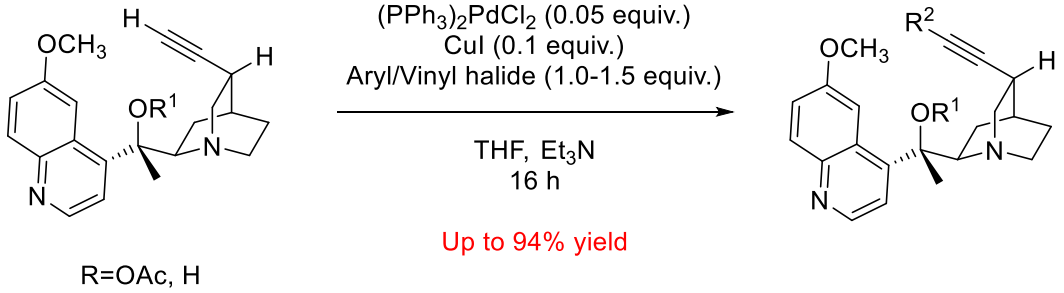
3.2 Project Aims

Like tropane, quinuclidine is a type of bridged nitrogen-containing bicyclic molecule. Quinuclidine derivatives have been commonly applied in the pharmaceutical industry and asymmetric catalysis. With four chiral carbon centres in quinine, 16 possible stereoisomers exist. Hence the stereoselective synthesis of quinine often required long steps and careful stereocontrol, with relatively low yields obtained. Therefore, efforts have been made to explore asymmetric reactions towards chiral quinuclidine derivatives.

Enantioenriched quinuclidine derivatives were often found more frequently as chiral catalysts in asymmetric cross-coupling reactions than as substrates, and previously reported cross-coupling reactions on quinuclidine type substrates were mostly not asymmetric proceeded without affecting any pre-existing stereocentres in the molecule. [184, 223-224]

For example, Jacobsen's work on catalytic asymmetric synthesis of quinine and quinidine described in Chapter 3.1.1 involved one step of Suzuki-Miyaura cross-coupling reactions, however, the stereochemistry was established by previous asymmetric step, and the cross-coupling reaction preserves the stereochemistry (Scheme 3.1.3). [210]

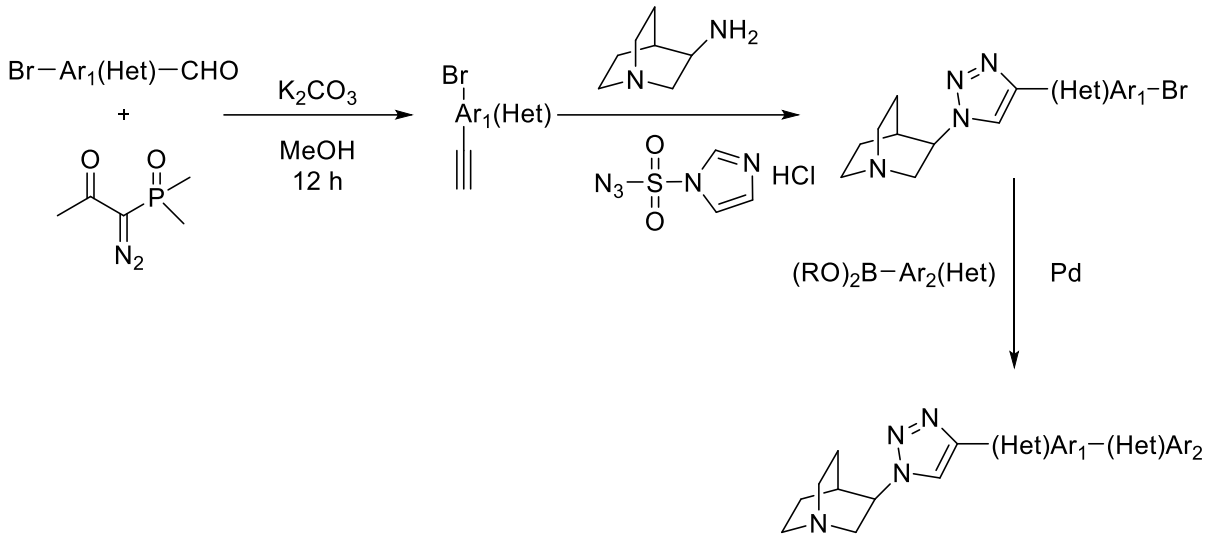
In Hoffmann and coworkers' work, they used Sonogashira cross-coupling on quinuclidine derivatives (Scheme 3.2.1), where the bond formation is at the end of alkyne group at the top, with all existing stereocentres remained intact. [225]



Scheme 3.2.1 Hoffmann's work on Sonogashira cross-coupling of chiral quinuclidine.

Another example was reported by Chalon, Routier, *et. al*., where synthesis of bis(het)aryl-1,2,3-triazole quinuclidine α7R ligands was done *via* a three-step sequence including a Suzuki-Miyaura cross coupling reaction (Scheme 3.2.2). Both the halide and the boron species were

specifically synthesised, and the synthesis of the aryl halide was from a chiral quinuclidine derivatised substrate. [226]



Scheme 3.2.2 Chalon and Routier's work on Suzuki-Miyaura cross-coupling of chiral quinuclidine.

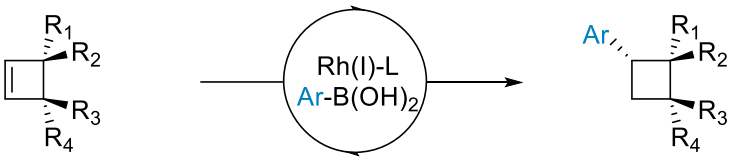
All reactions reported above focused on non-asymmetric cross-coupling reactions on chiral substrates with existing stereochemistry, and the bond formation only occur on substituents of the enantioenriched substrate and does not interfere with the pre-existing stereochemistry. Therefore, we wondered if we could develop catalytic asymmetric reactions from racemic or prochiral quinuclidine molecules towards chiral quinuclidines *via* stereoselective bond formation directly on the quinuclidine ring.

In Chapter 2, we have reported a highly stereoselective Rh-catalysed Suzuki-Miyaura cross-coupling type reactions between aryl- and heteroaryl-boronic pinacol esters with nortropane-derivatised allylic chloride. Consequently, we would like to expand the application of this methodology to quinuclidine, as it is also a bridged nitrogen-containing bicyclic moiety like tropane.

Because of its [2,2,2] bicyclic ring structure, we are unable to synthesise an allyl halide from quinuclidine according to Bredt's rule. [227-228] As our group has successfully performed Rh-catalysed arylation on cyclobutenes (Scheme 3.2.3a), [229] we proposed that dehydroquinuclidine could be a suitable substrate for investigation (Scheme 3.2.3b).

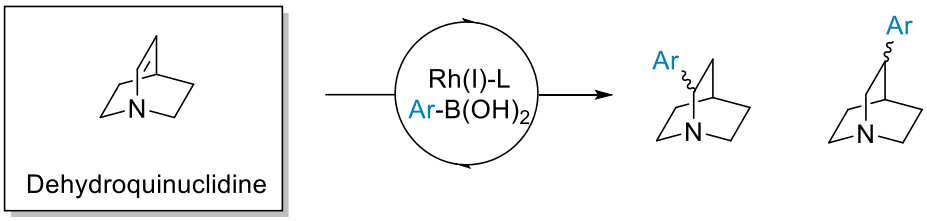
This project aims to apply the existing set of Rh-catalysed arylation conditions upon dehydroquinuclidine (Scheme 3.2.3b). Because the bridged bicyclic molecule is strained with the presence of a C=C double bond, our postulation is that the arylation reaction would be favoured with release of the ring strain by $C(sp^3)$–$C(sp^2)$ bond formation.

a.



Rh-catalysed
Asymmetric Arylation Reaction

b.



Rh-catalysed
Asymmetric Arylation Reaction

.

Scheme 3.2.3 Rh-catalysed asymmetric arylation reactions **a**. Asymmetric arylation on cyclobutene. **b**. Proposed asymmetric arylation on dehydroquinuclidine.

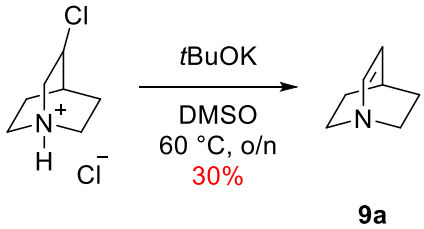
Firstly, we investigated different routes for the synthesis of proposed substrate, dehydroquinuclidine. Then, we attempted different reaction conditions on the substrate, exploring its reactivity towards this Rh-catalysed arylation reaction. We finally came to other dehydroquinuclidine-derivatised substrates, where we synthesised substrates with various substitutions on the nitrogen atom and investigated their different reactivities and stereoselectivities in the Rh-catalysed arylation reactions.

3.3 Results and Discussion

3.3.1 Substrate Synthesis

With the proposed dehydroquinuclidine substrate in mind, we started the target substrate synthesis. However, the existing methods of synthesis were either not reported with detailed procedure or not practically safe. [230-232] Therefore, we proposed several different synthetic routes, where elimination from substrates with different leaving groups at C3 positions could be performed.

We firstly performed the elimination reaction with commercially available 3-chloroquinuclidine hydrochloride salt and potassium *tert*-butoxide in DMSO (Scheme 3.3.1). [231-232] The reaction proceeded smoothly upon 60 °C heating overnight and the starting material was fully consumed.



9a

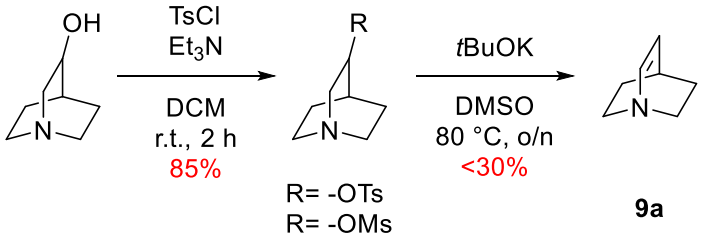
Scheme 3.3.1 Synthesis of **9a** from 3-chloroquinuclidine hydrochloride.

However, as the detailed procedure for purification could not be found in literature, we attempted a few methods to purify the product. Unfortunately, the initial attempt to purify the product *via* column chromatography failed to afford any product. Next, we tried Kugelrohr distillation which afforded only DMSO as the distillate. As **9a** has very similar molecular weight to quinuclidine, we realised that **9a** is highly volatile and potentially subject to sublimation. Consequently, we tried distillation under reduced pressure, and isolated the product successfully.

A common problem observed in purification was the presence of residual DMSO, hence extensive washing of the crude mixture was required during work-up. However, the high polarity of the product indicated aqueous wash should be avoided when possible. After several attempts of different work-up procedures, we found that aqueous wash with brine and sat. aq.

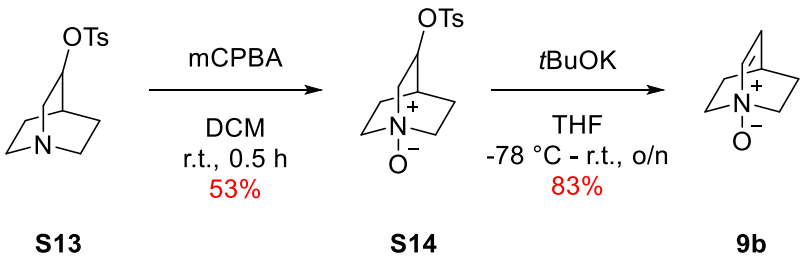
$NaHCO_3$ solution resulted in drastically decreased yield due to higher solubility of product in the aqueous phase. Finally, we found that washing >10 times with 1 M NaOH could efficiently remove excess DMSO without significant loss in yield of the product.

Later in the project, 3-chloroquinuclidine hydrochloride was discontinued by Sigma Aldrich, hence we went on to explore other synthesis routes of dehydroquinuclidine (Scheme 3.3.2). To form the C=C bond, elimination from other substrates were investigated, and we synthesised the substrate with a tosylate leaving group (**S13**) from 3-quinuclidol. Nevertheless, we experienced incomplete conversion in the elimination step. By heating the elimination reaction overnight at over 80 °C, only partial conversion was observed. We also tested the elimination of the corresponding mesylate substrate but achieved lower conversion. As full consumption of the starting material is desired due to the difficulty in purification of **9a**, further investigations of elimination on other substrates were not continued.



Scheme 3.3.2 Synthesis of **9a** from other substrates.

Later after screening on dehydroquinuclidine, we attempted synthesis of substrates with substitution on the nitrogen atom. Therefore, the *N*-oxide, the nitrogen-borane complex, and the HCl salt were synthesised.

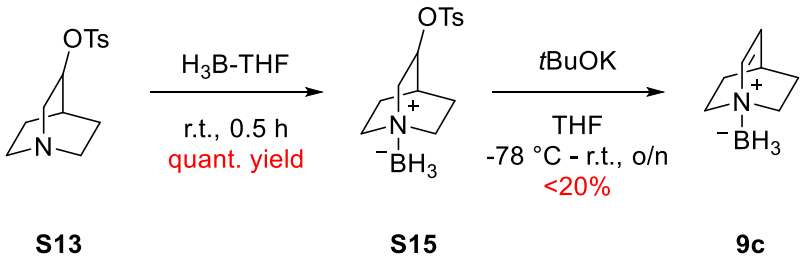


Scheme 3.3.3 Synthesis of **9b** from **S13**.

The *N*-oxide substrate **9b** was synthesised from tosylate **S13**. Oxidation of nitrogen was completed by the addition of *m*CPBA (Scheme 3.3.3). However, by addition of commercially

available ≤ 77% purity *m*CPBA, zero conversion was observed in the reaction even upon heating. By consulting the O'Neil group on their detailed experimental procedure, we realised that the purity of *m*CPBA was vital for the progression of oxidation. [222] Consequently, commercially available ≤ 77% purity *m*CPBA was purified by recrystallisation. The purified *m*CPBA successfully afforded the *N*-oxide **9b** in 30 min.

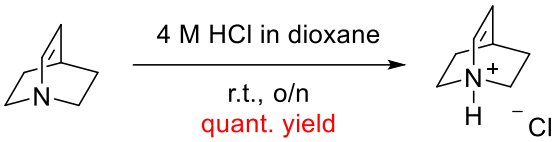
It was worth noticing that *N*-oxide product **9b** is highly polar, hence washing with any aqueous solution was avoided to prevent loss of product from work up, and the crude mixture was directly loaded onto a column for purification by silica gel chromatography. The side product in this reaction was washed out first with 60% EtOAc in hexane, while the product was eluted using 80% EtOAc and obtained as a white solid.



Scheme 3.3.4 Synthesis of **9c** from **S13**.

Likewise, the first step of synthesis of the nitrogen-borane complex involved addition of H_3B-THF solution to the tosylate **S13** (Scheme 3.3.4). [222] After several unsuccessful attempts with old H_3B-THF solution, it was noted that the freshness and purity for the H_3B-THF was also highly crucial for the reaction. The next step involved elimination of the tosylate group using potassium *tert*-butoxide to afford **9c**. Unlike the *N*-oxide substrates, the nitrogen-borane complex **S15** and **9c** were observed to decompose on silica, hence column chromatography was not used for purification.

The HCl salt **9d** could be synthesised easily by the addition of 4 M HCl in dioxane to **9a** and concentration and drying of the solvent (Scheme 3.3.5). In this route, **9a** was synthesised using the route shown in Scheme 3.3.1, and **9d** was subsequently synthesised using **9a**.



9a **9d**

Scheme 3.3.5 Synthesis of **9d** from **9a**.

3.3.2 Rh-Catalysed Arylation Reaction

After having successfully synthesised the substrates, we started testing the Rh-catalysed arylation reaction on **9a**. The reaction conditions we used were previously reported in the catalytic asymmetric cross-coupling reaction towards chiral cyclobutanes by Goetzke *et. al*., describe in detail below as 'General Procedure A' shown in Table 3.3.1. [229]

However, after stirring overnight at room temperature, no conversion was observed (Table 3.3.1, Entry 1). Elevated temperature (80 °C, overnight) also led to no product formation being observed (Table 3.3.1, Entry 2).

Next, because the presence of base was crucial in previous Rh-catalysed cross-coupling reactions reported by the group, [71, 118, 122, 229, 233-235] we tried the same reaction with the addition of 1 equiv. of CsOH as base. This time, trace product **10a** was observed in the NMR spectrum (Table 3.3.1, Entry 3). Purification was performed by column chromatography, but due to loss of mass from the minute quantity of **10a** and its high polarity, it could not be separated from other impurities.

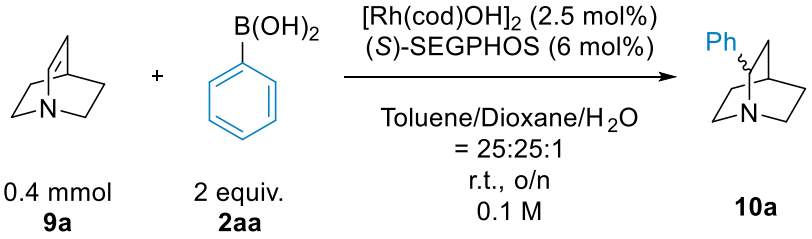
Next, the enantiomeric excess of the reaction was determined. The sample was run firstly on SFC, but the analytical columns on the SFC were unable to separate the two enantiomers of **10a**. Nevertheless, chiral HPLC columns separated the enantiomers and showed that around 93% ee was obtained. According to the relatively downfield chemical shift of the hydrogen atom connected to carbon at arylation position, we assume the regioselectivity of the reaction is shown as **10a** in Table 3.3.1, where the arylation occurs on the more electrophilic carbon.

To attempt to optimise the reaction yield, different reaction conditions were tested. To begin with, we tried increasing the reaction concentration from 0.1 M to 0.4 M, and no significant rise in yield was observed (Table 3.3.1, Entry 4). Meanwhile, a drop in ee was observed from 93% to 80%. We then tested the reaction at 100 °C, and again afforded trace product but with substantially reduced ee (58% ee, Table 3.3.1, Entry 5).

Next, we investigated whether the presence of water in the solvent system was required for the reaction. Anhydrous solvent was used without any addition of water, resulting in traces of product with only 51% ee, indicating that the presence of some water is necessary to achieve

good stereoselectivity in the reaction (Table 3.3.1, Entry 6). Other solvents were then investigated in combination to water including 1,4-dioxane, THF, and toluene which were commonly used solvents for Rh-catalysis by the Fletcher group. Nevertheless, no increase in yield or ee was observed (Table 3.3.1, Entries 7-9).

Table 3.3.1 Rh-catalysed arylation reaction of **9a**



General Procedure A

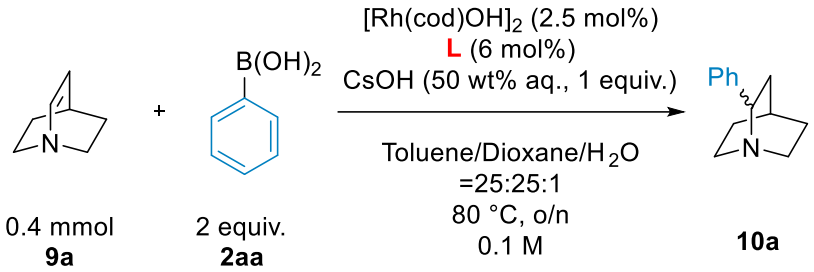
Entry	Deviation from General Procedure A	Yield /%[a]	ee/%[b]
1	-	N.R.	-
2	Heating to 80 °C	N.R.	-
3	1 equiv. of CsOH (50 wt% aq.), heating to 80 °C	Trace	93
4	1 equiv. of CsOH (50 wt% aq.), heating to 80 °C, 0.4 M	Trace	80
5	1 equiv. of CsOH (50 wt% aq.), heating to 100 °C	Trace	58
6	1 equiv. of CsOH (50 wt% aq.), toluene/dioxane as solvent	Trace	51
7	1 equiv. of CsOH (50 wt% aq.), dioxane/water as solvent	Trace	67
8	1 equiv. of CsOH (50 wt% aq.), toluene/water as solvent	Trace	86
9	1 equiv. of CsOH (50 wt% aq.), THF/water as solvent	Trace	84

a. Isolated yield with inseparable impurities. **b**. Enantiomeric excess determined by HPLC (High Performance Liquid Chromatography) analysis on a chiral non-racemic stationary phase.

The effect of ligand was then examined by ligand screening, with the various ligand tested shown in Table 3.3.2. Due to existing reactivity present with (*S*)-SEGPHOS in previous attempts, other ligands in the SEGPHOS family were tested together with other biphosphine ligands including BINAP (Table 3.3.2, Entries 1-12). Unfortunately, we could not achieve any increase in yield with the ligands screened above. Therefore, we went on to explore ligands that are structurally different (Table 3.3.2, Entries 13-19) and possess multiple coordinating sites, in order to minimise any negative effects of the lone pair on nitrogen. However, these

attempts failed to improve reaction yield.

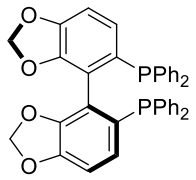
Table 3.3.2 Ligand screening on Rh-catalysed arylation reaction of **9a**



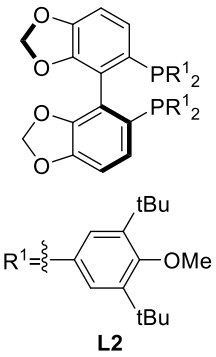
General Procedure B

Entry	Ligand used	Yield /%[a]	ee/%[b]
1	**L1**	Trace	93
2	**L2**	Trace	N.D.
3	**L3**	Trace	N.D.
4	**L4**	N.R.	-
5	**L5**	<15%	21
6	**L6**	Trace	N.D.
7	**L7**	Trace	N.D.
8	**L8**	Trace	N.D.
9	**L9**	N.R.	-
10	**L10**	<13%	N.D.
11	**L11**	Trace	N.D.
12	**L12**	Trace	N.D.
13	**L13**	N.R.	-
14	**L14**	Trace	N.D.
15	**L15**	N.R.	-
16	**L16**	N.R.	-
17	**L17**	Trace	N.D.
18	**L18**	N.R.	-
19	**L19**	Trace	N.D.

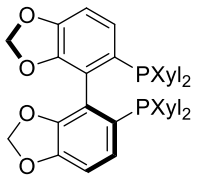
a. Isolated yield with inseparable impurities. **b**. Enantiomeric excess determined by HPLC (High Performance Liquid Chromatography) analysis on a chiral non-racemic stationary phase.



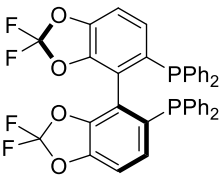
L1



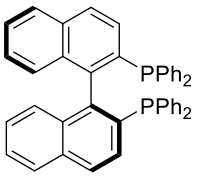
L2



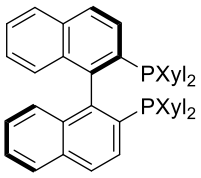
L3



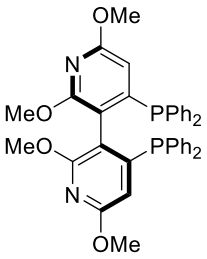
L4



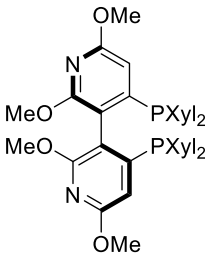
L5



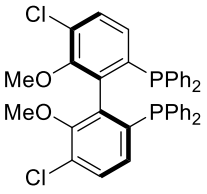
L6



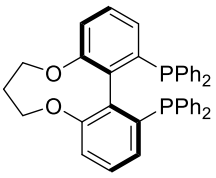
L7



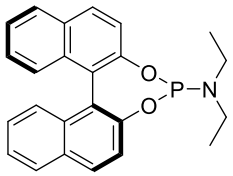
L8



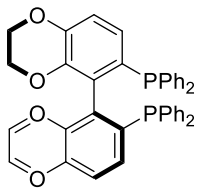
L9



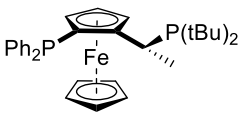
L10



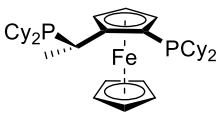
L11



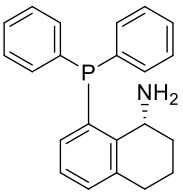
L12



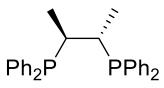
L13



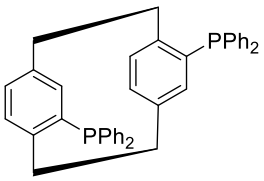
L14



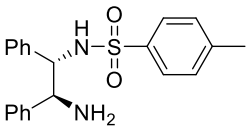
L15



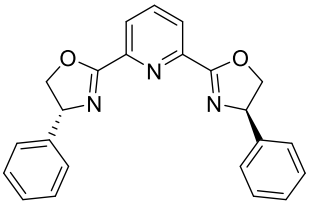
L16



L17



L18

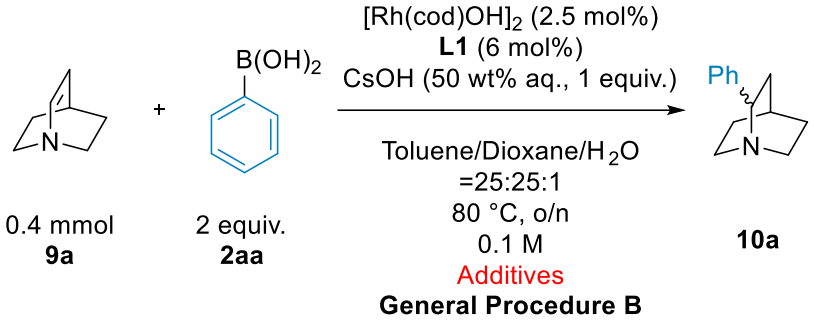


L19

To identify whether the lone pair on the nitrogen atom in **9a** was poisoning the reaction, we went on to screen Lewis acid additives, where various coordinating additives were added into the reaction before addition of the Rh-complex, to check if better conversion could be achieved. We started with zinc triflate in both catalytic and stoichiometric amounts, and after heating overnight, we observed the coordinated complex species by crude ^{1}H NMR spectroscopy instead of the arylation product **10a** (Table 3.3.3, Entries 2-3). This indicated that the additive

was effective in coordinating to the additive, but also exhibited potential inhibition to the Rh catalysis. Heating the reaction with 1.1 equiv. of zinc triflate at 120 °C overnight (Table 3.3.3, Entry 4) also gave no product by crude ^{1}H NMR spectroscopy, which we presume was caused by decomposition of the coordinated complex. With other additives including zinc bromide, lanthanum triflate, and silver perchlorate, no increase in reaction conversion was observed (Table 3.3.3, Entries 5-7).

Table 3.3.3 Additive screening on Rh-catalysed arylation reaction of **9a**

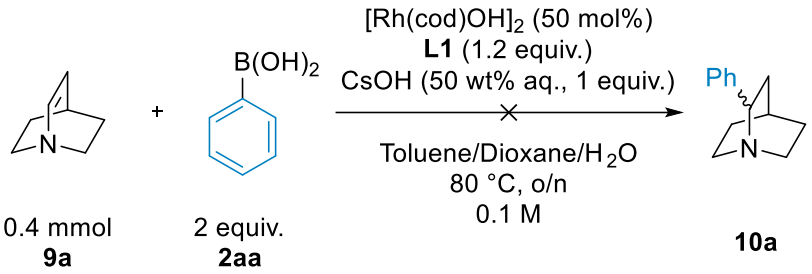


General Procedure B

Entry	Additive	Yield /%[a]
1	-	Trace
2	20 mol% $Zn(OTf)_2$	Coordination
3	1.1 equiv $Zn(OTf)_2$	Coordination
4	1.1 equiv $Zn(OTf)_2$, 120 °C	N.R.
5	20 mol% $ZnBr_2$	N.R.
6	40 mol% $La(OTf)_3$	N.R.
7	20 mol% $AgClO_4$	N.R.

a. Isolated yield with inseparable impurities.

In addition, we tested the reaction with a stoichiometric amount of $[Rh(cod)OH]_2$ and the ligand, as another method of probing whether catalyst poisoning was limiting the conversion of the reaction. Interestingly, after overnight stirring at 80 °C, no product formation was observed in the crude ^{1}H NMR spectra, and **9a** peaks were not found (Scheme 3.3.6). This indicated that catalyst poisoning was probably not the main reason for the limitation on reactivity, in addition to the possible decomposition of **9a** *via* ring-opening or other routes, as no olefinic proton peaks were observed in the crude ^{1}H NMR spectra.

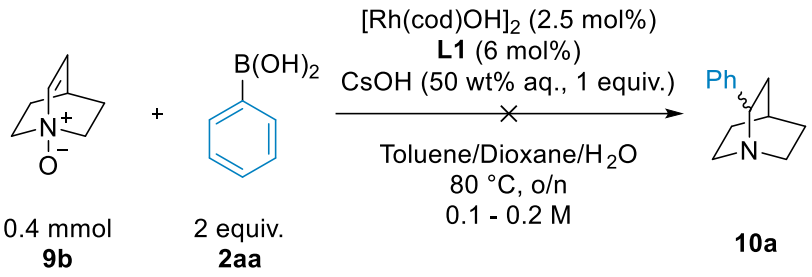


Scheme 3.3.6 Rh-catalysed arylation reaction on **9a** with stoichiometric catalysts.

3.3.3 Synthesis and Tests of Other Substrates

Next, we proposed that we could circumvent the possible inhibition problem by synthesising other substrates with *tetra*-substituted nitrogen atom. According to the work done by O'Neil and coworkers, [222] the *N*-oxide and nitrogen-borane complex equivalent of dehydro-quinuclidine have both been synthesised as shown in Scheme 3.3.3 and 3.3.4.

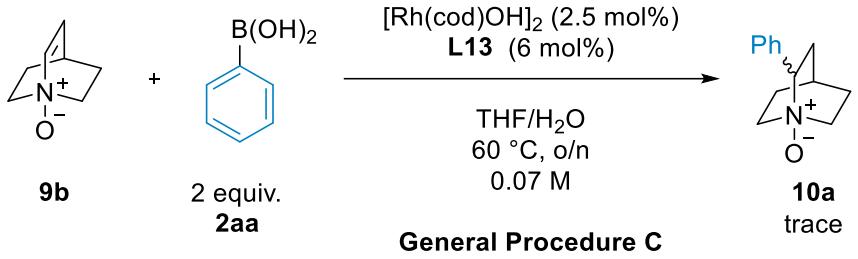
We firstly tested the *N*-oxide substrate **9b** in the Rh-catalysed arylation reaction. However, no product was observed in the crude NMR after overnight heating, and the situation was the same when we doubled the reaction concentration to 0.2 M (Scheme 3.3.7).



Scheme 3.3.7 Rh-catalysed arylation reaction on **9b**.

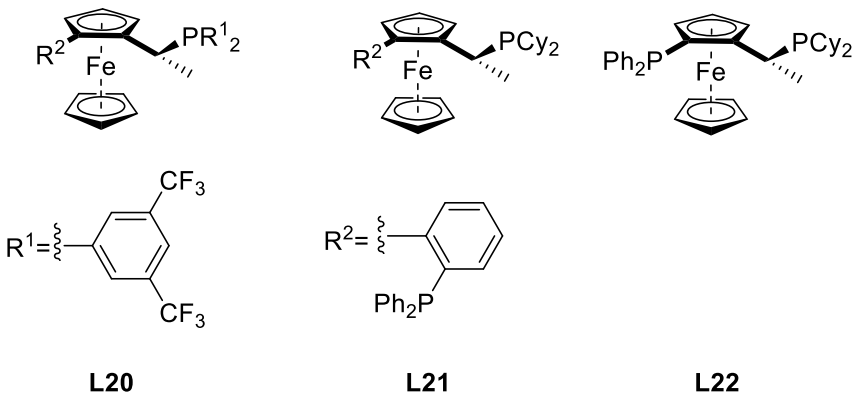
We subjected the reaction under other Rh-catalysed cross-coupling reaction conditions. Firstly, we tested the conditions from Lautens work (shown as General Procedure C), [236] using $[Rh(cod)OH]_2$ and Josiphos SL-J002-1 (**L13**) as the ligand in THF/H_2O heating at 60 °C overnight (Table 3.3.4, Entry 1). This time, we observed likely product formation by crude ^1H NMR spectroscopy. However, several attempts to isolate the product failed due to its presence in only trace amount.

Table 3.3.4 Reaction optimisation of Rh-catalysed arylation reaction of **9b**



Entry	Deviation from standard conditions	Yield /%[a]
1	-	Trace
2	Walphos SL-W001-1 **L20** as ligand	N.R.
3	Walphos SL-W003-1 **L21** as ligand	N.R.
4	1 equiv. of CsOH (50 wt% aq.)	Trace
5	Josiphos SL-J003-2 **L14** as ligand, 1 equiv. of CsOH (50 wt% aq.)	N.R.
6	Josiphos SL-J001-1 **L22** as ligand, 1 equiv. of CsOH (50 wt% aq.)	N.R.
7	(*S*)-SEGPHOS **L1** as ligand, 1 equiv. of CsOH (50 wt% aq.)	N.R
8	(*S*)-BINAP **L5** as ligand, 1 equiv. of CsOH (50 wt% aq.)	N.R
9	1 equiv. of CsOH (50 wt% aq.), Ph–Bpin as coupling partner	Trace
10	1 equiv. of CsOH (50 wt% aq.), toluene/water as solvent, 100 °C	Trace
11	1 equiv. of CsOH (50 wt% aq.), dioxane/water as solvent, 100 °C	N.R.
12	1 equiv. of Cs_2CO_3 (50 wt% aq.), mesitylene as solvent, 120 °C	N.R.
13	1 equiv. of CsOH (50 wt% aq.), 20 mol% $Zn(OTf)_2$ additive	Trace
14	1 equiv. of CsOH (50 wt% aq.), 1.1 equiv. $Zn(OTf)_2$ additive	N.R.

a. Isolated yield with inseparable impurities.



L20 **L21** **L22**

Further reaction optimisation was performed with the results shown above. We tested the same reaction with Walphos-type ligands including **L20** and **L21** (Table 3.3.4, Entries 2-3), but **L13** used by Lautens was the superior ligand as no reactivity was observed with the other ligands tested. Next, we tested the same reaction with 1.0 equiv. CsOH base addition, and afforded trace product (Table 3.3.4, Entry 4). More Josiphos-type ligands, including **L14** and **L22** were tested with the presence of base, but gave no reactivity, so were the biphosphine ligands including (*S*)-SEGPHOS and (*S*)-BINAP (Table 3.3.4, Entries 5-8).

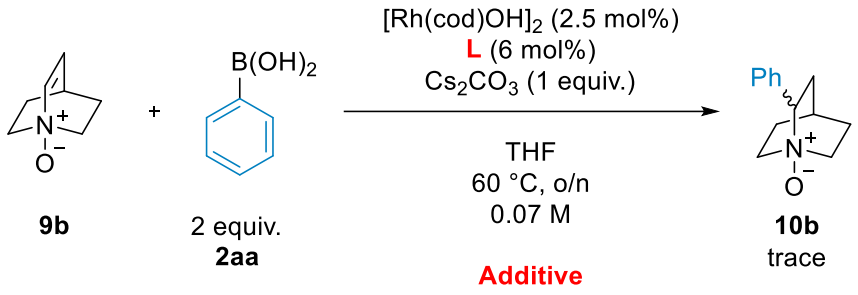
Substituting the coupling partner with phenyl boronic pinacol ester did not improve the yield (Table 3.3.4, Entry 9). Other solvent systems were also tested, including toluene/water and dioxane/water, where the first combination gave rise to trace product, and the latter one exhibited no reactivity at all (Table 3.3.4, Entries 10-11). Anhydrous conditions with Cs_2CO_3 as the base and mesitylene as solvent were also tested at 120 °C heating overnight, which gave no reactivity, potentially due to solubility issues of **9b** in non-polar solvent (Table 3.3.4, Entry 12). Poor reactivity when using dioxane and mesitylene as solvent was unexpected, as the former solvent should not pose a solubility issue to the polar substrate.

We again tested the effects of the addition of zinc triflate on the reaction, with amounts of 20 mol% and 1.1 equiv. Both appeared to be ineffective in increasing yield (Table 3.3.4, Entries 13-14).

Even though the lone pair on nitrogen atom in **9b** is no longer nucleophilic, the lone pairs and the negative charge on oxygen could potentially interfere with the catalyst. Therefore, we screened some additives that would associate with the oxygen atom, with the aim of reducing the nucleophilicity of oxygen and posing lower possibility in catalyst poisoning.

The additives were added into the substrate solution and stirred to allow reaction before the addition of catalytic species. However, unlike what we expected, the addition of acetic anhydride, sodium sulfite, boron trifluoride diethyl etherate, and zinc triflate were unsuccessful in promoting reactivity of the reaction by blocking the oxygen atom (Table 3.3.5, Entries 1-6). TMSOTf was observed to coordinate with the oxygen but was unable to increase reaction conversion (Table 3.3.5, Entries 7-8).

Table 3.3.5 Additive screening on Rh-catalysed arylation reaction of **9b**



Entry	Additive	Ligand	Yield /%[a]
1	1.5 equiv. acetic anhydride	**L13**	N.R.
2	1.5 equiv. Na_2SO_3	**L13**	N.R.
3	1.0 equiv F_3B-Et_2O	**L13**	N.R.
4	1.0 equiv F_3B-Et_2O	**L21**	N.R.
5	1.0 equiv $Zn(OTf)_2$	**L13**	N.R.
6	1.0 equiv $Zn(OTf)_2$	**L21**	N.R.
7	1.0 equiv. TMSOTf	**L13**	Coordination
8	1.0 equiv. TMSOTf	**L21**	Coordination

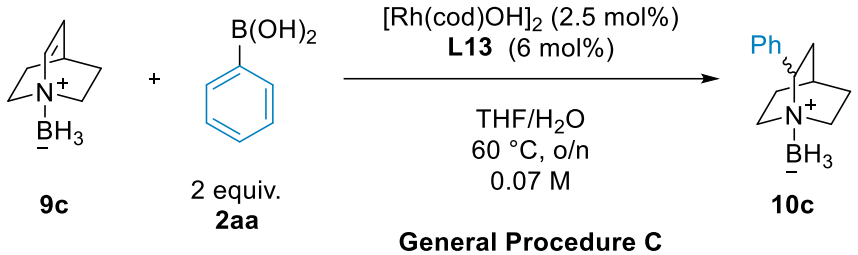
a. Isolated yield with inseparable impurities.

Two other sets of Rh-catalysed cross-coupling reaction conditions used by the Fletcher group members, shown as General Procedure E and F in Chapter 4.3.2 were tested on **9b**. Unfortunately, after initial screening, neither procedure provided a rise in reaction conversion (results not shown). Hence, we went on to investigate the reactivity of nitrogen-borane complex substrate **9c**. The synthesis of **9c** proceeded *via* a similar route to **9b** synthesis, where H_3B-THF was added to the tosylate **S13** to form the nitrogen-borane complex as shown in Scheme 3.3.5.

For **9c**, General Procedure C which proved to proceed to afford trace product in the **9b** reaction was used. After overnight stirring, we found out that no product was formed during the reaction, and only decomposition of **9c** to **9a** was observed (Table 3.3.6, Entry 1). We then tried the reaction with the addition of CsOH, and same results were obtained where only decomposition of **9c** to **9a** occurred (Table 3.3.6, Entry 2). We postulated the decomposition of **9c** could be due to the relatively weak N-B bond, therefore being hydrolysed by water in the reaction. Consequently, we went on to screen a few anhydrous conditions, where there was no addition

of water into the reaction and CsOH was replaced with Cs_2CO_3. Numerous different solvents were tested including THF, toluene, 2-methyl-THF, and dioxane. Among all, only dioxane rendered decomposition of **9c**, while other solvents listed above gave no reactivity (Table 3.3.6, Entries 3-6).

Table 3.3.6 Reaction optimisation of Rh-catalysed arylation reaction of **9c**



General Procedure C

Entry	Deviation from standard conditions	Yield /%[a]
1	-	Decomposition to **9a**
2	1 equiv. of CsOH (50 wt% aq.)	Decomposition to **9a**
3	1 equiv. of Cs_2CO_3, THF as solvent	N.R.
4	1 equiv. of Cs_2CO_3, toluene as solvent	N.R.
5	1 equiv. of Cs_2CO_3, dioxane as solvent	Decomposition to **9a**
6	1 equiv. of Cs_2CO_3, 2-methyl THF as solvent	N.R.
7	1 equiv. of Cs_2CO_3, THF as solvent, double catalyst loading	Decomposition to **9a**
8	1 equiv. of Cs_2CO_3, THF as solvent, 0.21 M concentration	Decomposition to **9a**
9	1 equiv. of Cs_2CO_3, THF as solvent, **L1** as ligand	Decomposition to **9a**
10	General Procedure B used, 0.07 M concentration	Decomposition to **9a**
11	General Procedure E used	Decomposition to **9a**
12	General Procedure F used	Decomposition to **9a**

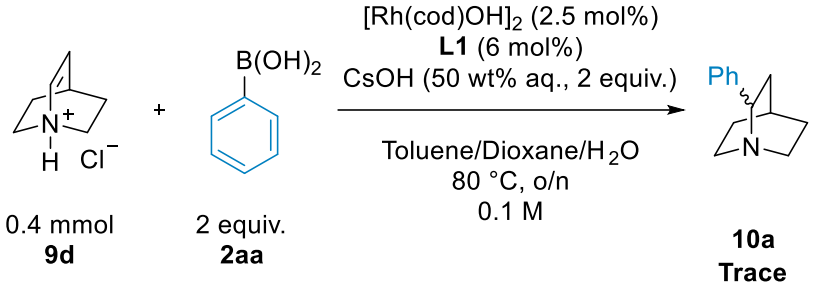
a. Isolated yield with inseparable impurities.

Next, we tested several different conditions that were regularly tested during screening to promote reactivity, including doubling catalyst loading, and tripling the reaction concentration (Table 3.3.6, Entries 7-8). Unfortunately, only decomposition was observed reactivity in these reactions. **L1** was also tested in the reaction as ligand, and we observed the same result (Table 3.3.6, Entry 9). Changing the reaction procedure to General Procedure B, E, and F also seemed

to give similar performance to the previous attempts (Table 3.3.6, Entries 10-12).

According to the screening results above, we summarised that the substrate **9c** was relatively unstable and susceptible to decomposition by hydrolysis. This indicated that **9c** is less as suitable as the substrate in this Rh-catalyse cross-coupling reaction, and substrates with higher stability could be synthesised and investigated.

Furthermore, the hydrochloride salt of dehydroquinuclidine **9d** was synthesised and tested in the reaction (Scheme 3.3.8). An extra equivalent of base was added to avoid any impacts due to acid-base neutralisation. In the reaction, trace product was again observed, and hence was not investigated further due to its high similarity in reactivity to **9a**.

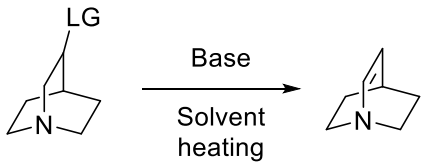


Scheme 3.3.8 Rh-catalysed arylation reaction on **9d**.

3.4 Conclusion and Future Work

In this project, we have synthesised various dehydroquinuclidine derivatised substrates and tested their reactivity in the Rh-catalysed Suzuki-Miyaura cross-coupling reaction. Both dehydroquinuclidine and its *N*-oxide derivative exhibited reactivity to form the arylation product but were only found in trace amounts and hence could not be isolated. The enantioselectivity of the reaction with dehydroquinuclidine was good with up to >90% ee. The nitrogen-borane complex equivalent did not proceed in the arylation reaction but decomposed to dehydroquinuclidine, potentially due to the low stability of nitrogen-boron bond. This reaction still requires significant improvement based on current results we have, and we propose several different approaches that could be investigated below.

Firstly, the synthesis and purification methods of the existing substrates could be optimised (Scheme 3.4.1). For **9a** synthesis, 3-chloroquinuclidine hydrochloride salt, the starting material for the current optimal route was discontinued by Sigma Aldrich. Therefore, to continue in reaction optimisation reaction on **9a**, we need to seek other routes that ideally, are short, effective, and clean. The other possible routes we have tested with tosylate and mesylate as the leaving groups did not afford full conversion, complicating isolation of product. Therefore, the existing reactions should be optimised, ideally with solvent that is more volatile than DMSO. A better purification method should also be sought, currently we afford the product with residual solvent from work-up by distillation. Consequently, it would be desirable if the optimal temperature of distillation could be determined by careful testing.

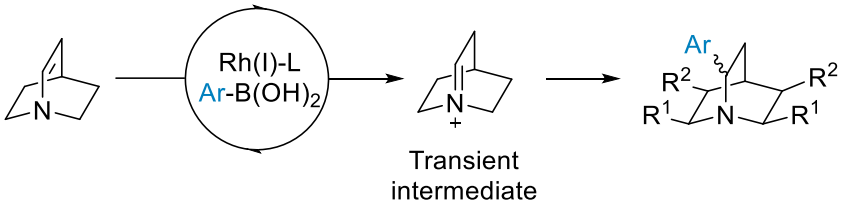


9a

Scheme 3.4.1 Optimisation of synthesis of **9a**.

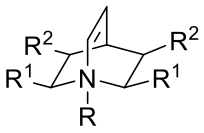
Secondly, other dehydroquinuclidine derivatives could be synthesised and investigated, as **9a-9d** experienced either difficulty in synthesis and purification or exhibited undesired reactivity in the Rh-catalysis. One of our possible postulations is that considering the necessity of water addition in the reaction (Table 3.3.1, Entry 6), the inhibition of the reactivity by the Lewis acid

additives (Table 3.3.3), together with the regioselectivity of aryl addition on the more electrophilic carbon atom, it is possible that even though with the violation with the Bredt's rule, it is possible that the reaction proceeded *via* a transient imine intermediate followed by aryl ring addition (Scheme 3.4.2). Therefore, as our previous attempts were made to eliminate the effects of the nitrogen lone pairs, possible attempts could be made to promote imine formation in the reaction, and hence without any substitutions on the nitrogen.



Scheme 3.4.2 Potential substrates for testing.

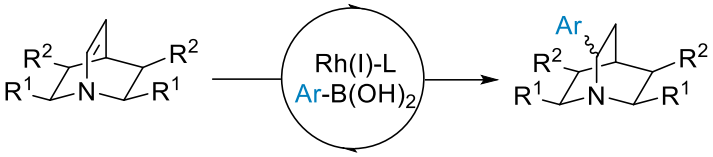
In addition, other substrates like **9e** with substitutions on the quinuclidine ring could also be synthesised and tested (Scheme 3.4.3). Ideally prochiral dehydroquinuclidine derivatives would be used with symmetrical substituents on the ring. This way, we could attempt synthetic routes towards chiral quinine and quinidine that would possess various biological and pharmacological activities. Additionally, different substitutions on the quinuclidine ring, especially one that are close to the enamine moiety, would likely have various effects on the stereoselectivity of the Rh-reactions.



9e

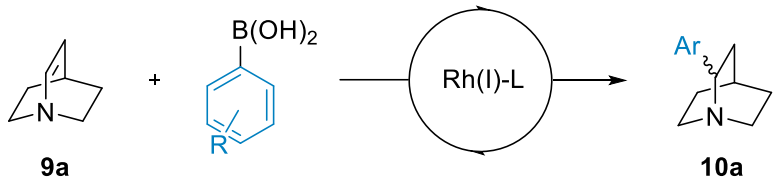
Scheme 3.4.3 Potential substrate for testing.

After more substrates are synthesised, we could continue our optimisation on the Rh-catalysed asymmetric arylation reaction. Procedures that have been tested could be investigated with new substrates, and for previously synthesised substrates, other Rh-catalysis reactions could be tested to allow improvement in reaction yield and stereoselectivity (Scheme 3.4.4).



Scheme 3.4.4 Optimisation of asymmetric Rh-catalysed arylation on quinuclidine-type substrates.

Finally, for the existing arylation reactions, different boronic acids could be probed and tested with various electronic and steric properties of the coupling partner (Scheme 3.4.5). With different coupling partner used, the reaction pathway may also differ. Previously, the Lautens group reported a Rh-catalysed ring-opening reaction of diazabicycles, where the reaction pathway could be switched to reductive arylation when certain boronic acids were used. [236]



Scheme 3.4.5 Optimisation of Rh-catalysed arylation on quinuclidine-type by use of different boronic acids.

Chapter 4: Experimental Procedures

4.1 General Information

All oxygen and moisture sensitive reactions were performed in flame-dried flasks under argon atmosphere with standard Schlenk techniques. Magnetic stirring was present throughout all reactions. All reactions performed with heating is performed utilizing DrySyn heating blocks. All the reactions at 0 ℃ were performed in ice-water cooling bath with cotton wool covering. Other reactions that required cooling were performed in appropriate cooling bath with cotton wool covering.

Nuclear Magnetic Resonance spectroscopy (^{1}H, ^{13}C, ^{19}F, COSY, HSQC, NOESY) was measured at room temperature in deuterated solvent (Sigma Aldrich) using Bruker AVIII HD 400 (400 MHz for ^{1}H NMR, 101 MHz for ^{13}C NMR, 376 MHz for ^{19}F NMR) or Bruker NOE600 (600/151 MHz) spectrometers. Chemical shifts were reported in parts per million (ppm) relative to residual solvent peak. Assignments were made in accordance with COSY and HSQC spectra.

Infrared spectroscopy was carried out on a Bruker Tensor 27 FT-IR spectrometer with internal calibration range of 4000-600 cm^{-1}.

Optical rotations ($[\alpha]^{25}_{D}$) were recorded using a Schmidt Haensch Unipol L2000 Polarimeter in a cell with a path length of 1 dm (using the sodium D line, 589 nm). Concentrations (c) are reported in g/100 mL. Temperatures are reported in °C.

Chiral SFC separation was conducted on Waters Acquity UPC2 system in Waters Empower software. Chiralpak columns (150 × 3 mm, particle size 3 μm) used for separation were specified in individual reactions. Analytical HPLC was carried out using an Agilent 1260 Infinity series normal phase unit equipped with an autosampler. HPLC grade solvent was used (Sigma Aldrich/Fisher Scientific).

High Resolution Mass spectra were carried out by internal service at the University of Oxford. Electron spray ionisation (ESI^{+}) was recorded on a Fisons Platform II. Analyses were

performed using a Thermo Exactive mass spectrometer equipped with Waters Acquity liquid chromatography system.

Commercially available reagents were purchased from: Sigma Aldrich, Alfa Aesar, Acros Organics, Fluorochem and Strem Chemical. All chemicals were used without further purifications unless otherwise stated. The ligands screened in catalytic reactions were either purchased or synthesised by group members. All the boronic pinacol esters were synthesised from the corresponding boronic acid and purified *via* column chromatography.

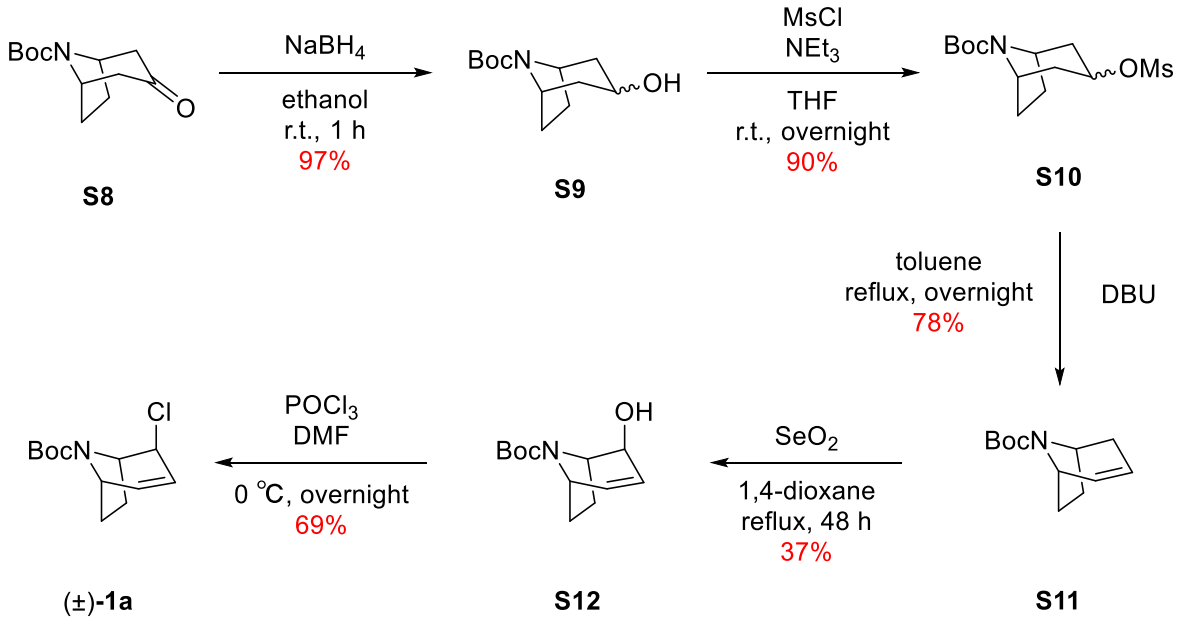
Anhydrous solvent was collected freshly from mBraun SPS-800 solvent purification system after passed through anhydrous alumina columns. Anhydrous THF for all Rh-catalysed reactions was purchased from Acros under molecular sieves.

Medium-pressure chromatography was performed on a CombiFlash Next Gen 100 system using a RediSep Gold® column. Manual Flash column chromatography was carried out using Merck 60 Å silica gel and VWR (40-63 μm) silica. Pressure was applied at the column head *via* a flow of nitrogen with the solvent system used in parentheses.

4.2 Chapter 2 Procedures

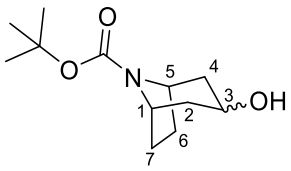
4.2.1 Substrate Synthesis

Synthesis of Nortropane-derived allyl chloride (±)-1a



Scheme 4.2.1 Overview of synthesis of allyl chloride (±)-**1a**.

Synthesis of S9



S9

Sodium borohydride (1.68 g, 44.4 mmol) was added portionwise to a solution of **S8** (5.00 g, 22.2 mmol) in ethanol (100 mL) at 0 °C, then the reaction mixture was allowed to warm up to r. t.. After stirring for 1h, NH_4Cl solution (sat. aq., 50 mL) followed by H_2O (50 mL) were added. The aqueous layer was extracted with EtOAc (100 mL × 3), and the combined organic layer was dried over $MgSO_4$. The resulting solution was concentrated in *vacuo* to afford **S9** as

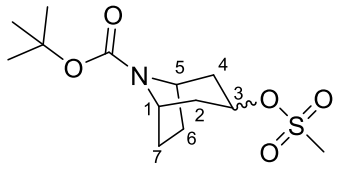
a mixture of diastereomers (d.r. ~ 1.1:1). **S2** was used directly in the next step without purification (4.85 g, 97% yield). The spectroscopic data are in agreement with the literature.[237]

^{1}H NMR ($CDCl_3$, 400 MHz, both diastereomers): δ (ppm) = 4.26-4.06 (m, 3H, C^1–H, C^3–H, C^5–H), 2.25-1.81 (m, 4H, C^2–H, C^4–H), 1.77-1.48 (m, 4H, C^6–H, C^7–H), 1.46/1.45 (2 × s, 9H, –$C(CH_3)_3$).

^{13}C NMR ($CDCl_3$, 101 MHz, both diastereomers): δ (ppm) = 153.6 (–C=O), 153.4 (–C=O), 79.5 (–$\underline{C}(CH_3)_3$), 79.2 (–$\underline{C}(CH_3)_3$), 65.5 (C^3), 64.2 (C^3), 53.3 (C^1/C^5), 52.8 (C^1/C^5), 40.7 (C^2/C^4), 38.6 (C^2/C^4), 28.66 (–$C(\underline{C}H_3)_3$), 28.65 (–$C(\underline{C}H_3)_3$), 28.1 (C^6, C^7).

HRMS (APCI): m/z calculated for $C_{12}H_{21}O_3NNa^+$ $[M+Na]^+$ 250.1414, found 250.1414.

Synthesis of S10



S10

According to a literature procedure by Nagase *et. al*., [238] triethylamine (4.7 mL, 36.8 mmol) was added to a solution of **S9** (5.57 g, 24.5 mmol) in tetrahydrofuran (50 mL) under an argon atmosphere. Methanesulfonyl chloride (2.1 mL, 29.6 mmol) was added dropwise at 0 °C. The reaction mixture was allowed to reach r. t. and stirred overnight. Then, H_2O (50 mL) was added, and the resulting mixture was extracted with EtOAc (50 mL × 3) and the combined organic layer was dried over $MgSO_4$. The solution was concentrated *in vacuo* and the crude product was purified by flash chromatography (hex/EtOAc=50/50) to afford **S10** (d.r. ~ 4.3:1, 64% yield) with recovered **S2** as a light yellow oil. The mixture of **S9** and **S10** was dissolved in THF (20 mL), followed by the addition of triethylamine (1.7 mL, 13.2 mmol) and methanesulfonyl chloride (0.76 mL, 8.82 mmol) were added dropwise at 0 °C. The reaction mixture was allowed to reach r. t. and stirred overnight. Then, H_2O (20 mL) was added, and the resulting mixture

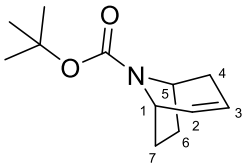
was extracted with EtOAc (20 mL x 3) and the combined organic layer was dried over $MgSO_4$. The solution was concentrated *in vacuo* and the crude product was purified by flash chromatography (hex/EtOAc=50/50) to afford **S10** (d.r. ~ 1.4:1, 90% yield) The spectroscopic data are in agreement with the literature.[238]

^{1}H NMR ($CDCl_3$, 400 MHz, major diastereomer): δ (ppm) = 4.98 (tt, J = 10.9, 6.2 Hz, 1H, C^3–H), 4.35-4.07 (m, 2H, C^1–H, C^5–H), 2.94 (s, 3H, –CH_3), 2.20-1.88 (m, 4H, C^2–H, C^4–H), 1.88-1.68 (m, 2H, C^6/C^7–H), 1.67-1.51 (m, 2H, C^6/C^7–H), 1.47 (s, 9H, –$C(CH_3)_3$), 1.45 (s, –$C(CH_3)_3$).

^{13}C NMR ($CDCl_3$, 101 MHz, major diastereomer): δ (ppm) = 153.2 (–C=O), 80.0 (–$\underline{C}(CH_3)_3$), 75.1 (C^3), 52.6 (C^1, C^5), 38.9 (–CH_3), 38.5 (C^2/C^4, C^6/C^7), 38.0 (C^2/C^4, C^6/C^7), 37.2 (C^2/C^4, C^6/C^7), 28.4 (–$C(\underline{C}H_3)_3$), 27.5 (C^2/C^4, C^6/C^7).

HRMS (APCI): m/z calculated for $C_{13}H_{23}O_5NSNa+$ $[M+Na]^+$ 328.1189, found 328.1188.

Synthesis of S11



S11

According to a literature procedure by Dallanoce and coworkers, [239] DBU (4.0 mL, 27 mmol) was added to a solution of **S10** (2.91g, 9.13 mmol) in toluene (11 mL), and the reaction mixture was stirred under reflux overnight. The reaction mixture was filtered over Celite® and concentrated *in vacuo.* Flash column chromatography (hex/EtOAc=85/15) afforded **S11** as a light yellow oil (1.56 g, 78% yield). The spectroscopic data are in agreement with the literature.[146]

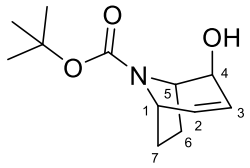
^{1}H NMR ($CDCl_3$, 400 MHz): δ (ppm) = 5.91 (s, 1H, C^2–H), 5.44 (dddd, J = 9.6, 4.1, 2.4, 1.3 Hz, 1H, C^3–H), 4.45-4.02 (m, 2H, C^1–H, C^5–H), 2.68 (s, 1H, C^4–H). 2.08 (m, 1H, C^6/C^7–H),

1.84 (tdd, J = 11.8, 10.2, 6.6 Hz, 2H, C^6/C^7–H), 1.71 (dd, J = 17.6, 4.4 Hz, 1H, C^4–H), 1.61 (m, 1H, C^6/C^7–H), 1.38 (s, 9H, –$C(CH_3)_3$).

^{13}C NMR ($CDCl_3$, 101 MHz): δ (ppm) = 154.1 (–C=O), 132.9 (C^2), 123.8 (C^3), 79.1 (–$\underline{C}(CH_3)_3$), 52.8 (C^1, C^5), 34.7 (C^4, C^6/C^7), 29.9 (C^6/C^7), 28.4 (–$C(\underline{C}H_3)_3$).

HRMS (APCI): m/z calculated for $C_{12}H_{19}O_2NNa^+$ $[M+Na]^+$ 232.1308, found 232.1309.

Synthesis of (±)-S12



(±)-**S12**

According to a related literature procedure by Chavan *et. al*., [240] SeO_2 (0.550 g, 4.96 mmol) was added to a solution of **S11** (0.944 g, 4.51mmol) in 1,4-dioxane (270 mL). The reaction mixture was stirred under reflux for 48 h. The reaction mixture was then cooled to r.t., filtered through Celite® and concentrated *in vacuo*. The crude product was dissolved in EtOAc (30 mL) and washed with $NaHCO_3$ (sat. aq., 20 mL); the aqueous layer was extracted with EtOAc (20 mL × 3), and the combined organic layer was washed with brine (20 mL) and dried over $MgSO_4$. The solution was concentrated *in vacuo* and the crude product was purified by flash column chromatography (hex/EtOAc= 70/30) to afford (±)-**S12** as a yellow oil (0.399 g, 37 % yield) as a single diastereomer (d.r. > 20:1).

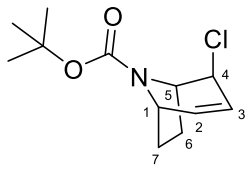
^{1}H NMR ($CDCl_3$, 400 MHz): δ (ppm) = 6.12 (dd, J = 9.6, 5.3 Hz, 1H, C^2–H), 5.78 – 5.59 (m, 1H, C^3–H), 4.46 (app. d, J = 8.2 Hz, 2H, C^1–H, C^5–H), 3.72 (dd, J = 9.7, 4.1 Hz, 1H, C^4–H), 3.27 (br. s, 1H, –OH), 2.23 – 2.07 (m, 1H, C^6/C^7–H), 1.98 – 1.72 (m, 1H, C^6/C^7–H), 1.72 – 1.54 (m, 1H, C^6/C^7–H), 1.46 (s, 9H, –$C(CH_3)_3$), 1.33 – 1.19 (m, 1H, C^6/C^7–H).

^{13}C NMR ($CDCl_3$, 101 MHz): δ (ppm) = 170.6 (–C=O), 133.7 (C^2), 126.2 (C^3), 79.6 (–$\underline{C}(CH_3)_3$), 71.1 (C^4), 58.0 (C^1/C^5), 53.5 (C^1/C^5), 30.2 (C^6/C^7), 28.1 (–$C(\underline{C}H_3)_3$), 24.3 (C^6/C^7).

HRMS (APCI): m/z calculated for $C_{12}H_{19}O_3NNa^+$ $[M+Na]^+$ 248.1257, found 248.1258.

IR: 3431, 2975, 1670, 1478, 1393, 1366, 1341, 1298, 1251, 1160, 11106, 1057, 1023, 957, 894, 868, 849, 831, 774, 718 cm^{-1}

Synthesis of (±)-1a



(±)-**1a**

According to a related literature procedure by Schäfer *et al*.,[119] (±)-**S12** (0.492 g, 2.18 mmol) was dissolved in DMF (3.5 mL) at 0 °C and cold $POCl_3$ (0.45 mL) in DMF (3.5 mL) was added dropwise. The reaction was allowed to reach r. t. overnight. Then, NaOH solution (1M in H_2O, 2.5 mL) was added, and the mixture was extracted with EtOAc (5 mL). The combined organic layer was dried over $MgSO_4$ and concentrated *in vacuo*. The crude product was purified *via* flash column chromatography (hexane/EtOAc = 85/15) to afford (±)-**1a** as a colourless oil, which solidified at –20°C (0.368 g, 69 % yield) to give an off-white solid. The product was afforded as a single diastereomer (d.r. > 20:1).

The relative stereochemistry was assigned *via* X-ray diffraction.

^{1}H NMR ($CDCl_3$, 400 MHz): δ (ppm) = 6.13 (m, 1H, C^2–H), 5.65 (d , *J* = 9.5 Hz, 1H, C^3–H), 4.57 (m, 2H, C^1–H, C^5–H), 4.23 (s, 1H, C^4–H), 2.29-2.06 (m, 1H, C^6/C^7–H), 1.85 (s, 1H, C^6/C^7–H), 1.77-1.65 (m, 1H, C^6/C^7–H), 1.60-1.52 (m, 1H, C^6/C^7–H), 1.47 (s, 9H, –$C(CH_3)_3$).

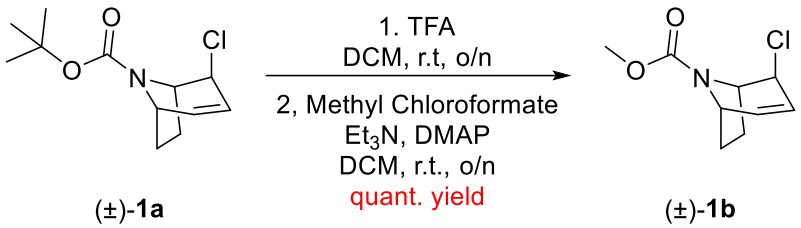
^{13}C NMR ($CDCl_3$, 101 MHz): δ (ppm) = 153.1 (–C=O), 134.9 (C^2), 124.6 (C^3), 80.0 (–$\underline{C}(CH_3)_3$), 59.1 (C^4), 58.7 (C^1/C^5), 58.1 (rot. C^1/C^5), 53.4 (rot. C^1/C^5), 51.7 (C^1/C^5), 31.6 (C^6/C^7), 28.5 (–$C(\underline{C}H_3)_3$), 27.5 (C^6/C^7).

HRMS (APCI): m/z calculated for $C_{12}H_{18}ClO_2NNa^+$ $[M+Na]^+$ 266.0918, found 266.0919.

IR: 2975, 2929, 2883, 1677, 1629, 1475, 1422, 1389, 1366, 1344, 1317, 1297, 1246, 1224, 1160, 1104, 1040, 1009, 969, 906, 891, 869 cm^{-1}

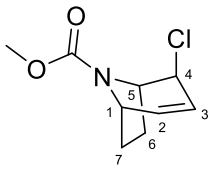
Melting Point: 55.7 – 59.1 °C

Synthesis of (±)-1b



Scheme 4.2.2 Overview of synthesis of allyl chloride (±)-**1b**.

According to related procedure by Karabiyikoglu *et al.*, [177] (±)-**1a** (0.546 g, 2.24 mmol) was dissolved in DCM (17 mL) at 0 °C and TFA (1.8 mL, 22.2 mmol) was added dropwise. The ice bath was removed and the reaction mixture was left stirring overnight. The crude mixture was concentrated *in vacuo*. DMAP (54.5 mg, 0.45 mmol) was added, followed by DCM (7.2 mL). Triethylamine (1.9 mL, 13.4 mmol) and methyl chloroformate (0.48 mL, 3.4 mmol) were added dropwise at 0 °C. The reaction mixture was allowed to reach r.t. overnight. DCM (60 mL) was added, and the organic layer was washed with $NaHCO_3$ (sat. aq. solution, 60 mL), brine (60 mL) and dried over $MgSO_4$. The reaction mixture was concentrated *in vacuo* and purified by flash column chromatography (hex/EtOAc = 90/10 to 80/20) to afford (±)-**1b** as a colourless oil (0.45 g, quant. yield).



(±)-**1b**

^{1}H NMR ($CDCl_3$, 400 MHz): δ (ppm) = 6.19 – 6.02 (m, 1H, C^2–H), 5.72 – 5.61 (m, 1H, C^3–H), 4.62 (s, 2H, C^1–H, C^5–H), 4.25 (s, 1H, C^4–H), 3.71 (s, 3H, –COOC$\underline{H}_3$), 2.19 (dddd, *J* =

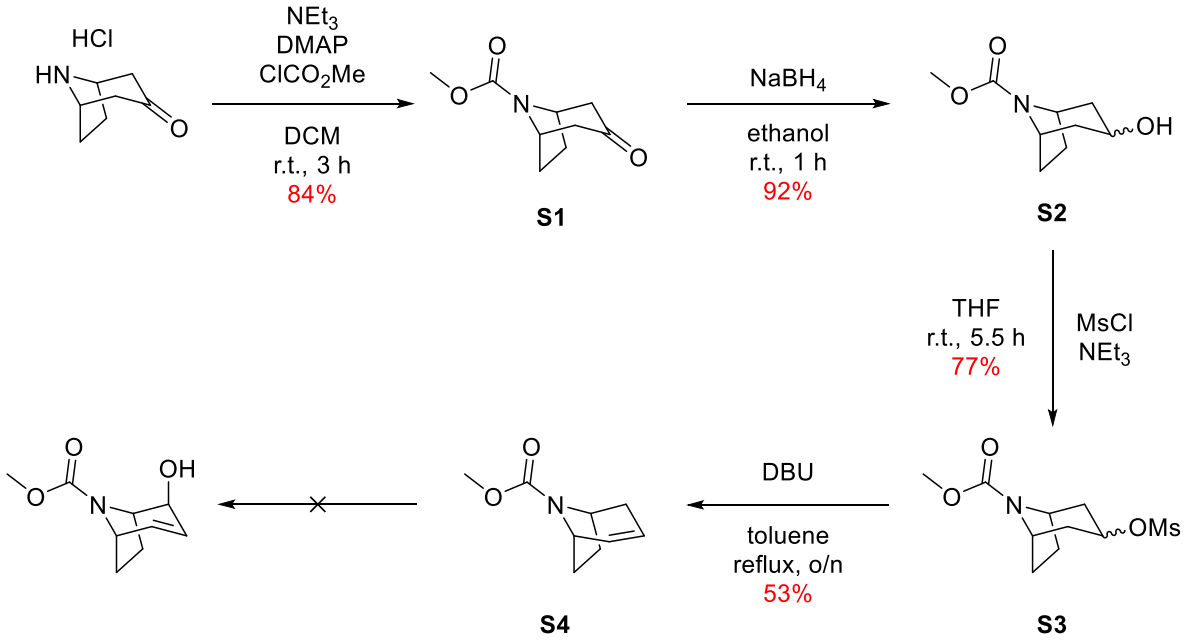
13.2, 10.8, 8.3, 2.4 Hz, 1H, C^6/C^7–H), 1.86 (d, J = 5.5 Hz, 1H, C^6/C^7–H), 1.79 – 1.72 (m, 1H, C^6/C^7–H), 1.63 – 1.50 (m, 1H, C^6/C^7–H).

^{13}C NMR ($CDCl_3$, 101 MHz): δ (ppm) = 154.5 (–C=O), 134.1 (C^2), 124.6 (C^3), 58.7 (C^4, C^1/C^5), 52.5 (–COO<u>C</u>H_3, C^1/C^5), 31.7 (C^6/C^7), 29.8, 27.3 (C^6/C^7).

HRMS (APCI): m/z calculated for $C^9H_{13}ClO_2N^+$ $[M+H]^+$ 202.0629, found 202.0632.

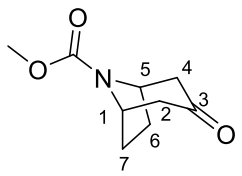
IR: 2955, 1703, 1453, 1405, 1340, 1298, 1223, 1193, 1109, 1045, 959, 904, 824, 801, 779, 744, 708, 675, 647, 628, 603 cm^{-1}

Prior to the synthesis shown in Scheme 4.2.2, attempts were also made to synthesise (±)-**1b** with the methyl carbamate protecting group attached at the beginning of the synthesis route (Scheme 4.2.3). We started from commercially available nortropinone hydrochloride salt and performed the protecting group switch to methyl carbamate. Then the following three steps were the same as the *N*-Boc substrate, where reduction–activation–elimination steps were completed in sequence. However, the next oxidation step remained unsuccessful after we experimented with several different oxidation conditions including epoxidation–ring opening and allylic oxidation.



Scheme 4.2.3 Overview of synthesis route of allyl chloride (±)-**1b** from nortropinone hydrochloride.

Synthesis of S1



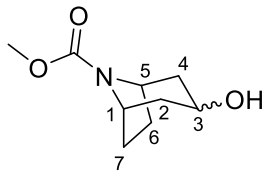
S1

According to procedure by Kubas *et. al*., [241] triethylamine (4.25 mL, 30.9 mmol) was added to a solution of nortropinone hydrochloride (1.00 g, 6.19 mmol) and DMAP (0.151 g, 1.24 mmol) in DCM (20 mL). The mixture was cooled to 0 °C, and methyl chloroformate (0.72 mL, 9.28 mmol) was added dropwise. The reaction mixture was stirred at r.t. overnight and diluted with DCM (20 mL), followed by washing with sat. aq. $NaHCO_3$ (20 mL), H_2O (20 mL) and drying over $MgSO_4$. Flash column chromatography (hex/EtOAC= 50/50 to 40/60) afforded the product **S1** as a white solid (0.961 g, 84% yield) as a single diastereomer (d.r. > 20:1). The spectroscopic data agrees with the literature. [241]

^{1}H NMR ($CDCl_3$, 400 MHz): δ (ppm) = 4.56 (s, 2H, C^1–H, C^5–H), 3.77 (s, 3H, –O$C\underline{H}_3$), 2.67 (s, 2H, C^2/C^4–H), 2.46 – 2.22 (m, 2H, C^2/C^4–H), 2.20 – 1.96 (m, 2H, C^6/C^7–H), 1.70 (t, J = 7.4 Hz, 2H, C^6/C^7–H).

^{13}C NMR ($CDCl_3$, 101 MHz) (two carbonyl carbons not observed due to low intensity of peaks): δ (ppm) = 53.3 (C^1, C^5), 52.6 (–O$\underline{C}H_3$), 49.2 (C^2, C^4), 28.9 (C^6, C^7).

Synthesis of S2



S2

According to a procedure by Baylis and coworkers, [242] $NaBH_4$ (0.508 g, 13.4 mmol) was added portionwise at 0 °C into a solution of **S1** (0.961 g, 5.25 mmol) in methanol (18 mL). The reaction mixture was stirred at r.t. for 1 h before quenching by dropwise addition of sat. aq. NH_4Cl (10 mL) at 0 °C. The reaction mixture was extracted with DCM (10 mL × 3) and dried

over $MgSO_4$. The solution was concentrated *in vacuo* and **S2** was afforded as a white solid (0.888 g, 92%) as mixture of diastereomers (d.r. ~1.6:1) and was directly used in the next step without purification.

^{1}H NMR ($CDCl_3$, 400 MHz): δ (ppm) = 4.45 – 4.14 (m, 2H, C^1–H, C^5–H), 4.10 (m, 1H, C^3–H), 3.69 (s, 3H, –O<u>C</u>H_3), 2.17 (t, *J* = 6.7 Hz, 2H, C^2/C^4–H), 2.03 – 1.87 (m, 2H, C^2/C^4–H), 1.72 (d, *J* = 15.1 Hz, 2H, C^6/C^7–H), 1.76 – 1.50 (m, 2H, C^6/C^7–H).

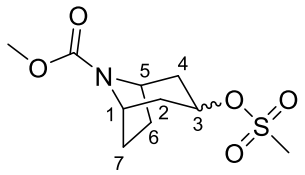
^{13}C NMR ($CDCl_3$, 101 MHz) (carbonyl carbon not observed due to low intensity of peaks): δ (ppm) = 65.4 (C^3), 53.2 (C^1, C^5), 52.3 (–O<u>C</u>H_3), 39.0 (C^2, C^4), 27.9 (C^6, C^7).

HRMS (APCI): m/z calculated for $C^9H_{14}O_2N^+$ $[M\text{-}OH]^+$ 168.10191, found 168.10210.

IR: 3421, 2925, 1673, 1455, 1398, 1363, 1330, 1193, 1112, 1085, 1043, 1016, 981, 943, 900, 870, 822, 769 cm^{-1}

Melting Point: 78.2 – 80.6 °C

Synthesis of S3



S3

According to a literature procedure by Nagase *et. al*., [238] triethylamine (1.02 mL, 7.27 mmol) was added into a solution of **S2** (0.888 g, 4.55 mmol) in DCM (14 mL). The mixture was cooled to 0 °C and methanesulfonyl chloride (0.44 mL, 5.46 mmol) was added dropwise. The reaction mixture was stirred at 0 °C for 3h before quenching with 1 M HCl (2.0 mL). The organic phase was washed with H_2O (5 mL) and brine (5 mL), dried over $MgSO_4$ and concentrated *in vacuo*. Flash column chromatography (hex/EtOAc=50/50 to 40/60) afforded **S3** as a white solid (0.972 g, 77% yield) as a mixture of diastereomers (d.r. ~1.6:1).

^{1}H NMR ($CDCl_3$, 400 MHz): δ (ppm) = 5.22 – 4.91 (m, 1H, C^3–H), 4.30 (s, 2H, C^1–H, C^5–H), 3.71 (s, 3H, –O<u>C</u>H_3), 3.00 (s, 3H, –OSO_2<u>C</u>H_3), 2.43 – 1.96 (m, 6H, C^2–H, C^4–H, C^6/C^7–H),

1.94 – 1.60 (m, 2H, C^6/C^7–H).

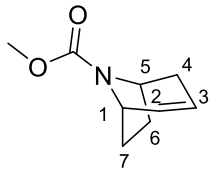
^{13}C NMR ($CDCl_3$, 101 MHz) (carbonyl carbon not observed due to low intensity of peaks): δ (ppm) = 74.8 (C^3), 52.6 (C^1, C^5), 52.5 (–O<u>C</u>H_3), 38.8 (–SO_2<u>C</u>H_3), 37.6 ($C^2/C^4/C^6/C^7$), 36.3 ($C^2/C^4/C^6/C^7$), 28.4 ($C^2/C^4/C^6/C^7$), 27.7 ($C^2/C^4/C^6/C^7$).

HRMS (APCI): m/z calculated for $C_{10}H_{17}O_5N_1NaS^+$ $[M+Na]^+$ 286.07196, found 286.07205.

IR: 3614, 3496, 2958, 1688, 1452, 1396, 1234, 1215, 1168, 1110, 1085, 1030, 943, 902, 854, 769, 671 cm^{-1}

Melting Point: 60.4 – 64.2 °C.

Synthesis of S4



S4

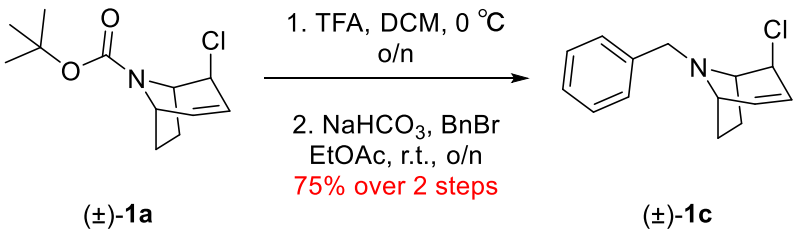
According to a literature procedure by Dallanoce and coworkers, [243] DBU (0.87 mL, 6.86 mmol) was added into a solution of **S3** (0.583 g, 2.29 mmol) in toluene (4.7 mL), and the mixture was stirred under reflux overnight. The reaction mixture was cooled to r.t. and directly loaded onto silica. Flash column chromatography (pet ether/EtOAc=85/15 to 50/50) afforded **S4** (0.202 g, 53% yield) as a single diastereomer (d.r. > 20:1).

^{1}H NMR ($CDCl_3$, 400 MHz): δ (ppm) = 5.98 (s, 1H, C^2–H), 5.52 (ddd, *J* = 10.0, 3.4, 1.5 Hz, 1H, C^3–H) 4.36 (m, 2H, C^1–H, C^5–H), 3.69 (s, 3H, –OC<u>H</u>$_3$), 2.74 (m, 3H, C^4–H), 2.17 (m, 2H, C^4–H), 2.01 – 1.87 (m, 2H, C^6/C^7–H), 1.81 (ddt, *J* = 17.7, 4.4, 1.5 Hz, 1H, C^6/C^7–H), 1.70 (d, *J* = 10.5 Hz, 2H, C^6/C^7–H).

^{13}C NMR ($CDCl_3$, 101 MHz) (C^4 and carbonyl carbon not observed due to low intensity): δ (ppm) = 132.8 (C^2), 124.3 (C^3), 53.5 (C^1, C^5), 52.4 (–O<u>C</u>H_3), 35.2 (C^6/C^7), 30.2 (C^6/C^7).

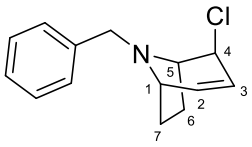
LRMS: m/z calculated for $C^9H_{14}O_2N_1^+$ $[M+H]^+$ 168.2.

Synthesis of Benzyl-Protected Allylic Chloride (±)-1c



Scheme 4.2.4 Overview of synthesis of (±)-**1c**.

According to a procedure by Karabiyikoglu *et al.*, [177] (±)-**1a** (0.134 g, 0.55 mmol) was dissolved in DCM (4.1 mL) and TFA (0.41 mL) was added dropwise at 0 °C. The ice bath was removed, and the reaction mixture was left stirring overnight. The crude mixture was concentrated *in vacuo* and dissolved in EtOAc (0.35 mL), and the solution was added dropwise into the solution of benzyl bromide (69 µL, 1.1 mmol) in EtOAc (0.88 mL) at 0 °C, and $NaHCO_3$ (0.69 g, 8.2 mmol) was added slowly portionwise to the solution. The reaction mixture was left stirring at room temperature overnight. The crude mixture was diluted with EtOAc (5 mL) and washed with H_2O (5 mL) and brine (5 mL). The mixture was extracted with EtOAc (5 mL × 3), and the organic phase was dried over $MgSO_4$, then concentrated under vacuum. The crude product was purified by flash column chromatography (hex/EtOAc = 90/10 to 80/20) to afford the product as a clear oil (97 mg, 75% yield).



(±)-**1c**

^{1}H NMR ($CDCl_3$, 400 MHz): δ (ppm) = 7.37 (d, *J* = 7.1 Hz, 2H, aryl–H), 7.29 – 7.13 (m, 3H, aryl–H), 6.02 (ddd, *J* = 9.5, 5.7, 1.0 Hz, 1H, C^2–H), 5.63 (ddd, *J* = 9.5, 4.0, 1.6 Hz, 1H, C^3–H), 4.10 (d, *J* = 3.9 Hz 1H, C^4–H), 3.76 (d, *J* = 13.6 Hz, 1H, –NC$\underline{H}_2$Ph), 3.54 (d, *J* = 13.6 Hz, 1H, –NC$\underline{H}_2$Ph), 3.48 (d, *J* = 7.9 Hz, 1H, C^1/C^5–H), 3.38 (t, *J* = 5.8 Hz, 1H, C^1/C^5–H), 2.25 – 2.03 (m, 1H, C^6/C^7–H), 2.05 – 1.80 (m, 1H, C^6/C^7–H), 1.67 – 1.56 (m, 1H, C^6/C^7–H), 1.44 – 1.32 (m, 1H, C^6/C^7–H).

^{13}C NMR ($CDCl_3$, 101 MHz): δ (ppm) = 135.8 (C^2), 128.9 (aryl–C), 128.2 (aryl–C), 126.9

(aryl–C), 123.9 (C^3), 64.0 C^1/C^5), 59.4 (C^4), 57.4 (C^1/C^5), 55.4 (–N<u>C</u>H_2Ph), 29.8 (C^6, C^7), 26.2 (C^6, C^7).

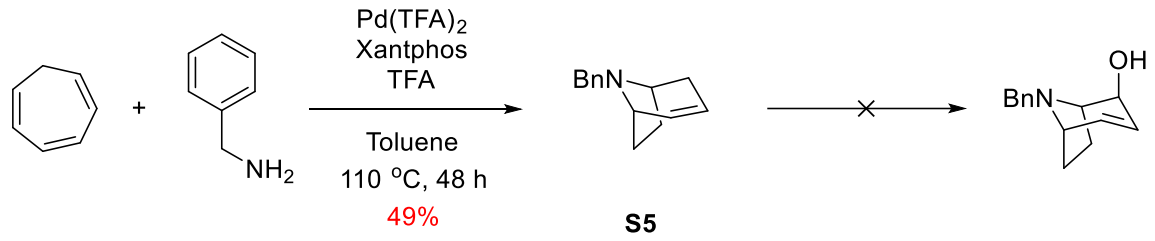
HRMS (APCI): m/z calculated for $C_{14}H_{17}ClN$ $[M+H]^+$ 234.1044, found 234.1046.

IR: 2957, 2871, 1703, 1495, 1452, 1389, 1356, 1318, 1297, 1273, 1256, 1226, 1207, 1153, 1106, 1073, 1044, 1030, 995, 959, 950, 887, 830, 799, 771, 739, 721, 696, 666 cm^{-1}

Melting Point: 46.7 – 47.1 °C.

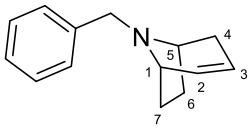
Attempted Synthesis of S5

Another route was investigated where consecutive inter- and intramolecular hydroamination of cycloheptatriene with benzylic amine occurred to form the benzyl-protected substrate **S10**. [172] The reaction proceeded nicely with 49%. Unfortunately, the following oxidation step failed to proceed, hence we continued to look into the synthesis of other possible substrates.



Scheme 4.2.5 Overview of synthesis of **S5**.

According to a literature procedure by Hartwig and coworkers, [172] $Pd(TFA)_2$ (0.199 g, 0.60 mmol), Xantphos (0.486 g, 0.84 mmol), and cycloheptatriene (4.9 mL, 48.0 mmol) were dissolved in toluene (12 mL) and the mixture was stirred for 2-3 min before benzylamine (1.3 mL, 12.0 mmol) was added. Trifluoroacetic acid (0.19 mL, 2.40 mmol) was added, and the reaction mixture was heated to 110 °C. The reaction was cooled to r.t. and quenched after 48 h by concentrating *in vacuo*. Flash column chromatography (hexane/acetone=99/1 to 96/4) afforded the product **S5** as a dark orange oil (1.17 g, 49% yield) as a single diastereomer (d.r. > 20:1). The spectroscopic data are in agreement with the literature. [172]



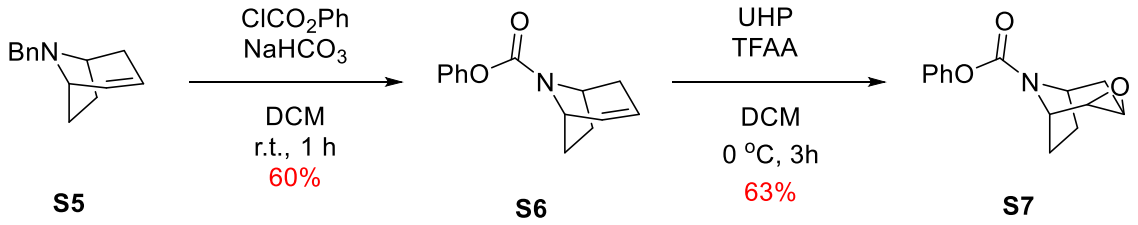
S5

^{1}H NMR ($CDCl_3$, 400 MHz): δ (ppm) = 7.42 – 7.35 (m, 2H, aryl–H), 7.34 – 7.27 (m, 2H, aryl–H), 7.26 – 7.20 (m, 1H, aryl–H), 5.78 (ddt, *J* = 9.4, 5.1, 2.0 Hz, 1H, C^2–H), 5.63 (m, 1H, C^3–H), 3.71 (d, *J* = 2.9 Hz, 2H, –N$C\underline{H}_2$–), 3.27 (ddt, *J* = 7.3, 4.5, 1.2 Hz, 1H, C^1/C^5–H), 3.21 (t, *J* = 5.5 Hz, 1H, C^1/C^5–H), 2.53 (ddd, *J* = 17.9, 4.7, 2.3 Hz, 1H, C^4–H), 2.25 – 2.10 (m, 1H, C^4–H), 2.08 – 1.93 (m, 1H, C^6/C^7–H), 1.85 (ddd, *J* = 11.9, 9.4, 2.8 Hz, 1H, C^6/C^7–H), 1.71 – 1.53 (m, 2H, C^6/C^7–H).

^{13}C NMR ($CDCl_3$, 101 MHz): δ (ppm) = 131.1 (C^2), 128.9 (aryl–C), 128.3 (aryl–C), 126.8 (aryl–C), 123.7 (C^3), 56.7 (C^1/C^5), 55.9 (C^1/C^5), 53.3 (–N$\underline{C}H_2$Bn), 34.3 (C^6/C^7), 31.9 (C^4), 30.2 (C^6/C^7).

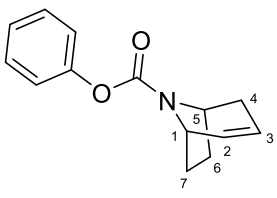
Due to the unsuccessful attempt to perform allylic oxidation on **S5**, we switched the protecting group from benzyl to phenyl carbamate to explore possibility to do selective oxidation on the phenyl carbamate-protected substrate **S6**.

Synthesis of S6 and S7



S5 **S6** **S7**

Scheme 4.2.6 Overview of synthesis of phenyl carbamate-protected substrate **S11** and **S12**.



S6

According to a procedure by Kotturi *et. al*.,[10] phenyl chloroformate (7.0 mL, 5.60 mmol) was added dropwise at 0 ℃ into a solution of **S5** (1.12 g, 5.60 mmol) and $NaHCO_3$ (2.83 g, 33.6 mmol) in DCM (13.4 mL). The ice bath was removed, and the reaction mixture was stirred at r.t. for 1 h before quenching with sat. aq. $NaHCO_3$ (10 mL). The mixture was extracted with EtOAc (10 ml × 3), and the combined organic layer was washed with H_2O (20 mL) and dried over $MgSO_4$. The solution was concentrated, and the crude product was purified by flash column chromatography (hex/DCM= 50/50 to 30/70) to afford the product **S6** as a white solid (0.767 g, 60% yield) as a single diastereomer (d.r. > 20:1).

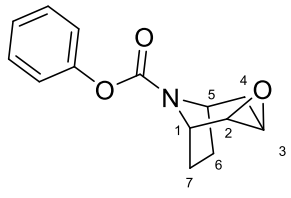
^{1}H NMR ($CDCl_3$, 400 MHz): δ (ppm) = 7.40 – 7.28 (m, 2H, aryl–H), 7.23 – 7.14 (m, 1H, aryl–H), 7.15-7.04 (m, 1H, aryl–H), 6.06 (ddt, *J* = 9.5, 5.1, 2.1 Hz, 1H, C^2–H), 5.66 – 5.52 (m, 1H, C^3–H), 4.64 – 4.31 (m, 2H, C^1–H, C^5–H), 2.89 (d, *J* = 17.9 Hz, 1H, C^4–H), 2.41 – 2.14 (m, 1H, C^4–H), 2.14 – 1.92 (m, 2H, C^6/C^7–H), 1.92 – 1.62 (m, 2H, C^6/C^7–H).

^{13}C NMR ($CDCl_3$, 101 MHz) (carbonyl carbon not observed due to low intensity): δ (ppm) = 132.4 (C^2), 129.3 (aryl–C), 125.2 (aryl–C), 124.5 (C^3), 121.8 (aryl–C), 53.7 (C^1, C^5), 34.5 (C^4, C^6/C^7), 29.6 (C^6/C^7).

HRMS (APCI): m/z calculated for $C_{14}H_{15}O_2N_1Na^+$ $[M+Na]^+$ 252.09950, found 252.09965.

IR: 3366, 2977, 1713, 1594, 1493, 1396, 1341, 1319, 1203, 1182, 1163, 1127, 1061, 996, 963, 914, 873, 831, 746, 705, 689, 671 cm^{-1}

Melting Point: 81.7 – 84.2 ℃.



S7

According to a procedure by Goeztke *et al*., [71] a solution of TFAA (0.43 mL, 10.0 mmol) in DCM (1.6 mL) was added dropwise into a solution of UHP (0.943 g, 10.0 mmol) in DCM (2.6 mL) at 0 ℃ and the mixture was stirred for 1 h, before a solution of **S6** (0.767 g, 3.34 mmol) in DCM (1.6 mL) was added. The mixture was stirred for another 3 h before diluting with DCM

(20 mL) and washing with sat. aq. $NaHCO_3$ (10 mL) and dried over $MgSO_4$. Flash column chromatography (hex/EtOAc=70/30) afforded **S7** as a white solid (0.517 g, 63% yield) as a single diastereomer (d.r. > 20:1).

^{1}H NMR ($CDCl_3$, 400 MHz): δ (ppm) = 7.40 – 7.29 (m, 2H, aryl–H), 7.23 – 7.09 (m, 3H, aryl–H), 4.64 – 4.52 (m, 1H, C^2–H), 4.27 – 4.06 (m, 1H, C^4–H), 3.09 (m, 2H, C^1–H, C^6–H), 2.57 (dd, *J* = 15.5, 5.4 Hz, 1H, C^5–H), 2.34 – 2.03 (m, 2H, C^4–H), 2.03 – 1.90 (m, 1H, C^6/C^7–H), 1.80 – 1.64 (m, 2H, C^6/C^7–H).

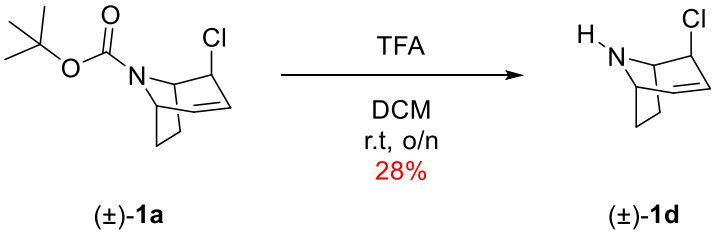
^{13}C NMR ($CDCl_3$, 101 MHz) (carbonyl carbon not observed due to low intensity): δ (ppm) = 129.3 (aryl–C), 125.2 (aryl–C), 122.0, 121.8 (aryl–C), 53.2 (C^2), 50.9 (C^4), 48.0 (C^1), 29.3 (C^5/C^6/C^7), 28.9 (C^5/C^6/C^7), 26.1 (C^5/C^6/C^7).

HRMS (APCI): m/z calculated for $C_{14}H_{15}O_3N_1Na^+$ $[M+Na]^+$ 268.09441, found 268.09436.

IR: 2980, 1714, 1594, 1492, 1394, 1362, 1319, 1195, 1159, 990, 965, 943, 885, 839, 782, 741, 691 cm^{-1}

Melting Point: 92.4 – 95.5 °C.

Synthesis of (±)-1d

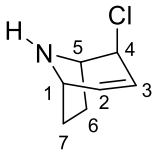


(±)-**1a** (±)-**1d**

Scheme 4.2.7 Overview of synthesis (±)-**1d**.

According to a procedure by Karabiyikoglu *et al.*, [177] (±)-**1a** (0.244 g, 1.00 mmol) was dissolved in DCM (5.0 mL) and TFA (2.5 mL) was added dropwise at 0 °C. The ice bath was removed, and the reaction mixture was left stirring overnight. DCM (5.0 mL) was added to the reaction, followed by dropwise addition of $NaHCO_3$ (sat. aq. solution, 10 mL) at 0 °C. The crude mixture was extracted with EtOAc (15 mL × 3) and dried over $MgSO_4$. The organic layer was concentrated under vacuum. The crude product was purified by flash column

chromatography (Acetone/MeOH/Et_3N = 99/1/1 to 86/10/4) to afford the product as a yellow oil (38.2 mg, 28 % yield).



(±)-**1d**

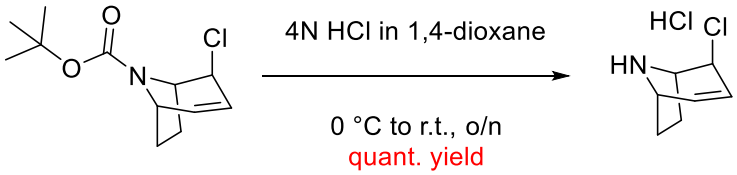
^{1}H NMR ($CDCl_3$, 400 MHz): δ (ppm) = 6.12 (ddd, *J* = 9.6, 5.1, 0.9 Hz, 1H, C^2–H), 5.59 (ddd, *J* = 9.5, 4.2, 1.8 Hz, 1H, C^3–H), 4.15 – 4.04 (m, 1H, C_4–H), 3.81 – 3.74 (m, 1H, C^1/C^5–H), 3.70 – 3.63 (m, 1H, C^1/C^5–H), 2.63 (br. s, 1H, -NH), 2.21 – 2.07 (m, 1H), 1.98 – 1.84 (m, 1H), 1.72 – 1.62 (m, 1H, C^6/C^7–H), 1.53 – 1.41 (m, 1H, C^6/C^7–H).

^{13}C NMR ($CDCl_3$, 101 MHz): δ (ppm) = 138.6 (C^2), 124.89 (C^3), 69.0 (C^1/C^5), 59.4 (C^1/C^5), 53.7 (C_4), 29.8 (C^6, C^7), 24.5 (C^6, C^7).

HRMS (APCI): m/z calculated for $C^7H_{11}ClN$ $[M+H]^+$ 144.0575, found 144.0575.

IR: 3384, 2973, 1640, 1467, 1380, 13432, 1308, 1163, 1130, 953, 817 cm^{-1}

Synthesis of (±)-**1e**

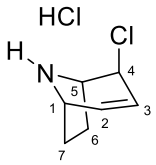


(±)-**1a** (±)-**1e**

Scheme 4.2.8 Overview of synthesis (±)-**1e**.

According to the procedure performed by Han and coworkers, [244] HCl (4 N in 1,4-dioxane, 40 mL) was added portionwise to (±)-**1a** (0.487g, 2.00 mmol) was at 0 °C. The ice bath was removed, and the reaction mixture was left stirring overnight. The reaction mixture was

concentrated *in vacuo*. The residue was washed with dry diethyl ether (10 mL × 3) and collected by vacuum filtration. The product was afforded as a light-yellow solid (0.360 g, quant. yield).



(±)-**1e**

^{1}H NMR (D_2O, 400 MHz): δ = 6.19 (ddd, *J* = 9.8, 5.6, 1.0 Hz, 1H, C^2–H), 5.96 (ddd, *J* = 9.8, 4.4, 1.6 Hz, 1H, C^3–H), 4.79 (m, 1H, C^4–H), 4.40 (m, 2H, C^1–H, C^5–H), 2.39 (m, 1H, C^6/C^7–H), 2.24 – 2.01 (m, 2H, C^6/C^7–H), 1.91 (m, 1H, C^6/C^7–H).

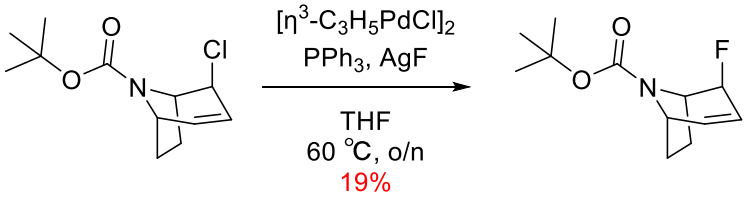
^{13}C NMR (D_2O, 101 MHz): δ (ppm) = 131.7 (C^2), 127.2 (C^3), 63.0 (C^1/C^5), 58.1 (C^4), 56.4 (C^1/C^5), 31.7 (C^6/C^7), 26.8 (C^6/C^7).

HRMS (APCI): m/z calculated for $C^7H_{12}Cl_2N$ $[M+H]^+$ 179.0269 and $C^7H_{11}ClN$ $[M–HCl+H]^+$ 144.0575, found 144.0575.

IR: 2884, 2753, 2593, 2470, 1666, 1590, 1498, 1450, 1352, 1212, 1147, 1054, 928, 901, 812, 772, 730, 698 cm^{-1}

Melting Point: 130.7 – 131.8 °C

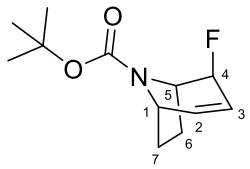
Synthesis of Allylic Fluoride (±)-**1f**



(±)-**1a** (±)-**1f**

Scheme 4.2.9 Overview of synthesis (±)-**1f**.

According to a procedure by Katcher *et al.*, [245] (±)-**1a** (0.244 g, 1.00 mmol) was added in THF (10 mL) to a mixture of $[PdCl(C_3H_5)]_2$ (18.3 mg, 5.0 mol %), PPh_3 (39.3 mg, 15 mol %), and AgF (0.254 g, 2.00 mmol). The reaction mixture wad heated to 60 °C and stirred overnight. The crude mixture was warmed to r.t. and filtered over Celite® and the solution was concentrated *in vacuo*. The crude product was purified by flash column chromatography (hexane/EtOAc = 90/10 to 80/20) to afford the product as a clear oil (44 mg, 19 % yield).



(±)-**1f**

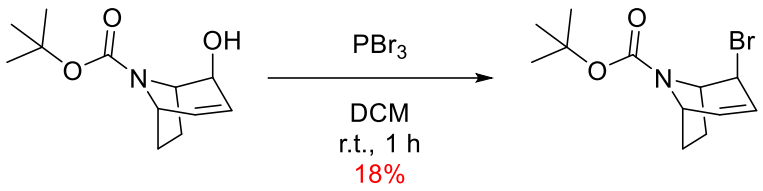
^{1}H NMR ($CDCl_3$, 400 MHz): δ (ppm) = 6.06 (s, 1H, C^2–H), 5.55– 5.37 (m, 1H, C^3–H), 4.55 – 3.96 (m, 3H, C^1/C^5–H, C^4–H), 2.29 – 1.97 (m, 1H, C^6/C^7–H), 2.00 – 1.88 (m, 1H, C^6/C^7–H), 1.87 – 1.73 (m, 1H, C^6/C^7–H), 1.79 – 1.62 (s, 1H, C^6/C^7–H), 1.39 (s, 9H, –$C(CH_3)_3$).

^{13}C NMR ($CDCl_3$, 101 MHz): δ (ppm) = 153.5 (–C=O), 136.1 (C^2), 123.8 (C^3), 80.0 (–$\underline{C}(CH_3)_3$), 56.0 (C^4), 55.5 (C^1/C^5), 53.2 (rot. C^1/C^5), 53.2 (rot. C^1/C^5), 52.9 (C^1/C^5), 34.7 (C^6, C^7), 28.4 (–$C(\underline{C}H_3)_3$), 21.8 (C^6, C^7).

HRMS (APCI): m/z calculated for $C_{12}H_{18}FNNaO_2$ $[M+Na]^+$ 250.1213, found 250.1214.

IR: 2987, 2359, 2340, 1638, 1403, 1335, 1260, 1177, 1024, 947, 894, 871, 849, 804, 774, 750, 727, 711, 684, 666, 648, 630, 620, 606 cm^{-1}

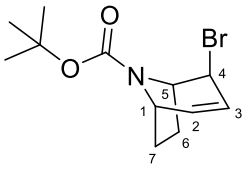
Synthesis of Allylic Bromide (±)-**1g**



(±)-**S5** (±)-**1g**

Scheme 4.2.10 Overview of synthesis (±)-**1g**.

According to a procedure by Zhang *et al.*, [246] (±)-**S5** (0.113 g, 0.50 mmol) was dissolved in DCM (0.5 mL), and PBr_3 (25 µL, 0.28 mmol) was added slowly over 15 min at 0 °C. The ice bath was removed, and the reaction mixture was left stirring for 1 h. DCM (1.0 mL) was added to quench the reaction, and the reaction mixture was washed with cold H_2O (1.5 mL × 2) and brine (sat. aq. solution, 1.5 mL × 2), followed by extraction with DCM (2.0 mL × 2). The organic layer was dried over $MgSO_4$ and concentrated *in vacuo*. The crude product was purified by quick flash column chromatography (hexane/EtOAc = 90/10 to 85/15) to afford the product as a clear oil (26 mg, 18 % yield).



(±)-**1f**

^{1}H NMR ($CDCl_3$, 400 MHz): δ (ppm) = 5.98 (s, 1H, C^2–H), 5.72 – 5.65 (m, 1H, C^3–H), 4.62 (s, 1H, C^1/C^5–H), 4.54 (s, 1H, C^1/C^5–H), 4.38 (s, 1H, C^4–H), 2.15 – 2.05 (m, 1H, C^6/C^7–H), 1.69 – 1.59 (m, 1H, C^6/C^7–H), 1.55 – 1.43 (m, 1H, C^6/C^7–H), 1.42 (s, 9H, –$C(CH_3)_3$), 1.18 (s, 1H, C^6/C^7–H).

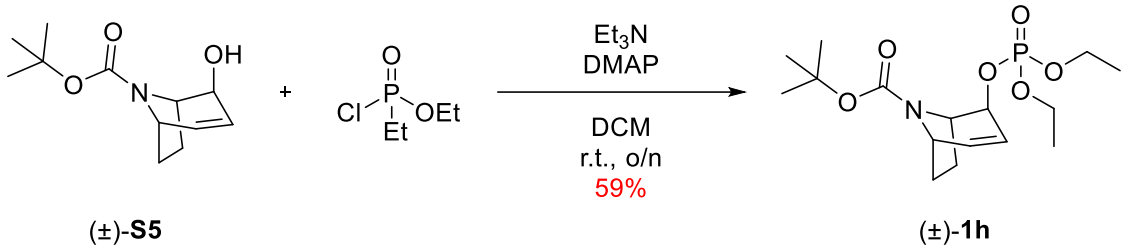
^{13}C NMR ($CDCl_3$, 101 MHz): δ (ppm) = 152.1 (–C=O), 132.2 (C^2), 125.5 (C^3), 80.0 (–$\underline{C}(CH_3)_3$), 56.8 (C^1/C^5), 55.5 (rot. C^1/C^5), 52.5 (rot. C^1/C^5), 51.4 (C^1/C^5), 50.8 (C^4), 30.7 (C^6, C^7), 28.5 (–$C(\underline{C}H_3)_3$), 26.5 (C^6, C^7).

HRMS (APCI): m/z calculated for $C_{12}H_{18}BrNO_2$ 287.0521 and 289.0500, molecular ion not

found.

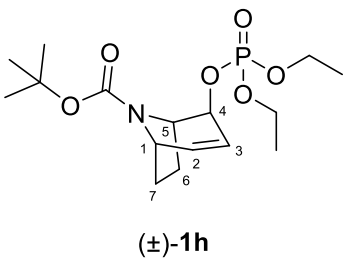
IR: 2980, 1702, 1605, 1439, 1392, 1361, 1165, 1145, 1092, 1042, 1028, 964, 860, 817, 765, 731, 673, 657, 627 cm^{-1}

Synthesis of Allylic Phosphate (±)-**1h**



Scheme 4.2.11 Overview of synthesis (±)-**1h**.

According to a procedure by Jacques *et al.*, [69] (±)-**S5** (0.264 g, 1.17 mmol) was dissolved in DCM (5.4 mL) and added dropwise to DMAP (7.46 mg, 0.06 mmol) at 0 °C. Diethyl chlorophosphite (0.26 mL, 1.76 mmol) was added dropwise into the reaction mixture at 0 °C. The ice bath was removed, and the reaction mixture was left stirring overnight. H_2O (4.0 mL) was slowly added to quench the reaction, and the reaction mixture was extracted with DCM (10 mL × 2) and the organic layer was washed with brine (sat. aq. solution, 5.0 mL). The organic layer was dried over $MgSO_4$ and concentrated *in vacuo*. The crude product was purified by flash column chromatography (hexane/EtOAc = 80/20 to 20/80) to afford the product as a clear oil (0.281 g, 59 % yield).



^{1}H NMR ($CDCl_3$, 400 MHz): δ (ppm) = 6.21 (s, 1H, C^2–H), 5.67 – 5.58 (m, 1H, C^3–H), 4.65 – 4.42 (m, 2H, C^1–H, C^5–H), 4.36 (s, 1H, C^4–H), 4.15 – 3.96 (m, 4H,-($OC\underline{H}_2CH_3$)$_2$), 1.63 –

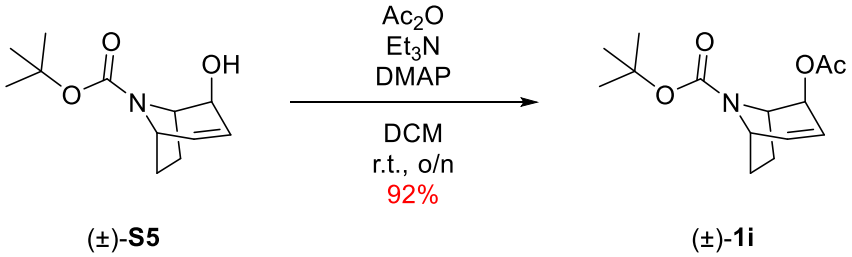
1.53 (m, 1H, C^6/C^7–H), 1.38 (s, 9H, –$C(CH_3)_3$), 1.36 – 1.28 (m, 1H, C^6/C^7–H), 1.31 – 1.17 (m, 7H, ,-($OCH_2C\underline{H}_3)_2$, C^6/C^7–H).

^{13}C NMR ($CDCl_3$, 101 MHz): δ (ppm) = 153.3 (–C=O), 137.2 (C^2), 122.2 (C^3), 79.5 (–$\underline{C}(CH_3)_3$), 74.5 (C^4), 63.7 (-($O\underline{C}H_2CH_3)_2$), 56.8 (C^1/C^5), 56.1 (rot. C^1/C^5), 53.0 (rot. C^1/C^5), 51.7 (C^1/C^5), 30.1 (C^6, C^7), 28.3 (–$C(\underline{C}H_3)_3$), 24.5 (C^6, C^7), 16.1 (-($OCH_2\underline{C}H_3)_2$).

HRMS (APCI): m/z calculated for $C_{16}H_{29}NO_6P$ $[M+H]^+$ 361.1727, found 362.1727.

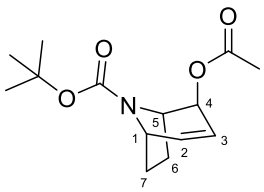
IR: 2981, 1697, 1478, 1420, 1367, 1343, 1322, 1260, 1167, 1106, 1070, 1017, 999, 972, 910, 884, 778, 719 cm^{-1}

Synthesis of Allylic Acetate (±)-**1i**



Scheme 4.2.12 Overview of synthesis (±)-**1i**.

According to a procedure by Nagata *et al.*, [247] (±)-**S5** (0.138 g, 0.61 mmol) was dissolved in DCM (4.1 mL) and added dropwise to DMAP (7.46 mg, 0.06 mmol) at 0 °C. Et_3N was added slowly into the reaction mixture, followed by dropwise addition of Ac_2O (87 µL, 0.92 mmol) at 0 °C. The ice bath was removed, and the reaction mixture was left stirring overnight. Et_2O (15 mL) was added to the reaction, and the reaction mixture was wash with brine (sat. aq. solution, 5.0 mL) followed by Et_2O extraction (10 mL × 2). The organic layer was dried over $MgSO_4$ and concentrated *in vacuo*. The crude product was purified by flash column chromatography (hexane/EtOAc = 90/10 to 70/30) to afford the product as a white solid (0.147 g, 92 % yield).



^{1}H NMR ($CDCl_3$, 400 MHz): δ (ppm) = 6.23 (s, 1H, C^2–H), 5.53 (s, 1H, C^3–H), 4.72 (s, 1H, C^4–H), 4.48 (s, 2H, C^1–H, C^5–H), 2.10 – 2.04 (m, 1H, C^6/C^7–H), 2.01 (s, 3H, -OCOCH_3), 1.66 – 1.51 (m, 2H, C^6/C^7–H), 1.38 (s, 9H, –$C(CH_3)_3$).

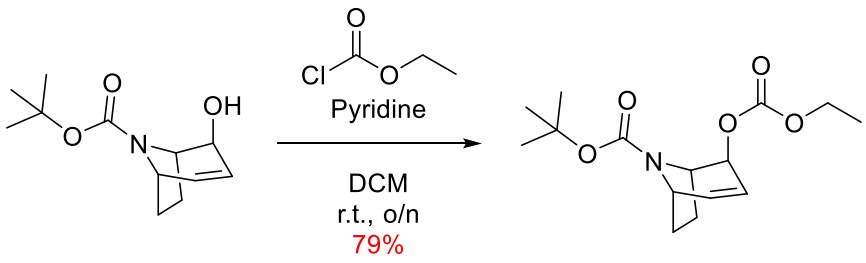
^{13}C NMR ($CDCl_3$, 101 MHz): δ (ppm) = 153.0 (–C=O), 137.7 (C^2), 121.6 (C^3), 79.4 (–$\underline{C}(CH_3)_3$), 71.6 (C^4), 55.4 (C^1/C^5), 54.7 (rot. C^1/C^5), 53.3 (rot. C^1/C^5), 51.8 (C^1/C^5), 30.5 (C^6, C^7), 28.4 (–$C(\underline{C}H_3)_3$), 25.1 (C^6, C^7), 21.3 (-OCO$\underline{C}H_3$).

HRMS (APCI): m/z calculated for $C_{14}H_{21}NNaO_4$ $[M+Na]^+$ 290.1363, found 290.1362.

IR: 2957, 2871, 1703, 1495, 1452, 1389, 1356, 1297, 1273, 1257, 1226, 1207, 1153, 1106, 1044, 1030, 995, 959, 887, 799, 771, 739, 721, 696, 666 cm^{-1}

Melting Point: 64.8 – 66.7 °C

Synthesis of Allylic Ethyl Carbonate (±)-**1j**

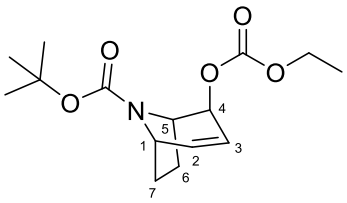


(±)-**S5** (±)-**1j**

Scheme 4.2.13 Overview of synthesis (±)-**1j**.

According to a procedure by Almehmadi *et. al.*, [248] (±)-**S5** (0.338 g, 1.50 mmol) was added in DCM (7.5 mL), and pyridine (0.15 mL, 1.80 mmol) was added dropwise into the solution at 0 °C, followed by dropwise addition of ethyl chloroformate (0.16 mL, 1.65 mmol). The ice bath was removed, and the reaction was stirred overnight. $KHSO_4$ (1 M aq. Solution, 5.0 mL) was added to quench the reaction, and the reaction mixture was extracted with DCM (10 mL × 2) and washed with brine (sat. aq. Solution, 5.0 mL). The organic layer was dried over $MgSO_4$ and concentrated *in vacuo*. Purification by automated medium-pressure chromatography

(hexane/EtOAc = 100/0 to 85/15) afforded the product as a white solid (0.354 g, 79 % yield).



(±)-**1j**

^{1}H NMR ($CDCl_3$, 400 MHz): δ (ppm) = 6.30 (s, 1H, C^2–H), 5.62 – 5.54 (m, 1H, C^3–H), 4.59 – 4.47 (m, 1H, C^1–H, C^5–H), 4.25 – 4.09 (m, 1H, C^4–H), 2.19 – 2.11 (m, 1H, C^6/C^7–H), 1.64 (ddd, *J* = 11.6, 8.9, 2.4 Hz, 1H, C^6/C^7–H), 1.47 (s, 11H, C^6/C^7–H, –$C(CH_3)_3$).

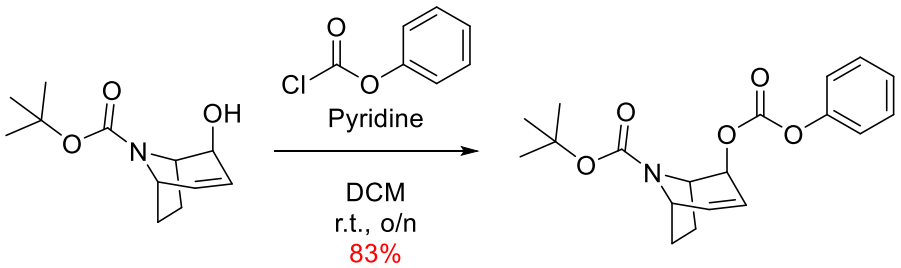
^{13}C NMR ($CDCl_3$, 101 MHz): δ (ppm) = 154.6 (–C=O), 154.1 (–C=O), 138.3 (C^2), 120.9 (C^3), 80.0 (–$\underline{C}(CH_3)_3$), 74.5 (C^4), 63.8 (–COO$\underline{C}H_2CH_3$), 55.2 (C^1/C^5), 51.8 (C^1/C^5), 30.3 (C^6, C^7), 28.2 (–$C(\underline{C}H_3)_3$), 24.8 (C^6, C^7), 14.2 (–$COOCH_2\underline{C}H_3$).

HRMS (APCI): m/z calculated for $C_{15}H_{23}NNaO_5$ $[M+Na]^+$ 320.1468, found 320.1470.

IR: 2982, 2348, 1738, 1698, 11392, 1371, 1339, 1295, 1258, 1173, 1105, 1047, 1010, 978, 865, 837, 794, 659, 645, 629, 615 cm^{-1}

Melting Point: 38.2 – 40.3 °C

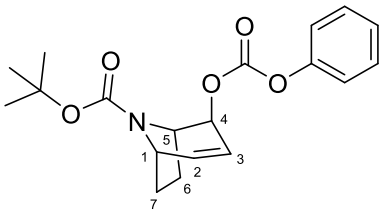
Synthesis of Allylic Phenyl Carbonate (±)-**1k**



(±)-**S5** (±)-**1k**

Scheme 4.2.14 Overview of synthesis (±)-**1k**.

According to a procedure by Almehmadi *et. al.*, [248] (±)-**S5** (0.338 g, 1.50 mmol) was added in DCM (7.5 mL), and pyridine (0.15 mL, 1.80 mmol) was added dropwise into the solution at 0 °C, followed by dropwise addition of phenyl chloroformate (0.21 mL, 1.65 mmol). The ice bath was removed, and the reaction was stirred overnight. $KHSO_4$ (1 M aq. Solution, 5.0 mL) was added to quench the reaction, and the reaction mixture was extracted with DCM (10 mL × 2) and washed with brine (sat. aq. Solution, 5.0 mL). The organic layer was dried over $MgSO_4$ and concentrated *in vacuo*. Purification by automated medium-pressure chromatography (hexane/EtOAc = 100/0 to 85/15) afforded the product as a white solid (0.432 g, 83 % yield).



(±)-**1k**

^{1}H NMR ($CDCl_3$, 400 MHz): δ (ppm) = 7.37 (t, *J* = 7.7 Hz, 2H, aryl–H), 7.27 – 7.16 (m, 3H, aryl–H), 6.38 (s, 1H, C^2–H), 5.69 (ddd, *J* = 9.7, 4.3, 1.8 Hz, 1H, C^3–H), 4.73 (d, *J* = 4.2 Hz, 1H, C^4–H), 4.69 – 4.44 (m, 2H, C^1–H, C^5–H), 2.24 – 2.14 (m, 1H, C^6/C^7–H), 1.68 (ddd, *J* = 11.6, 8.9, 2.4 Hz, 1H, C^6/C^7–H), 1.47 (s, 11H, C^6/C^7–H, –$C(CH_3)_3$).

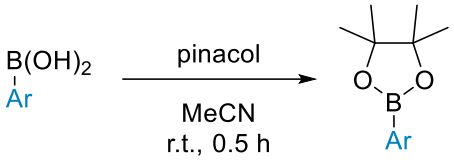
^{13}C NMR ($CDCl_3$, 101 MHz): δ (ppm) = 153.2 (–C=O), 151.2 (–C=O), 138.5 (C^2), 128.9 (aryl–C), 125.5 (aryl–C), 121.6 (C^3), 120.6 (aryl–C), 79.8 (–$\underline{C}(CH_3)_3$), 75.0 (C^4), 54.7 (C^1/C^5), 54.4 (rot. C^1/C^5), 53.2 (rot. C^1/C^5), 51.4 (C^1/C^5), 29.8 (C^6, C^7), 27.8 (–$C(\underline{C}H_3)_3$), 24.5 (C^6, C^7).

HRMS (APCI): m/z calculated for $C_{19}H_{24}NO_5$ $[M+H]^+$ 346.1649, found 346.1646.

IR: 2996, 2976, 1753, 1698, 1593, 1484, 1456, 1415, 1368, 1342, 1320, 1294, 1247, 1211, 1163, 1106, 1076, 1044, 1021, 974, 958, 908, 838, 769, 732, 688, 650, 633 cm^{-1}

Melting Point: 81.4 – 82.4 °C

Synthesis of Aryl- and Heteroaryl Boronic Acid Pinacol Esters



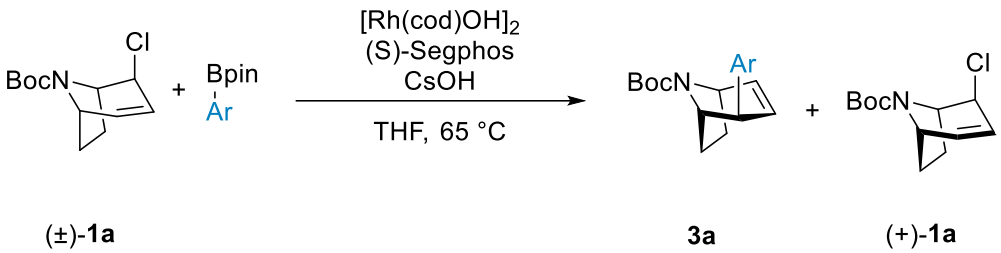
2b - 2t

Scheme 4.2.15 Overview of synthesis of boronic acid pinacol esters **2b** – **2t**.

According to the previous procedure by González *et al.*,[233] boronic acid (1.0 equiv.) and pinacol (1.02 equiv.) are dissolved in MeCN (1.2 M) and stirred under open air for 0.5 h until the solution became clear. The result solution was concentrated *in vacuo* and the crude product was purified using automated medium-pressure chromatography (hexane/EtOAc = 95/5 to 85/15) afforded the boronic pinacol ester as a solid (>90% yield).

4.2.2 Rh–Catalysed Allylic Arylation Reactions

General Procedure A



(±)-**1a** **3a** (+)-**1a**

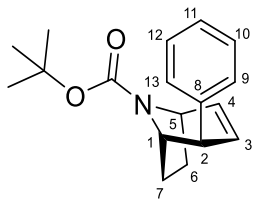
Scheme 4.2.16 Rh–Catalysed Suzuki-Miyaura cross–Coupling reaction between (±)-**1a** and boronic acid pinacol esters.

$[Rh(cod)OH]_2$ (2.3 mg, 2.5 mol%) and (*S*)-Segphos (7.3 mg, 6.0 mol%) were dissolved in THF (0.5 mL) under an argon atmosphere and CsOH (50 wt% aq., 70 µL, 0.40 mmol) was added. This catalyst solution was heated to 65 °C. After 0.5 h, a solution of boronic pinacol ester (0.40 mmol) and (±)-**1a** (48.7 mg, 0.20 mmol) in THF (0.40 mL) was added into the mixture. THF (0.10 mL) was used to rinse the flask. The reaction mixture was stirred at 65 °C for 1 h. The reaction mixture was cooled to r.t.. Hexane (2 mL) and silica (1 g) were added, and the solvent was removed under reduced pressure. Automated liquid chromatography was performed to purify the product using hexane/EtOAc as eluent.

Racemic samples of the products were synthesised with *rac*-BINAP (purchased from commercial suppliers) or *rac*-Segphos (mixed by manually mixing the *R* and *S*-Segphos in 1:1 ratio) as the ligand.

4.2.3 Product Characterisations

Synthesis of 3a



3a

The corresponding compound was prepared following General Procedure A using (±)-**1a** and phenyl boronic pinacol ester **2a**. Purification by automated medium-pressure chromatography (hexane/EtOAc = 95/5 to 90/10) afforded the product **3a** as a white solid (29 mg, 50% yield). SFC analysis showed an enantiomeric excess of 95%.

Further, (+)-**1a** was isolated as a white solid (19 mg, 39% yield). SFC analysis showed an enantiomeric excess of >99%.

^{1}H NMR ($CDCl_3$, 400 MHz): δ (ppm) = 7.35-7.26 (m, 2H, aryl–H), 7.25-7.15 (m, 3H, aryl–H), 6.24 (d, *J* = 8.3 Hz, 1H, C^4–H), 5.59 (ddd, *J* = 9.6, 4.1, 1.7 Hz, 1H, C^3–H), 4.70-4.48 (m, 1H, C^1/C^5–H), 4.31 (d, *J* = 7.9 Hz, 1H, C^1/C^5–H), 3.22 (dt, *J* = 3.6, 1.6 Hz, 1H, C^2–H), 2.22 (dt, *J* = 17.4, 5.7 Hz, 1H, C^6/C^7–H), 1.94-1.68 (m, 2H, C^6/C^7–H), 1.34 (m, 1H, C^6/C^7–H), 1.04 (s, 9H, –$C(CH_3)_3$)

^{13}C NMR ($CDCl_3$, 101 MHz): δ (ppm) = 152.5 (–C=O), 142.6 (C^8), 133.3 (C^4), 131.9 (rot. C^4), 128.5 (C^9, C^{13}), 128.4 (C^{10}, C^{12}), 126.5 (C^{11}), 125.5 (C^3), 78.8 (–$\underline{C}(CH_3)_3$) ,59.0 (C^1/C^5), 57.5 (rot. C^1/C^5), 53.6 (rot. C^1/C^5), 52.0 (C^1/C^5), 51.5 (C^2), 34.0 (C^6/C^7), 30.1 (C^6/C^7), 28.5 (rot. –$C(\underline{C}H_3)_3$), 28.05 (–$C(\underline{C}H_3)_3$).

HRMS (APCI): m/z calculated for $C_{18}H_{23}O_2NNa^+$ $[M+Na]^+$ 308.1621, found 308.1621.

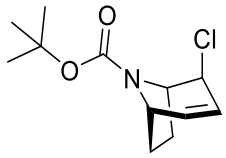
IR: 2969, 2927, 2868, 1678, 1478, 1425, 1390, 1363, 1344, 1308, 1247, 1171, 1130, 1105, 1040, 1005, 968, 896, 875, 856, 829, 750, 717, 700, 633 cm^{-1}

Melting Point: 96- 99 °C

SFC Chiralpak ® IF; 1500 psi, 30 °C; flow: 1.5 ml/min; from 1% to 20% MeOH in 5 min (major enantiomer t_R = 2.63 min; minor enantiomer t_R = 2.93 min)

[α]$^{25}_D$ = −106.7 (c = 1.0, $CHCl_3$).

Analytical data for enantioenriched (+)-1a

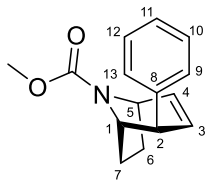


(+)-**1a**

SFC Chiralpak ® IG; 1500 psi, 30 °C; flow: 1.5 ml/min; from 1% to 30% MeOH in 5 min (major enantiomer t_R = 2.33 min)

[α]$^{25}_D$ = +217.6 (c = 1.0, $CHCl_3$, ee >99%).

Synthesis of 3ab



3ab

The corresponding compound was prepared following General Procedure A using (±)-**1b** and phenyl boronic pinacol ester **2a**. heating the reaction overnight. Purification by flash column chromatography (hexane/EtOAc = 100/0 to 80/20) afforded the product **3ab** as a colourless oil (33 mg, 67% yield). ^{1}H NMR showed a diastereomeric excess of 5.9:1. SFC analysis showed an enantiomeric excess of 94%.

^{1}H NMR ($CDCl_3$, 400 MHz): δ (ppm) = 7.34 – 7.28 (m, 2H, aryl–H), 7.20 (td, *J* = 7.0, 1.3 Hz, 3H, aryl–H), 6.24 (s, 1H, C^4–H), 5.60 (ddd, *J* = 9.7, 4.2, 1.7 Hz, 1H, C^3–H), 4.67 – 4.23 (m, 2H, C^1–H, C^5–H), 3.61 (s, 1H, C^2–H), 3.34 – 2.99 (m, 3H, –$COOCH_3$), 2.27 – 2.20 (m, 1H, C^6/C^7–H), 2.00 – 1.88 (m, 2H, C^6/C^7–H), 1.85 – 1.80 (m, 1H, C^6/C^7–H).

^{13}C NMR ($CDCl_3$, 101 MHz): δ (ppm) = 154.4 (–C=O), 132.9 (C^4), 128.4 (C^8), 128.3 (aryl–C), 126.7 (aryl–C), 125.6 (C^3), 59.0 (C^1/C^5), 52.9 (C^2), 51.6 (–$COOCH_3$), 34.0 (C^6/C^7), 30.0 (C^6/C^7).

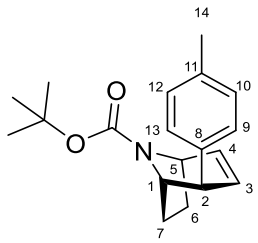
HRMS (APCI): m/z calculated for $C_{15}H_{18}O_2N^+$ $[M+H]^+$ 244.1332, found 244.1333.

IR: 2923, 2854, 1703, 1453, 1405, 1334, 1194, 1109, 1045, 752, 715, 700, 665, 656, 601 cm^{-1}

SFC Chiralpak ® IE; 1500 psi, 30 °C; flow: 1.5 ml/min; from 1% to 30% MeOH in 5 min (major enantiomer t_R = 3.46 min; minor enantiomer t_R = 3.35 min)

$[\alpha]^{25}_D$ = −47.0 (c = 1.0, $CHCl_3$).

Synthesis of 3b



3b

The corresponding compound was prepared following General Procedure A using (±)-**1a** and **2b**. Purification by automated medium-pressure chromatography (hexane/EtOAc = 100/0 to 90/10) afforded the product **3b** as a white solid (26 mg, 44% yield). SFC analysis showed an enantiomeric excess of 96%.

Further, (+)-**1a** was isolated as a white solid (approx. 15 mg, 30% yield), contaminated with small amounts of **2b.** SFC analysis showed an enantiomeric excess of >99%.

^{1}H NMR ($CDCl_3$, 600 MHz) δ (ppm) = 7.10 (s, 4H, aryl–H), 6.30 – 6.04 (m, 1H, C^4–H), 5.58 (ddd, *J* = 9.7, 4.2, 1.7 Hz, 1H, C^3–H), 4.65 – 4.19 (m, 2H, C^1–H, C^5–H), 3.18 (d, *J* = 4.2 Hz, 1H, C^2–H), 2.32 (s, 3H, C^{14}–H), 2.27 – 2.12 (m, 1H, C^6/C^7–H), 1.97 – 1.85 (m, 2H, C^6/C^7–H), 1.85 – 1.74 (m, 1H, C^6/C^7–H), 1.05 (s, 9H, –$C(CH_3)_3$).

^{13}C NMR ($CDCl_3$, 151 MHz) δ (ppm) = 152.5 (–C=O), 139.6 (C^8), 135.9 (C^{11}), 133.1 (C^4), 131.66 (rot. C^4), 129.0 (aryl–C), 128.3 (aryl–C), 128.1 (aryl–C), 126.8 (rot. C^3), 125.7 (C^3), 79.1 (–$\underline{C}(CH_3)_3$), 59.0 (C^1/C^5), 57.6 (rot. C^1/C^5), 53.5 (rot. C^1/C^5), 52.0 (C^1/C^5), 51.2 (C^2), 34.5 (rot. C^6/C^7), 34.0 (C^6/C^7), 30.0 (C^6/C^7), 29.2 (rot. C^6/C^7), 28.5 (rot. –$C(\underline{C}H_3)_3$), 28.0 (–$C(\underline{C}H_3)_3$), 21.1 (C^{14}).

HRMS (APCI): m/z calculated for $C_{19}H_{25}O_2NNa^+$ $[M+Na]^+$ 322.1778, found 322.1775.

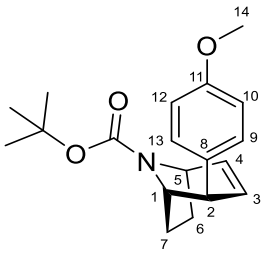
IR: 2974, 2928, 2871, 2360, 2341, 1693, 1513, 1478, 1422, 1391, 1365, 1339, 1303, 1251, 1230, 1173, 1132, 1104, 1062, 1042, 1022, 1007, 971, 912, 803, 783, 686, 640 cm^{-1}

Melting Point: 91.8 - 92.6 °C

SFC Chiralpak ® IB; 1500 psi, 30 °C; flow: 1.5 ml/min; from 1% to 30% MeOH in 5 min (major enantiomer t_R = 1.81 min; minor enantiomer t_R = 1.72 min)

$[\alpha]^{25}_D$ = −114.0 (c = 1.0, $CHCl_3$).

Synthesis of 3c



3c

The corresponding compound was prepared following General Procedure A using (±)-**1a** and

2c. Purification by automated medium-pressure chromatography (hexane/EtOAc = 100/0 to 90/10) afforded the product **3c** as a white solid (20 mg, 32% yield). SFC analysis showed an enantiomeric excess of 94%.

Further, (+)-**1a** was isolated as a white solid (18 mg, 37% yield). SFC analysis showed an enantiomeric excess of >99%.

^{1}H NMR ($CDCl_3$, 600 MHz) δ (ppm) = 7.12 (d, *J* = 8.4 Hz, 2H, aryl–H), 6.83 (d, *J* = 8.2 Hz, 2H, aryl–H), 6.28 – 6.04 (m, 1H, C^4–H), 5.56 (ddd, *J* = 9.6, 4.2, 1.6 Hz, 1H, C^3–H), 4.63 – 4.21 (m, 2H, C^1–H, C^5–H), 3.78 (s, 3H, C^{14}–H), 3.17 (d, *J* = 4.1 Hz, 1H, C^2–H), 2.26 – 2.12 (m, 1H, C^6/C^7–H), 1.98 – 1.81 (m, 2H, C^6/C^7–H), 1.81 – 1.64 (m, 1H, C^6/C^7–H), 1.08 (s, 9H, –$C(CH_3)_3$).

^{13}C NMR ($CDCl_3$, 151 MHz) δ (ppm) = 158.5 (–C=O), 152.5 (C^{11}), 134.9 (C^8), 132.9 (C^4), 131.6 (rot. C^4), 129.4 (C^9/C^{13}), 129.2 (C^9/C^{13}), 126.8 (rot. C^3), 125.8 (C^3), 113.8 (C^9, C^{12}), 78.7 (–$\underline{C}(CH_3)_3$), 59.0 (C^1/C^5), 57.6 (rot. C^1/C^5), 55.5 (C^{14}), 53.5 (rot. C^1/C^5), 52.0 (C^1/C^5), 50.8 (C^2), 34.0 (C^6/C^7), 29.8 (C^6/C^7), 29.0 (rot. C^6/C^7), 28.5 (rot. –$C(\underline{C}H_3)_3$), 28.1 (–$C(\underline{C}H_3)_3$).

HRMS (APCI): m/z calculated for $C_{19}H_{25}O_3NNa^+$ $[M+Na]^+$ 338.1726, found 338.1724.

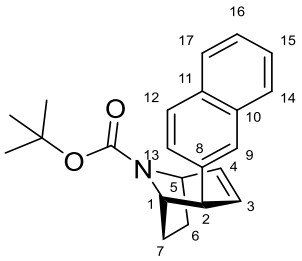
IR: 2934, 2835, 2349, 1689, 1611, 1510, 1423, 1340, 1246, 1177, 1106, 1038, 1007, 895, 861, 824, 786, 760, 706 cm^{-1}

Melting Point: 93.3- 94.3 °C

SFC Chiralpak ® IC; 1500 psi, 30 °C; flow: 1.5 ml/min; from 1% to 5% MeOH in 5 min (major enantiomer t_R = 4.27 min; minor enantiomer t_R = 4.08 min)

$[\alpha]^{25}_D$ = −115.1 (c = 1.0, $CHCl_3$).

Synthesis of 3d



3d

The corresponding compound was prepared following General Procedure A using (±)-**1a** and **2d**. Purification by automated medium-pressure chromatography (hexane/EtOAc = 100/0 to 90/10) afforded the product **3d** as a white solid (34 mg, 51% yield). SFC analysis showed an enantiomeric excess of 95%.

Further, (+)-**1a** was isolated as a white solid (15 mg, 31% yield). SFC analysis showed an enantiomeric excess of >99%.

^{1}H NMR ($CDCl_3$, 600 MHz) δ (ppm) = 7.89 – 7.68 (m, 3H, aryl–H), 7.60 (s, 1H, aryl–H), 7.51 – 7.34 (m, 3H, aryl–H), 6.38 – 6.11 (m, 1H, C^4–H), 5.70 (dd, *J* = 10.2, 4.1 Hz, 1H, C^3–H), 4.67 – 4.37 (m, 2H, C^1–H, C^5–H), 3.38 (d, *J* = 4.0 Hz, 1H, C^2–H), 2.36 – 2.17 (m, 1H, C^6/C^7–H), 2.08 – 1.91 (m, 2H, C^6/C^7–H), 1.91 – 1.72 (m, 1H, C^6/C^7–H), 1.08 (s, 9H, –$C(CH_3)_3$).

^{13}C NMR ($CDCl_3$, 151 MHz) δ (ppm) = 152.5 (–C=O), 134.0 (C^8), 133.7 (C^4), 133.6 (aryl–C), 132.5 (rot. C^4), 132.2 (aryl–C), 128.0 (aryl–C), 127.9 (aryl–C), 127.5 (aryl–C), 127.1 (aryl–C), 126.9 (aryl–C), 126.0 (aryl–C), 125.5 (C^3), 125.4 (aryl–C), 78.6 (–$\underline{C}(CH_3)_3$), 58.6 (C^1/C^5), 57.4 (rot. C^1/C^5), 53.6 (rot. C^1/C^5), 52.1 (C^1/C^5), 51.6 (C^2), 34.0 (C^6/C^7), 30.1 (C^6/C^7), 28.5 (rot. –$C(\underline{C}H_3)_3$), 27.8 (–$C(\underline{C}H_3)_3$).

HRMS (APCI): m/z calculated for $C_{22}H_{25}O_2NNa^+$ $[M+Na]^+$ 358.1777, found 358.1774.

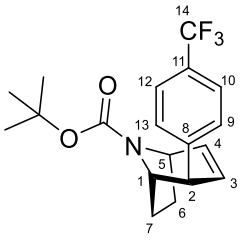
IR: 2974, 1689, 1421, 1339, 1305, 1247, 1174, 1133, 1104, 1043, 1008, 973, 897, 859, 815, 786, 746, 713, 626, 607 cm^{-1}

Melting Point: 134.4 – 135.0 °C

SFC Chiralpak ® IB; 1500 psi, 30 °C; flow: 1.5 ml/min; from 1% to 30% MeOH in 5 min (major enantiomer t_R = 3.00 min; minor enantiomer t_R = 2.63 min)

[α]$^{25}_D$ = −228.2 (c = 1.0, $CHCl_3$).

Synthesis of 3e



3e

The corresponding compound was prepared following General Procedure A using (±)-**1a** and **2e**. Purification by automated medium-pressure chromatography (hexane/EtOAc = 100/0 to 90/10) afforded the product **3e** as a white solid (31 mg, 44% yield). SFC analysis showed an enantiomeric excess of 94%.

Further, (+)-**1a** was isolated as a white solid (10 mg, 21% yield). SFC analysis showed an enantiomeric excess of >99%.

^{1}H NMR ($CDCl_3$, 600 MHz) δ (ppm) = 7.55 (d, *J* = 8.0 Hz, 2H, aryl–H), 7.34 (d, *J* = 8.0 Hz, 2H, aryl–H), 6.34 – 6.10 (m, 1H, C^4–H), 5.57 (ddd, *J* = 9.6, 4.2, 1.7 Hz, 1H, C^3–H), 4.66 – 4.19 (m, 2H, C^1–H, C^5–H), 3.28 (d, *J* = 4.4 Hz, 1H, C^2–H), 2.35 – 2.18 (m, 1H, C^6/C^7–H), 1.99 – 1.84 (m, 2H, C^6/C^7–H), 1.84 – 1.72 (m, 1H, C^6/C^7–H), 1.02 (s, 9H, –$C(CH_3)_3$).

^{13}C NMR ($CDCl_3$, 151 MHz) δ (ppm) = 152.3 (–C=O), 146.7 (C^8), 134.1 (C^4), 132.7 (rot. C^4), 129.2 (d, *J* = 129.18 Hz, C^{11}), 128.9 (C^9/C^{13}), 128.6 (C^9/C^{13}), 125.3 (q, *J* = 3.8 Hz, C^{10}, C^{12}), 124.5 (C^3), 124.5 (q, *J* = 271.9 Hz, –CF_3), 79.1 (–$\underline{C}(CH_3)_3$), 58.8 (C^1/C^5), 57.3 (rot. C^1/C^5), 53.6 (rot. C^1/C^5), 52.1 (C^1/C^5), 51.1 (C^2), 34.4 (rot. C^6/C^7), 33.9 (C^6/C^7), 30.0 (C^6/C^7), 29.2 (rot. C^6/C^7), 28.4 (rot. –$C(\underline{C}H_3)_3$), 28.0 (–$C(\underline{C}H_3)_3$).

^{19}F NMR (376 MHz, $CDCl_3$) δ (ppm) = −62.48 (s, rot. $–CF_3$), −62.57 (s, $–CF_3$).

HRMS (APCI): m/z calculated for $C_{19}H_{22}F_3O_2NNa^+$ $[M+Na]^+$ 376.1495, found 376.1495.

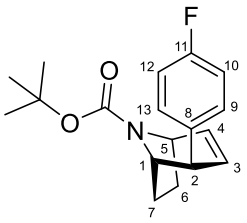
IR: 2360. 2341. 1678. 1477. 142. 1330, 1160, 1109, 1069, 1019, 863, 825, 778, 756, 716, 669, 655 cm^{-1}

Melting Point: 99.2 – 100.5 °C

SFC Chiralpak ® IF; 1500 psi, 30 °C; flow: 1.5 ml/min; from 1% to 5% MeOH in 5 min (major enantiomer t_R = 2.25 min; minor enantiomer t_R = 2.34 min)

$[\alpha]^{25}_D$ = −80.1 (c = 1.0, $CHCl_3$).

Synthesis of 3f



3f

The corresponding compound was prepared following General Procedure A using (±)-**1a** and **2f**. The reaction was stirred for 4 h. Purification by automated medium-pressure chromatography (hexane/EtOAc = 100/0 to 90/10) afforded the product **3f** as a white solid (30 mg, 49% yield). SFC analysis showed an enantiomeric excess of 98%.

Further, (+)-**1a** was isolated as a white solid (approx. 19 mg, 38% yield), contaminated with small amounts of **3f**. SFC analysis showed an enantiomeric excess of >99%.

^{1}H NMR ($CDCl_3$, 600 MHz) δ (ppm) = 7.23 – 7.11 (m, 2H, aryl–H), 6.98 (t, *J* = 8.7 Hz, 2H, aryl–H), 6.35 – 6.04 (m, 1H, C^4–H), 5.55 (ddd, *J* = 9.6, 4.3, 1.7 Hz, 1H, C^3–H), 4.68 – 4.18 (m, 2H, C^1–H, C^5–H), 3.20 (d, *J* = 4.2 Hz, 1H, C^2–H), 2.31 – 2.14 (m, 1H, C^6/C^7–H), 1.98 – 1.84

(m, 2H, C^6/C^7–H), 1.84 – 1.65 (m, 1H, C^6/C^7–H), 1.08 (s, 9H, –$C(CH_3)_3$).

^{13}C NMR ($CDCl_3$, 151 MHz) δ (ppm) = 161.8 (d, *J* = 244.5 Hz, C^{11}), 152.4 (–C=O), 138.2 (C^8), 133.2 (C^4), 132.0 (rot. C^4), 129.8 (d, *J* = 7.8 Hz, C^9, C^{13}), 126.2 (rot. C^3), 125.2 (C^3), 115.0 (d, *J* = 20.8 Hz, C^{10}, C^{12}), 78.8 (–$\underline{C}(CH_3)_3$), 58.8 (C^1/C^5), 57.5 (rot. C^1/C^5), 53.4 (rot. C^1/C^5), 51.9 (C^1/C^5), 50.6 (C^2), 34.3 (rot. C^6/C^7), 33.8 (C^6/C^7), 29.7 (C^6/C^7), 28.9 (rot. C^6/C^7), 28.3 (rot. –$C(\underline{C}H_3)_3$), 28.0 (–$C(\underline{C}H_3)_3$).

^{19}F NMR (376 MHz, $CDCl_3$) δ (ppm) = -116.72 (s, rot. C–F), -117.21 (s, C–F).

HRMS (APCI): m/z calculated for $C_{18}H_{22}FO_2NNa^+$ $[M+Na]^+$ 326.1527, found 326.1524.

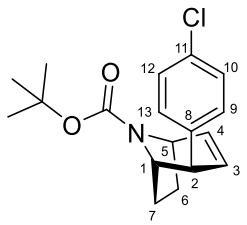
IR: 2941, 2360, 2341, 1678, 1508, 1430, 1345, 1224, 1176, 1109 862, 724, 685 cm^{-1}

Melting Point: 91.6 - 92.5 °C

SFC Chiralpak ® IB; 1500 psi, 30 °C; flow: 1.5 ml/min; from 1% to 5% MeOH in 5 min (major enantiomer t_R = 1.91 min; minor enantiomer t_R = 1.82 min)

$[\alpha]^{25}_D$ = −113.0 (c = 1.0, $CHCl_3$).

Synthesis of 3g



3g

The corresponding compound was prepared following General Procedure A using (±)-**1a** and **2g**. Purification by automated medium-pressure chromatography (hexane/EtOAc = 100/0 to 90/10) afforded the product **3g** as a white solid (30 mg, 47% yield). SFC analysis showed an enantiomeric excess of 96%.

Further, (+)-**1a** was isolated as a white solid (12 mg, 25% yield). SFC analysis showed an enantiomeric excess of >99%.

^{1}H NMR ($CDCl_3$, 600 MHz) δ (ppm) = 7.38 – 7.18 (m, 2H, aryl–H), 7.21 – 7.05 (m, 2H, aryl–H), 6.35 – 6.03 (m, 1H, C^4–H), 5.62 – 5.49 (m, 1H C^3–H), 4.76 – 4.13 (m, 2H, C^1–H, C^5–H), 3.21 (d, J = 4.1 Hz, 1H, C^2–H), 2.31 – 2.17 (m, 1H, C^6/C^7–H), 1.96 – 1.88 (m, 2H, C^6/C^7–H), 1.88 – 1.73 (m, 1H, C^6/C^7–H), 1.10 (s, 9H, –$C(CH_3)_3$).

^{13}C NMR ($CDCl_3$, 151 MHz) δ (ppm) = 152.4 (–C=O), 141.1 (C^8), 133.6 (C^4), 132.4 (C^{11}), 129.9 (aryl–C), 129.6 (aryl–C), 128.4 (aryl–C), 126.1 (rot. C^3), 125.0 (C^3), 79.0 (–$\underline{C}(CH_3)_3$), 58.8 (C^1/C^5), 57.4 (rot. C^1/C^5), 53.5 (rot. C^1/C^5), 52.1 (C^1/C^5), 50.8 (C^2), 34.4 (rot. C^6/C^7), 29.9 (C^6/C^7), 29.1 (rot. C^6/C^7), 28.5 (rot. –$C(\underline{C}H_3)_3$), 28.1 (–$C(\underline{C}H_3)_3$).

HRMS (APCI): m/z calculated for $C_{18}Cl_1H_{22}O_2NNa^+$ $[M+Na]^+$ 342.1231, found 342.1229.

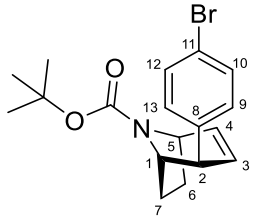
IR: 2943, 2834, 1676, 1427, 1109, 1025, 689 cm^{-1}

Melting Point: 117.8 – 119.4 °C

SFC Chiralpak ® IB; 1500 psi, 30 °C; flow: 1.5 ml/min; from 1% to 30% MeOH in 5 min (major enantiomer t_R = 1.98 min; minor enantiomer t_R = 1.88 min)

$[\alpha]^{25}_D$ = −80.6 (c = 1.0, $CHCl_3$).

Synthesis of 3h



3h

The corresponding compound was prepared following General Procedure A using (±)-**1a** and

2h. Purification by automated medium-pressure chromatography (hexane/EtOAc = 100/0 to 90/10) afforded the product **3h** as a white solid (28 mg, 39% yield). SFC analysis showed an enantiomeric excess of 96%.

Further, (+)-**1a** was isolated as a white solid (approx. 17 mg, 35% yield), contaminated with small amounts of **2h**. SFC analysis showed an enantiomeric excess of >99%.

^{1}H NMR ($CDCl_3$, 600 MHz) δ (ppm) = 7.48 – 7.32 (m, 2H, aryl–H), 7.12 – 7.05 (m, 2H, aryl–H), 6.29 – 6.07 (m, 1H, C^4–H), 5.54 (ddd, *J* = 9.6, 4.2, 1.7 Hz, 1H, C^3–H), 4.68 – 4.13 (m, 2H, C^1–H, C^5–H), 3.18 (d, *J* = 4.2 Hz, 1H, C^2–H), 2.28 – 2.16 (m, 1H, C^6/C^7–H), 1.97 – 1.82 (m, 2H, C^6/C^7–H), 1.82 – 1.68 (m, 1H, C^6/C^7–H), 1.24 (s, 9H, –C(CH_3)$_3$).

^{13}C NMR ($CDCl_3$, 151 MHz) δ (ppm) = 152.4 (–C=O), 141.6 (C^8), 133.7 (C^4), 132.3 (rot. C^4), 131.4 (aryl–C), 130.3 (aryl–C), 126.0 (rot. C^3), 124.9 (C^3), 120.4 (C^{11}), 79.1 (–C(CH_3)$_3$), 58.8 (C^1/C^5), 57.4 (rot. C^1/C^5), 53.6 (rot. C^1/C^5), 52.1 (C^1/C^5), 50.9 (C^2), 34.4 (rot. C^6/C^7), 33.9 (C^6/C^7), 29.9 (C^6/C^7), 29.1 (rot. C^6/C^7), 28.5 (rot. –C(CH_3)$_3$), 28.1 (–C(CH_3)$_3$).

HRMS (APCI): m/z calculated for $C_{18}H_{22}BrO_2NNa^+$ $[M+Na]^+$ 386.0726 and 388.0706, found 386.0725 and 388.0704.

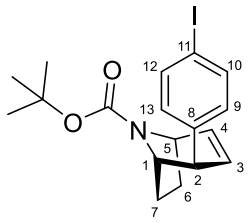
IR: 2974, 1692, 1487, 1420, 1339, 1171, 1132, 1105, 1072, 1043, 1010, 972, 894, 858, 818, 758, 724, 658 cm^{-1}

Melting Point: 103.6 – 104.1 °C

SFC Chiralpak ® IB; 1500 psi, 30 °C; flow: 1.5 ml/min; from 1% to 30% MeOH in 5 min (major enantiomer t_R = 2.17 min; minor enantiomer t_R = 2.07 min)

$[\alpha]^{25}_D$ = −85.7 (c = 1.0, $CHCl_3$).

Synthesis of 3i



3i

The corresponding compound was prepared following General Procedure A using (±)-**1a** and **2i**. Purification by automated medium-pressure chromatography (hexane/EtOAc = 100/0 to 90/10) afforded the product **3i** as a white solid (18 mg, 22% yield). SFC analysis showed an enantiomeric excess of 96%.

Further, (+)-**1a** was isolated as a white solid (approx. 32 mg, 66% yield), contaminated with small amounts of **2i**. SFC analysis showed an enantiomeric excess of 59%.

^{1}H NMR ($CDCl_3$, 600 MHz) δ (ppm) = 7.75 – 7.50 (m, 2H, aryl–H), 7.07 – 6.87 (m, 2H, aryl–H), 6.29 – 6.09 (m, 1H, C^4–H), 5.54 (ddd, *J* = 9.6, 4.2, 1.7 Hz, 1H, C^3–H), 4.70 – 4.07 (m, 2H, C^1–H, C^5–H), 3.16 (d, *J* = 4.1 Hz, 1H, C^2–H), 2.31 – 2.10 (m, 1H, C^6/C^7–H), 1.96 – 1.81 (m, 2H, C^6/C^7–H), 1.81 – 1.59 (m, 1H, C^6/C^7–H), 1.24 (s, 9H, –$C(CH_3)_3$).

^{13}C NMR ($CDCl_3$, 151 MHz) δ (ppm) = 152.4 (–C=O), 142.4 (C^8), 137.4 (C^{10}, C^{12}), 133.8 (C^4), 132.4 (rot. C^4), 130.6 (C^9, C^{13}), 126.0 (rot. C^3), 124.8 (C^3), 91.8 (C^{11}), 79.1 (–$\underline{C}(CH_3)_3$), 58.8 (C^1/C^5), 57.4 (rot. C^1/C^5), 53.6 (rot. C^1/C^5), 52.1 (C^1/C^5), 50.9 (C^2), 34.4 (rot. C^6/C^7), 33.9 (C^6/C^7), 29.9 (C^6/C^7), 29.2 (rot. C^6/C^7), 28.5 (rot. –$C(\underline{C}H_3)_3$), 28.1 (–$C(\underline{C}H_3)_3$).

HRMS (APCI): m/z calculated for $C_{18}H_{22}IO_2NNa^+$ $[M+Na]^+$ 434.0587, found 434.0583.

IR: 2974, 1690, 1482, 1365, 1300, 1248, 1172, 1132, 1104, 1062, 1042, 1006, 972, 894, 857, 817, 758, 723, 650 cm^{-1}

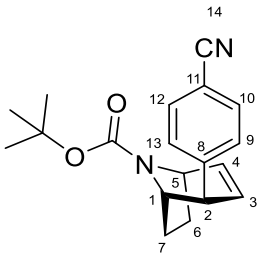
Melting Point: 104.7 – 105.3 °C

SFC Chiralpak ® IB; 1500 psi, 30 °C; flow: 1.5 ml/min; from 1% to 30% MeOH in 5 min

(major enantiomer t_R = 2.41 min; minor enantiomer t_R = 2.33 min)

[α]$^{25}_D$ = −99.6 (c = 1.0, $CHCl_3$).

Synthesis of 3j



3j

The corresponding compound was prepared following General Procedure A using (±)-**1a** and **2j**. The reaction was stirred overnight at 80 °C in 1,4-dioxane. Purification by automated medium-pressure chromatography (hexane/EtOAc = 100/0 to 90/10) afforded the product **3j** as a white solid (14 mg, 23% yield). ^{1}H NMR integration showed a diastereomeric ratio of 18:1. SFC analysis showed an enantiomeric excess of 97%.

Further, (+)-**1a** was isolated as a white solid (approx. 22 mg, 46% yield), contaminated with small amounts of **2j**. SFC analysis showed an enantiomeric excess of 39%.

^{1}H NMR ($CDCl_3$, 600 MHz) δ (ppm) = 7.69 – 7.48 (m, 2H, aryl–H), 7.34 (d, *J* = 7.9 Hz, 2H, aryl–H), 6.36 – 6.13 (m, 1H, C^4–H), 5.55 (ddd, *J* = 9.6, 4.2, 1.7 Hz, 1H, C^3–H), 4.67 – 4.18 (m, 2H, C^1–H, C^5–H), 3.27 (d, *J* = 4.1 Hz, 1H, C^2–H), 2.28 – 2.18 (m, 1H, C^6/C^7–H), 1.96 – 1.86 (m, 2H, C^6/C^7–H), 1.86 – 1.71 (m, 1H, C^6/C^7–H), 1.16 (s, 9H, –$C(CH_3)_3$).

^{13}C NMR ($CDCl_3$, 151 MHz) δ (ppm) = 152.3 (–C=O), 148.2 (C^8), 134.4 (C^4), 132.2 (aryl–C), 129.4 (aryl–C), 124.1 (C^3), 119.2 (–CN), 110.4 (C^{11}), 79.2 (–$\underline{C}(CH_3)_3$), 58.7 (C^1/C^5), 53.6 (rot. C^1/C^5), 52.2 (C^1/C^5), 51.3 (C^2), 34.4 (rot. C^6/C^7), 33.9 (C^6/C^7), 30.1 (rot. C^6/C^7), 29.9 (C^6/C^7), 28.4 (rot. –$C(\underline{C}H_3)_3$), 28.1 (–$C(\underline{C}H_3)_3$).

HRMS (APCI): m/z calculated for $C_{19}H_{22}O_2N_2Na^+$ $[M+Na]^+$ 333.1573, found 333.1573.

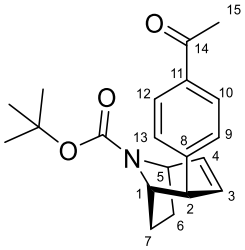
IR: 2974, 1690, 1482, 1365, 1300, 1248, 1172, 1132, 1104, 1062, 1042, 1006, 972, 894, 857, 817, 758, 723, 650 cm^{-1}

Melting Point: 103.8 – 104.9 °C

SFC Chiralpak ® IB; 1500 psi, 30 °C; flow: 1.5 ml/min; from 1% to 30% MeOH in 5 min (major enantiomer t_R = 2.24 min; minor enantiomer t_R = 2.17 min)

$[\alpha]^{25}_D$ = −104.4 (c = 0.5, $CHCl_3$).

Synthesis of 3k



3k

The corresponding compound was prepared following General Procedure A using (±)-**1a** and **2k**. Purification by automated medium-pressure chromatography (hexane/EtOAc = 100/0 to 75/25) afforded the product **3k** as a white solid (12 mg, 19% yield). SFC analysis showed an enantiomeric excess of 98%.

Further, (+)-**1a** was isolated as a white solid (approx. 32 mg, 65% yield), contaminated with small amounts of **2k**. SFC analysis showed an enantiomeric excess of 31%.

^{1}H NMR ($CDCl_3$, 600 MHz) δ (ppm) = 7.89 (d, *J* = 7.9 Hz, 2H, aryl–H), 7.32 (d, *J* = 8.0 Hz, 2H, aryl–H), 6.36 – 6.15 (m, 1H, C^4–H), 5.58 (ddd, *J* = 9.7, 4.3, 1.5 Hz, 1H, C^3–H), 4.79 – 4.27 (m, 2H, C^1–H, C^5–H), 3.27 (d, *J* = 4.1 Hz, 1H, C^2–H), 2.58 (s, 3H, C^{15}–H), 2.30 – 2.12 (m, 1H, C^6/C^7–H), 1.98 – 1.83 (m, 2H, C^6/C^7–H), 1.83 – 1.69 (m, 1H, C^6/C^7–H), 1.20 (s, 9H, –$C(CH_3)_3$).

^{13}C NMR ($CDCl_3$, 151 MHz) δ (ppm) = 198.1 (C^{14}), 152.4 (–C=O), 148.2 (C^8), 135.7 (C^{11}),

133.9 (C^4), 132.7 (rot. C^4), 128.8 (aryl–C), 128.5 (aryl–C), 125.6 (rot. C^3), 124.7 (C^3), 79.0 (–$\underline{C}(CH_3)_3$), 58.7 (C^1/C^5), 57.3 (rot. C^1/C^5), 53.6 (rot. C^1/C^5), 52.2 (C^1/C^5), 51.4 (C^2), 34.5 (rot. C^6/C^7), 34.0 (C^6/C^7), 30.1 (C^6/C^7), 29.3 (rot. C^6/C^7), 28.5 (rot. –$C(\underline{C}H_3)_3$), 28.1 (–$C(\underline{C}H_3)_3$), 26.8 (C^{15}).

HRMS (APCI): m/z calculated for $C_{20}H_{25}O_3NNa^+$ $[M+Na]^+$ 350.1727, found 350.1728.

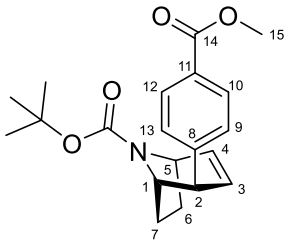
IR: 2974, 1684, 1606, 1422, 1365, 1340, 1269, 1173, 1105, 1043, 973, 861, 755, 664 cm^{-1}

Melting Point: 116.7 – 117.4 °C

SFC Chiralpak ® IF; 1500 psi, 30 °C; flow: 1.5 ml/min; from 1% to 30% MeOH in 5 min (major enantiomer t_R = 3.58 min; minor enantiomer t_R = 3.46 min)

$[\alpha]^{25}_D$ = −112.2 (c = 0.5, $CHCl_3$).

Synthesis of 3l



3l

The corresponding compound was prepared following General Procedure A using (±)-**1a** and **2l**. Purification by automated medium-pressure chromatography (hexane/EtOAc = 100/0 to 75/25) afforded the product **3l** as a white solid (41 mg, 59% yield). SFC analysis showed an enantiomeric excess of 96%.

Further, (+)-**1a** was isolated as a white solid (approx. 13 mg, 27% yield), contaminated with small amounts of **2l**. SFC analysis showed an enantiomeric excess of >99%.

^{1}H NMR ($CDCl_3$, 600 MHz) δ (ppm) = 7.96 (d, *J* = 7.9 Hz, 2H, aryl–H), 7.29 (d, 2H, aryl–H), 6.33 – 6.13 (m, 1H, C^4–H), 5.57 (ddd, *J* = 9.6, 4.1, 1.7 Hz, 1H, C^3–H), 4.65 – 4.19 (m, 2H, C^1–H, C^5–H), 3.90 (s, 3H, C^{15}–H), 3.33 – 3.21 (m, 1H, C^2–H), 2.36 – 2.15 (m, 1H, C^6/C^7–H), 1.97 – 1.86 (m, 2H, C^6/C^7–H), 1.86 – 1.71 (m, 1H, C^6/C^7–H), 1.14 (s, 9H, –$C(CH_3)_3$).

^{13}C NMR ($CDCl_3$, 151 MHz) δ (ppm) = 167.3 (C^{14}), 152.4 (–C=O), 148.0 (C^8), 133.8 (C^4), 132.6 (rot. C^4), 129.7 (2 × aryl–C), 128.6 (2 × aryl–C), 128.4 (C^{11}), 125.7 (rot. C^3), 124.8 (C^3), 79.0 (–$\underline{C}(CH_3)_3$), 58.7 (C^1/C^5), 57.4 (rot. C^1/C^5), 53.6 (rot. C^1/C^5), 52.2 (C^1/C^5), 52.1 (C^2), 51.4 (C^{15}), 34.4 (rot. C^6/C^7), 33.9 (C^6/C^7), 30.2 (C^6/C^7), 29.3 (rot. C^6/C^7), 28.5 (rot. –$C(\underline{C}H_3)_3$), 28.1 (–$C(\underline{C}H_3)_3$).

HRMS (APCI): m/z calculated for $C_{20}H_{25}O_4NNa^+$ $[M+Na]^+$ 366.1676, found 366.1673.

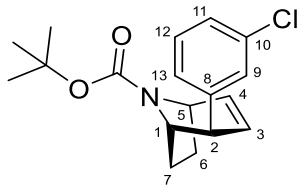
IR: 2974, 2926, 2874, 1721, 1693, 1574, 1477, 1420, 1391, 1366, 1340, 1312, 1279, 1174, 1157, 1132, 1104, 1062, 1043, 1020, 1008, 971, 913, 895, 877, 862, 826, 762, 720, 707, 662 cm^{-1}

Melting Point: 98.5 – 98.8 °C

SFC Chiralpak ® IC; 1500 psi, 30 °C; flow: 1.5 ml/min; from 1% to 30% MeOH in 5 min (major enantiomer t_R = 3.58 min; minor enantiomer t_R = 3.46 min)

$[\alpha]^{25}_D$ = −102.9 (c = 1.0, $CHCl_3$).

Synthesis of 3m



3m

The corresponding compound was prepared following General Procedure A using (±)-**1a** and

2m. Purification by automated medium-pressure chromatography (hexane/EtOAc = 100/0 to 90/10) afforded the product **3m** as a white solid (24 mg, 38% yield). SFC analysis showed an enantiomeric excess of 96%.

Further, (+)-**1a** was isolated as a white solid (6 mg, 12% yield). SFC analysis showed an enantiomeric excess of >99%.

^{1}H NMR ($CDCl_3$, 600 MHz) δ (ppm) = 7.24 – 7.16 (m, 3H, aryl–H), 7.15 – 7.08 (m, 1H, aryl–H), 6.30 – 6.13 (m, 1H, C^4–H), 5.55 (ddd, *J* = 9.6, 4.1, 1.7 Hz, 1H, C^3–H), 4.66 – 4.22 (m, 2H, C^1–H, C^5–H), 3.19 (d, *J* = 4.0 Hz, 1H, C^2–H), 2.30 – 2.16 (m, 1H, C^6/C^7–H), 1.95 – 1.79 (m, 2H, C^6/C^7–H), 1.84 – 1.67 (m, 1H, C^6/C^7–H), 1.08 (s, 9H, –$C(CH_3)_3$).

^{13}C NMR ($CDCl_3$, 151 MHz) δ (ppm) = 152.4 (–C=O), 144.8 (C^8), 134.3 (C^{10}), 133.9 (C^4), 132.7 (rot. C^4), 129.6 (aryl–C), 128.6 (aryl–C), 127.0 (aryl–H), 126.7 (aryl–H), 125.7 (rot. C^3), 124.8 (C^3), 79.0 (–$\underline{C}(CH_3)_3$), 58.8 (C^1/C^5), 57.4 (rot. C^1/C^5), 53.5 (rot. C^1/C^5), 52.1 (C^1/C^5), 51.0 (C^2), 34.4 (rot. C^6/C^7), 33.9 (C^6/C^7), 30.0 (C^6/C^7), 29.1 (rot. C^6/C^7), 28.5 (rot. –$C(\underline{C}H_3)_3$), 28.1 (–$C(\underline{C}H_3)_3$).

HRMS (APCI): m/z calculated for $C_{18}H_{22}ClO_2NNa^+$ $[M+Na]^+$ 342.1231, found 342.1230.

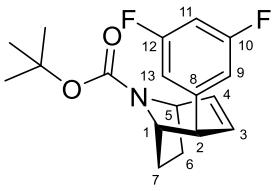
IR: 2974, 2928, 2872, 2362, 1692, 1596, 1572, 1476, 1421, 1391, 1366, 1339, 1315, 1294, 1249, 1230, 1173, 1157, 1133, 1104, 1080, 1061, 1043, 1008, 974, 921, 892, 864, 846, 829, 772, 729, 690 cm^{-1}

Melting Point: 90.7 – 91.8 °C

SFC Chiralpak ® ID; 1500 psi, 30 °C; flow: 1.5 ml/min; from 1% to 30% MeOH in 5 min (major enantiomer t_R = 2.29 min; minor enantiomer t_R = 2.42 min)

$[\alpha]^{25}_D$ = −128.6 (c = 1.0, $CHCl_3$).

Synthesis of 3n



3n

The corresponding compound was prepared following General Procedure A using (±)-**1a** and **2n**. Purification by automated medium-pressure chromatography (hexane/EtOAc = 100/0 to 90/10) afforded the product **3n** as a white solid (31 mg, 49% yield). SFC analysis showed an enantiomeric excess of 97%.

Further, (+)-**1a** was isolated as a white solid (approx. 22 mg, 46% yield), contaminated with small amounts of **2n**. SFC analysis showed an enantiomeric excess of >99%.

^{1}H NMR ($CDCl_3$, 600 MHz) δ (ppm) = 6.76 (d, *J* = 7.7 Hz, 2H, aryl–H), 6.70 – 6.59 (m, 1H, aryl–H), 6.31 – 6.13 (m, 1H, C^4–H), 5.53 (ddd, *J* = 9.6, 4.3, 1.7 Hz, 1H, C^3–H), 4.68 – 4.20 (m, 2H, C^1–H, C^5–H), 3.18 (d, *J* = 4.2 Hz, 1H, C^2–H), 2.31 – 2.16 (m, 1H, C^6/C^7–H), 1.97 – 1.82 (m, 2H, C^6/C^7–H), 1.82 – 1.68 (m, 1H, C^6/C^7–H), 1.26 (s, 9H, –$C(CH_3)_3$).

^{13}C NMR ($CDCl_3$, 151 MHz) δ (ppm) = 163.1 (dd, *J* = 247.8, 12.7 Hz, C^{10}, C^{12}), 152.7 (–C=O), 152.6 (d, *J* = 87.3 Hz, C^9/C^{13}), 146.5 (d, *J* = 77.0 Hz, C^9/C^{13}), 134.4 (C^4), 133.2 (rot. C^4), 125.17 (rot. C^3), 124.3 (C^3), 111.3 (d, *J* = 25.5 Hz, C^8), 101.93 (t, *J* = 25.5 Hz, C^{11}), 79.1 (–$\underline{C}(CH_3)_3$), 58.6 (C^1/C^5), 57.3 (rot. C^1/C^5), 53.5 (rot. C^1/C^5), 52.07 (C^1/C^5), 50.9 (C^2), 34.3 (rot. C^6/C^7), 33.8 (C^6/C^7), 30.0 (C^6/C^7), 29.1 (rot. C^6/C^7), 28.4 (rot. –$C(\underline{C}H_3)_3$), 28.1 (–$C(\underline{C}H_3)_3$).

^{19}F NMR (377 MHz, $CDCl_3$) δ (ppm) = −110.71 to −110.75 (br. m, C–F).

HRMS (APCI): m/z calculated for $C_{18}H_{21}F_2O_2NNa^+$ $[M+Na]^+$ 344.1433, found 344.1430.

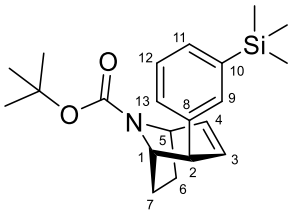
IR: 2929,1684, 1625, 1597, 1456, 1428, 1392, 1367, 1343, 1319, 1216, 1172, 1116, 1045 993, 952, 894, 845, 754, 684, 667, 628 cm^{-1}

Melting Point: 78.3 – 79.2 °C

SFC Chiralpak ® ID; 1500 psi, 30 °C; flow: 1.5 ml/min; from 1% to 30% MeOH in 5 min (major enantiomer t_R = 1.73 min; minor enantiomer t_R = 1.93 min)

[α]$^{25}_D$ = −97.4 (c = 1.0, $CHCl_3$).

Synthesis of 3o



3o

The corresponding compound was prepared following General Procedure A using (±)-**1a** and **2o**. Purification by automated medium-pressure chromatography (hexane/EtOAc = 100/0 to 90/10) afforded the product **3o** as a colourless oil (33 mg, 46% yield). SFC analysis showed an enantiomeric excess of 97%.

Further, (+)-**1a** was isolated as a white solid (18 mg, 36% yield). SFC analysis showed an enantiomeric excess of >99%.

^{1}H NMR ($CDCl_3$, 600 MHz) δ (ppm) = 7.40 – 7.31 (m, 2H, aryl–H), 7.28 (t, *J* = 7.4 Hz, 1H, aryl–H), 7.19 (d, *J* = 7.8 Hz, 1H, aryl–H), 6.30 – 6.18 (m, 1H, C^4–H), 5.65 – 5.52 (m, 1H, C^3–H), 4.67 – 4.22 (m, 2H, C^1–H, C^5–H), 3.32 – 3.20 (m, 1H, C^2–H), 2.32 – 2.09 (m, 1H, C^6/C^7–H), 1.96 – 1.86 (m, 2H, C^6/C^7–H), 1.86 – 1.77 (m, 1H, C^6/C^7–H), 1.20 (s, 9H, –$C(CH_3)_3$), 0.25 (s, 9H, -$Si(CH_3)_3$).

^{13}C NMR ($CDCl_3$, 151 MHz) δ (ppm) = 152.4 (–C=O), 141.7 (C^{10}), 140.3 (C^8), 133.4 (C^4), 133.3 (aryl–C), 131.5 (aryl–C), 129.0 (aryl–C), 127.9 (aryl–C), 126.9 (rot. C^3), 125.4 (C^3), 78.6 (–$\underline{C}(CH_3)_3$), 59.2 (C^1/C^5), 57.4 (rot. C^1/C^5), 53.6 (rot. C^1/C^5), 52.1 (C^1/C^5), 51.5 (C^2), 34.5 (rot. C^6/C^7), 30.0 (C^6/C^7), 29.4 (rot. C^6/C^7), 28.6 (rot. –$C(\underline{C}H_3)_3$), 28.0 (–$C(\underline{C}H_3)_3$), −0.9 (-$Si(CH_3)_3$).

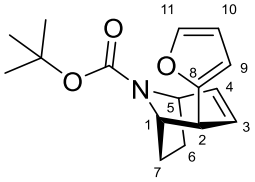
HRMS (APCI): m/z calculated for $C_{21}H_{31}O_2NSiNa^+$ $[M+Na]^+$ 380.2016, found 380.2014.

IR: 2951, 2871, 1745, 1695, 1613, 1422, 1366, 1340, 1296, 1249, 1172, 1105, 1052, 1015, 977, 946, 867, 838, 771, 753, 713, 693 cm^{-1}

SFC Chiralpak ® IC; 1500 psi, 30 °C; flow: 1.5 ml/min; from 1% to 20% MeOH in 5 min (major enantiomer t_R = 2.33 min; minor enantiomer t_R = 2.24 min)

$[\alpha]^{25}_D$ = −54.9 (c = 1.0, $CHCl_3$).

Synthesis of 3p



3p

The corresponding compound was prepared following General Procedure A using (±)-**1a** and **2p**. The reaction was stirred for 2 h. Purification by automated medium-pressure chromatography (hexane/EtOAc = 100/0 to 90/10) afforded the product **3p** as a white solid (31 mg, 56% yield). SFC analysis showed an enantiomeric excess of 97%.

Further, (+)-**1a** was isolated as a white solid (14 mg, 28% yield). SFC analysis showed an enantiomeric excess of >99%.

^{1}H NMR ($CDCl_3$, 600 MHz) δ (ppm) = 7.37 (s, 1H, aryl–H), 6.33 – 6.25 (m, 1H, C^4–H), 6.24 – 5.93 (m, 2H, aryl–H), 5.60 (dd, *J* = 9.9, 4.0 Hz, 1H, C^3–H), 4.69 – 4.38 (m, 2H, C^1–H, C^5–H), 3.24 (d, *J* = 4.2 Hz, 1H, C^2–H), 2.31 – 2.18 (m, 1H, C^6/C^7–H), 1.97 – 1.85 (m, 2H, C^6/C^7–H), 1.82 – 1.68 (m, 1H, C^6/C^7–H), 1.20 (s, 9H, –$C(CH_3)_3$).

^{13}C NMR ($CDCl_3$, 151 MHz) δ (ppm) = 155.6 (–C=O), 152.6 (C^8), 141.5 (C^{11}), 134.6 (C^4), 133.0 (rot. C^4), 123.8 (rot. C^3), 122.9 (C^3), 110.5 (C^{10}), 107.0 (C^9), 79.0 (–$\underline{C}(CH_3)_3$), 55.7 (C^1/C^5), 55.1 (rot. C^1/C^5), 53.5 (rot. C^1/C^5), 52.0 (C^1/C^5), 44.9 (C^2), 34.3 (rot. C^6/C^7), 33.9 (C^6/C^7), 29.4 (C^6/C^7), 28.5 (rot. –$C(\underline{C}H_3)_3$), 28.1 (–$C(\underline{C}H_3)_3$).

HRMS (APCI): m/z calculated for $C_{16}H_{21}O_3NNa^+$ $[M+Na]^+$ 298.1414, found 298.1414.

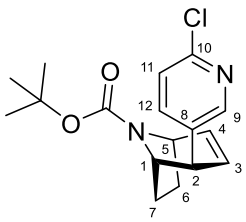
IR: 2360, 2344, 1694, 1421, 1340, 1249, 1227, 1175, 1141, 1106, 1044, 1005, 971, 870, 830, 791, 734, 668, 647, 640, 635, 625, 618, 608 cm^{-1}

Melting Point: 224.1 – 226.3 °C

SFC Chiralpak ® ID; 1500 psi, 30 °C; flow: 1.5 ml/min; from 1% to 20% MeOH in 5 min (major enantiomer t_R = 3.50 min; minor enantiomer t_R = 3.89 min)

$[\alpha]^{25}_D$ = −30.8 (c = 1.0, $CHCl_3$).

Synthesis of 3q



3q

The corresponding compound was prepared following General Procedure A using (±)-**1a** and **2q**. The reaction was stirred for 2 h. Purification by automated medium-pressure chromatography (hexane/EtOAc = 100/0 to 70/30) afforded the product **3q** as a white solid (27 mg, 42% yield). SFC analysis showed an enantiomeric excess of 97%.

Further, (+)-**1a** was isolated as a white solid (approx. 13 mg, 26% yield), contaminated with small amounts of **2q**. SFC analysis showed an enantiomeric excess of >99%.

^{1}H NMR ($CDCl_3$, 600 MHz) δ (ppm) = 8.25 (s, 1H, aryl–H), 7.51 (dd, *J* = 8.0, 2.5 Hz, 1H, aryl–H), 7.40 – 7.15 (m, 1H, aryl–H), 6.35 – 6.09 (m, 1H, C^4–H), 5.52 (ddd, *J* = 9.6, 4.2, 1.7 Hz, 1H, C^3–H), 4.76 – 4.17 (m, 2H, C^1–H, C^5–H), 3.23 (d, *J* = 4.1 Hz, 1H, C^2–H), 2.33 – 2.08 (m, 1H, C^6/C^7–H), 2.04 – 1.82 (m, 2H, C^6/C^7–H), 1.82 – 1.75 (m, 1H, C^6/C^7–H), 1.25 (s, 9H, –$C(CH_3)_3$).

^{13}C NMR ($CDCl_3$, 151 MHz) δ (ppm) = 152.4 (–C=O), 149.8 (C^{10}), 149.6 (C^9), 138.9 (Aryl–C), 137.0 (aryl–C), 134.5 (C^4), 133.2 (rot. C^4), 124.9 (rot. C^3), 123.9 (aryl–C, C^3), 79.5 (–$\underline{C}(CH_3)_3$), 58.7 (C^1/C^5), 57.3 (rot. C^1/C^5), 53.6 (rot. C^1/C^5), 52.2 (C^1/C^5), 48.2 (C^2), 34.3 (rot. C^6/C^7), 33.8 (C^6/C^7), 30.5 (rot. C^6/C^7), 29.9 (C^6/C^7), 29.1 (rot. –C($\underline{C}H_3)_3$), 28.2 (–C($\underline{C}H_3)_3$).

HRMS (APCI): m/z calculated for $C_{17}H_{22}ClO_2N_2^+$ $[M+H]^+$ 321.1364, found 321.1362.

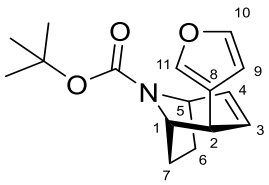
IR: 2981, 1683, 1426, 1216, 1107, 753, 668 cm^{-1}

Melting Point: 106.0 – 106.7 °C

SFC Chiralpak ® IA; 1500 psi, 30 °C; flow: 1.5 ml/min; from 1% to 30% MeOH in 5 min (major enantiomer t_R = 3.30 min; minor enantiomer t_R = 3.17 min)

$[\alpha]^{25}_D$ = −106.8 (c = 1.0, $CHCl_3$).

Synthesis of 3r



3r

The corresponding compound was prepared following General Procedure A using (±)-**1a** and **2r**. The reaction was stirred for 2 h. Purification by automated medium-pressure chromatography (hexane/EtOAc = 100/0 to 90/10) afforded the product as a white solid (8 mg, 15% yield). ^{1}H NMR integration showed a diastereomeric ratio of 17:1. SFC analysis showed an enantiomeric excess of 98%.

Further, (+)-**1a** was isolated as a white solid (32 mg, 65% yield). SFC analysis showed an enantiomeric excess of 26%.

^{1}H NMR ($CDCl_3$, 600 MHz) δ (ppm) = 7.40 (s, 1H, aryl–H), 7.17 (s, 1H, aryl–H), 6.39 – 6.32 (m, 1H, aryl–H), 6.20 – 5.96 (m, 1H, C^4–H), 5.60 (ddd, *J* = 9.6, 4.2, 1.7 Hz, 1H, C^3–H), 4.74 – 4.13 (m, 2H, C^1–H, C^5–H), 3.09 (s, 1H, C^2–H), 2.29 – 2.12 (m, 1H, C^6/C^7–H), 1.96 – 1.81 (m, 2H, C^6/C^7–H), 1.81 – 1.66 (m, 1H, C^6/C^7–H), 1.31 (s, 9H, –C(CH_3)$_3$).

^{13}C NMR ($CDCl_3$, 151 MHz) δ (ppm) = 152.8 (–C=O), 142.8 (C^{10}), 140.2 (C^{11}), 132.9 (C^4), 131.3 (rot. C^4), 126.6 (C^8), 126.4 (rot. C^3), 125.2 (C^3), 110.8 (C^9), 79.0 (–<u>C</u>(CH_3)$_3$), 57.5 (C^1/C^5), 56.3 (rot. C^1/C^5), 53.6 (rot. C^1/C^5), 52.1 (C^1/C^5), 42.9 (C^2), 34.3 (rot. C^6/C^7), 34.0 (C^6/C^7), 29.6 (C^6/C^7), 28.8 (rot. C^6/C^7), 28.5 (rot. –C(<u>C</u>H_3)$_3$), 28.2 (–C(<u>C</u>H_3)$_3$).

HRMS (APCI): m/z calculated for $C_{16}H_{21}O_3NNa^+$ $[M+Na]^+$ 298.1414, found 298.1412.

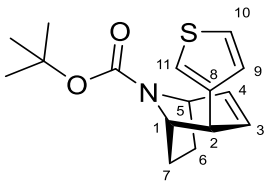
IR: 2974, 2924, 2872, 2852, 1692, 1500, 1477, 1421, 1391, 1366, 1339, 1248, 1220, 1172, 1159, 1133, 1104, 1066, 1045, 1024, 1006, 956, 907, 893, 874, 850, 829, 777 cm^{-1}

Melting Point: 63.6 – 64.0 °C

SFC Chiralpak ® IC; 1500 psi, 30 °C; flow: 1.5 ml/min; from 1% to 30% MeOH in 5 min (major enantiomer t_R = 2.15 min; minor enantiomer t_R = 2.22 min)

[α]$^{25}_D$ = −93.4 (c = 0.5, $CHCl_3$).

Synthesis of 3s



3s

The corresponding compound was prepared following General Procedure A using (±)-**1a** and **2s**. The reaction was stirred for 2 h. Purification by automated medium-pressure chromatography (hexane/EtOAc = 100/0 to 90/10) afforded the product **3s** as a white solid (27

mg, 44% yield). ^{1}H NMR integration showed a diastereomeric ratio of 19:1. SFC analysis showed an enantiomeric excess of 88%.

Further, (+)-**1a** was isolated as a white solid (19 mg, 40% yield). SFC analysis showed an enantiomeric excess of >99%.

^{1}H NMR ($CDCl_3$, 600 MHz) δ (ppm) = 7.28 – 7.26 (m, 1H, aryl–H), 7.15 – 6.99 (m, 1H, aryl–H), 6.99 – 6.91 (m, 1H, aryl–H), 6.27 – 5.97 (m, 1H, C^4–H), 5.66 (ddd, *J* = 9.7, 4.2, 1.7 Hz, 1H, C^3–H), 4.62 – 4.29 (m, 2H, C^1–H, C^5–H), 3.31 (d, *J* = 4.1 Hz, 1H, C^2–H), 2.31 – 2.12 (m, 1H, C^6/C^7–H), 1.96 – 1.84 (m, 2H, C^6/C^7–H), 1.84 – 1.68 (m, 1H, C^6/C^7–H), 1.17 (s, 9H, –$C(CH_3)_3$).

^{13}C NMR ($CDCl_3$, 151 MHz) δ (ppm) = 152.6 (–C=O), 132.9 (C^4), 131.3 (rot. C^4), 127.9 (aryl–C), 127.5 (aryl–C), 126.7 (rot. C^3), 125.6 (C^3), 125.2 (aryl–C), 121.8 (aryl–C), 78.9 (–$\underline{C}(CH_3)_3$), 58.1 (C^1/C^5), 56.6 (rot. C^1/C^5), 53.6 (rot. C^1/C^5), 52.0 (C^1/C^5), 47.0 (C^2), 34.4 (rot. C^6/C^7), 34.0 (C^6/C^7), 29.9 (rot. C^6/C^7), 29.7 (C^6/C^7), 28.5 (rot. –C($\underline{C}H_3)_3$), 28.2 (–C($\underline{C}H_3)_3$).

HRMS (APCI): m/z calculated for $C_{16}H_{21}O_2SNNa^+$ $[M+Na]^+$ 314.1185, found 314.1183.

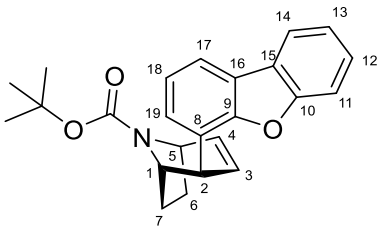
IR: 2959, 2923, 2852, 1677, 1634, 1475, 1432, 1390, 1363, 1344, 1311, 1292, 1274, 1251, 1229, 1179, 1163, 1132, 1110, 1041, 1007, 974, 947, 906, 891, 871, 849, 837, 763, 715, 695, 675, 652, 631 cm^{-1}

Melting Point: 78.1 - 79.4 °C

SFC Chiralpak ® IC; 1500 psi, 30 °C; flow: 1.5 ml/min; from 1% to 30% MeOH in 5 min (major enantiomer t_R = 2.14 min; minor enantiomer t_R = 2.23 min)

$[\alpha]^{25}_D$ = −106.4 (c = 0.5, $CHCl_3$).

Synthesis of 3t



3t

The corresponding compound was prepared following General Procedure A using (±)-**1a** and **2t**. The reaction was stirred for 2 h. Purification by automated medium-pressure chromatography (hexane/EtOAc = 100/0 to 90/10) afforded the product **3t** as a white solid (16 mg, 21% yield). SFC analysis showed an enantiomeric excess of 88%.

Further, (+)-**1a** was isolated as a white solid (27 mg, 56% yield). SFC analysis showed an enantiomeric excess of 38%.

^{1}H NMR ($CDCl_3$, 600 MHz) δ (ppm) = 7.99 (d, *J* = 7.7 Hz, 1H, aryl–H), 7.87 (d, *J* = 7.3 Hz, 1H, aryl–H), 7.64 (d, *J* = 8.3 Hz, 1H, aryl–H), 7.49 (t, *J* = 7.8 Hz, 1H, aryl–H), 7.37 (t, *J* = 7.5 Hz, 1H, aryl–H), 7.32 – 7.26 (m, 2H, aryl–H), 6.46 – 6.19 (m, 1H, C^4–H), 5.72 (dd, *J* = 9.8, 4.2 Hz, 1H, C^3–H), 4.84 – 4.38 (m, 2H, C^1–H, C^5–H), 4.13 – 3.81 (m, 1H, C^2–H), 2.47 – 2.27 (m, 1H, C^6/C^7–H), 2.10 – 1.86 (m, 3H, C^6/C^7–H), 0.88 (s, 9H, –$C(CH_3)_3$).

^{13}C NMR ($CDCl_3$, 151 MHz) δ (ppm) = 156.2 (–C=O), 154.2 (C^9), 152.4 (C^{10}), 134.3 (C^4), 132.9 (rot. C^4), 127.3 (aryl–C), 127.0 (aryl–C), 126.8 (aryl–C), 125.4 (aryl–C), 124.7 (rot. C^3), 124.5 (C^3), 123.7 (aryl–C), 123.0 (aryl–C), 122.8 (aryl–C), 120.8 (aryl–C), 119.0 (aryl–C), 111.8 (aryl–C), 78.6 (–$\underline{C}(CH_3)_3$), 56.8 (C^1/C^5), 56.3 (rot. C^1/C^5), 53.7 (rot. C^1/C^5), 52.3 (C^1/C^5), 45.1 (C^2), 34.5 (rot. C^6/C^7), 34.1 (C^6/C^7), 30.0 (C^6/C^7), 29.3 (rot. C^6/C^7), 28.5 (rot. –$C(\underline{C}H_3)_3$), 27.8 (–$C(\underline{C}H_3)_3$).

HRMS (APCI): m/z calculated for $C_{24}H_{25}O_3NNa^+$ $[M+Na]^+$ 398.1727, found 398.1723.

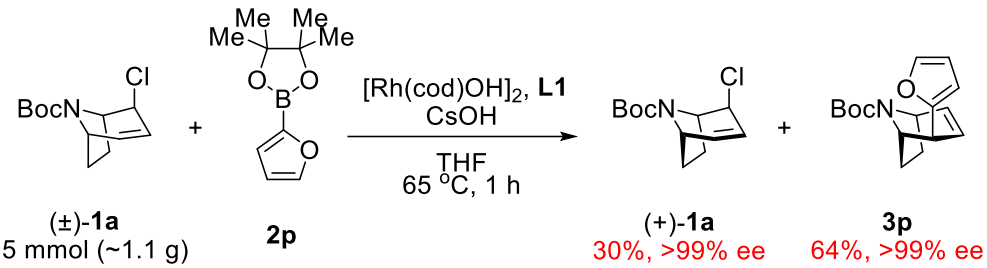
IR: 2975, 1690, 1476, 1451, 1423, 1390, 1365, 1340, 1302, 1264, 1183, 1134, 1105, 1042, 1008, 976, 894, 845, 754, 713, 624 cm^{-1}

Melting Point: 93.8 – 94.6 °C

SFC Chiralpak ® IB; 1500 psi, 30 °C; flow: 1.5 ml/min; from 1% to 30% MeOH in 5 min (major enantiomer t_R = 2.95 min; minor enantiomer t_R = 3.18 min)

$[\alpha]^{25}_D$ = +74.5 (c = 1.0, $CHCl_3$).

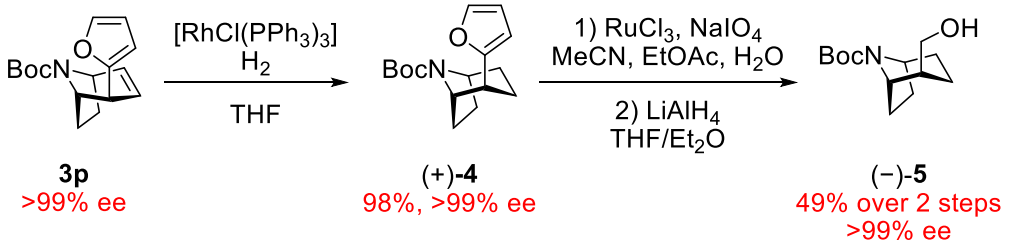
4.2.4 Upscale and Derivatisation of Product



Scheme 4.2.17 Upscale Rh–Catalysed Suzuki-Miyaura cross–Coupling reaction between (±)-**1a** and **2p**.

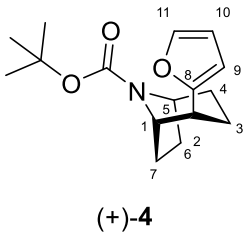
General Procedure A was used for the upscale reaction of (±)-**1a** (1.10 g, 4.5 mmol) and **2t** (2.60 g, 13.5 mmol) with reaction time of 2 h. Purification by automated medium-pressure chromatography (hexane/EtOAc = 100/0 to 90/10) afforded the product **3p** as a white solid (0.793 g, 64% yield) and enantiopure (+)-**1a** (0.326 g, 30%). SFC analysis showed an enantiomeric excess of >99% for both **3p** and (+)-**1a**.

Derivatisation of product



Scheme 4.2.18 Overview of derivatisation of cross–Coupling product **3p**.

Synthesis of (+)-4



(+)-**4**

3p (0.165 g, 0.60 mmol) and [$Rh(PPh_3)_3Cl$] (55.5 mg, 10 mol%) was dissolved in THF (0.5 mL) and H_2 was bubbled through the solution for 3 min and the reaction was left stirring under

H_2 overnight at r.t.. The crude product was loaded on to hydromatrix bulk material and purified by flash column chromatography to afford the product **of** (+)-**4** as a white solid (0.115 g, 98% yield). SFC analysis showed an enantiomeric excess of >99%.

^{1}H NMR ($CDCl_3$, 600 MHz) δ (ppm) = 7.39 – 7.31 (m, 1H, aryl–H), 6.43 – 6.24 (m, 1H, aryl–H), 6.23 – 6.01 (m, 1H, aryl–H), 4.64 – 4.42 (m, 1H, C^1/C^5–H), 4.42 – 4.17 (m, 1H, C^1/C^5–H), 2.93 – 2.81 (m, 1H, C^2–H), 2.18 – 1.81 (m, 6H, C^3–H, C^4–H, C^6/C^7–H), 1.80 – 1.57 (m, 2H, C^6/C^7–H), 1.43 – 1.23 (s, 9H, –$C(CH_3)_3$).

^{13}C NMR ($CDCl_3$, 151 MHz) δ (ppm) = 157.4 (–C=O), 153.0 (aryl–C), 140.6 (aryl–C), 110.3 (aryl–C), 105.5 (aryl–C), 78.8 (–$\underline{C}(CH_3)_3$), 56.6 (C^1/C^5), 55.5 (rot. C^1/C^5), 53.9 (rot. C^1/C^5), 52.7 (C^1/C^5), 39.8 (C^2), 29.1 (C^6/C^7), 28.5 (C^3), 28.3 (–$C(\underline{C}H_3)_3$), 27.9 (rot. –$C(\underline{C}H_3)_3$), 27.2 (C^6/C^7), 20.0 (C^4).

HRMS (APCI): m/z calculated for $C_{16}H_{23}O_3NNa^+$ $[M+Na]^+$ 300.1570, found 300.1566.

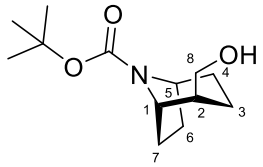
IR: 2974, 1688, 1506, 1478, 1418, 1391, 1365, 1340, 1232, 1170, 1105, 1024, 953, 923, 874, 854, 759, 731, 600 cm^{-1}

Melting Point: 44.3 – 45.4 °C

SFC Chiralpak ® ID; 1500 psi, 30 °C; flow: 1.5 ml/min; from 1% to 5% MeOH in 5 min (major enantiomer t_R = 3.15 min)

$[\alpha]^{25}_D$ = +41.0 (c = 1.0, $CHCl_3$).

Synthesis of (−)-5



(−)-**5**

$RuCl_3$ (10.5 mg, 10 mol%) and $NaIO_4$ (1.62 g, 7.56 mmol) was dissolved in H_2O (4.0 mL), EtOAc (2.0 mL) and MeCN (0.40 mL) and stirred for 30 min until the mixture turned orange. A solution of (+)-**4** (0.111 g, 0.40 mmol) in DCM (2.0 mL) was added dropwise at 0 °C (each addition was made after the colour of the reaction mixture turned back orange). After stirring the mixture for 2 h, brine (5 mL) was added and the aqueous layer was extracted with EtOAc (10 mL × 3). The organic layer was dried over $MgSO_4$ and concentrated *in vacuo*. The mixture was purified *via* flash column chromatography (DCM/MeOH/AcOH = 94/5/1), then concentrated *in vacuo* to afford a black solid which was directly used in the next step. The black solid was dissolved in THF/Et_2O (1.3 mL / 0.86 mL) and added dropwise to solution of $LiAlH_4$ (3.0 equiv., 1.3 mL (1 M in THF)) in Et_2O (0.86 mL) at 0 °C. The reaction mixture was slowly allowed to reach r.t.. After 4 h, EtOAc (2.0 mL) and potassium sodium tartrate solution (sat.aq., 8 mL) were added and stirring was continued overnight. The reaction mixture was extracted with EtOAc (10 mL × 3) and dried over $MgSO_4$ and concentrated *in vacuo*. Purification by flash column chromatography afforded the product as a colourless oil (47 mg, 49 % yield). SFC analysis showed an enantiomeric excess of >99%.

^{1}H NMR ($CDCl_3$, 600 MHz) δ (ppm) = 4.47 – 3.97 (m, 2H, C^1–H, C^5–H), 3.57 – 3.27 (m, 2H, C^8–H), 2.13 – 2.03 (m, 1H, C^4/C^6/C^7–H), 2.03 – 1.91 (m, 1H, C^4/C^6/C^7–H), 1.90 – 1.78 (m, 2H, C^2–H, C^4/C^6/C^7–H), 1.73 – 1.62 (m, 3H, C^4/C^6/C^7–H), 1.47 (s, 9H, –$C(CH_3)_3$), 1.35 – 1.23 (m, 1H, C^3–H), 1.23 – 1.10 (m, 1H, C^3–H).

^{13}C NMR ($CDCl_3$, 151 MHz) δ (ppm) = 154.5 (–C=O), 79.8 (–$\underline{C}(CH_3)_3$), 63.1 (rot. C^8), 62.5 (C^8), 54.3 (C^1/C^5), 53.6 (rot. C^1/C^5), 52.4 (C^1/C^5), 42.4 (rot. C^2), 42.0 (C^2), 28.6 (–$C(\underline{C}H_3)_3$), 28.0 (C^4/C^6/C^7), 27.8 (C^4/C^6/C^7), 27.6 (C^4/C^6/C^7), 18.4 (C^3).

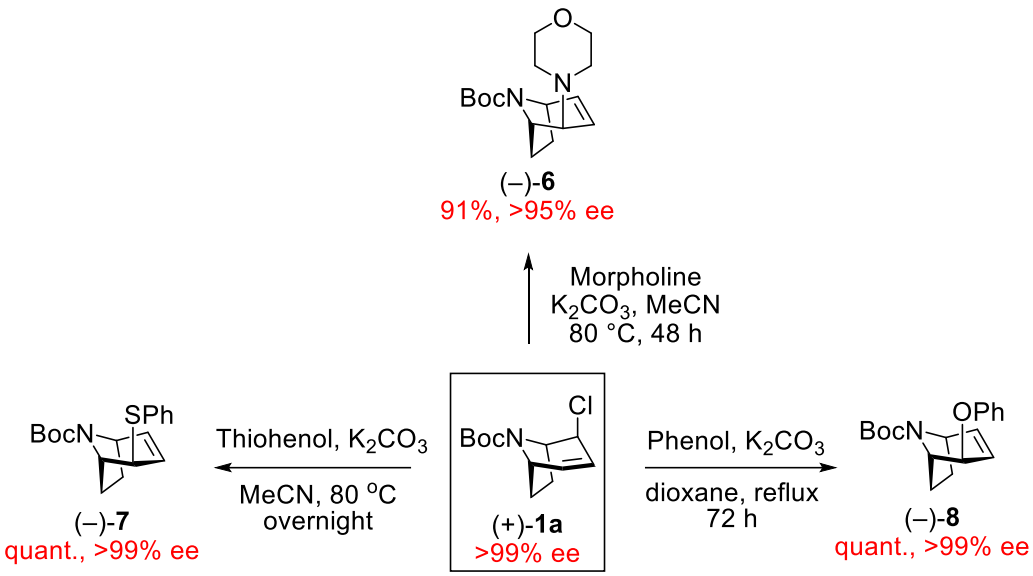
HRMS (APCI): m/z calculated for $C_{13}H_{23}O_3NNa^+$ $[M+Na]^+$ 264.1570, found 264.1567.

IR: 3441, 2933, 1690, 1667, 1476, 1422, 1365, 1322, 1241, 1164, 1112, 1042, 986, 959, 942, 920, 869, 763 cm^{-1}

SFC Chiralpak ® IG; 1500 psi, 30 °C; flow: 1.5 ml/min; from 1% to 20% MeOH in 5 min (major enantiomer t_R = 3.62 min; minor enantiomer t_R = 3.21 min)

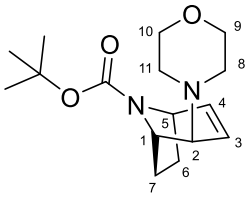
$[\alpha]^{25}_D$ = −1.3 (c = 1.0, $CHCl_3$).

4.2.5 Derivatisation of Enantiopure Allyl Chloride



Scheme 4.2.19 Overview of derivatisation of resolved enantiopure allyl chloride (+)-**1a**.

Synthesis of (−)-6



(−)-**6**

According to a previous procedure by the group with modified conditions,[177] (+)-**1a** (57.6 mg, 0.24 mol), K_2CO_3 (98.1 mg, 0.71 mmol) was dissolved in MeCN (2.4 mL) and morpholine (29 µL, 0.34 mmol) was added. The reaction mixture was heated to 80 °C and stirred for 48 h before cooling to r.t. and dry loading onto silica. Purification by automated medium-pressure chromatography (hexane/acetone = 100/0 to 60/40) afforded the product (−)-**6** as a white solid (mg, 91% yield). SFC analysis showed an enantiomeric excess of >95% due to inability to find a gradient to separate two peaks.

^{1}H NMR ($CDCl_3$, 600 MHz) δ (ppm) = 6.16 (s, 1H, C^4–H), 5.52 (s, 1H, C^3–H), 4.74 – 4.36 (m, 2H, C^1–H, C^5–H), 3.75 – 3.57 (m, 4H, C^8–H, C^{11}–H), 2.75 (ddd, *J* = 14.8, 7.3, 4.3 Hz, 3H, C^2–

H, C^9/C^{10}–H), 2.68 – 2.57 (m, 2H, C^9/C^{10}–H), 2.09 – 1.96 (m, 1H, C^6/C^7–H), 1.73 (d, *J* = 9.5 Hz, 3H, C^6/C^7–H), 1.53 – 1.28 (m, 9H, –$C(CH_3)_3$).

^{13}C NMR ($CDCl_3$, 151 MHz) δ (ppm) = 152.9 (–C=O), 135.1 (C^4), 134.5 (rot. C^4), 124.7 (rot. C^3), 124.3 (C^3), 79.8 (–$\underline{C}(CH_3)_3$), 67.8 (C^8, C^{11}), 67.6 (C^2), 53.5 (rot. C^1/C^5), 52.4 (C^1/C^5), 52.2 (C^1/C^5), 51.2 (rot. C^1/C^5), 49.7 (C^9, C^{10}), 28.7 (–$C(\underline{C}H_3)_3$), 28.0 (C^6/C^7), 27.4 (C^6/C^7).

HRMS (APCI): m/z calculated for $C_{16}H_{27}O_3N_2^+$ $[M+H]^+$ 295.2016, found 295.2016.

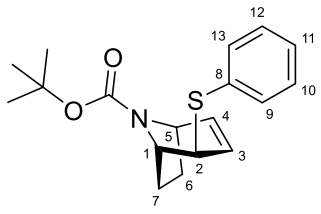
IR: 2955, 2920, 2851, 1693, 1477, 1452, 1420, 1392, 1366, 1338, 1296, 1253, 1228, 1166, 1135, 1116, 1100, 1069, 1043, 1004, 979, 957, 924, 905, 893, 869, 830, 770, 712, 697, 662, 647, 619, 607 cm^{-1}

Melting Point: 89.6 – 90.7 °C

SFC Chiralpak ® IG; 1500 psi, 30 °C; flow: 1.5 ml/min; from 1% to 20% MeOH in 5 min (major enantiomer t_R = 3.01 min).

$[\alpha]^{25}_D$ = −34.3 (c = 1.0, $CHCl_3$).

Synthesis of (−)-7



(−)-**7**

According to a previous procedure by the group with modified conditions,[177] (+)-**1a** (37.4 mg, 0.125 mmol), K_2CO_3 (0.11 g, 0.25 mmol) was dissolved in MeCN (1.6 mL) and thiophenol (38.0 μL) was added (0.04 mL, 0.375 mmol). Then, the reaction mixture was heated at 80 °C overnight before cooling to r.t. and dry loading onto silica. Purification by automated medium-pressure chromatography (hexane/EtOAc = 100/0 to 90/10) afforded the product (−)-**7** as a

white solid (39 mg, quantitative yield). SFC analysis showed an enantiomeric excess of >99%.

^{1}H NMR ($CDCl_3$, 600 MHz) δ (ppm) = 7.64 – 7.40 (m, 2H, aryl–H), 7.30 (t, *J* = 7.6 Hz, 2H, aryl–H), 7.24 (t, *J* = 7.4 Hz, 1H, aryl–H), 6.14 – 5.97 (m, 1H, C^4–H), 5.69 – 5.50 (m, 1H, C^3–H), 4.63 – 4.42 (m, 2H, C^1–H, C^5–H), 3.62 – 3.43 (m, 1H, C^2–H), 2.18 – 2.02 (m, 1H, C^6/C^7–H), 1.90 – 1.75 (m, 2H, C^6/C^7–H), 1.62 – 1.55 (m, 1H, C^6/C^7–H), 1.46 (s, 9H, –$C(CH_3)_3$).

^{13}C NMR ($CDCl_3$, 151 MHz) δ (ppm) = 153.6 (–C=O), 136.0 (C^4), 135.3 (rot. C^4), 134.1 (C^8), 133.4 (aryl–C), 131.4 (aryl–C), 129.1 (aryl–C), 127.0 (aryl–C), 124.2 (rot. C^3), 123.5 (C^3), 79.8 (–$\underline{C}(CH_3)_3$), 56.2 (rot. C^1/C^5), 54.0 (C^2), 53.1 (rot. C^1/C^5), 52.4 (C^1/C^5), 33.4 (C^6/C^7), 29.1 (C^6/C^7), 28.5 (–$C(\underline{C}H_3)_3$), 28.5 (rot. –$C(\underline{C}H_3)_3$).

HRMS (APCI): m/z calculated for $C_{18}H_{23}O_2SNNa^+$ $[M+Na]^+$ 340.1342, found 340.1341.

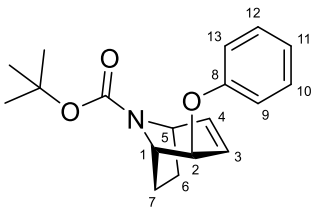
Melting Point: 76.3 – 77.8 °C

IR: 2974, 2929, 2870, 2360, 1693, 1584, 1478, 1420, 1391, 1366, 1338, 1298, 1250, 1225, 1168, 1102, 1065, 1042, 1026, 1003, 966, 892, 872, 835, 785, 742, 693, 650, 627 cm^{-1}

SFC Chiralpak ® IA; 1500 psi, 30 °C; flow: 1.5 ml/min; from 1% to 30% MeOH in 5 min (major enantiomer t_R = 2.59 min; minor enantiomer t_R = 2.47 min)

$[\alpha]^{25}_D$ = −57.9 (c = 1.0, $CHCl_3$).

Synthesis of (−)-8



(−)-**8**

According to a previous procedure by the group with modified conditions,[177] (+)-**1a** (32.3 mg,

0.13 mmol), K_2CO_3 (72.3 mg, 0.52 mmol) and phenol (21.8 mg, 0.30 mmol) was dissolved in 1,4-dioxane (2 mL) and the reaction mixture was heated to reflux for 72 h before cooling to r.t. Acetyl chloride (0.04 mL) was added dropwise and the reaction was wash with brine followed by extraction with EtOAc (10 mL × 3). The crude product was loaded onto silica and purification by automated medium-pressure chromatography (hexane/EtOAc = 100/0 to 90/10) afforded the product (−)-**8** as a white solid (38 mg, quantitative yield). SFC analysis showed an enantiomeric excess of >99%.

^{1}H NMR ($CDCl_3$, 600 MHz) δ (ppm) = 7.32 – 7.26 (m, 2H, aryl–H), 7.05 – 6.87 (m, 3H, aryl–H), 6.33 (s, 1H, C^4–H), 5.84 – 5.68 (m, 1H, C^3–H), 4.68 (d, *J* = 7.8 Hz, 1H, C^1/C^5–H), 4.64 – 4.51 (m, 1H, C^1/C^5–H), 4.30 (d, *J* = 4.4 Hz, 1H, C^2), 2.23 – 2.07 (m, 1H, C^6/C^7–H), 1.87 (s, 1H, C^6/C^7–H), 1.71 (ddd, *J* = 11.5, 8.9, 2.4 Hz, 1H, C^6/C^7–H), 1.52 – 1.24 (m, 10H, –$C(CH_3)_3$, C^6/C^7–H).

^{13}C NMR ($CDCl_3$, 151 MHz) δ (ppm) = 157.7 (–C=O), 153.4 (C^8), 137.1 (C^4), 129.6 (aryl–C), 122.5 (aryl–C), 121.1 (aryl–C), 117.0 (rot. C^3), 115.7 (C^3), 79.5 (–$\underline{C}(CH_3)_3$), 54.3 (C^2), 53.6 (C^1/C^5), 51.9 (C^1/C^5), 30.8 (C^6/C^7), 29.8 (rot. C^6/C^7), 28.5 (rot. –$C(\underline{C}H_3)_3$), 28.3 (–$C(\underline{C}H_3)_3$), 24.82 (C^6/C^7).

HRMS (APCI): m/z calculated for $C_{18}H_{23}O_3NNa^+$ $[M+Na]^+$ 324.1570, found 324.1570.

Melting Point: 72.5 – 73.4 °C

IR: 2975, 2360, 1693, 1596, 1493, 1420, 1390, 1365, 1347, 1319, 1292, 1229, 1174, 1105, 1072, 1050, 1027, 1010, 990, 911, 872, 840, 821, 753, 718, 693, 608 cm^{-1}

SFC Chiralpak ® IG; 1500 psi, 30 °C; flow: 1.5 ml/min; from 1% to 30% MeOH in 5 min (major enantiomer t_R = 2.85 min; minor enantiomer t_R = 3.02 min)

$[\alpha]^{25}_D$ = −26.4 (c = 1.0, $CHCl_3$).

4.2.6 Calculation of Apparent S-Factors

The ee of the remaining allyl chloride (+)-**1a** and product **3a** – **3t** are determined by Super Fluid Chromatography (SFC).

Two different conversion values of **1a** were used for calculation of apparent *s*-factors: Conversion 1 (C1) was determined by (1− isolated yield of **1a** after reaction), Conversion 2 (C2) was determined by (1− isolated yield of product after reaction) taking into account the competitive hydrolysis of **1a**.

The apparent *s*-factors were calculated using formula (1) below (C1/C2: Conversion; ee: ee of **1a**).[249]

$$s = \frac{\ln [(1-C)(1-ee)]}{\ln [(1-C)(1+ee)]} \qquad (1)$$

The calculated apparent *s*-factors are shown below in Table 4.2.1.

Some of the apparent s-factor values give what might be unexpected values, likely due to one or both of the following reasons:

1. Competitive hydrolysis resulted in an inaccurate conversion during calculation, as consumption of **1a** did not all result in product formation.

2. The Rh–Catalysed cross–Coupling reaction does not proceed like classical kinetic resolutions, where one enantiomer of the starting material is converted to product much faster than the other enantiomer so that the less reactive enantiomer of the substrate and the product are both highly enantioenriched. In our case, there is potentially equilibration of intermediates arising from both enantiomers of **1a**, and a partial DyKAT-like mechanism. Therefore, the S-factor cannot be used to meaningfully measure the efficiency of the observed kinetic resolution, and so the values given here are the 'apparent s-factor'.

Table 4.2.1 Yields and ee of products and calculated conversion and *s*-factor.

Entry	Product	Product yield/%	Product ee/%	% of SM recovered	**1a** ee/%	C1/%	C2/%	Apparent s-factor 1	Apparent s-factor 2
1	**3a**	50	95	39	>99	61	50	21.88	1057.01
2	**3b**	44	96	30	>99	70	56	11.26	40.85
3	**3c**	32	94	37	>99	63	68	18.29	12.73
4	**3d**	51	95	31	>99	69	49	11.96	-356.90
5	**3e**	44	94	21	>99	79	56	7.07	40.85
6	**3f**	49	98	38	>99	62	51	19.94	210.92
7	**3g**	47	96	25	>99	75	53	8.58	80.14
8	**3h**	39	96	35	>99	65	61	15.64	21.88
9	**3i**	22	96	66	59	34	78	-27.11	2.29
10	**3j**	23	97	46	39	54	77	2.84	1.72
11	**3k**	19	98	65	31	35	81	4.99	1.46
12	**3l**	59	96	27	>99	73	41	9.52	-31.98
13	**3m**	38	96	12	>99	88	62	4.70	19.94
14	**3n**	49	97	46	>99	54	51	60.88	210.92
15	**3o**	46	97	36	>99	64	54	16.87	60.88
16	**3p**	56	97	28	>99	72	44	10.05	-47.87
17	**3q**	42	97	26	>99	74	58	9.03	30.51
18	**3r**	15	98	65	26	35	85	3.67	1.32
19	**3s**	44	88	40	>99	60	56	24.20	40.85
20	**3t**	21	88	56	38	44	79	4.10	1.65

4.2.7 X-Ray Crystallographic Analysis

Low temperature single crystal X-ray diffraction data were collected using a (Rigaku) Oxford Diffraction SuperNova diffractometer. Raw frame data were reduced using CrysAlisPro and the structures were solved using 'Superflip' [250] before refinement with CRYSTALS as per the SI (CIF). [251-252] Crystallographic data have been deposited with the Cambridge Crystallographic Data Centre as supplementary publication no. CCDC 2156812, 2156553, 2156805 and can be obtained *via* www. ccdc.cam.ac.uk/data_request/cif.

Table 4.2.2 Crystal data and structure refinement for **(+)-1a**.

CCDC number	2156812
Temperature	150 K
Wavelength	1.54184 Å
Crystal system / Space group	Orthorhombic / $P2_12_12_1$
Unit cell dimensions	a = 7.16900(10) Å α = 90°.
	b = 10.31260(10) Å β = 90°.
	c = 17.30370(10) Å γ = 90°.
Volume	1279.28(2) $Å^3$
Z	4
Independent reflections	2649 [R(int) = 0.032]
Data / restraints / parameters	2649 / 0 / 147
Goodness-of-fit on F^2	1.0129
Final R indices [I>2sigma(I)]	R1 = 0.0202, wR2 = 0.0542
R indices (all data)	R1 = 0.0204, wR2 = 0.0544
Absolute structure parameter	-0.003(3)
Extinction coefficient	41(4)

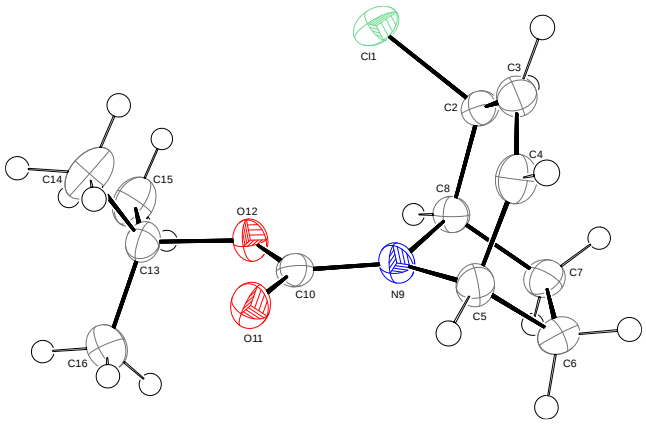


Table 4.2.3 Crystal data and structure refinement for **3p**.

CCDC number	2156553	
Temperature	150 K	
Wavelength	1.54184 Å	
Crystal system / Space group	Monoclinic / $P2_1$	
Unit cell dimensions	a = 8.00800(10) Å	α= 90°.
	b = 16.0984(3) Å	β = 103.3911(18)°.
	c = 11.7605(2) Å	γ = 90°.
Volume	1474.90(4) $Å^3$	
Z	4	
Independent reflections	6078 [R(int) = 0.041]	
Data / restraints / parameters	6076 / 1 / 363	
Goodness-of-fit on F^2	1.0043	
Final R indices [I>2sigma(I)]	R1 = 0.0345, wR2 = 0.0833	
R indices (all data)	R1 = 0.0376, wR2 = 0.0868	
Absolute structure parameter	0.01(8)	
Extinction coefficient	13(3)	

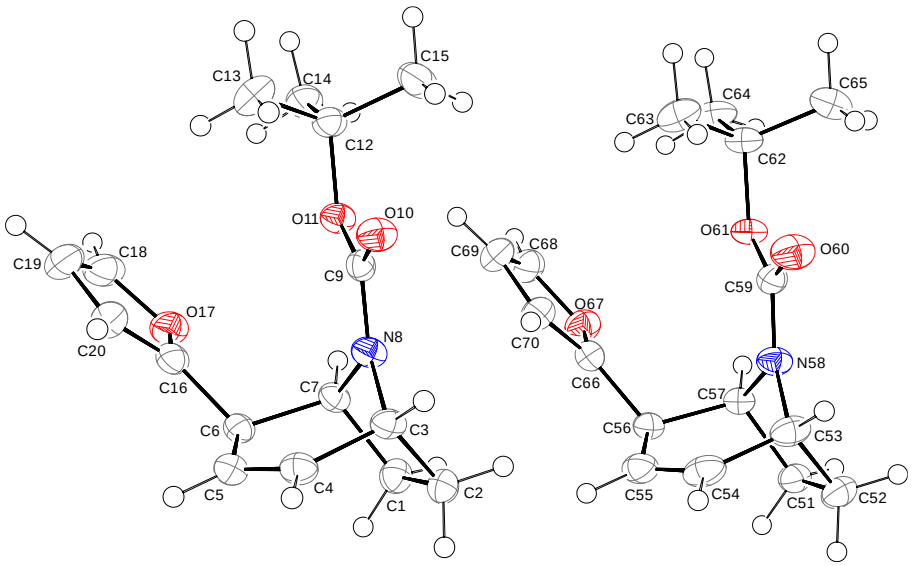
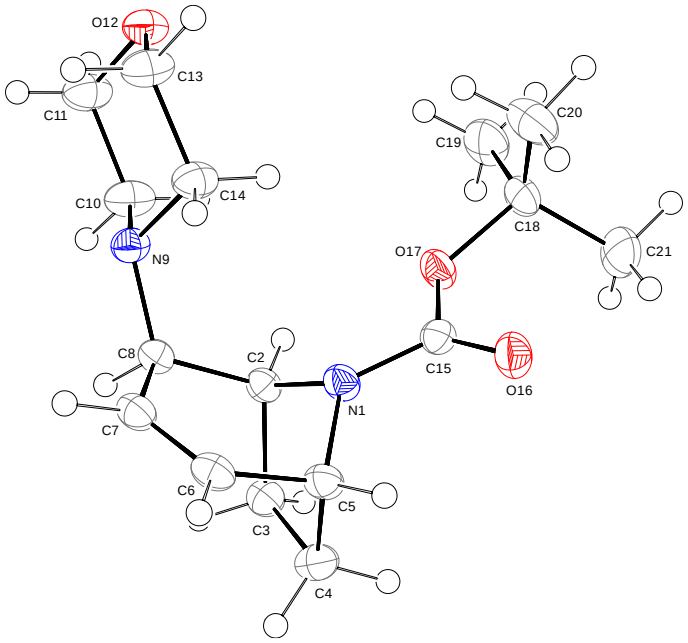


Table 4.2.4. Crystal data and structure refinement for (–)-**6**.

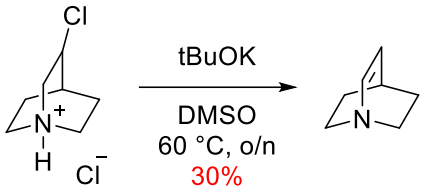
CCDC number	2156805
Temperature	150 K
Wavelength	1.54184 Å
Crystal system / Space group	Orthorhombic / $P2_12_12_1$
Unit cell dimensions	a = 6.13100(10) Å α = 90°.
	b = 15.83460(10) Å β = 90°.
	c = 16.66730(10) Å γ = 90°.
Volume	1618.09(3) $Å^3$
Z	4
Independent reflections	3363 [R(int) = 0.026]
Data / restraints / parameters	3363 / 0 / 191
Goodness-of-fit on F^2	1.0052
Final R indices [I>2sigma(I)]	R1 = 0.0266, wR2 = 0.0710
R indices (all data)	R1 = 0.0270, wR2 = 0.0715
Absolute structure parameter	-0.03(3)
Largest diff. peak and hole	0.06 and -0.07 $e.Å^{-3}$



4.3 Chapter 3 Procedures

4.3.1 Substrate Synthesis

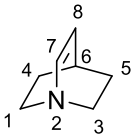
Synthesis of 9a



Scheme 4.3.1 Overview of synthesis **9a**.

According to a procedure by Lasne and coworkers, [231] the hydrochloride salt of 3–Chloroquinuclidine (1.82 g, 10.0 mmol) and potassium *tert*-butoxide (3.36 g, 30.0 mmol) was dissolved in dimethyl sulfoxide (20 mL), and the reaction mixture was stirred at 60 °C overnight. Diethyl ether (10 mL) was added to the flask and the crude mixture was washed with 1 M NaOH solution (15 mL × 10), and the aqueous phase was washed with diethyl ether (20 mL × 10). The organic layer was dried over $MgSO_4$ and concentrated at 400 mbar in 25 °C water bath. The crude mixture was purified by distillation at 150 mbar up to 80 °C, and the product **9a** was collected at -78 °C as a white solid (up to 30%).

The product is highly volatile and exhibits oily character at room temperature, therefore exhibited higher yield upon larger scale due to loss in distillation. The product is sensitive towards air and oxidation and turned yellow under air exposure at room temperature.



9a

^{1}H NMR ($CDCl_3$, 400 MHz) δ (ppm) = 6.50 – 6.44 (m, 2H, C^7–H, C^8–H), 3.02 – 2.65 (m, 2H, C^1/C^3–H), 2.65 – 2.44 (m, 3H, C^1/C^3–H, C^6–H), 1.66 – 1.53 (m, 2H, C^4–H, C^5–H), 1.50 – 1.38 (m, 2H, C^4–H, C^5–H).

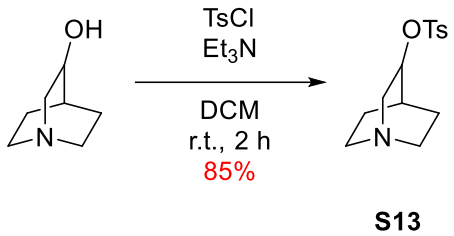
^{13}C NMR ($CDCl_3$, 151 MHz) δ (ppm) = 142.5 (C^7), 135.8 (C^8), 48.8 (C^1/C^3), 47.8 (C^1/C^3), 42.4 (C^6), 27.8 (C^4/C^5), 26.5 (C^4/C^5).

HRMS (APCI): m/z calculated for $C^7H_{12}N$ $[M+H]^+$ 110.0964, found 110.0967.

IR: 3037, 2943, 2867, 1604, 1455, 1365, 1313, 1158, 1060, 1036, 1011, 987, 970, 878, 835, 811, 787, 731, 607 cm^{-1}

Melting Point: 69.1 – 71.3 °C.

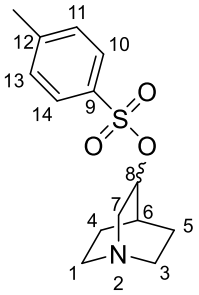
Synthesis of S13



S13

Scheme 4.3.2 Overview of synthesis **S13**.

Following the procedure by O'Neil *et al*., [222] 3-quinuclidinol (2.52 g, 20.0 mmol) and 4-toluenesulfonyl chloride (7.64 g, 40.0 mmol) was dissolved in DCM (54 mL) and triethylamine (5.2 mL, 36.6 mmol) was added dropwise at 0 °C. The ice bath was removed, and the reaction was stirred at room temperature for 2 h. The reaction was quenched by addition of 1 M NaOH (20 mL). The crude mixture was extracted with DCM (40 mL × 3) and dried over $MgSO_4$. The combined organic layer was concentrated in vacuo and the crude product was purified by flash column chromatography (DCM/MeOH = 100/0 to 95/5) to afford the product **S13** as light-yellow solid (4.77 g, 85% yield).



S13

^{1}H NMR ($CDCl_3$, 400 MHz) δ (ppm) = 7.85 – 7.78 (m, 2H, C^{10}–H, C^{14}–H), 7.36 (d, *J* = 7.9 Hz, 2H, C^{11}–H, C^{13}–H), 4.67 – 4.57 (m, 1H, C^{8}–H), 3.14 – 3.03 (m, 1H, C^{7}–H), 2.97 – 2.58 (m, 5H, C^{4}–H, C^{5}–H, C^{7}–H), 2.47 (s, 3H, -PhC<u>H</u>$_3$), 2.05 – 1.97 (m, 1H, C^{6}–H), 1.87 (dddt, *J* = 12.0, 10.1, 5.0, 2.0 Hz, 1H, C^{1}/C^{3}–H), 1.74 – 1.61 (m, 1H, C^{1}/C^{3}–H), 1.53 – 1.31 (m, 2H, C^{1}/C^{3}–H).

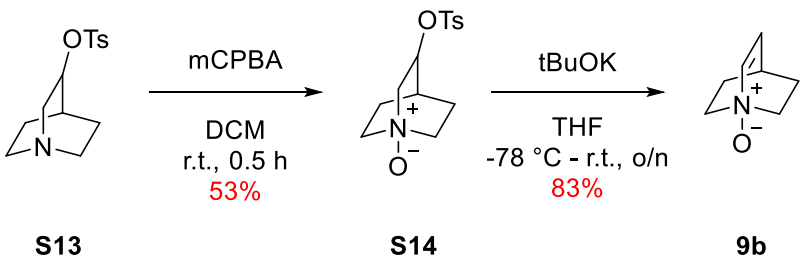
^{13}C NMR ($CDCl_3$, 151 MHz) δ (ppm) = 129.9 (C^{10}, C^{14}), 127.5 (C^{11}, C^{13}), 79.3 (C^{8}), 55.1 (C^{7}), 47.1 (C^{4}/C^{5}), 46.1 (C^{4}/C^{5}), 26.2 (C^{6}), 24.5 (C^{1}/C^{3}), 21.5 (-PhC<u>H</u>$_3$), 18.8 (C^{1}/C^{3}), 18.5 (C^{1}/C^{3}).

HRMS (APCI): m/z calculated for $C_{14}H_{20}NO_3S$ $[M+H]^+$ 282.1158, found 282.1154.

IR: 3399, 2988, 1598, 1493, 1463, 1358, 1190, 1175, 1122, 1093, 1034, 1011, 987, 952, 899, 818, 785, 731, 710, 681, 668 cm^{-1}

Melting Point: 92.7 – 93.6 °C

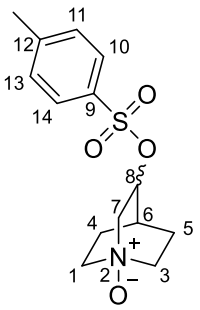
Synthesis of *N*-oxide substrate 9b



S13 **S14** **9b**

Scheme 4.3.3 Overview of synthesis **9b**.

Synthesis of S14



S14

Based on the procedure by O'Neil *et al*., [222] **S13** (1.12 g, 3.76 mmol) was dissolved in DCM (20 mL), and *m*CPBA (1.03 g, 5.64 mmol) was added portionwise at 0 °C. The ice bath was removed, and the reaction was stirred at room temperature for 30 min. The crude mixture was loaded directly on to column and the crude product was purified by flash column chromatography (EtOAc/MeOH = 100/0 to 20/80) to afford the product **S14** as a white solid (0.63 g, 53% yield). The acid side product was washed out at EtOAc/MeOH = 80/20.

The progression of reaction required high purity *m*CPBA, potentially because the impurities including *m*-chlorobenzoic acid and water in commercial *m*CPBA inhibited the reaction. Therefore, the commercial *m*CPBA (~77% purity) was purified by recrystallisation before use in the reaction.

^{1}H NMR ($CDCl_3$, 400 MHz) δ (ppm) = 7.85 – 7.78 (m, 2H, C^{10}–H, C^{14}–H), 7.36 (d, *J* = 7.9 Hz, 2H, C^{11}–H, C^{13}–H), 4.67 – 4.57 (m, 1H, C^8–H), 3.14 – 3.03 (m, 1H, C^7–H), 2.97 – 2.58 (m, 5H, C^4–H, C^5–H, C^7–H), 2.47 (s, 3H, -PhC$\underline{H}_3$), 2.05 – 1.97 (m, 1H, C^6–H), 1.87 (dddt, *J* = 12.0, 10.1, 5.0, 2.0 Hz, 1H, C^1/C^3–H), 1.74 – 1.61 (m, 1H, C^1/C^3–H), 1.53 – 1.31 (m, 2H, C^1/C^3–H).

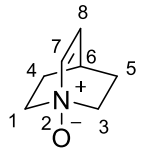
^{13}C NMR ($CDCl_3$, 151 MHz) δ (ppm) = 129.9 (C^{10}, C^{14}), 127.5 (C^{11}, C^{13}), 79.3 (C^8), 55.1 (C^7), 47.1 (C^4/C^5), 46.1 (C^4/C^5), 26.2 (C^6), 24.5 (C^1/C^3), 21.5 (-Ph$\underline{C}H_3$), 18.8 (C^1/C^3), 18.5 (C^1/C^3).

HRMS (APCI): m/z calculated for $C_{14}H_{20}NO_4S$ $[M+H]^+$ 298.1108, found 298.1105.

IR: 3392, 3248, 1599, 1494, 1459, 1367, 1174, 1095, 1073, 976, 947, 900, 815, 788, 666 cm^{-1}

Melting Point: 108.3 – 109.0 °C

Synthesis of 9b



9b

Based on the procedure by O'Neil *et al*., [222] **S14** (0.157 g, 0.53 mmol) was dissolved in THF (1.1 mL), and potassium *tert*-butoxide (89.0 mg, 0.79 mmol) was added portion-wise at -78 °C. The cooling bath was left to warm up to room temperature and the reaction mixture was stirred overnight. The crude mixture was loaded directly onto the column and purified by flash column chromatography (EtOAc/MeOH = 80/20 to 60/40) to afford the product **9b** as an oil (66.1 mg, 83% yield).

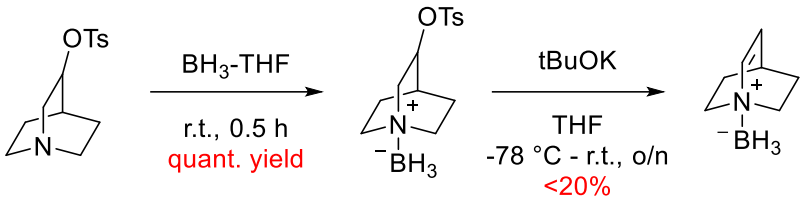
^{1}H NMR ($CDCl_3$, 400 MHz) δ (ppm) = 6.66 (d, J = 1.0 Hz, 1H, C^7–H), 6.45 (t, J = 6.6 Hz, 1H, C^8–H), 3.58 – 3.47 (m, 2H, C^1/C^3–H), 3.32 – 3.18 (m, 2H, C^1/C^3–H), 2.87 – 2.77 (m, 1H, C^6–H), 2.03 – 1.91 (m, 2H, C^4/C^5–H), 1.87 – 1.73 (m, 2H, C^4/C^5–H).

^{13}C NMR ($CDCl_3$, 151 MHz) δ (ppm) = 146.2 (C^7), 129.9 (C^8), 65.7 (C^1, C^3), 26.5 (C^4, C^5), 25.5 (C^6).

HRMS (APCI): m/z calculated for $C^7H_{12}NO$ $[M+H]^+$ 126.0913, found 126.0915.

IR: 3661, 2981, 2885, 1461, 1386, 1251, 1151, 1081, 966, 946, 898, 815, 709, 667, 630 cm^{-1}

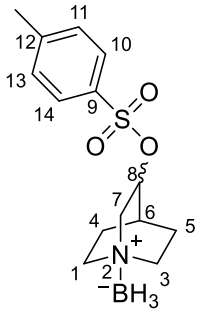
Synthesis of the Nitrogen-Borane substrate 9c



S13 **S15** **9c**

Scheme 4.3.4 Overview of synthesis **9b**.

Synthesis of S15



S15

Based on the procedure by O'Neil *et al.*, [222] H_3B-THF (1 M, 3.8 mL) solution was added dropwise to **S13** (0.700 g, 2.49 mmol) at 0 °C, and the ice bath was removed and the reaction mixture was left stirring at room temperature. The reaction was monitored by TLC and stirring was stopped after 2.5 h with the reaction mixture concentrated to afford **S15** (0.735 g, quant. yield), which is used directly in the next step without further purifications.

The product was observed to decompose on 2D TLC hence column chromatography was not used as purification method.

^{1}H NMR ($CDCl_3$, 400 MHz) δ (ppm) = 7.85 – 7.75 (m, 2H, C^{10}–H, C^{14}–H), 7.43 – 7.35 (m, 2H, C^{11}–H, C^{13}–H), 4.76 – 4.67 (m, 1H, C^8–H), 3.17 (ddt, *J* = 15.1, 8.5, 1.6 Hz, 1H), 3.09 – 2.98 (m, 2H, C^4/C^5–H), 3.02 – 2.90 (m, 2H, C^7–H), 2.94 – 2.84 (m, 1H, C^4/C^5–H), 2.88 – 2.78 (m, 1H, C^4/C^5–H), 2.47 (s, 3H, -PhC$\underline{H}_3$), 2.29 (tp, *J* = 4.3, 2.4 Hz, 1H, C^6–H), 2.15 – 2.01 (m, 1H, C^1/C^3–H), 1.86 (ddt, *J* = 14.2, 10.1, 4.4 Hz, 1H, C^1/C^3–H), 1.72 – 1.56 (m, 2H, C^1/C^3–H),

1.50 (s, 3H, -B<u>H</u>$_3$).

^{13}C NMR ($CDCl_3$, 151 MHz) δ (ppm) = 130.2 (C^{11}, C^{13}), 127.5 (C^{10}, C^{14}), 75.7 (C^8), 59.7 (C^4/C^5), 53.4 (C^4/C^5), 52.4 (C^7), 25.8 (C^6), 22.5 (C^1/C^3), 21.8 (-Ph<u>C</u>H$_3$), 18.5 (C^1/C^3).

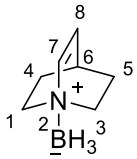
^{11}B NMR ($CDCl_3$, 193 MHz) δ (ppm) = -2.85 (s).

HRMS (APCI): m/z calculated for $C_{14}H_{22}BNNaO_3S$ $[M+Na]^+$ 318.1306, found 318.1306.

IR: 2956, 2925, 2365, 2276, 1597, 1456, 1401, 1361, 1338, 1192, 1172, 1095, 1036, 1107, 977, 957, 912, 875, 861, 834, 822, 813, 786, 739, 706, 666, 647, 634, 620 cm^{-1}

Melting Point: 84.2 – 86.4 ℃.

Synthesis of 9c



9c

Based on the procedure by O'Neil *et al*., [222] a solution of **S15** (0.735 g, 2.49 mmol) in THF (15 mL) was added dropwise to potassium *tert*-butoxide (0.559 g, 4.98 mmol) at -78 ℃. The cooling bath was removed after 2 h, and THF (3 mL) was added to quench the reaction. The reaction mixture was filtered under reduced pressure, and the white solid was collected washed with NaOH (5 mL) and extracted with DCM (10 mL × 3) and concentrated to afford the product **9c** as off-white solid (<20% yield).

The product appeared to be stable on 2D TLC but decomposition was observed during column chromatography purification. TsOH was observed to be the side product, purification by distillation under reduced pressure only afforded **9a**, indicating that **9c** was sensitive towards heating.

^{1}H NMR (D_2O, 400 MHz) δ (ppm) = 7.06 (d, *J* = 6.9 Hz, 1H, C^8–H), 6.79 (s, 1H, C^7–H), 5.40 (d, *J* = 3.5 Hz, 2H,), 3.85 – 3.70 (m, 2H, C^1/C^3–H), 3.47 (s, 2H, C^1/C^3–H), 3.17 (s, 1H, C^6–H), 2.44 (s, 3H, -B$\underline{H}_3$), 2.18 (s, 2H, C^4/C^5–H), 1.91 (d, *J* = 13.9 Hz, 2H, C^4/C^5–H).

^{13}C NMR (D_2O, 151 MHz) δ (ppm) = 137.8 (C^8), 131.3 (C^7), 58.2 (C^1/C^3), 57.7 (C^1/C^3), 25.7 (C^6), 23.7 (C^4/C^5), 23.3 (C^4/C^5).

^{11}B NMR (D_2O, 193 MHz) δ (ppm) = -2.87 (s).

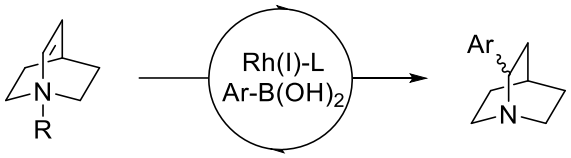
HRMS (APCI): m/z calculated for $C^7H_{14}BN$ 123.1219, molecular ion not found.

IR: 3017, 1627, 1479, 1422, 1188, 1127, 1036, 1011, 945, 826, 813, 726, 685, 636 cm^{-1}

Melting Point: > 200 °C.

4.3.2 Rh–Catalysed Asymmetric Arylation Reactions

Substrates **9a** – **9c** were tested with different Rh–Catalysed arylation procedures, which are summarised below. All reactions were carried out under an inert argon atmosphere using standard Schlenk techniques with all reagents weighed open to air.



Scheme 4.3.4 Rh–Catalysed arylation reaction on dehydroquinuclidine derivatives.

General Procedure A

According to the procedure by Goetzke *et. al*.,[229] $[Rh(cod)OH]_2$ (2.3 mg, 2.5 mol%) and (*S*)-Segphos (7.3 mg, 6.0 mol%) were dissolved in THF (1.0 mL) under an argon atmosphere stirred at 60 °C for 30 min. The dark-orange complex was left to reach room temperature over 10 min maximum and was then added to a solution of phenyl boronic acid (0.40 mmol, 2.0 equiv.) and

9a (0.20 mmol, 1.0 equiv.) in toluene (1.0 mL) and H_2O (0.04 mL) under an argon atmosphere. The resulting mixture was stirred at 80 °C overnight. The crude mixture was then cooled to room temperature and diluted with hexane (1 mL) and directly loaded onto silica for purification.

Racemic samples of the products were synthesised with *rac*-BINAP (purchased from commercial suppliers).

General Procedure B

The procedure is same to **General Procedure A** with CsOH (0.40 mmol, 1.0 equiv) added into the reaction mixture after addition of Rh-ligand complex solution.

General Procedure C

According to a procedure by Lautens and coworkers, [236] $[Rh(cod)OH]_2$ (4.6 mg, 2.5 mol%), *tert*-Bu-Josiphos (SL-J002-1) (13.0 mg, 6.0 mol%) was added to a 10 mL round-bottom flask equipped with a magnetic stir bar. The flask was flushed with argon and THF (1.5 mL) and H_2O (0.3 mL) were added. The clear orange solution was stirred at room temperature for 15-20 min. Substrate **9a** (0.2 mmol, 1.0 equiv.) and phenylboronic acid (0.4 mmol, 2.0 equiv) were added together as a solution in THF (1.2 mL). The reaction mixture was allowed to react at 60 °C overnight and allowed to cool to room temperature before quenching with hexane dilution (1 mL). The reaction mixture was filtered on a short silica gel pipette and directly loaded onto the column for purification.

Racemic samples of the products were synthesised with *rac*-BINAP (purchased from commercial suppliers).

General Procedure D

The procedure is same to **General Procedure C** with CsOH (0.20 mmol, 1.0 equiv) added into the reaction mixture after addition of Rh-ligand complex solution.

General Procedure E

According to a procedure by the Fletcher group member, $[Rh(cod)OH]_2$ (4.6 mg, 2.5 mol%), (*S*)-Segphos (14.6 mg, 6.0 mol%) was added to a 5 mL round-bottom flask equipped with a magnetic stir bar. THP (0.2 mL) and toluene (0.2 mL) were added into the flask and the reaction mixture was heated at 60 °C for 30 min. The complex was allowed to cool to room temperature before being added to a solution of substrate **9a** (0.4 mmol, 1.0 equiv.) and phenylboronic acid (0.8 mmol, 2.0 equiv) in H_2O (0.2 mL). The reaction was stirred overnight at 60 °C, and then cooled to room temperature before quenching with hexane dilution (1 mL). The reaction mixture was filtered on a short silica gel pipette and directly loaded onto the column for purification.

General Procedure F

According to a procedure by the Fletcher group member, $[Rh(cod)OH]_2$ (4.6 mg, 2.5 mol%), Walphos (SL-W003-1, 16.1 mg, 6.0 mol%) was added to a 5 mL round-bottom flask equipped with a magnetic stir bar. THP (0.3 mL) was added into the flask and the reaction mixture was heated at 60 °C for 30 min. The complex solution was then allowed to cool to room temperature before addition to the solution of substrate **9a** (0.4 mmol, 1.0 equiv.), phenylboronic acid (1.2 mmol, 3.0 equiv), Cs_2CO_3 (130 mg, 1.0 equiv.), and $Zn(OTf)_2$ (14.5 mg, 0.2 equiv.) in THP (0.1 mL). The reaction was stirred overnight at 60 °C, and then cooled to room temperature before quenching with hexane dilution (1 mL). The reaction mixture was filtered on a short silica gel pipette and directly loaded onto the column for purification.

5. References

[1] J. March, *Advanced organic chemistry*, **1968**.

[2] E. J. Corey, *Angew. Chem., Int. Ed. Engl.* **1991**, *30*, 455-465.

[3] E. J. Corey, *The logic of chemical synthesis*, Рипол Классик, **1991**.

[4] A. De Meijere, F. Diederich, A. de Meijere, *Metal-catalyzed cross-coupling reactions, Vol. 1*, Wiley-VCH Weinheim, **2004**.

[5] E.-i. Negishi, A. De Meijere, *Handbook of organopalladium chemistry for organic synthesis*, John Wiley & Sons, **2003**.

[6] R. F. Heck, *J. Am. Chem. Soc.* **1969**, *91*, 6707-6714.

[7] K. Tamao, K. Sumitani, M. Kumada, *J. Am. Chem. Soc.* **1972**, *94*, 4374-4376.

[8] K. Sonogashira, *J. Organomet. Chem.* **2002**, *653*, 46-49.

[9] A. O. King, N. Okukado, E.-i. Negishi, *J. Chem. Soc., Chem. Commun.* **1977**, 683-684.

[10] J. K. Stille, *Angew. Chem., Int. Ed. Engl.* **1986**, *25*, 508-524.

[11] N. Miyaura, A. Suzuki, *Chem. Rev.* **1995**, *95*, 2457-2483.

[12] N. Miyaura, A. Suzuki, *J. Chem. Soc., Chem. Commun.* **1979**, 866-867.

[13] N. Miyaura, K. Yamada, A. Suzuki, *Tetrahedron Lett.* **1979**, *20*, 3437-3440.

[14] D. Zhang, Q. Wang, *Coord. Chem. Rev.* **2015**, *286*, 1-16.

[15] A. Suzuki, *Angew. Chem. Int. Ed.* **2011**, *50*, 6722-6737.

[16] D. G. Hall, *Boronic acids: preparation, applications in organic synthesis and medicine*, John Wiley & Sons, **2006**.

[17] F. Lovering, J. Bikker, C. Humblet, *J. Med. Chem.* **2009**, *52*, 6752-6756.

[18] F. Lovering, *MedChemComm* **2013**, *4*, 515-519.

[19] D. C. Blakemore, L. Castro, I. Churcher, D. C. Rees, A. W. Thomas, D. M. Wilson, A. Wood, *Nat. Chem.* **2018**, *10*, 383-394.

[20] E. L. Eliel, S. H. Wilen, *Stereochemistry of organic compounds*, John Wiley & Sons, **1994**.

[21] G. Bringmann, T. Gulder, T. A. M. Gulder, M. Breuning, *Chem. Rev.* **2011**, *111*, 563-639.

[22] H. Yang, J. Sun, W. Gu, W. Tang, *J. Am. Chem. Soc.* **2020**, *142*, 8036-8043.

[23] A. Joncour, A. Décor, J. M. Liu, M. E. Tran Huu Dau, O. Baudoin, *Chem. Eur. J.* **2007**, *13*, 5450-5465.

[24] E. Kumarasamy, R. Raghunathan, M. P. Sibi, J. Sivaguru, *Chem. Rev.* **2015**, *115*, 11239-

11300.

[25] F. W. Goetzke, L. Dijk, S. P. Fletcher, in *PATAI'S Chemistry of Functional Groups*, **2019**, pp. 1-54.

[26] T. Hayashi, K. Hayashizaki, T. Kiyoi, Y. Ito, *J. Am. Chem. Soc.* **1988**, *110*, 8153-8156.

[27] A. N. Cammidge, K. V. L. Crépy, *ChemComm* **2000**, 1723-1724.

[28] J. Yin, S. L. Buchwald, *J. Am. Chem. Soc.* **2000**, *122*, 12051-12052.

[29] X. Shen, G. O. Jones, D. A. Watson, B. Bhayana, S. L. Buchwald, *J. Am. Chem. Soc.* **2010**, *132*, 11278-11287.

[30] G. Hedouin, S. Hazra, F. Gallou, S. Handa, *ACS Catal.* **2022**, *12*, 4918-4937.

[31] M. Uemura, K. Kamikawa, *J. Chem. Soc., Chem. Commun.* **1994**, 2697-2698.

[32] K. Kamikawa, T. Watanabe, M. Uemura, *J. Org. Chem.* **1996**, *61*, 1375-1384.

[33] S. G. Nelson, M. A. Hilfiker, *Org. Lett.* **1999**, *1*, 1379-1382.

[34] K. Nicolaou, H. Li, C. N. Boddy, J. M. Ramanjulu, T. Y. Yue, S. Natarajan, X. J. Chu, S. Bräse, F. Rübsam, *Chem. Eur. J.* **1999**, *5*, 2584-2601.

[35] B. H. Lipshutz, J. M. Keith, *Angew. Chem. Int. Ed.* **1999**, *38*, 3530-3533.

[36] A. Joncour, A. Décor, S. Thoret, A. Chiaroni, O. Baudoin, *Angew. Chem.* **2006**, *118*, 4255-4258.

[37] F. Colobert, V. Valdivia, S. Choppin, F. R. Leroux, I. Fernández, E. Álvarez, N. Khiar, *Org. Lett.* **2009**, *11*, 5130-5133.

[38] Y.-N. Ma, S.-D. Yang, *Chem. Eur. J.* **2015**, *21*, 6673-6677.

[39] Y.-N. Ma, S.-D. Yang, *Chem. Rec.* **2016**, *16*, 977-986.

[40] Y.-I. Jo, C.-Y. Lee, C.-H. Cheon, *Org. Lett.* **2020**, *22*, 4653-4658.

[41] J. F. Jensen, M. Johannsen, *Org. Lett.* **2003**, *5*, 3025-3028.

[42] Y. Zhou, X. Zhang, H. Liang, Z. Cao, X. Zhao, Y. He, S. Wang, J. Pang, Z. Zhou, Z. Ke, L. Qiu, *ACS Catal.* **2014**, *4*, 1390-1397.

[43] Y. Li, B. Pan, X. He, W. Xia, Y. Zhang, H. Liang, C. V. Subba Reddy, R. Cao, L. Qiu, *Beilstein J. Org. Chem.* **2020**, *16*, 966-973.

[44] W. Tang, N. D. Patel, G. Xu, X. Xu, J. Savoie, S. Ma, M.-H. Hao, S. Keshipeddy, A. G. Capacci, X. Wei, Y. Zhang, J. J. Gao, W. Li, S. Rodriguez, B. Z. Lu, N. K. Yee, C. H. Senanayake, *Org. Lett.* **2012**, *14*, 2258-2261.

[45] G. Xu, W. Fu, G. Liu, C. H. Senanayake, W. Tang, *J. Am. Chem. Soc.* **2014**, *136*, 570-573.

[46] X. Yang, G. Xu, W. Tang, *Tetrahedron* **2016**, *72*, 5178-5183.

[47] A. Bermejo, A. Ros, R. Fernández, J. M. Lassaletta, *J. Am. Chem. Soc.* **2008**, *130*,

15798-15799.

[48] S.-S. Zhang, Z.-Q. Wang, M.-H. Xu, G.-Q. Lin, *Org. Lett.* **2010**, *12*, 5546-5549.

[49] D. Shen, Y. Xu, S.-L. Shi, *J. Am. Chem. Soc.* **2019**, *141*, 14938-14945.

[50] M. C. Willis, L. H. Powell, C. K. Claverie, S. J. Watson, *Angew. Chem. Int. Ed.* **2004**, *43*, 1249-1251.

[51] X. Urbaneja, A. Mercier, C. Besnard, E. P. Kündig, *ChemComm* **2011**, *47*, 3739-3741.

[52] G. Zou, J. Falck, *Tetrahedron Lett.* **2001**, *42*, 5817-5819.

[53] Y. Yamamoto, S. Takada, N. Miyaura, *Chem. Lett.* **2006**, *35*, 1368-1369.

[54] Y. Yamamoto, S. Takada, N. Miyaura, T. Iyama, H. Tachikawa, *Organometallics* **2009**, *28*, 152-160.

[55] C. Sun, B. Potter, J. P. Morken, *J. Am. Chem. Soc.* **2014**, *136*, 6534-6537.

[56] Y. Yang, S. L. Buchwald, *J. Am. Chem. Soc.* **2013**, *135*, 10642-10645.

[57] C. H. Schuster, J. R. Coombs, Z. A. Kasun, J. P. Morken, *Org. Lett.* **2014**, *16*, 4420-4423.

[58] K.-G. Chung, Y. Miyake, S. Uemura, *J. Chem. Soc., Perkin trans. 1* **2000**, 15-18.

[59] B. Saito, G. C. Fu, *J. Am. Chem. Soc.* **2007**, *129*, 9602-9603.

[60] B. Saito, G. C. Fu, *J. Am. Chem. Soc.* **2008**, *130*, 6694-6695.

[61] N. A. Owston, G. C. Fu, *J. Am. Chem. Soc.* **2010**, *132*, 11908-11909.

[62] P. M. Lundin, G. C. Fu, *J. Am. Chem. Soc.* **2010**, *132*, 11027-11029.

[63] Z. Lu, A. Wilsily, G. C. Fu, *J. Am. Chem. Soc.* **2011**, *133*, 8154-8157.

[64] S. L. Zultanski, G. C. Fu, *J. Am. Chem. Soc.* **2011**, *133*, 15362-15364.

[65] A. Wilsily, F. Tramutola, N. A. Owston, G. C. Fu, *J. Am. Chem. Soc.* **2012**, *134*, 5794-5797.

[66] P. Tian, H.-Q. Dong, G.-Q. Lin, *ACS Catal.* **2012**, *2*, 95-119.

[67] F. Menard, T. M. Chapman, C. Dockendorff, M. Lautens, *Org. Lett.* **2006**, *8*, 4569-4572.

[68] F. Menard, D. Perez, D. Sustac Roman, T. M. Chapman, M. Lautens, *J. Org. Chem.* **2010**, *75*, 4056-4068.

[69] R. Jacques, A. M. L. Hell, R. D. C. Pullin, S. P. Fletcher, *Tetrahedron* **2019**, *75*, 130560.

[70] L. Dong, Y.-J. Xu, L.-F. Cun, X. Cui, A.-Q. Mi, Y.-Z. Jiang, L.-Z. Gong, *Org. Lett.* **2005**, *7*, 4285-4288.

[71] F. W. Goetzke, M. Mortimore, S. P. Fletcher, *Angew. Chem. Int. Ed.* **2019**, *58*, 12128-12132.

[72] R. Kučera, F. W. Goetzke, S. P. Fletcher, *Org. Lett.* **2020**, *22*, 2991-2994.

[73] S. Mishra, F. C. T. Modicom, C. L. Dean, S. P. Fletcher, *Commun. Chem.* **2022**, *5*, 154.

[74] L. Cunningham, S. Mishra, L. Matthews, S. P. Fletcher, *Org. Lett.* **2022**, *24*, 8886-8889.

[75] S.-P. Jiang, X.-Y. Dong, Q.-S. Gu, L. Ye, Z.-L. Li, X.-Y. Liu, *J. Am. Chem. Soc.* **2020**, *142*, 19652-19659.

[76] T. Iwamoto, C. Okuzono, L. Adak, M. Jin, M. Nakamura, *ChemComm* **2019**, *55*, 1128-1131.

[77] J. Y. Hamilton, D. Sarlah, E. M. Carreira, *Angew. Chem.* **2013**, *125*, 7680-7683.

[78] Y. Zheng, B.-B. Yue, K. Wei, Y.-R. Yang, *Org. Lett.* **2018**, *20*, 8035-8038.

[79] E. Vitaku, D. T. Smith, J. T. Njardarson, *J. Med. Chem.* **2014**, *57*, 10257-10274.

[80] N. Kerru, L. Gummidi, S. Maddila, K. K. Gangu, S. B. Jonnalagadda, *Molecules* **2020**, *25*, 1909.

[81] D. W. Old, J. P. Wolfe, S. L. Buchwald, *J. Am. Chem. Soc.* **1998**, *120*, 9722-9723.

[82] A. F. Littke, C. Dai, G. C. Fu, *J. Am. Chem. Soc.* **2000**, *122*, 4020-4028.

[83] R. A. Batey, T. D. Quach, *Tetrahedron Lett.* **2001**, *42*, 9099-9103.

[84] G. A. Morris, S. T. Nguyen, *Tetrahedron Lett.* **2001**, *42*, 2093-2096.

[85] W. Goodall, K. Wild, K. J. Arm, J. G. Williams, *J. Chem. Soc., Perkin trans. II* **2002**, 1669-1681.

[86] D. J. Wallace, C.-y. Chen, *Tetrahedron Lett.* **2002**, *43*, 6987-6990.

[87] G. A. Molander, B. Biolatto, *J. Org. Chem.* **2003**, *68*, 4302-4314.

[88] K. M. L. Daku, R. F. Newton, S. P. Pearce, J. Vile, J. M. Williams, *Tetrahedron Lett.* **2003**, *44*, 5095-5098.

[89] A.-S. Rebstock, F. Mongin, F. Trécourt, G. Quéguiner, *Tetrahedron* **2003**, *59*, 4973-4977.

[90] T. E. Barder, S. L. Buchwald, *Org. Lett.* **2004**, *6*, 2649-2652.

[91] P. Appukkuttan, A. B. Orts, R. P. Chandran, J. L. Goeman, J. Van der Eycken, W. Dehaen, E. Van der Eycken, *Eur. J. Org. Chem.* **2004**, *2004*, 3277-3285.

[92] J. W. Dankwardt, *Angew. Chem. Int. Ed.* **2004**, *43*, 2428-2432.

[93] C. Y. Legault, Y. Garcia, C. A. Merlic, K. Houk, *J. Am. Chem. Soc.* **2007**, *129*, 12664-12665.

[94] Y.-Q. Fang, M. Lautens, *J. Org. Chem.* **2008**, *73*, 538-549.

[95] M. A. Düfert, K. L. Billingsley, S. L. Buchwald, *J. Am. Chem. Soc.* **2013**, *135*, 12877-12885.

[96] W. Liu, X. Yu, Y. Li, C. Kuang, *ChemComm* **2014**, *50*, 9291-9294.

[97] W. Miura, K. Hirano, M. Miura, *Org. Lett.* **2016**, *18*, 3742-3745.

[98] J. Zhong, Y. Long, X. Yan, S. He, R. Ye, H. Xiang, X. Zhou, *Org. Lett.* **2019**, *21*, 9790-

9794.

[99] M. Zhou, J. Tsien, T. Qin, *Angew. Chem. Int. Ed.* **2020**, *59*, 7372-7376.

[100] N. Kudo, M. Perseghini, G. C. Fu, *Angew. Chem. Int. Ed.* **2006**, *45*, 1282-1284.

[101] X. A. F. Cook, A. de Gombert, J. McKnight, L. R. E. Pantaine, M. C. Willis, *Angew. Chem. Int. Ed.* **2021**, *60*, 11068-11091.

[102] C. Fischer, G. C. Fu, *J. Am. Chem. Soc.* **2005**, *127*, 4594-4595.

[103] F. O. Arp, G. C. Fu, *J. Am. Chem. Soc.* **2005**, *127*, 10482-10483.

[104] S. Son, G. C. Fu, *J. Am. Chem. Soc.* **2008**, *130*, 2756-2757.

[105] X. Dai, N. A. Strotman, G. C. Fu, *J. Am. Chem. Soc.* **2008**, *130*, 3302-3303.

[106] S. W. Smith, G. C. Fu, *J. Am. Chem. Soc.* **2008**, *130*, 12645-12647.

[107] P. Pomarański, S. Samanta, P. Roszkowski, J. K. Maurin, Z. Czarnocki, *Tetrahedron Lett.* **2016**, *57*, 4713-4717.

[108] N. Haddad, H. P. R. Mangunuru, K. R. Fandrick, B. Qu, J. D. Sieber, S. Rodriguez, J.-N. Desrosiers, N. D. Patel, H. Lee, D. Kurouski, N. Grinberg, N. K. Yee, J. J. Song, C. H. Senanayake, *Adv. Synth. Catal.* **2016**, *358*, 3522-3527.

[109] W. Xia, Y. Li, Z. Zhou, H. Chen, H. Liang, S. Yu, X. He, Y. Zhang, J. Pang, Z. Zhou, L. Qiu, *Adv. Synth. Catal.* **2017**, *359*, 1656-1662.

[110] W. Xia, Z.-W. Zhang, Y. Li, X. Jiang, H. Liang, Y. Zhang, R. Cao, L. Qiu, *Org. Biomol. Chem.* **2019**, *17*, 2351-2355.

[111] M. E. Welsch, S. A. Snyder, B. R. Stockwell, *Curr. Opin. Chem. Biol.* **2010**, *14*, 347-361.

[112] R. D. Taylor, M. MacCoss, A. D. G. Lawson, *J. Med. Chem.* **2014**, *57*, 5845-5859.

[113] J. Ding, T. Rybak, D. G. Hall, *Nat. Commun.* **2014**, *5*, 5474.

[114] X. Ma, H. Zhao, M. Binayeva, G. Ralph, M. Diane, S. Zhao, C.-Y. Wang, M. R. Biscoe, *Chem* **2020**, *6*, 781-791.

[115] R. Firestein, A. J. Bass, S. Y. Kim, I. F. Dunn, S. J. Silver, I. Guney, E. Freed, A. H. Ligon, N. Vena, S. Ogino, *Nature* **2008**, *455*, 547-551.

[116] R. Firestein, K. Shima, K. Nosho, N. Irahara, Y. Baba, E. Bojarski, E. L. Giovannucci, W. C. Hahn, C. S. Fuchs, S. Ogino, *Int. J. Cancer.* **2010**, *126*, 2863-2873.

[117] A. S. Adler, M. L. McCleland, T. Truong, S. Lau, Z. Modrusan, T. M. Soukup, M. Roose-Girma, E. M. Blackwood, R. Firestein, *Cancer Res.* **2012**, *72*, 2129-2139.

[118] M. Sidera, S. P. Fletcher, *Nat. Chem.* **2015**, *7*, 935-939.

[119] P. Schäfer, T. Palacin, M. Sidera, S. P. Fletcher, *Nat. Comm.* **2017**, *8*, 15762.

[120] G. Ison, L. J. Howie, L. Amiri-Kordestani, L. Zhang, S. Tang, R. Sridhara, V. Pierre, R.

Charlab, A. Ramamoorthy, P. Song, F. Li, J. Yu, W. Manheng, T. R. Palmby, S. Ghosh, H. N. Horne, E. Y. Lee, R. Philip, K. Dave, X. H. Chen, S. L. Kelly, K. G. Janoria, A. Banerjee, O. Eradiri, J. Dinin, K. B. Goldberg, W. F. Pierce, A. Ibrahim, P. G. Kluetz, G. M. Blumenthal, J. A. Beaver, R. Pazdur, *Clin. Cancer Res.* **2018**, *24*, 4066-4071.

[121] X. Shu, D. Zhong, Y. Lin, X. Qin, H. Huo, *J. Am. Chem. Soc.* **2022**, *144*, 8797-8806.

[122] Y. Zhang, F. W. Goetzke, K. E. Christensen, S. P. Fletcher, *ACS Catal.* **2022**, *12*, 8995-9002.

[123] G. Fodor, R. Dharanipragada, *Nat. Prod. Rep.* **1994**, *11*, 443-450.

[124] S. Afewerki, J.-X. Wang, W.-W. Liao, A. Córdova, in *The Alkaloids: Chemistry and Biology, Vol. 81* (Ed.: H.-J. Knölker), Academic Press, **2019**, pp. 151-233.

[125] S. Rodriguez, U. Uria, E. Reyes, L. Prieto, M. Rodríguez-Rodríguez, L. Carrillo, J. L. Vicario, *Org. Biomol. Chem.* **2021**, *19*, 3763-3775.

[126] B. Dräger, *Nat. Prod. Rep.* **2004**, *21*, 211-223.

[127] G. Grynkiewicz, M. Gadzikowska, *Pharmacol. Rep.* **2008**, *60*, 439.

[128] M. Gadzikowska, G. Grynkiewicz, *Acta Pol. Pharm.* **2001**, *58*, 481-492.

[129] M. Lounasmaa, T. Tamminen, in *The Alkaloids: Chemistry and Pharmacology*, **1993**, pp. 1-114.

[130] K. L. Kohnen-Johannsen, O. Kayser, *Molecules* **2019**, *24*, 796.

[131] R. Willstätter, A. Bode, *Ber. Dtsch. Chem. Ges.* **1901**, *34*, 1457-1461.

[132] R. Robinson, *J. Chem. Soc., Trans.* **1917**, *111*, 762-768.

[133] C. Schopf, G. Lehmann, *Justus Liebigs Ann. Chem.* **1935**, *518*, 1-37.

[134] C. Schöpf, *Angew. Chem.* **1937**, *50*, 797-805.

[135] R. Willstätter, O. Wolfes, H. Mäder, *Justus Liebigs Ann. Chem.* **1923**, *434*, 111-139.

[136] W. Parker, R. A. Raphael, D. I. Wilkinson, *J. Chem. Soc.* **1959**, 2433-2437.

[137] G. P. Pollini, S. Benetti, C. De Risi, V. Zanirato, *Chem. Rev.* **2006**, *106*, 2434-2454.

[138] O. Duclos, A. Duréault, J. Depezay, *Tetrahedron Lett.* **1992**, *33*, 1059-1062.

[139] F.-D. Boyer, J.-Y. Lallemand, *Synlett* **1992**, 969-971.

[140] F. o.-D. Boyer, J.-Y. Lallemand, *Tetrahedron* **1994**, *50*, 10443-10458.

[141] P. R. Skaanderup, R. Madsen, *ChemComm* **2001**, 1106-1107.

[142] J. Marco-Contelles, E. de Opazo, *J. Org. Chem.* **2002**, *67*, 3705-3717.

[143] A. S. Hernández, A. Thaler, J. Castells, H. Rapoport, *J. Org. Chem.* **1996**, *61*, 314-323.

[144] R. Lin, J. Castells, H. Rapoport, *J. Org. Chem.* **1998**, *63*, 4069-4078.

[145] S. C. Turner, H. Zhai, H. Rapoport, *J. Org. Chem.* **2000**, *65*, 861-870.

[146] V. K. Aggarwal, C. J. Astle, M. Rogers-Evans, *Org. Lett.* **2004**, *6*, 1469-1471.

[147] M. Majewski, G.-Z. Zheng, *Synlett* **1991**, *1991*, 173-175.
[148] M. Majewski, R. Lazny, *Tetrahedron Lett.* **1994**, *35*, 3653-3656.
[149] M. Majewski, R. Lazny, *J. Org. Chem.* **1995**, *60*, 5825-5830.
[150] M. Majewski, R. Lazny, *Synlett* **1996**, *1996*, 785-786.
[151] M. Majewski, R. Lazny, A. Ulaczyk, *Can. J. Chem.* **1997**, *75*, 754-761.
[152] R. Lazny, M. Sienkiewicz, T. Olenski, Z. Urbanczyk-Lipkowska, P. Kalicki, *Tetrahedron* **2012**, *68*, 8236-8244.
[153] J. C. Lee, K. Lee, J. K. Cha, *J. Org. Chem.* **2000**, *65*, 4773-4775.
[154] Y. Yu, X.-F. Yang, C.-F. Xu, C.-H. Ding, X.-L. Hou, *Org. Lett.* **2013**, *15*, 3880-3883.
[155] K. Kulkarni, A. Y. Zhao, A. W. Purcell, P. Perlmutter, *Synlett* **2008**, *2008*, 2209-2212.
[156] N. Cramer, S. Laschat, A. Baro, W. Frey, *Synlett* **2003**, *2003*, 2175-2177.
[157] D. M. Mans, W. H. Pearson, *Org. Lett.* **2004**, *6*, 3305-3308.
[158] J. H. Xu, S. C. Zheng, J. W. Zhang, X. Y. Liu, B. Tan, *Angew. Chem. Int. Ed.* **2016**, *55*, 11834-11839.
[159] H. M. Davies, N. J. Huby, *Tetrahedron Lett.* **1992**, *33*, 6935-6938.
[160] H. M. L. Davies, J. J. Matasi, L. M. Hodges, N. J. S. Huby, C. Thornley, N. Kong, J. H. Houser, *J. Org. Chem.* **1997**, *62*, 1095-1105.
[161] R. Narayan, J. O. Bauer, C. Strohmann, A. P. Antonchick, H. Waldmann, *Angew. Chem. Int. Ed.* **2013**, *52*, 12892-12896.
[162] B. Hu, X. Zhang, Y. Mo, J. Li, L. Lin, X. Liu, X. Feng, *Org. Lett.* **2020**, *22*, 1034-1039.
[163] D. C. Marcote, I. Varela, J. Fernández-Casado, J. L. Mascareñas, F. López, *J. Am. Chem. Soc.* **2018**, *140*, 16821-16833.
[164] R. P. Reddy, H. M. L. Davies, *J. Am. Chem. Soc.* **2007**, *129*, 10312-10313.
[165] Z. J. Jia, G. Shan, C. G. Daniliuc, A. P. Antonchick, H. Waldmann, *Angew. Chem. Int. Ed.* **2018**, *57*, 14493-14497.
[166] H. Suga, M. Yoshiwara, T. Yamaguchi, T. Bando, M. Taguchi, A. Inaba, Y. Goto, A. Kikuchi, K. Itoh, Y. Toda, *ChemComm* **2019**, *55*, 1552-1555.
[167] S. Rodriguez, U. Uria, E. Reyes, L. Carrillo, T. Tejero, P. Merino, J. L. Vicario, *Angew. Chem.* **2020**, *132*, 6846-6850.
[168] G.-J. Lin, X. Zheng, P.-Q. Huang, *ChemComm* **2011**, *47*, 1545-1547.
[169] H. Xu, C. Golz, C. Strohmann, A. P. Antonchick, H. Waldmann, *Angew. Chem.* **2016**, *128*, 7892-7896.
[170] L. Melzig, A. Gavryushin, P. Knochel, *Org. Lett.* **2007**, *9*, 5529-5532.
[171] M. Hassine, H. B. Jannet, N. Ghermani, M. Alami, S. Messaoudi, *Synth.* **2020**, *52*, 450-

458.

[172] N. Sakai, A. Ridder, J. F. Hartwig, *J. Am. Chem. Soc.* **2006**, *128*, 8134-8135.

[173] J. Buter, R. Moezelaar, A. J. Minnaard, *Org. Biomol. Chem.* **2014**, *12*, 5883-5890.

[174] P. A. Cox, A. G. Leach, A. D. Campbell, G. C. Lloyd-Jones, *J. Am. Chem. Soc.* **2016**, *138*, 9145-9157.

[175] H. Y. W. He, S. L.; Zhang, Y.; Ma, B.; Chen, Y.; Wang, Y. H.et al., *Vol. WO2015131773A1*, **2015**.

[176] Z. Zeng, J. Zhang, M. Jia, B. Wu, X. Cai, X. Zhang, Y. Feng, Y. Ma, Q. Gao, Z. Fei, *Org. Process Res. Dev.* **2022**, *26*, 447-457.

[177] S. Karabiyikoglu, A. V. Brethomé, T. Palacin, R. S. Paton, S. P. Fletcher, *Chem. Sci.* **2020**, *11*, 4125-4130.

[178] L. N. Yakhontov, in *Advances in Heterocyclic Chemistry, Vol. 11* (Eds.: A. R. Katritzky, A. J. Boulton), Academic Press, **1970**, pp. 473-523.

[179] M. D. Mashkovsky, L. N. Yakhontov, M. E. Kaminka, E. E. Mikhlina, in *Progress in Drug Research / Fortschritte der Arzneimittelforschung / Progrès des recherches pharmaceutiques* (Ed.: E. Jucker), Birkhäuser Basel, Basel, **1983**, pp. 9-61.

[180] N. M. Hext, J. Hansen, A. J. Blake, D. E. Hibbs, M. B. Hursthouse, O. V. Shishkin, M. Mascal, *J. Org. Chem.* **1998**, *63*, 6016-6020.

[181] W. S. Hamama, O. M. A. El-Magid, H. H. Zoorob, *J. Heterocycl. Chem.* **2006**, *43*, 1397-1420.

[182] S. Wawzonek, M. F. Nelson, Jr., P. J. Thelen, *J. Am. Chem. Soc.* **1951**, *73*, 2806-2808.

[183] K. C. Bharadwaj, T. Gupta, R. M. Singh, in *Synthesis of Medicinal Agents from Plants* (Eds.: A. Tewari, S. Tiwari), Elsevier, **2018**, pp. 205-227.

[184] P. J. Boratyński, M. Zielińska-Błajet, J. Skarżewski, in *The Alkaloids: Chemistry and Biology, Vol. 82*, **2019**, pp. 29-145.

[185] P. J. Boratyński, M. Zielińska-Błajet, J. Skarżewski, in *The Alkaloids: Chemistry and Biology, Vol. 82* (Ed.: H.-J. Knölker), Academic Press, **2019**, pp. 29-145.

[186] H. M. Staines, S. Krishna, *Treatment and prevention of malaria: antimalarial drug chemistry, action and use*, Springer Science & Business Media, **2012**.

[187] A. U. Krettli, SciELO Brasil, **2001**.

[188] T. S. Kaufman, E. A. Rúveda, *Angew. Chem. Int. Ed.* **2005**, *44*, 854-885.

[189] A. A. Grace, A. J. Camm, *N. Engl. J. Med.* **1998**, *338*, 35-45.

[190] H. Jang, J. Lee, C. Song, Wiley-VCH, Weinheim, **2009**.

[191] C. E. Song, in *The Alkaloids: Chemistry and Biology, Vol. 53*, Academic Press, **1999**,

pp. 1-56.

[192] E. N. Jacobsen, I. Marko, W. S. Mungall, G. Schroeder, K. B. Sharpless, *J. Am. Chem. Soc.* **1988**, *110*, 1968-1970.

[193] K. Hoi-Lun, C. Sorato, Y. Ogino, C. Hou, K. B. Sharpless, *Tetrahedron Lett.* **1990**, *31*, 2999-3002.

[194] K. B. Sharpless, W. Amberg, Y. L. Bennani, G. A. Crispino, J. Hartung, K. S. Jeong, H. L. Kwong, K. Morikawa, Z. M. Wang, *J. Org. Chem.* **1992**, *57*, 2768-2771.

[195] H. C. Kolb, M. S. VanNieuwenhze, K. B. Sharpless, *Chem. Rev.* **1994**, *94*, 2483-2547.

[196] K. Kacprzak, **2013**, pp. 605-641.

[197] P. Pelletier, *Ann. Chim. Phys.* **1819**, *10*, 142-177.

[198] É. Henry, A. Delondre, *J. Pharm.* **1833**, *19*, 623-625.

[199] É. Henry, A. Delondre, *J. Pharm.* **1834**, *20*, 157-162.

[200] R. B. Turner, R. Woodward, in *The Alkaloids: Chemistry and Physiology, Vol. 3*, Elsevier, **1953**, pp. 1-63.

[201] L. Andersson, M. L. Kawasaki, *Revision of the genus Cinchona (Rubiaceae-Cinchoneae)*, New York Botanical Garden, **1997**.

[202] A. Strecker, *Justus Liebigs Ann. Chem.* **1854**, *91*, 349-351.

[203] P. Rabe, W. Schneider, E. Ackermann, *Ber. Dtsch. Chem. Ges.* **1907**, *40*, 3655.

[204] P. Rabe, K. Kindler, *Ber. Dtsch. Chem. Ges.* **1918**, *51*, 466-467.

[205] P. Rabe, *Justus Liebigs Ann. Chem.* **1932**, *492*, 242-266.

[206] A. C. Smith, R. M. Williams, *Angew. Chem., Int. Ed.* **2008**, *47*, 1736-1740.

[207] R. B. Woodward, W. E. Doering, *J. Am. Chem. Soc.* **1944**, *66*, 849-849.

[208] R. B. Woodward, W. E. Doering, *J. Am. Chem. Soc.* **1945**, *67*, 860-874.

[209] G. Stork, D. Niu, A. Fujimoto, E. R. Koft, J. M. Balkovec, J. R. Tata, G. R. Dake, *J. Am. Chem. Soc.* **2001**, *123*, 3239-3242.

[210] I. T. Raheem, S. N. Goodman, E. N. Jacobsen, *J. Am. Chem. Soc.* **2004**, *126*, 706-707.

[211] M. Arshad, M. A. Fernández, E. M. McGarrigle, V. K. Aggarwal, *Tetrahedron Asymmetry* **2010**, *21*, 1771-1776.

[212] O. Illa, M. Arshad, A. Ros, E. M. McGarrigle, V. K. Aggarwal, *J. Am. Chem. Soc.* **2010**, *132*, 1828-1830.

[213] G. K. Friestad, A. Ji, C. S. Korapala, J. Qin, *Org. Biomol. Chem.* **2011**, *9*, 4039-4043.

[214] G. K. Friestad, A. Ji, J. Baltrusaitis, C. S. Korapala, J. Qin, *J. Org. Chem.* **2012**, *77*, 3159-3180.

[215] J. Igarashi, M. Katsukawa, Y.-G. Wang, H. P. Acharya, Y. Kobayashi, *Tetrahedron Lett.*

2004, *45*, 3783-3786.

[216] J. Igarashi, Y. Kobayashi, *Tetrahedron Lett.* **2005**, *46*, 6381-6384.

[217] S. Sarkar, P. K. Chatterjee, L. H. Cumbal, A. K. SenGupta, *Chem. Eng. J.* **2011**, *166*, 923-931.

[218] P. Webber, M. J. Krische, *J. Org. Chem.* **2008**, *73*, 9379-9387.

[219] Z. Luo, Z. Wang, G. Sun, W. Jian, F. Jiang, B. Luan, R. Li, L. Zhang, *Org. Lett.* **2020**, *22*, 4322-4326.

[220] H. Brunner, J. Bügler, B. Nuber, *Tetrahedron Asymmetry* **1995**, *6*, 1699-1702.

[221] I. A. O'Neil, J. Hitchin, I. Bhamra, A. P. Chorlton, D. J. Tapolczay, *Tetrahedron Lett.* **2008**, *49*, 7416-7418.

[222] I. A. O'Neil, D. Wynn, J. Y. Q. Lai, *Tetrahedron Lett.* **2000**, *41*, 271-274.

[223] V. K. Aggarwal, I. Emme, S. Y. Fulford, *J. Org. Chem.* **2003**, *68*, 692-700.

[224] W. Xiao, X. Wang, R. Liu, J. Wu, *Chin Chem Lett* **2021**, *32*, 1847-1856.

[225] J. Frackenpohl, W. M. Braje, H. M. R. Hoffmann, *J. Chem. Soc., Perkin trans. 1* **2001**, 47-65.

[226] A. Ouach, J. Vercouillie, E. Bertrand, N. Rodrigues, F. Pin, S. Serriere, L. Boiaryna, A. Chartier, N. Percina, P. Tangpong, Z. Gulhan, C. Mothes, J.-B. Deloye, D. Guilloteau, G. Page, F. Suzenet, F. Buron, S. Chalon, S. Routier, *Eur. J. Med. Chem.* **2019**, *179*, 449-469.

[227] J. Bredt, *Justus Liebigs Ann. Chem.* **1924**, *437*, 1-13.

[228] J. Bredt, J. Houben, P. Levy, *Ber. Dtsch. Chem. Ges.* **1902**, *35*, 1286-1292.

[229] F. W. Goetzke, A. M. Hell, L. van Dijk, S. P. Fletcher, *Nat. Chem.* **2021**, *13*, 880-886.

[230] C. A. Grob, A. Kaiser, E. Renk, *Helv. Chim. Acta.* **1957**, *40*, 2170-2185.

[231] M.-C. Lasne, J.-L. Ripoll, J.-C. Guillemin, J.-M. Denis, *Tetrahedron Lett.* **1984**, *25*, 3847-3848.

[232] J.-C. Guillemin, J.-M. Denis, M.-C. Lasne, J.-L. Ripoll, *Tetrahedron* **1988**, *44*, 4447-4455.

[233] J. González, L. van Dijk, F. W. Goetzke, S. P. Fletcher, *Nat. Protoc.* **2019**, *14*, 2972-2985.

[234] L. van Dijk, R. Ardkhean, M. Sidera, S. Karabiyikoglu, Ö. Sari, T. D. W. Claridge, G. C. Lloyd-Jones, R. S. Paton, S. P. Fletcher, *Nat. Catal.* **2021**, *4*, 284-292.

[235] F. W. Goetzke, S. P. Fletcher, *Synlett* **2021**, *32*, 1816-1825.

[236] J. Panteleev, F. Menard, M. Lautens, *Adv. Synth. Catal.* **2008**, *350*, 2893-2902.

[237] F. W. Friese, A. Studer, *Angew. Chem. Int. Ed.* **2019**, *58*, 9561-9564.

[238] T. Nagase, T. Takahashi, T. Sasaki, A. Nagumo, K. Shimamura, Y. Miyamoto, H. Kitazawa, M. Kanesaka, R. Yoshimoto, K. Aragane, *J. Med. Chem.* **2009**, *52*, 4111-4114.

[239] C. Dallanoce, F. Frigerio, G. Martelli, G. Grazioso, C. Matera, D. Y. Pomè, L. Pucci, F. Clementi, C. Gotti, M. De Amici, *Bioorg. Med. Chem.* **2010**, *18*, 4498-4508.

[240] S. P. Chavan, N. B. Dumare, K. P. Pawar, *RSC Adv.* **2014**, *4*, 32594-32598.

[241] H. Kubas, U. Meyer, M. Hechenberger, K.-U. Klein, P. Plitt, R. Zemribo, H. W. Spexgoor, S. G. van Assema, U. Abel, *Bioorganic Med. Chem. Lett.* **2013**, *23*, 6370-6376.

[242] A. M. Baylis, E. J. Thomas, *Tetrahedron* **2007**, *63*, 11666-11671.

[243] C. Dallanoce, F. Frigerio, G. Martelli, G. Grazioso, C. Matera, D. Y. Pomè, L. Pucci, F. Clementi, C. Gotti, M. D. Amici, *Bioorg. Med. Chem.* **2010**, *18*, 4498-4508.

[244] G. Han, M. Tamaki, V. J. Hruby, *Pept. Res.* **2001**, *58*, 338-341.

[245] M. H. Katcher, A. G. Doyle, *J. Am. Chem. Soc.* **2010**, *132*, 17402-17404.

[246] Z. Zhang, F. Wang, X. Mu, P. Chen, G. Liu, *Angew. Chem. Int. Ed.* **2013**, *52*, 7549-7553.

[247] H. Nagata, M. Kawamura, K. Ogasawara, *Synth.* **2000**, *2000*, 1825-1834.

[248] Y. A. Almehmadi, F. G. West, *Org. Lett.* **2020**, *22*, 6091-6095.

[249] E. Vedejs, M. Jure, *Angew. Chem. Int. Ed.* **2005**, *44*, 3974-4001.

[250] L. Palatinus, G. Chapuis, *J. Appl. Crystallogr.* **2007**, *40*, 786-790.

[251] P. Parois, R. I. Cooper, A. L. Thompson, *Chem. Cent. J.* **2015**, *9*, 30-30.

[252] R. I. Cooper, A. L. Thompson, D. J. Watkin, *J. Appl. Crystallogr.* **2010**, *43*, 1100-1107.